ZHI LI

Regulatory mechanisms of the bivalve mantle and their association with shell biomineralization

UNIVERSIDADE DO ALGARVE

Faculdade de Ciências e Tecnologia

Faro, 2024

ZHI LI

Regulatory mechanisms of the bivalve mantle and their association with shell biomineralization

Doutoramento em Ciências Biológicas

Especialidade em Biologia de Desenvolvimento, Funcional e Integrativa

Trabalho efetuado sob a orientação de:

Prof. Doutora Deborah M. Power

Prof. Doutora João Carlos dos Reis Cardoso

UNIVERSIDADE DO ALGARVE

Faculdade de Ciências e Tecnologia

Faro, 2024

ZHI LI

Regulatory mechanisms of the bivalve mantle and their association with shell biomineralization

Doctoral Programme in Biological Sciences

Specialty in Developmental, Functional and Integrative Biology

Supervisors:

Prof. Doctor Deborah M. Power

Prof. Doctor João Carlos dos Reis Cardoso

UNIVERSIDADE DO ALGARVE

Faculdade de Ciências e Tecnologia

Faro, 2024

Título | Thesis title

Regulatory mechanisms of the bivalve mantle and their association with shell biomineralization

Declaração de autoria de trabalho:

Declaro ser a autora deste trabalho que é original e inédito. Autores e trabalhos consultados estão devidamente citados no texto e constam da listagem de referências incluída.

Declaration of authorship:

This work has not previously been submitted for a degree in any university. To the best of my knowledge and belief, the thesis contains no material previously published or written by another person except where due reference is made in the thesis itself.

Zhi Li

Copyright: Zhi Li. A Universidade do Algarve reserva para si o direito, em conformidade com o disposto no Código do Direito de Autor e dos Direitos Conexos, de arquivar, reproduzir e publicar a obra, independentemente do meio utilizado, bem como de a divulgar através de repositórios científicos e de admitir a sua cópia e distribuição para fins meramente educacionais ou de investigação e não comerciais, conquanto seja dado o devido crédito ao autor e editor respetivos".

Copyright: Zhi Li. According to the code of authors copyright and related rights, the University of Algarve reserves the legal right, to file, reproduce and publish this work, regardless the means of disclosure, as well to divulge through scientific repositories and to allow its copy and distribution, for educational or research purposes, if due credit is given to the respective author and publisher.

Support

This study received Portuguese national funds from FCT - Foundation for Science and Technology through institutional projects UIDB/04326/2020, UIDP/04326/2020 and LA/P/0101/2020, and from the operational programmes CRESC Algarve 2020 and COMPETE 2020 through projects EMBRC.PT ALG-01-0145-FEDER-022121 and BIODATA.PT ALG-01-0145-FEDER-022231 and from FCT-funded project FCT-AGAKHAN/ 541666287/2019HealthyBi4 Namibe project. ZL was supported by a PhD scholarship from the China Scholarship Council.

Acknowledgments

I always thought there was plenty of time, and graduation seemed far away. Now, it's finally my turn to write here. On Christmas Eve in 2020, I arrived in this unfamiliar country. In pursuit of higher academic knowledgement, I came to a place 10,000 kilometers away from my hometown. These four years, so different from my previous experiences, have left a unique mark on the canvas of my life.

Completing this doctoral thesis has been a journey full of challenges and rewards, made possible through the inspiration and meticulous guidance of my supervisor, Professor Deborah Mary Power. I am deeply grateful to her for the help and care she provided during my Ph.D. research. In terms of academic research, she helped me gain a deeper understanding and appreciation of this field. She respected each of my viewpoints, offering suggestions, support, and guidance. Her expertise significantly enriched my knowledge and expanded my research experience. In terms of daily life, she provided me with great reassurance. When I first arrived in this completely unfamiliar environment, I was cautious about everything, but my supervisor told me, 'To do what you want.' I always remember this phrase; it encouraged me to communicate and be bold in facing challenges. I am deeply grateful to my supervisor for her invaluable feedback, patience, and dedication towards my academic and my life. These are priceless. I am truly fortunate, and her guidance will always be remembered.

I am fortunate to have met my second supervisor, Professor João Carlos dos Reis Cardoso. He is not only my tutor but also my best friend. In my experiments, he

always observed meticulously and paid attention to details. In writing papers and my dissertation, he not only scrutinized every word but also taught me step by step how to write a polished paper, raising my writing skills to a higher level. He was not just my mentor; he was more like a friend. Approachable, friendly, and sometimes joking around, he brought a relaxed atmosphere to the serious research environment. As a student, I am deeply grateful for his unwavering support.

I would like to extend special thanks to my colleagues and friends at CCMAR, whose camaraderie and insightful discussions made these four years both enjoyable and inspiring. I am particularly grateful to Professor Adelino Vicente Mendonça Canário, Rute Felix, Hamed Abdollahpour, Naghmeh Jafari Pastaki, Teresa Correia, Carina Mónico, and others for their help, support, and friendship in both my experiments and daily life. I also thank the China Scholarship Council for providing me with a four-year scholarship.

I am fortunate to have been raised by open-minded parents. I am grateful to my family for their unconditional trust, respect, and support. For twenty-eight years, they have prioritized my health and happiness, allowing me to follow my heart. When I decided to leave and travel thousands of kilometers away, they firmly told me that I had the freedom to make mistakes. Throughout these four years, I have always remembered my father's words at the boarding gate: 'If you can't keep going, come home.' These words have been my spiritual pillar over the past four years. In this thorny world, only your love remains an unsolvable enigma.

I save the most romantic thanks for last, to my fiancé Mr. Maoxiao Peng. We've

been in love for several years, supporting each other's studies, and have traveled together for many years, promising to explore the world hand in hand. Meeting you has been the greatest fortune of my life, sharing the warmth of every season. From dawn to dusk, through all our journeys, your presence brings comfort. Our love is like a gentle stream, and I am grateful to love you.

Finally, thank you all for being part of this journey. This is my graduation season - the past is still with me, and the future is also already here.

Abstract

The significance of bivalves lies both in their economic importance to the aquaculture and food industry and their ecological roles in marine environments. Biomineralized shells are a hallmark of bivalves, enclosing their soft bodies and being crucial for their survival. Although various neuropeptide precursors have been described, their role in biomineralization has not been emphasized. The primary objective of this paper is to explore the role of neuropeptides in the nervous system and mantle, and to investigate how the nervous system regulates mantle function. It aims to study how the nervous system regulates the biomineralization process and elucidate the complex mechanisms controlling mantle physiology and shell formation. The experimental methods used in this study include omics analysis. Additionally, the symmetrical marine bivalve, Mediterranean mussel (*Mytilus galloprovincialis*), was selected as the experimental subject, and verification experiments were conducted at the immunohistochemical, molecular, and functional levels. The results of this study suggest that: 1) Neuropeptide gene expression at the mantle edge and in the cerebropleural ganglia (CPG) regulates shell regrowth. 2) Severing the CPG commissure inhibits shell regrowth and alters neuropeptide gene expression as well as the spatial organization of nerve fibers in the ganglia and mantle. 3) In the symmetrical bivalve *M. galloprovincialis*, gene expression in the left and right sides of the mantle is not completely symmetrical. 4) The CPG regulates the expression of genes related to biomineralization, with lncRNAs appearing to play an important role in the biomineralization process. This paper provides strong evidence that neuropeptides and

the nervous system influence mantle function and shell growth in bivalves. These findings contribute to our understanding of the role of the neuroendocrine system and neuropeptides in the mantle biomineralization toolbox of bivalves.

Keywords: bivalve, cerebropleural ganglia (CPG), lncRNA, mantle, neuropeptide, regrowth, shell biomineralization, symmetrical

Resumo

Os bivalves são um dos principais grupos de organismos invertebrados compreendendo aproximadamente 23% das espécies identificadas no ambiente marinho. A sua importância reside não só no seu papel económico para a aquicultura e para a indústria alimentar como também no seu papel ecológico como filtradores de água ambiental e no ciclo de nutrientes. Os bivalves fazem parte da classe Mollusca e todas as espécies identificadas nesta classe possuem uma concha biomineralizada que é uma das principais características da sua fisionomia. A concha nos bivalves funciona como o seu exoesqueleto. Esta é formada por duas valvas que isolam o corpo mole do meio exterior e desempenha um papel extremamente importante na sua sobrevivência, pois fornece proteção contra predadores e agressões ambientais, além de reduzir a perda de água e funcionar como um importante armazém de mineral. A concha dos bivalves é principalmente constituída por cristais biomineralizados de carbonato de cálcio ($CaCO_3$, constituindo cerca de 95% da concha) que se encontram complexados com uma matriz proteica que confere a estrutura característica à concha. O manto dos bivalves é o tecido que envolve e protege o seu corpo mole e está em contato direto com a parte interna da concha. Este é o principal órgão formador de conchas, e o crescimento da concha dependendo da atividade secretora da margem do manto. Para além do manto também já foi sugerido que os hemócitos (células circulantes) presentes no fluido circulante possuem também um papel importante na formação da estrutura biomineralizada da concha. Os mecanismos pelos quais os bivalves e outros moluscos com estruturas biomineralizadas produzem as suas

conchas biomineralizadas têm sido alvo de vários estudos e um conjunto de proteínas envolvidas na formação da concha já foram descritas (*biomineralization toolbox*), fornecendo recursos moleculares importantes para a compreensão dos mecanismos de produção de conchas. No entanto, ainda permanece por esclarecer como este mecanismo tão importante é regulado e quais são os fatores que contribuem para formação e crescimento da concha.

Os neuropéptidos são um grupo de moléculas mensageiras que estão envolvidas na regulação de vários processos fisiológicos em animais, incluindo em moluscos. Recentemente em moluscos gastrópodes foi sugerido que poderia existir um potencial envolvimento do neuropéptidos e do sistema neuroendócrino na regulação do crescimento da concha. No entanto o seu papel na regulação da biomineralização ainda não foi estudado. Em bivalves genomas e transcritomas existem para várias espécies e vários precursores para neuropéptidos já foram identificados com base em ferramentas bioinformáticas e genómica comparativa, mas, no entanto, a sua função para a maioria das moléculas permanece ainda por descobrir.

O manto em bivalves é um tecido que é inervado pelos gânglios nervosos descentralizados que se encontram em pares e existem ao longo do corpo do bivalve e análise do transcritoma do manto revela que existe uma variedade enorme de transcritos para neuropéptidos e para recetores de neuropéptidos a serem expressos o que sugere que este sistema (péptidos e seus recetores) possuem um potencial envolvimento na regulação da sua função e fisiologia do manto incluindo na formação e biomineralização da concha.

O objetivo principal desta tese consiste em determinar qual o papel dos neuropéptidos no sistema nervoso e no manto, e investigar como o sistema nervoso regula a função do manto usando como modelo o bivalve marinho comercial e economicamente importante, o mexilhão Mediterrâneo (*Mytillus galloprovincialis*) que é um bivalve simétrico onde as duas valvas da concha são idênticas. Esta tese foca-se em três objetivos principais: 1) Identificação dos precursores de neuropéptidos expressos no manto do mexilhão e desenvolver experiências de dano e reparação da concha biomineralizada e a resposta dos gânglios nervosos para caracterizar a expressão dos neuropéptidos do manto e identificar candidatos durante o processo de regeneração. 2) Determinar qual o papel sobre a regulação da biomineralização da concha no mexilhão pelo sistema nervoso - através da análise do transcritoma do manto, identificar transcritos envolvidos no crescimento da concha e caracterizar as suas potenciais funções reguladas pelo sistema nervoso. 3) Caracterizar a evolução do sistema dos neuropéptidos da família das Alatostatinas (ASTs), grupo característicos dos invertebrados e bastante estudado em insetos, e caracterizar a sua potencial função no manto dos bivalves através da análise comparativa e evolutiva entre diferentes membros desta família e caracterização da sua função. Os métodos experimentais utilizados neste estudo incluem a realização e desenvolvimento de várias experiências, análises da ômica (transcritoma e genoma) com base em informação disponível em bases de dados ou através de NGS de amostras de manto e do gânglio, bem como estudos bioquímicos e moleculares e de expressão para caracterizar a função dos genes candidatos.

Os resultados obtidos neste estudo sugerem que: 1) A expressão dos genes para os neuropéptidos na margem do manto e nos gânglios cerebropleurais (CPG) regulam o crescimento da concha. 2) A rutura através do corte da comissura nervosa que liga os dois gânglios CPG inibe a regeneração do crescimento da concha após dano e isto altera a expressão dos genes para os neuropéptidos, bem como a organização e distribuição espacial das fibras nervosas quer nos gânglios como no manto. 3) No mexilhão, que é um bivalve com concha simétrica, a expressão dos genes no manto do lado esquerdo e direito de cada valva não é completamente simétrica. 4) O gânglio CPG regula a expressão de genes relacionados com a biomineralização e os transcritos não codificantes lncRNAs parecem que desempenham um papel importante no processo de biomineralização. Os resultados obtidos nesta tese providenciam fortes evidências de que os neuropéptidos e o sistema nervoso estão envolvidos na regulação da função do manto e consequentemente o crescimento da concha biomineralizada nos bivalves. Estas descobertas contribuem para uma melhor compreensão sobre o papel do sistema neuroendócrino e dos neuropéptidos como importantes fatores reguladores do *biomineralization toolbox* kit no manto em bivalves.

Palavras chave: Bivalve, gânglios cerebropleurais (CPG), lncRNA, manto, neuropeptidos, regeneração da concha, biomineralização da concha, concha simétrica

Contents

List of Tables

Chapter 2

Chapter 4

List of Figures

Chapter 1

Chapter 2

Chapter 3

Chapter 4

CHAPTER 1

General Introduction and main goals

1.1 General introduction and main goals

Members of the Mollusca phylum in particular the bivalves are gaining more attention from the scientific community and societal stakeholders because of their ecological importance, likely impact of climate change and increasing economic importance for the aquaculture and the food industry (Talmage and Gobler, 2010; Rodolfo-Metalpa et al., 2011). Bivalves are a major proportion of global benthic organisms in marine ecosystems, comprising approximately 23% of the marine species identified to date. The hard mineralized shell is one of the hallmarks of bivalves. This calcified structure is their exoskeleton and plays an important role in their survival because it provides protection from predators and environmental aggressions, and also reduces water loss and functions as an important mineral store (Vermeij, 1983). The bivalve shell and equivalent structures in other molluscs are mostly biomineralized crystals of calcium carbonate ($CaCO_3$, approximately 95% of the shell) deposited in an organic layer composed of proteins and polysaccharides that create the shell matrix. The mantle, a tegument that is in direct contact with the inner side of the shell secretes the organic matrix and minerals and is responsible for the response of the shell to biotic and abiotic factors and for the remarkable diversity of bivalve shells.

The ability of an organism to respond to biotic and abiotic factors in their environment can result in the expression of highly variable phenotypes in the absence of genetic differentiation. This flexibility of response is called phenotypic plasticity and has a significant impact on their fitness and survival (Miner et al., 2005). Very

clear examples of phenotypic plasticity have been described from within the Mollusca, where shell shape and thickness vary with habitat as illustrated in a variety of studies, e.g. *Littorina striata* (Wolf et al., 1998), *Littorina obtusata* (Trussell and Nicklin, 2002), *Siphonaria species* (Teske et al., 2007), *Isognomom alatus* (Wilk and Bieler, 2009), *Nacella concinna* (Hoffman et al., 2010), and *Unio pictorum* (Zieritz et al., 2011). In some studies, detailed examination has proven a causal link between the production of thicker shells in response to damage by predators (Johannesson, 1986; Trussell and Smith, 2000) or environmental perturbation such as tidal immersion and ice impacts (Wilk and Bieler, 2009; Hoffman et al., 2010). However, the underlying mechanisms that explain the change in the shell, such as calcium regulatory proteins and pathways or calcium handling and turnover, are generally poorly described (or absent) in taxa other than vertebrates.

The mantle serves as the primary shell-forming organ in both juvenile and adult bivalves, and shell growth depends on the secretory activity of the mantle (Clark et al., 2010; Marin et al., 2012; Suzuki and Nagasawa, 2013). The formation of the shell begins within the pallial space, a narrow, sealed cavity formed between the mantle and shell. Insights into the potential regulatory mechanisms of shell growth in bivalves have been derived from studies of another class of molluscs, the gastropods, where studies of the nervous system have highlighted a role for the neuroendocrine system in shell formation. Studies have found that shell damage altered the appearance of neurosecretory cells in the visceral ganglion (VG) of the snail *Helisoma duryi* (Dillaman et al., 1976), and differences in shell growth have been associated

with neurosecretory activity in the snail brain (Saleuddin and Kunigelis, 1984). As a first step towards understanding the mechanism of bivalve shell production, the malacological community have been developing molecular resources for bivalves and a shell toolbox was derived in recent years, but research on the regulatory factors influencing shell formation remain scarce. The focus of the present thesis is to investigate regulatory factors of shell production in bivalves. This introduction starts with a general consideration of the Mollusca then looks at the bivalves in more depth highlighting, the nervous system, neuroendocrine factors and salient features of relevance for the contextualization of the shell and its regulation.

1.2 The Mollusca phylum

1.2.1 The Molluscs

Molluscs are a highly diverse phylum and is the second most species rich after the Arthropods (Figure 1.1), with an estimated 93,000 known living species (extant) and approximately 70,000 known fossil records (Brusca & Brusca, 2003). In phylogenetic terms the Molluscs are envolutionary closely related with the Annelids, Nemerteans, and Brachiopods and all these phyla belong to the Lophotrochozoa superphylum, which together with the Ecdysozoa (that contain the Arthropods and Nematodes and other small phyla) are part of the Protostomes (Dunn et al., 2008). Most of the living extant mollusc species inhabit the oceans, but there are also many species adapted to terrestrial and freshwater environments (Leal & Harasewych, 1999).

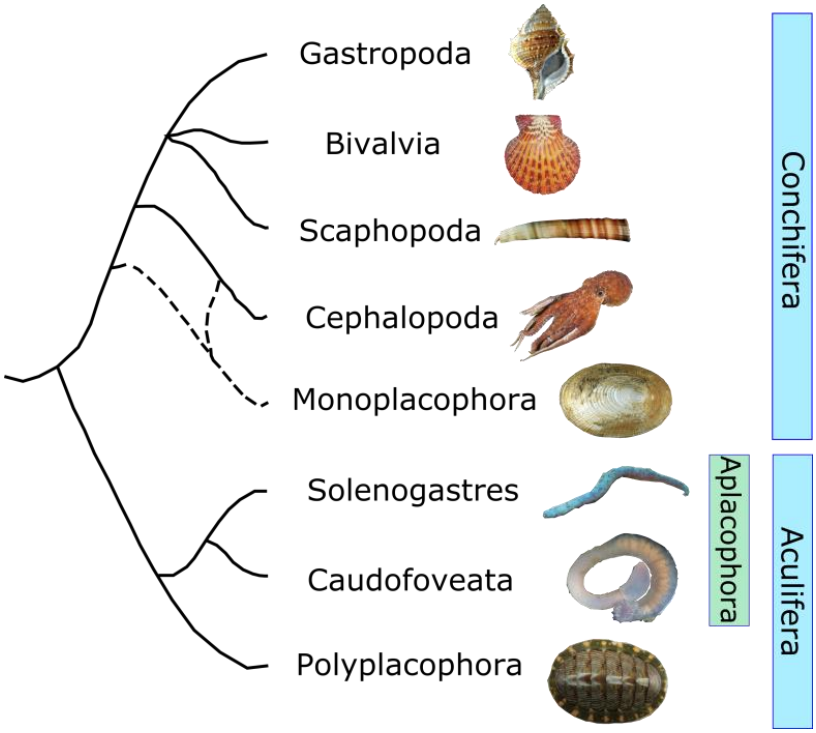

Figure 1.1. The main lineages of the Mollusca phyla. Phylogenetic relationships are based on (Kocot et al., 2011; Smith et al., 2011; Vinther et al., 2012). [The figure was taken from (McDougall and Degnan, 2018)].

Extant molluscs are classified into 8 classes: Gastropoda; Bivalvia; Scaphopoda; Cephalopoda; Monoplacophora; Solenogastres; Caudofoveata and Scaphopoda. The most diverse Mollusca class are the gastropods with 40,000 - 90,000 living species and at least 13,000 extant and fossil genera (Ponder et al., 2019) and the second most diverse class are the bivalves with 50,000 living species (estimates of the diversity of living species range from 7500 to about 50,000 (Frank et al., 2019; Huber, 2010) and over 42,000 fossil species (Pojeta, 1987). They all share common features, such as an unsegmented soft body, a hard biomineralized shell that is their skeleton (internal or external), a radula for feeding, and a foot for movement (Stöger et al., 2013). The most distinctive feature between the different members of each class is the exuberant diversity of their shell morphology, including its colour and patterns and anatomical

structure. The presence or absence of the shell is used for classification. Molluscs without a shell are classified as Aculifera, which includes the Aplacophoran clades Solenogastres (Neomeniomorpha) and Caudofoveata (Chaetodermomorpha). The sister clade Conchifera includes all other shelled molluscs that derived from a uni-shelled ancestor and some species that are thought to have lost their shell during evolution (eg: aplysia) (Smith et al., 2011; Wanninger & Wollesen, 2019). The shell of molluscs is a calcium-based structure that covers part or all of the soft body surface. It is typically covered by a thin outer organic layer (periostracum), the structure and formation are similar to the keratin layer of shell-less animals (Checa et al., 2017). The hard part of the shell is composed of layers of calcium carbonate, organized into aragonite and calcite crystals.

Additionally, from a socioeconomic perspective products derived from the shell, such as pearls, have high economic value (Zenger et al., 2019). Furthermore, the unique characteristics of the shell mean the materials composing it and its structure are studied in materials science (Meyers et al., 2008) and military technology research (Muzzarelli, 2011). Another important contribution of the calcareous shells of molluscs is their role in the Earth's carbon cycle.

1.2.2 The Bivalves

Bivalve animals encompass numerous species, yet they exhibit typical common anatomical features such as a laterally compressed soft body, a biomineralized shell composed of two valves, and a hinge on the dorsal side where the shell articulates. The two biomineralized valves are connected on the dorsal side by an elastic, partially

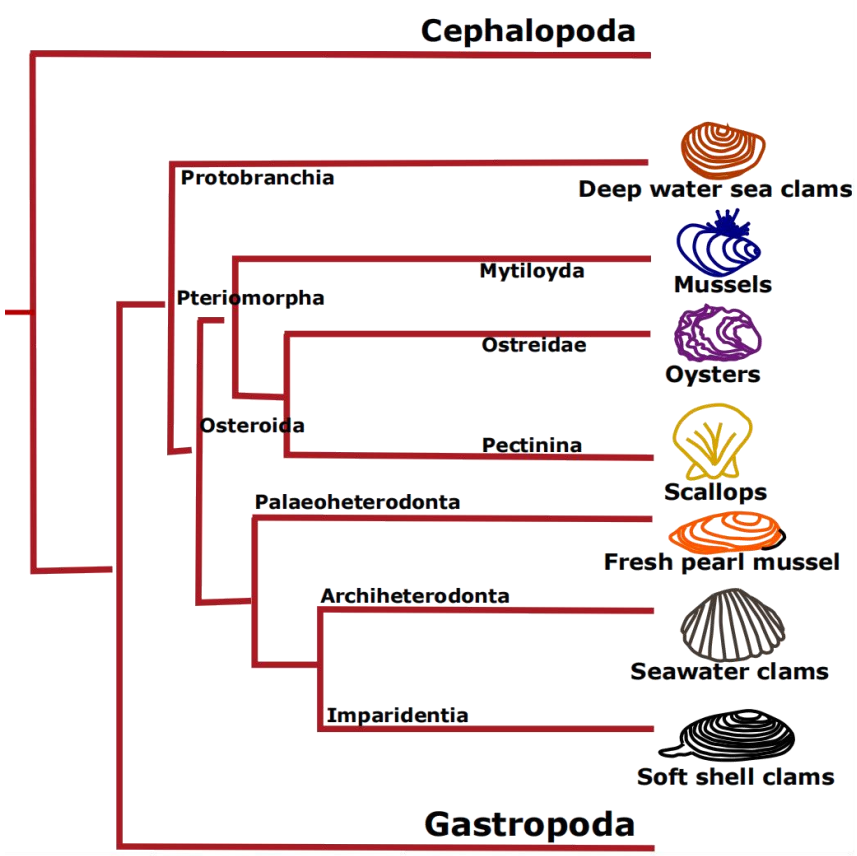

Figure 1.2. An overview of the phylogenetic distribution of well-known bivalves across different Bivalve orders.

calcified, or chitinous external or internal ligament, and they are joined together by one or two adductor muscles (Seilacher, 1985). Unlike other Mollusca members the bivalve head is underdeveloped and lacks jaws and a radula. No eyes exist and the majority of the sensory systems are located in the mantle edge which contains the cilia that are primarily used for feeding. They comply anatomically with their classification as protostomes, since their mouth and anus are situated at opposite ends of their body, and their digestive system is typically complex.

The foot is used for movement, and in some bivalves (e.g. razor clams), it is also used for burrowing. Bivalves are predominantly marine organisms, and fertilization

usually occurs externally, and is followed by the trochophore and veliger larval stages, and eventually metamorphose into the adult form (Venkatesan & Mohamed, 2015).

The soft body in the bivalves is not normally visible externally as it is covered by the outer hard shells (a.k.a. valves) and the shell secreting mantle is attached along the edge of the shell. An image of the macroscopic anatomy of a bivalve is provided in Figure 1.3. Each valve's interior has two muscles, namely the large posterior and the small anterior adductor muscles. The anterior and posterior retractor muscles are also attached to the shell and control the movement of the foot. The ventral surface or 'sole' of the foot is covered in cilia and in the mussel *Mytilus* there are as many as nine different kinds of gland, each of which plays its own specific role in crawling and attachment (Lane and Nott, 1975). In *Mytilus*, the foot secretes byssal threads, which pass through a ventral fissure between the shells and serves to attach and anchor the bivalve to the substrate and the shells of other proximate bivalves. The gills have a large surface area and their rich haemolymph supply makes them well suited for gas exchange, so they have a respiratory function as well as a role in feeding. The labial palps main efficient gill function by continuously removing material from the food tracts on the gills, and preventing gill saturation. The reproductive system of bivalves is extremely simple and the paired gonads are closely connected and play an important role in reproduction and propagation (Gosling, 2015).

The mantle is a bilateral symmetrical structure associated with the right and left valve and is composed of a double layered epithelium that surrounds the animals' body and is localized beneath the shell and is the main organ involved in shell

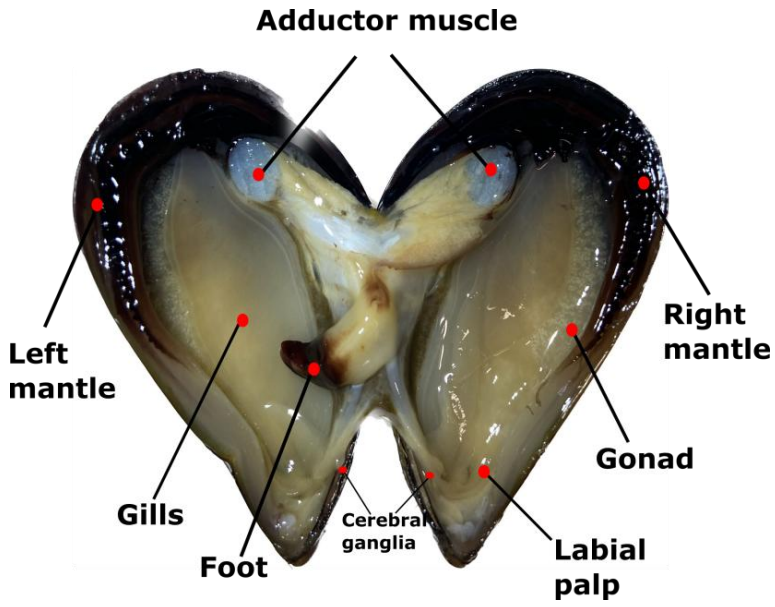

Figure 1.3. Photograph of the internal anatomy of a bivalve. In the image the mussel *M. galloprovinciallis* is represented and the main organs are indicated. The figure was created using Inkscape software v1.2.

production. The mantle contains most of the reproductive glands, where gametes proliferate. After the mussel releases gametes, the outer mantle becomes thin and transparent. The mantle not only plays an important role in gamete production but is also the primary site for storing nutrients (especially glycogen). Therefore, the nutritional reserves of mussels typically accumulate during the summer months when food is abundant and are used for reproduction in the fall and winter when less food is available (Zwaan and Mathieu, 1992).

The edge of the mantle is divided into three layers, the outer, middle and inner fold. The outer mantle fold, close to the shell, has a direct relationship with shell secretion. The middle mantle fold has sensory functions, and this fold often contains short tentacles with tactile and chemoreceptor cells (Figure 1.4) and both cell types

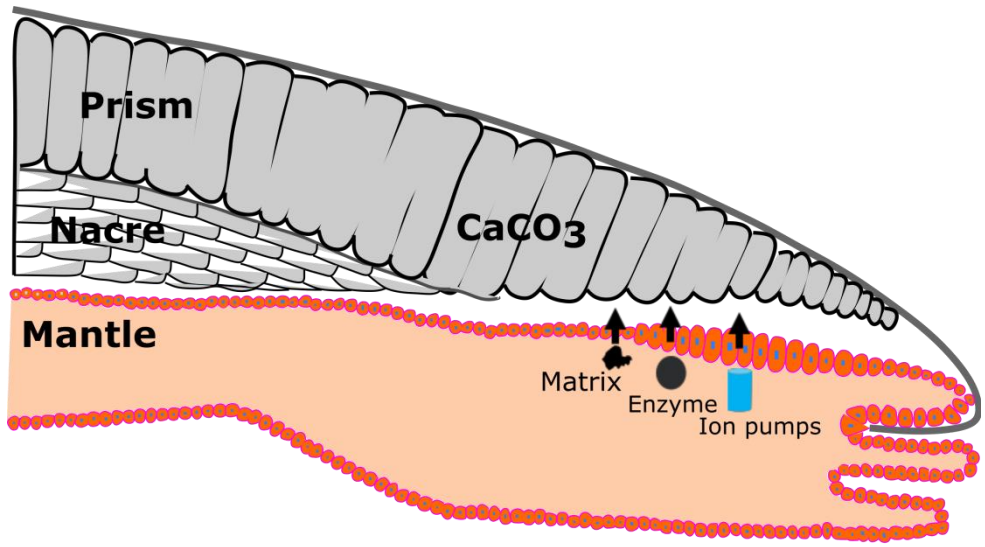

Figure 1.4. Schematic representation of the mantle and shell in Bivalvia. The figure was created using Inkscape software v1.2, and the mantle schematic was adapted from (Kauffman, 1979). The main shell mineral constituent and structural form are indicated along with the key molecules found in the mantle secretory epithelium that contribute to shell formation.

play a crucial role in predator detection and avoidance. The inner mantle fold is the largest of the three mantle folds, and it has well-developed muscles primarily responsible for controlling water flow in the mantle cavity (Gosling, 2008). The mantle has various functions, including sensory activities, secretory activities, and it contributes to shell growth, and shell repair (Saleuddin and Wilbur, 2012). Huang et al (Huang et al., 2022) proposed another possibility regarding mantle function since the outer mantle epithelial cells secrete immune-related molecules into the outer shell space through vesicle transport and that the mantle complements the role of the hemocytes has an important immunological organ. This possibility raises new questions for basic research on mantle function.

Bivalves also have a nervous system that is composed of ganglia and nerve fibers that innervate a variety of tissues. Three pairs of ganglia have been identified and a

more detailed description of the nervous system is provided below since it is central to understanding how the mantle and its diverse functions are regulated.

1.2.2.1 The ecological, aquaculture and commercial importance of bivalves

Increased interest in bivalves and their biology is linked, in part, to their interest for aquaculture since they represent a sustainable food source. Aquaculture of bivalve molluscs has a history of over 50 years (Korringa, 1976) and during this time has achieved a moderate level of technological development. New varieties of economically relevant bivalves are being selected and bred for traits of interest for aquaculture (growth, disease resistance etc) (Nell and Hand, 2003; Zhang et al., 2003). In fact, harvest and aquaculture production of bivalves yielded a global capture of 17.3 million tonnes in 2018 (Food and Agriculture Organization (FAO), 2020). Additionally, bivalves are used for monitoring pollution in aquatic ecosystems (Gosling, 2008) and to assess the health of aquatic ecosystems. Some bivalves are also cultured for pearl production, which contributes to their general commercial value. Therefore, research on the anatomy, physiology, behavior, and ecology of bivalve molluscs is of high relevance.

1.2.2.1.1 Ecological importance

Bivalves are widely distributed in coastal waters, shallow subtidal waters, and deep-sea hydrothermal vent rock substrates (Lutz and Kennish, 1993; Gosling, 2008) and they play crucial ecological roles in the marine environment. They primarily function as filter-feeding benthic organisms, and this feeding habit enhances their

ecological significance because when feeding they “clean” environmental waters. Because of this feeding behaviour they accumulate from the environment pollutants and other substances in their soft tissues and in their shells and thus are important organisms for environmental monitoring (Sheehan and McDonagh, 2008). Bivalves filter feed on primary producers (bacteria and phytoplankton) and transform the energy captured into proteins, lipids and carbohydrates. In this way, bivalves connect primary producers with other higher trophic organisms such as fish in the aquatic food web. This connection facilitates energy transfer and material cycling through the ecosystem and maintains the balance and stability of aquatic ecosystems (Newell, 2004; Vaughn and Hoellein, 2018). For these reasons bivalves are important accumulators of calcium and carbon in ecosystems and have a key role in nutrient cycles, creating and altering habitats, and impacting food webs (Vaughn and Hoellein, 2018).

In marine environments, radioactive nucleotides and metals accumulate in mussel shells, and for this reason they are frequently used to assess environmental pollution (Boisson et al., 1998). Bivalves exhibit adaptability to diverse environments (Loker et al., 2004; Song et al., 2010; Venier et al., 2011), however, climate change and pollution can severely impact their health, potentially compromising their immune system and increase their susceptibility to disease (Bayne, 1979; Dyrynda et al., 1998, 2000; Cherkasov et al., 2007).

1.2.2.1.2 Aquaculture and commercial of bivalves

Most mollusc farming techniques rely on the traditional method of collecting seed from the wild and transplanting them to farms. However, various farming systems (Samonte et al., 1992) have been developed: 1) Bottom culture methods for relatively shallow waters, 2) Stake culture that varies with water flow intensity and depth, offering low costs and easy harvesting, 3) Raft culture that is used for adults of 2 - 3 months, and 4) Rope culture methods (Rosell, 1991) are now the most commonly used techniques for mussel farming. Oysters and scallops are among the most important species in global aquaculture. Bivalves are widely consumed worldwide, and are particularly popular in Europe and Asia (Avdelas et al., 2021). Mussels, along with oysters and clams, are considered delicacies. The global market value of bivalves exceeds 23.9 billion USD, and is expected to grow in the coming years (van der Schatte Olivier et al., 2020). In Asia some bivalves are also cultured for pearl production, and this contributes significantly to their commercial value.

Nonetheless, bivalves have the ability to adapt to adverse conditions and possess a rich array of factors that can combat the effects of environmental stressors such as bioactive compounds with anti-inflammatory, anticancer, and antiviral properties, making them of potential interest for industrial and pharmaceutical products (Eghianruwa et al., 2019). Bivalves are also utilized as a source of biological molecules for cosmetics and personal care products. For instance, chitosan, a compound extracted from the shells of crustaceans and bivalves, has moisturizing and anti-aging properties, making it of interest for human skincare products (Aranaz et al.,

2018; Odeleye et al., 2019; Hosseini et al., 2022). Therefore, bivalves play a crucial role in marine and freshwater ecosystems and have high added value for the blue economy since they provide a range of other services for humans.

1.3 The biomineralized shell in bivalves

Biomineralization is a biologically controlled process through which organisms can produce various mineralized structures (Saleuddin and Wilbur, 2012). It is a widespread and evolutionary ancient process that can occur in prokaryotes, eukaryotes, plants, and animals (Knoll, 2003; Yoshida et al., 2010) and the necessary minerals are naturally occurring, inorganic substances. Biomineralization generates a diversity of crystal structures that serve a variety of functions such as tissue support, protection against the environment, feeding, and sensing (Miyamoto et al., 2013). The shell of bivalves and other Mollusca is composed of highly ordered calcium carbonate crystals in an organic matrix. The calcium carbonate crystals found in mollusc mineralized structures exists as aragonite or calcite, embedded within a softer organic matrix composed of proteins, acidic polysaccharides, and chitin (Marin, 2020). The organic matrix constitutes up to 5% of the dry shell weight and is crucial for crystal nucleation events and crystal growth (Marin et al., 2005; Suzuki et al., 2009; Fang et al., 2011). Additionally, the shell contains trace amounts of magnesium, strontium, fluoride and other minerals that can influence its strength, durability and resistance to erosion and dissolution (Keihan et al., 2020; Sharma et al., 2021).

From an evolutionary perspective, Kobayashi (Kobayashi et al., 2006) has categorized the microstructure of bivalve shells into three layers (Figure 1.5):

(1) the periostracum, (2) the prismatic layer, and (3) the nacreous shell layer. The outermost layer of the shell is a thin periostracum composed of matrix proteins and chitin (Saleuddin et al., 2012). The periostracum (organic matrix of the shell) is an outer layer secreted by the mantle that covers the external side of the calcium carbonate shell.

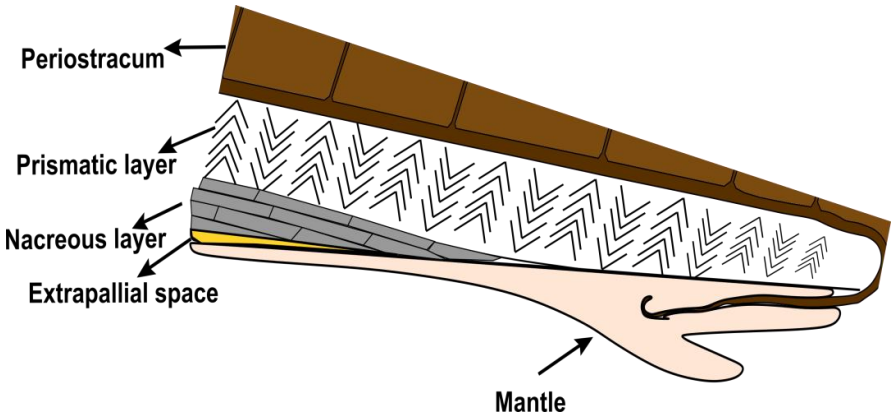

Figure 1.5. Schematic diagram of bivalve shell microstructure. Figure drawn in Inkscape software v1.2.

This organic membrane consists of various proteins, glycoproteins, and polysaccharides. The periostracum serves to protect the shell from dissolution in corrosive environments (Tevesz and Carter, 1980) and from biological aggressions (Bottjer, 1981; Harper and Skelton, 1993). Beneath the periostracum is the mineralized layer, consisting of elongated crystals that develop perpendicular to the shell surface and delineate the prismatic layer. The prisms in the prismatic layer are made of aragonite (Taylor et al., 1969). Below the prismatic layer, the main layer, constituting approximately 50% of the shell's thickness, is the nacreous layer, which

is composed of tiny crystals. It is made up of $CaCO_3$ in the form of aragonite (Checa, 2000). It is evident that during the formation of the different layers of the shell, calcium carbonate merges into various crystalline and intermediate forms, that are characteristic of the distinct layering of the shell. The arrangement of the shell microstructure in bivalves depends on shell matrix proteins that are secreted by the mantle (Taylor et al., 1969; Carter, 1990). Bivalve shells exhibit superior mechanical properties, so understanding the formation and mineralization of shells can provide inspiration for various fields such as the search for novel synthetic materials (Kaplan, 1998; Paula et al., 2010), biomedical applications (Westbroek and Marin, 1998; Liao et al., 2000; Berland et al., 2005), and marine ecosystems (Harayashiki et al., 2020).

1.3.1 The shell mineralization process

Shell mineralization consists of two main steps. In the first step ions pass through mantle epithelial cells and then proteins are synthesized by the mantle cells and second step involve the grow of secreted $CaCO_3$ crystals grow together with the surrounding organic matrix (Saleuddin and Wilbur, 2012). Calcium carbonate is secreted by the mantle cells that also secrete Ca^{2+}, CO_3^{2-} and other ions and a diversity of proteins that are part of the shell matrix and provide the scaffolding structure for the biomineralized crystals to nucleate and form the shell (Cuif et al., 2010). The most active region of the mantle involved in shell production is the mantle edge, which as explained above is divided into three folds, that each have specific functions (Yonge, 1957, 1983). The mantle transports the ions, organic matrix proteins, and carbohydrates required for shell biomineralization (Richardson et al., 1981; Addadi

and Weiner, 1992; Morton and Peharda, 2008; Audino et al., 2015). The process of biomineralization is still not well understood but it is thought that an amorphous calcium carbonate precursor phase (ACC) is formed in mantle cells and then exocytosed and incorporated into the growing shell front (Weiss et al., 2002; Jacob et al., 2011). However, the regulation of these processes by biotic and abiotic factors is uncharacterized.

Transcriptomics and proteomics studies have contributed a growing list of genes and proteins present in the mantle and involved in shell formation but how their production is regulated in molluscs is unknown (Joubert et al., 2010; Zhang et al., 2012; Bjärnmark et al., 2016; Arivalagan et al., 2017). The identification by transcriptomics of genes involved in biomineralization (or more accurately, functional protein domains) has been derived by comparative transcriptomics of different tissues and of larval stages before and after initiation of shell formation (Zhang et al., 2012; Herlitze et al., 2018; Zhao et al., 2018).

The experimental paradigm used in my study to permit real-time studies of biomineralization in living organisms was to induce shell damage and then use transcriptomics and other complimentary approaches to analyse shell repair. Using a diversity of approaches, it was possible to identify functional domains associated with biomineralization but also with other important processes during shell formation such as cellular calcium/ion transport, and the identification of genes encoding novel proteins with putative biomineralization domains through consulting biomineralization databases. However, associating shell microstructure with proteins

is not easy since studies so far suggest shell microstructure is proposed to be determined by a relatively small set of shared genes (Jackson et al., 2010; Marin, 2020). Additional complexity arises from the fact some genes, proteins, or domains with divergent representation in different species of bivalve have a long evolutionary history related to biomineralization, such as carbonic anhydrase and tyrosinase (Aguilera et al., 2014; Le Roy et al., 2014).

Currently, a minimal biomineralization toolbox has been proposed, consisting of a set of functional protein domains considered to be critical for production of aragonite microstructures in molluscs (Arivalagan et al., 2017). This toolkit was elaborated and guided by shell proteomics and is currently limited to four domains that are shared between evolutionary divergent species with different microstructures in their shells (Arivalagan et al., 2017). Therefore, at the molecular level, there are still many unknowns. The development and testing of experimental models for mantle regulation is a priority as it will extend understanding of shell biomineralization, mollusc evolution and the likely impact of climate change. Comparative approaches based on genomics, proteomics, transcriptomics and related approaches can contribute to enrich the toolbox by identifying factors, variability, and plasticity of the regulatory toolbox affecting bivalve biomineralization and shell production.

There is currently great concern over the acidification of the world's oceans and the effects on a wide range of life forms. In the 250 years since the beginning of the industrial revolution, atmospheric CO_2 levels have risen from 280 to > 390 ppm (Canadell et al., 2007) and average surface ocean pH has fallen from an average of

8.16 to 8.05 (Cao and Caldeira, 2008) with a consequent reduction in the degree of saturation with respect to calcium carbonate. This has led to mounting concern about the potential impact(s) of ocean acidification and warming on organisms with calcareous skeletons and their ability to precipitate calcium carbonate, which is central to constructing and maintaining robust skeletons and shells (Doney et al., 2009; Peng et al., 2017).

Ocean acidification can affect the biomineralization toolbox of bivalves by disrupting ion transport and secretion of organic matrices. Decreased pH levels can impact the transport of calcium ions (Ca^{2+}) within bivalve bodies, which are essential for shell formation (Chandra Rajan et al., 2021), leading to a slowdown in shell growth (Thomsen et al., 2013). Research also indicates that ocean acidification can affect the secretion of organic matrices in bivalves by altering the expression of SMP-coding genes (Gazeau et al., 2010), which influences the biomineralization process. However, the full extent of the impact of OA and climate change on bivalve shells and the biomineralization toolbox remains unresolved.

Reports have mentioned that shell damage can alter the secretory cells in the nervous system (Dillaman et al., 1976). In the ganglia of the slug *Agriolimax reticulatus*, neuropeptides are believed to regulate shell growth (Smit et al., 1988). This intriguing suggestion about a link between the nervous system and shell growth offers new possibilities for the regulation of bivalve shells and biomineralization.

1.4 The nervous system in Mollusca

The nervous system in Mollusca (Figure 1.6) exhibits considerable diversity and complexity probably due to their high plasticity, diverse habitats and adaptability to different environments and lifestyles (Bullock and Horridge, 1965). The nervous

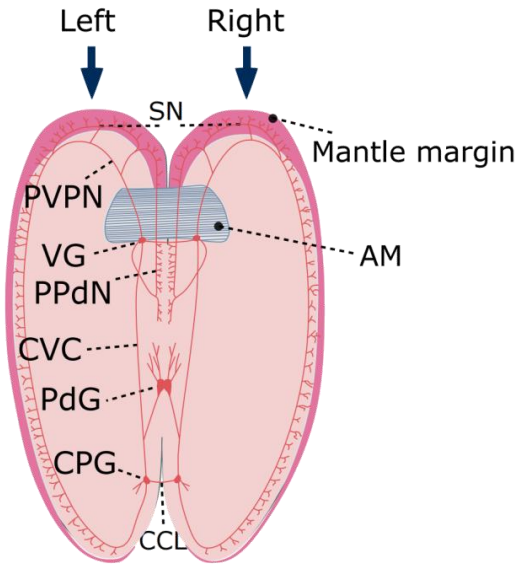

Figure 1.6. Anatomy of the mussel neuronal structures. SN - syphonal nerve, PVPN - posterior renal nerve, VG - visceral ganglia, PPdN - posterior dorsal pallial nerve, CVC - cerebrovisceral commissure, PdG - Pedal ganglia, CPG - cerebrupleural ganglia, AM - adductor muscle, CCL - cerebral commissure linkage. The figure was drawn using Inkscape software v1.2. and is an adaptation of an image adapted from (Field, 1922).

system in Mollusca consists of a network of ganglia and nerve fibers, and sensory structures that regulate various physiological functions and behaviors. The ganglia are the main organs of their central nervous system (CNS), and they are in general symmetrical on both sides of the molluscs. The CNS typically consists of four major pairs of neuronal ganglia: the cerebral ganglia (CG), the pleural ganglia, the pedal ganglia (PG), and the buccal ganglia. Another set of ganglia, known as the visceral ganglia (VG), is present in cephalopods, gastropods, and bivalves.

1.4.1 The mollusc nervous system

The nervous system of the molluscs is more diverse than that of other protostomes. However, their central nervous system typically does not have a brain divided into distinct regions (Faller et al., 2012), unlike other protostomes such as the annelids and the arthropods. The nervous system of molluscs, like vertebrates, is primarily composed of two essential parts: the CNS, which includes the 'brain' with sensory and motor cells, and the PNS (peripheral nervous system). The PNS comprises the somatic nervous system, controlling muscle movements, and the autonomic nervous system, responsible for the involuntary movements of the heart, intestines, vessels, and certain glands (Ponder et al., 2019). The CNS in molluscs is concentrated in the head region, with cell bodies clustered in ganglia. The CNS typically consists of four major pairs of neuronal ganglia as outlined above. The pairs of ganglions are interconnected by nerve commissures and the different ganglia are connected to each other by a complex network of fibers. The PNS includes paired lateral nerve cords and pedal nerve cords that innervate the mantle and the foot, respectively, in cephalopods, bivalves, gastropods, and some other mollusc, but these structures are absent in monoplacophorans and patellogastropods (Frank et al., 2019). The CNS and main components of the sensory organs are primarily located in the head region of gastropods and cephalopods, where sensory organs such as the eyes and tentacles are present. But not in bivalve where head region is non-exist and they are distributed along their body. A diversity of organizations exist across the Mollusca and the basic arrangement of the nervous system plan in Mollusca Classes is

represented in Figure 1.7. The Mollusca nerve cords consist of axon clusters, with their cell bodies forming clusters along their body. Their axons lack the myelin sheath unlike the myelinated nerves in some arthropods and annelids (Roots, 2008).

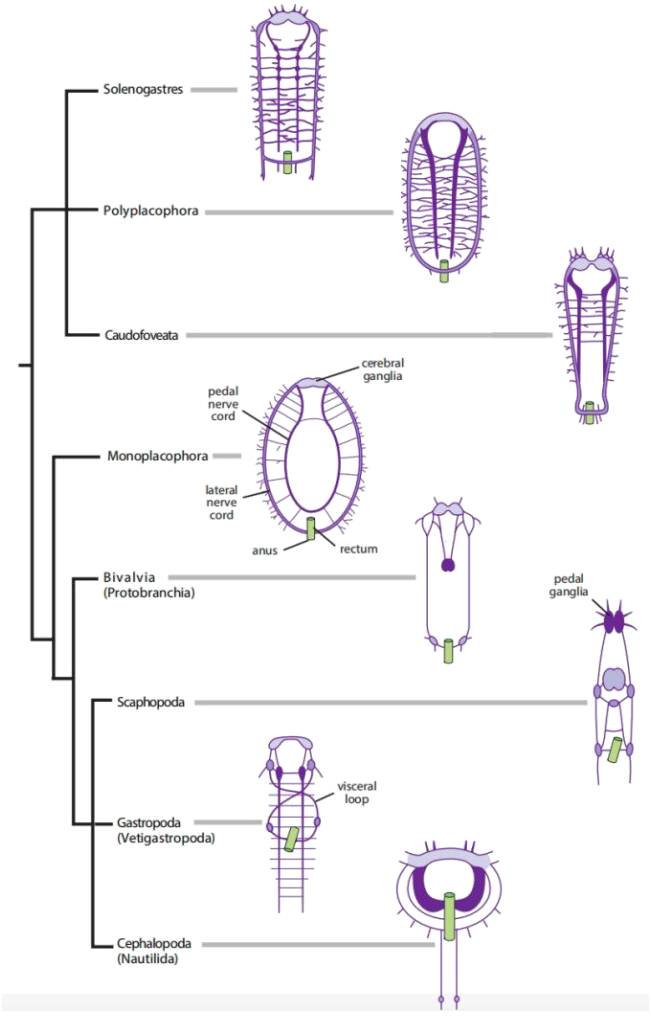

Figure 1.7. Structural pattern of the nervous system in the different mollusca classes. Taken from the book Biology and Evolution of the Mollusca (Frank et al., 2019), (and redrawn and modified from Salvini-Plawen, 1972).

Some major molluscan nerves are single axons, and the nerve cord extends from the anterior ganglia or nerve clusters to the viscera and through the foot.

During larval development stages, an anterior circum buccal nerve ring is formed with neural connections to the head region. Subsequently, during larvae development

the paired pedal nerve cords (controlling the foot) and visceral nerve cords (controlling the vicera and mantle) emerge. In most Mollusca, the anterior nerve ring (composed of CG, pleural ganglia, and PG cells, including the buccal ganglia) is located at the anterior end of the buccal mass. In gastropods, the CG resides in front of the buccal mass, but in cephalopods, and some other gastropods of the opisthobranch subclass (such as sea slugs and sea hares) the CG migrates in a posterior direction during development (Ponder and Lindberg, 1997). In molluscs with a more advanced nervous systems such as the gastropods (e.g. *slugs*) and the cephalopods (e.g. *Nautilus*), the CG dominates the head region where eyes and tactile organs such as tentacles are present, the buccal ganglia controls the buccal region, salivary glands, esophagus, and stomach, the PG controls the foot, the pleural ganglia regulates the external body wall and mantle, and the VG innervates the internal organs, posterior gut and posterior body.

In molluscs, the nervous system of different species originates from their various developmental stages. In gastropods the origin of the nervous system is the delamination of cells from the ectoderm, with the CG originating from the initially formed head plates by the neurons of the larval apical sense organ (ASO) (Raven, 2013). In polyplacophorans, in the posthatching trochophores the earliest elements of the nervous system are peripheral neurons projecting to the apical organ. Among these neurons, two pairs of exceptionally large lateral cells layout the pathway of the developing adult nervous system (Voronezhskaya et al., 2002). The PG and the lateral nerve trunk project anterior from the cerebral ganglia, and the pedal nerve

masses are connected by the commissure. The more peripheral ganglia, including the buccal ganglia and, if present, the subradular ganglia emerge larvae ocelli during development (Friedrich et al., 2002). The conservation and functional homology of the visceral nerve cord in molluscs is questionable due to its divergent anatomical localization. There is no specific descriptions of homology for the CG and PG in molluscs. For example, in aplacophorans (molluscs with no shells) such as the Solenogastres, the visceral nerve cord lies between the dorso-ventral muscles, while in monoplacophorans, polyplacophorans, bivalves and scaphopods, it exists outside the shell muscles. While in cephalopods and gastropods, it is located inside the shell muscle.

1.4.2 The nervous system in bivalves

The structure of the nervous system in bivalves is among the simplest and best conserved in the molluscs and is bilaterally symmetrical. Due to the sedentary (attached) lifestyle of the bivalves, their nervous system is inherently simple. In bilaterally symmetrical bivalves, the CNS consists of 3 pairs of ganglia: the cerebropleural ganglia (CPG), VG, PG, and bundles of paired bilaterally symmetrical nerve fibers that connect the different ganglia and that also project throughout their bodies (Gosling, 2008; Meechonkit et al., 2010; Crook and Walters, 2011). These three pairs of ganglia play a crucial role in coordinating the activity of bivalves and in early stages of the blue mussel (*M. edulis*) the cilia on the outer surface of the mantle are controlled by nervous innervation from the ganglia (Catapane et al., 1979, 1980). The CPG is also known as the brain-pleural ganglia because it combines the cerebral

ganglia and pleural ganglia found in other molluscs. This pair of ganglia is suggested to be the homologue of the two independent ganglia in other molluscs and it is located on both sides of the esophagus and a nerve commissure connects them on the dorsal side of the esophagus and connects them to the VG through paired cerebral-pedal nerve projections. The PG pair is located within the visceral mass at the bottom of the foot and the VG pair (or visceral apex or posterior) is located on the ventral side of the posterior adductor muscle (Figure 1.5). These three pairs of ganglia innervate different organs and tissues in bivalves and regulate different functions. The CPG ganglia mainly innervate and control the activity of the anterior adductor muscle and the anterior mantle, and the VG innervates the gills through the gill nerves and many of the internal organs including the pericardium, kidneys and the posterior mantle. The PG is suggested to innervate the foot through relatively few (3 to 6) nerves. While there have been initial studies on the characterization of the nervous system in bivalves, research on the specific function of the ganglia and the organization of the nervous system in adult bivalves remains poorly studied.

In bivalves the development of the nervous system is conserved. However, in some protobranch bivalves (such as Nucula and Leda) the CG and pleural ganglia are partially fused, and they have lost the buccal ganglia. The CPG of bivalves are similar to the pleural ganglia of gastropods because they innervate some of the same areas (shell muscles, visceral nerve loop) (Frank et al., 2019). The anterior pallial nerve aligns with the posterior pallial nerve from the VG, and the merged nerve cords forms

the extrapallial nerve that surrounds the edge of the mantle. The CPG also innervates the labial tentacles, mouth, and esophagus.

The VG is the largest among the three pairs of ganglia, extending horizontally from near the kidneys to the posterior mantle region of the body. In certain species, such as representatives of the *Spondylus* and *Lima genus*, the cerebral ganglia is fused with the VG, and a long cerebral commissure is present (Pelseneer, 1931). From the large VG numerous nerve projections innervation many of the internal organs including the gills, heart, pericardium, kidneys, digestive tract, gonads, posterior mantle, and the sensory organs of the mantle, siphon, and cerebral mantle cortex. In the scallops, the paired VG are completely fused, forming a rudimentary 'brain' with noticeable eyes at the edge of the mantle (Bullough, 1958; Galtsoff, 1964; Beninger and Le Pennec, 2006; Gosling, 2015). The PG nerves innervate the foot as well as the anterior and some posterior muscle tissues and the foot retractor muscles.

Currently, classical histological methods have been employed to localize the neuroanatomy of individual bivalve ganglia (Galtsoff, 1964). As neurotransmitters play a crucial role in the nervous system, subsequent studies have focused on the use of immunohistochemical methods to determine the distribution of neurotransmitters in the ganglia of individual molluscs (Too and Croll, 1995; Meechonkit et al., 2010; Tantiwisawaruji et al., 2014). However, the types of neurons in the ganglia, the combinations of neurotransmitters, and the individual expression of neurotransmitters remains largely undocumented.

1.4.3 Neuroendocrine signalling molecules

In vertebrates, the neuroendocrine system regulates reproduction, development, and growth. Model organisms (such as goldfish) have been used to depict models of neuroendocrine signaling (Richard et al., 1986). In the CNS of fish and mice, the interactions between the neuropeptide gonadotropin-releasing hormone (GnRH), catecholamine DA, and the amino acid γ-aminobutyric acid (GABA) form the core

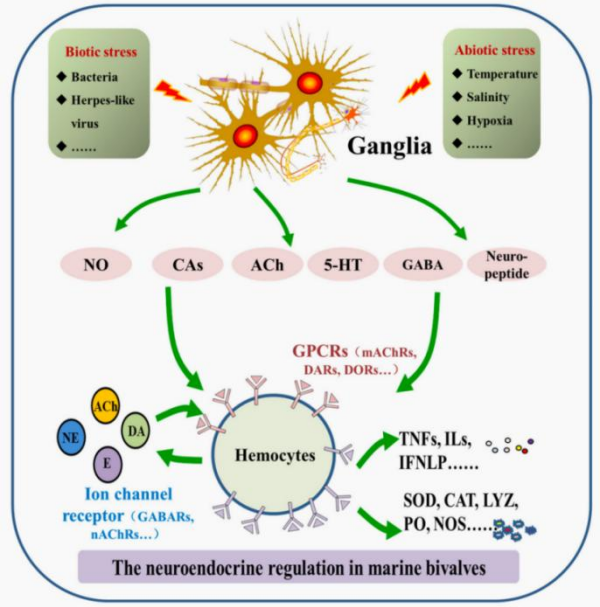

Figure 1.8. Molecular features of the neuroendocrine-immune (NEI) system in marine bivalves. Quoted from (Liu, Li, et al., 2018).

understanding of the comprehensive control of luteinizing hormone (LH) (Trudeau, 1997; Popesku et al., 2008). To date, the diversity of neuropeptides and receptors, as well as the central role of GnRH, has been extensively reviewed in vertebrates (Klausen et al., 2002; Lethimonier et al., 2004; Guilgur et al., 2006). Furthermore, recent advances in transcriptome analysis suggest that neurotransmitters not only control the release of pituitary hormones but also have rapid and profound

receptor-mediated effects that regulate gene expression in the neuroendocrine brain (Popesku et al., 2008). In fish, the concept of neuroendocrine-immune interactions has also been validated (Barreda et al., 2004; Hanington et al., 2006; Metz et al., 2006).

In marine bivalves, various hormones, neurotransmitters, their receptors, and key enzymes involved in synthesis have been identified (Song et al., 2015; Wang et al., 2018). The neuroendocrine system responds to various environmental stressors by regulating immune activity, energy allocation, growth, and locomotion (Lacoste, Jalabert, et al., 2001; Lacoste, Malham, et al., 2001). Marine bivalves are also considered suitable models for studying the basic mechanisms of neuroendocrine regulation in response to environmental stressors (Malagoli et al., 2017). In this section, molecular features of the neuroendocrine system identified in marine bivalves are described (Figure 1.8).

1.4.3.1 Neurotransmitters

Neurotransmitters are endogenous chemical molecules that play crucial roles in the communication within the nervous system involved in regulating various physiological processes, including behavior, cognition, locomotion, feeding and other essential body functions. To date, the catecholaminergic, cholinergic, enkephalinergic, serotonergic, γ-aminobutyric acid (GABA ergic), and neuropeptide systems of marine bivalves have been characterized, and they share similar molecular bases with their counterparts in vertebrates (Wang et al., 2018).

The catecholaminergic system (CA) is an important neurotransmitter system composed of dopamine (DA), norepinephrine (NE), and epinephrine (E) (Kvetnansky et al., 2009). DA, NE, and E are present in many marine bivalves and exhibit biological activity (Goh and Davey, 1976; O'Connor et al., 1982; Franchini et al., 1985). They are detected at the highest levels in ganglia and hemocytes (Liu et al., 2018b). This indicates that bivalves possess a complete CA neuroendocrine network. Interestingly, the nematode *Caenorhabditis elegans* only has a dopaminergic neuroendocrine system (Suo et al., 2004; Felton and Johnson, 2014). Therefore, the CA neuroendocrine system found in molluscs may represent the most primitive but functionally complex structure that evolved.

In bivalves, the cholinergic nervous system has been identified and characterized (Shi et al., 2014). Enzyme activity of AChE has been observed in hemocytes of *Crassostrea gigas*(renamed *Magallana gigas*) and in tissues such as the gills, mantle, intestines, and muscles of *Crassostrea. hongkongensis* (Zha et al., 2013). A form of AChE has also been found in *Chlamys Farreri* (Shi, 2012). This indicates that in bivalves, the cholinergic nervous system has acquired a structure and function that suits the physiological processes it regulates.

The monoamine neurotransmitters, serotonin (5-HT) and DA, as well as the enzymes involved in their synthesis and degradation, have been described in the ganglia, gill nerves, and gill tissues of the Blue mussel (*M. edulis*) (Blaschko and Milton, 1960; Stefano et al., 1976; Stefano and Catapane, 1979; Catapane, 1982c). Serotonergic and dopaminergic neurons were identified in both CPG and VG in the

mussel and they were found to be activated through electrical stimulation or direct neurotransmitter perfusion into the ganglia (Stefano and Aiello, 1975; Stefano et al., 1976). Serotonergic and dopaminergic nerve fibers found in the gill nerves extend into branches beneath the ciliated cells on the outer surface of the gill (Catapane, 1982b; Aiello, 1990). Extensive morphological, pharmacological, neurochemical, and physiological studies have demonstrated that 5-HT and DA, both peripheral and ganglionic control ciliary activity in the mussel gills (Aiello, 1970; Catapane et al., 1979, 1981; Catapane, 1982a). Ciliary excitation is activated by serotonergic nerve fibers, while ciliary inhibition occurs through dopaminergic fibers and these excitatory and inhibitory effects are blocked by serotonin and dopamine antagonists such as mescaline (MS) and ergonovine (ERG), respectively (Catapane et al., 1980; Catapane, 1983).

In the early studies of the bivalve nervous system, there was extensive research on the neurotransmitter opioid. For example, opioid receptors and their endogenous effector are believed to play a crucial role in the regulation of neurotransmitter release in the mollusc nervous system (Stefano and Catapane, 1979). Moreover, opioid peptides were found to increase the concentration of DA in bivalve (*M. edulis*) ganglia. DA release stimulated by potassium in the CPG, VG, and PG can be inhibited by morphine and other sequence and structurally related opioid peptides (Stefano et al., 1981). Opioid receptors were found to be expressed in the VG and enhance the beating of lateral cilia through 5-HT (Cadet, 2004) . Opioid signaling is

not confined to the bivalve CNS (ganglia) but was also detected in gills (Mantione et al., 2006).

To better understand the nervous system of bivalves, in situ analysis has been conducted, including the localization of secretory cells and the expression of neurotransmitters (Karhunen et al., 1993; Liu et al., 2018a; Kotsyuba et al., 2020; Kotsyuba and Dyachuk, 2023). Early studies suggested that the CNS of bivalve larvae was relatively simple in terms of tissue organization (Bayne, 1971; Hickman and Gruffydd, 1971; Waller, 1981). In the last two decades, the nervous system of bivalve has been investigated using immunohistochemical techniques. This includes the presence and distribution of 5-HT (Kreiling et al., 2001), FMRFamide (Voronezhskaya et al., 2002), AchE (Raineri and Ospovat, 1994; Raineri, 1995) and CA (Croll et al., 1997). For example, Kotsyuba et al examined immunohistochemically the distributions of neurons containing signaling molecules

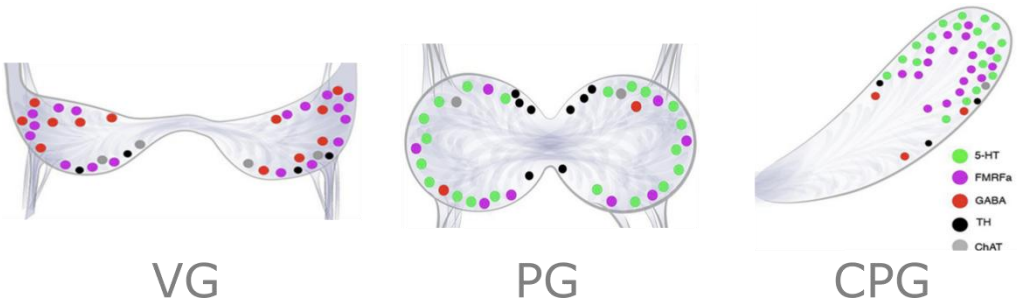

Figure 1.9. Schematic representation of the distribution of neurons in three pairs of ganglia. 5-HT, 5-hydroxytryptamine; GABA, γ-aminobutyric acid; TH, tyrosine hydroxylase. Quoted from the (Kotsyuba et al., 2020).

(including FMRFamide, 5-HT, ChAT, GABA and TH) as well as the proliferative status of neurons in the ganglia (CPG, VG and PG) of the mussel *Crenomytilus*

grayanus (Kotsyuba et al., 2020) (Figure 1.9). While immunolabeling was used to study circuits related to the nervous system and its active substances, but the functionality of neurotransmitters and neuromodulators remains to be investigated.

1.4.3.2 Neuropeptides

Neuropeptides are a large group of signaling molecules that are synthesized by short sequences of amino acids (generally 3 - 100) and released by the neurons through regulated secretory pathways. They are initially synthesized as part of large, inactive precursor proteins called prepropeptides and bioactive neuropeptides are released by proteolytic cleavage post-translation and sometimes undergo further modifications to yield the mature peptide. They can act as neurotransmitters, neuromodulators or neurohormones. A single neuropeptide precursor molecule can produce a single neuropeptide, multiple different neuropeptides, multiple copies of a single neuropeptide, or any combination thereof (Li et al., 2008). Many neuropeptide sequences are short and structurally similar, making it difficult to generate specific antibodies and achieve specific expression of a particular neuropeptide. Neuropeptide binding to G-protein specific receptors (G-protein-coupled receptors, GPCRs) on the surface of target cells, trigger their effect. Once the ligand is bound, the receptor undergoes a conformational change, activating associated G proteins and leading to an intracellular signaling cascade which is a key mechanism in cellular signal transduction, especially in the nervous system (Wen et la., 2010; Jurenka and Nusawardani, 2011).

Invertebrates, including members of the phylum Mollusca, are a rich source for isolating neuropeptides and testing their physiological effects (Kobayashi and Muneoka, 1990; Muneoka, 1994; Kiss and Pirger, 2006; Nässel and Wegener, 2011). Molluscs have been successfully utilized as model systems to study the molecular and cellular mechanisms underlying behavioral generation and plasticity (Kandel and Abel, 1995; Bailey et al., 1996). Currently, over 100 different peptides have been identified and partially sequenced in gastropod molluscs. They exhibit remarkable complexity, selectivity, and adaptability as chemical signaling molecules (Kobayashi and Muneoka, 1990; Muneoka et al., 2000; Kiss and Pirger, 2006).

In molluscs, neuropeptides of bivalves are predominantly studied in a few species, and have mostly been identified in ganglia. In 1977, Price and Greenber (Price and Greenberg, 1977) identified a new cardioexcitatory substance, now commonly known as FMRFamide (Phe-MetArg-Phe amide), in the ganglia of the clam *Macrocallista nimbosa*. This was the first neuropeptide identified in Mollusca tissues. In mussels, several types of neurosecretory cells have been discovered, with the majority located in the CPG (Illanes–Bucher,1979). These neurosecretory cells can produce peptides that are released into the circulatory system.

In bivalves, such as the Akoya pearl oyster (*P. fucata*), 74 predicted neuropeptide genes have been identified (Zhang et al., 2012; Stewart et al., 2014). In the CNS of Pacific oyster (such as *M. gigas*) transcriptome analysis identified neuropeptide transcripts (Bigot et al., 2014). In the transcriptomic analysis of the VG in *M. gigas* during the reproductive cycle, it was found that among the complete neuropeptide

library, 25 novel regulatory peptides were discovered, supporting their involvement in gametogenesis or related metabolic control (Réalis-Doyelle et al., 2021). Through transcriptomic and proteomic analyses of the nerve ganglia in *Patinopecten yessoensis*, neuropeptides were identified and characterized (Zhang et al., 2018).

Although a large diversity of neuropeptide transcripts has been identified in bivalves their functional characterization remains mostly unexplored. Currently, at least four different neuropeptides have been discovered to modulate the reproductive system of bivalve animals (Morishita et al., 2010). One of them is GnRH, which is a neurohormone that plays a crucial regulatory role in the reproduction of vertebrates (Marques et al., 2022). Insulin-related peptides have also been identified in the neurosecretory cells of several bivalve species. In the Pacific oyster *M. gigas*, it has been demonstrated that insulin-related peptides are involved in growth regulation by stimulating protein synthesis pathways in mantle edge cells involved in shell growth (Gricourt et al., 2003, 2006). In the study of the mollusc Aplysia, injections of insulin-like peptides reduced hemolymph glucose levels, indicating their role in regulating metabolic functions in Aplysia (Floyd et al., 1999). Additionally, the neuropeptides GnRH and Kisspeptin were shown to participate in the reproductive regulation of many vertebrates (Tsutsui et al., 2010; Gopurappilly et al., 2013). Neuropeptides are also one of the most crucial components of the Neuro-endocrine-immune (NEI) system in marine molluscs. Additionally, methionine-enkephalin ([Met5]-ENK), an opioid peptide has been measured in

hemocytes of *M. gigas* (Liu et al., 2008) and its receptors are also widely expressed in important tissues of oysters (Guo et al., 2013; Liu et al., 2015).

1.4.3.3 Neuropeptide - GPCR system in the mantle

The neuropeptide signaling system is ancient in evolution, appearing to have emerged in early deuterostomes, possibly even before bilaterians (Jékely, 2013; Mirabeau and Joly, 2013; Elphick et al., 2018). Neuropeptides primarily exert their effects through GPCRs (Hökfelt et al., 2000). Emerging evidence suggests that the related neuropeptide-receptor pairs exhibit evolutionary conservation in regulating animal physiology and conspecific behaviors (Jékely et al., 2018).

The mantle, which regulates shell formation in molluscs, is interconnected to the overall nervous system through complex neural endings. Evidence for the presence of several neuropeptides in the mantle exists and we recently identified a homologue of the vertebrate CALC system in the shell forming mantle of bivalves, this system in vertebrates is involved in calcium homeostasis by regulating calcium uptake and bone turnover (Naot and Cornish, 2008; Naot et al., 2019). The CALC system in bivalves arose through lineage and species-specific duplications and we have demonstrated that this system is a candidate regulator of shell mineralization (Cardoso et al., 2020). The CALC receptors are members of the GPCRs, the most extensive receptor family known, and regulates a vast diversity of physiological processes in vertebrates and non-vertebrates. Bivalve mantle transcriptomes are rich in GPCRs and by analogy

with the CALC system they and their ligands (many receptors are still orphans) presumably regulate mantle function.

1.5 Objectives of the thesis

Marine bivalves are ecological and economically important Mollusca species. The shell is a hallmark of bivalves and this naturally biomineralized structure is essential for their survival. However, climate changes and anthropogenic pollution are affecting the bivalve shell and in this way threatening their survival. The mantle plays an important role in the secretion of the shell and the shell "biomineralization toolbox" has been characterized, However, how shell growth and biomineralization is regulated remains poorly described. The mantle is innervated by the ganglia and mantle transcriptomes indicate a high abundance of neuropeptides and neuropeptide receptors. However, their role in regulating mantle function and shell production remains unclear. Therefore, it is crucial to identify neuropeptides and receptors in the mantle and the role of the nervous system in mantle function to understand the intricate mechanisms governing mantle physiology and shell formation. The main goal of this thesis is to explore the regulatory role of neuropeptides on mantle function and shell regulation in bivalves using as a model the commercially and economically important marine bivalve, the Mediterranean mussel (*M. galloprovincialis*). This thesis is organized with a general introduction that provides an overview of the state of the art and then has three chapters dedicated to the results and a section providing a final discussion and highlighting future perspectives.

Chapter 2- Identifies the diversity of neuropeptide precursors that are expressed in the mussel mantle and the influence of the nerve ganglia on mantle neuropeptide expression and function during shell regeneration after damage.

Chapter 3- Determines the overall changes in the mantle transcriptome in mussels with intact and damage ganglia commissure focusing on neuropeptide and GPCR transcripts during the process of shell repair.

Chapter 4- Characterize the allatostatin neuropeptide system in the mussel mantle and allocates a putative role, based on preliminary analysis that suggests it was most likely associated with the immune response and then the putative function was confirmed using a bacterial challenge.

CHAPTER 2

Neuropeptides regulate shell growth in the Mediterranean mussel (*Mytilus galloprovincialis*)

Neuropeptides regulate shell growth in the Mediterranean mussel (*Mytilus galloprovincialis*)

Manuscript submitted to the International Journal of Biological Macromolecules (2024, under review)

Acknowledgements

The authors would like to thank to Dr. Telmo Nunes from the microscopy unit of the Faculdade de Ciências da Universidade de Lisboa for the shell SEM images. This study received Portuguese national funds from FCT - Foundation for Science and Technology through institutional projects UIDB/04326/2020, UIDP/04326/2020 and LA/P/0101/2020, and from the operational programmes CRESC Algarve 2020 and COMPETE 2020 through the projects EMBRC.PT ALG-01-0145-FEDER-022121 and BIODATA .PT ALG-01-0145-FEDER-022231 and from the FCT-funded project FCT-AGAKHAN/ 541666287/2019HealthyBi4 Namibe. ZL was supported by a PhD scholarship from the China Scholarship Council.

Neuropeptides regulate shell growth in the Mediterranean mussel (*Mytilus galloprovincialis*)

Zhi Li[1], Maoxiao Peng[1], Rute C Félix[1], João CR Cardoso[1*] and Deborah M Power[1,2,3*]

[1]Comparative Endocrinology and Integrative Biology, Centre of Marine Sciences, Universidade do Algarve, Campus de Gambelas, 8005-139 Faro, Portugal

[2]International Research Center for Marine Biosciences, Ministry of Science and Technology, Shanghai Ocean University, Shanghai, China

[3]Key Laboratory of Exploration and Utilization of Aquatic Genetic Resources, Ministry of Education, Shanghai Ocean University, Shanghai, China

2.1. Abstract

In bivalves, which are molluscs enclosed in a biomineralized shell, a diversity of neuropeptide precursors has been described but their involvement in shell growth has been largely neglected. Here, using a symmetric marine bivalve, the Mediterranean mussel (*Mytilus galloprovinciallis*), we uncover a role for the neuroendocrine system and neuropeptides in shell production. We demonstrate that the mantle is rich in neuropeptide precursors and that a complex network of neuropeptide-secreting fibres innervates the mantle edge a region highly involved in shell growth. We show that shell damage and shell repair significantly modify neuropeptide gene expression in the mantle edge and the nervous ganglia (cerebropleural ganglia, CPG). When the CPG nerve commissure was severed, shell production was impaired after shell damage, and modified neuropeptide gene expression, the spatial organization of nerve fibres in the ganglia and mantle and biomineralization enzyme activity in the mantle edge. Injection of CALCIa and CALCIIa peptides rescued the impaired shell repair phenotype providing further support for their role in biomineralization. We propose that the regulatory mechanisms identified are likely to be conserved across bivalves and other shelled molluscs since they all share a similar nervous system, a common mantle biomineralization toolbox, and shell structure.

Keywords: bivalves, mantle innervation, neuropeptidome

2.2. Introduction

The Molluscs are one of the most diverse groups of soft-bodied invertebrate animals and the second most specious phyla after the insects (Kocot et al., 2011; Smith et al., 2011; Vinther, 2015; Wanninger and Wollesen, 2019). They belong to the lophotrochozoans and are found in nearly all ecosystems on Earth playing a vital role in the maintenance of the structure and function of many ecosystems and as a source of food for humans and other taxa. The Mollusca phyla is composed of two major subclades, Aculifera (shell-less molluscs) and Conchifera (shell-bearing molluscs), which diversified 546 million years ago (MYA) (Kocot et al., 2020). The Conchifera molluscs (Bivalvia, Cephalopoda, Gastropoda, Monoplacophora, and Scaphopoda), are the most diverse subclade and are proposed to have diversified 540 MYA, and their calcified uni- or bivalved shells are equated with their evolutionary success and widespread distribution (Vinther, 2015; Ponder et al., 2019). The evolution of molecules that regulate the rate of shell formation such as chitin was proposed to be a crucial step in Conchifera diversification (Weiss et al., 2006, 2013; Weiss, 2012). Surprisingly little attention has been paid to the contribution of regulatory molecules and processes to mollusc evolution.

The vast diversity of forms, lifestyles and ecological niches of the Mollusca is matched by the high diversity and plasticity of their nervous systems including a centralized brains in cephalopods through to scattered ganglia in bivalves (Budelmann, 1995; Ellis and Kempf, 2011). Studies of the giant squid axon generated seminal insights into nerve cell excitability (Hodgkin and Huxley, 1939, 1945) and

gastropod slugs and snails continue to be important models for neurobiology (Benjamin et al., 2021). Other Mollusca are less well studied although the basic architecture of the nervous system in most classes has been characterized (Salvini-Plawen, 1972; Haszprunar, 1988; Hartenstein, 2016). The bivalves are the experimental model of the present study, and have a bilaterally symmetrical, decentralized, nervous system. In bivalves, three bilateral pairs of interconnected ganglia, the cerebropleural ganglia (CPG), visceral ganglia (VG) and pedal ganglia (PG) innervate and regulate tissue function in the organism (Beninger and Le Pennec, 2006). The CPG in bivalves is similar to the pleural ganglia of gastropods and innervates some of the same anatomical structures including the adductor muscle and visceral nerve loop. The CPG in bivalves also innervates the anterior mantle, the labial tentacles, the mouth, and the oesophagus via the anterior pallial nerves (Ponder et al., 2019). The large paired VGs innervate many of the internal organs including the gills, heart, pericardium, kidneys, digestive tract, gonads, posterior mantle, and the sensory organs of the mantle, siphon, and cerebral mantle cortex (Ponder et al., 2019). In the scallops, the paired VGs are completely fused, forming a rudimentary 'brain' (Beninger and Le Pennec, 2006; Gosling, 2015). The PG nerves in the scallop innervate the foot as well as the anterior and posterior muscle tissues (Ponder et al., 2019). In oysters, the PG is reduced in dimension, and this has been associated with the loss of the foot after metamorphosis. Available transcriptomes and proteomes of the ganglia in a) the bivalves, the Yesso scallop (*Patinopecten yessoensi*) and oysters (*Magallana gigas* and *Pinctata fucata*), b) the gastropods, the grey garden slug

(*Deroceras reticulatum)*, giant triton snail (*Charonia tritonis*), freshwater snail (*Biomphalaria glabrata*) and land snail (*Theba pisana*) and c) the cephalopod (*Sepia officinalis*) reveals the ganglia and neurons express a broad spectrum of proteins and neuropeptides.

Studies of a handful of neuropeptides identified before the advent of high throughput gene/protein sequencing assigned their functions mainly to growth, reproduction, and metabolism (O'Shea and Schaffer, 1985). The first neuropeptide to be sequenced was isolated from the salivary glands of the octopus *Eledone muschata* (Erspamer and Anastasi, 1962). Since then, a large neuropeptide repertoire has been identified in molluscs using omics and reveals relatively good conservation with the repertoire in Arthropods and Vertebrates (Oliveira et al., 2019), but the function of only a few have been characterized (Zhang et al., 2018). For example, in the Sydney Rock oyster (*Saccostrea glomerata*), the neuropeptides CCAP and APGW-amide are proposed to regulate reproduction (Van In et al., 2016) and in the gastropod, *Lymnaea stagnalis*, NPF/NPY neuropeptides are proposed to be involved in energy balance (Jong-Brink et al., 2001). The FMRF-amide-like peptides in Mollusca are suggested to regulate the cardiovascular system, osmoregulation, reproduction, digestion, and feeding behaviour (Zatylny-Gaudin and Favrel, 2014). In the gastropods, the land snail (*Otala lacteal*) and the planorbid snail (*Helisoma duryi*), and a bivalve, the Pacific oyster (*M. gigas*), insulin-like peptides (ILP) are proposed to regulate mantle edge cell growth and shell growth (Saleuddin et al., 1992; Abdraba and Saleuddin, 2000; Gricourt et al., 2003).

The intriguing observation that neuropeptides can modulate shell growth in the Pacific oyster is supported by reports in other molluscs. For example, in the freshwater air-breathing snail *Helisoma*, shell damage modified the appearance of neurosecretory cells in the VG (Dillaman et al., 1976) and neurosecretory activity by the snail brain was associated with shell growth (Saleuddin and Kunigelis, 1984). In the pond snail *Lymnaea stagnalis* two groups of neurosecretory light green cells (LGC) in the CPG secreted a hormone that stimulated shell and soft tissue growth and was later proposed to be an ILP (Geraerts, 1976; Smit et al., 1988).

The importance of the bivalve shell for survival means considerable attention has been focused on shell construction, which occurs in the extrapallial space (EPS) a narrow-sealed cavity between the shell and mantle (Taylor and Layman, 1972; Marin et al., 2012; Louis et al., 2022). The mantle epithelial cells secrete chitin, and shell matrix proteins and provide a scaffold where Ca^{2+} and carbonate (CO_3^{2-}) ions secreted from the ciliated mantle and haemocytes can nucleate and crystalise to create the hard mineralised shell (Clark et al., 2010; Marin et al., 2012; Alves and Oliveira, 2013; Suzuki and Nagasawa, 2013; Louis et al., 2022). To improve understanding of shell production mantle transcriptomes and proteomes from bivalve species have been produced (Bjärnmark et al., 2016; Yarra et al., 2016; Carini et al., 2019) and a biomineralization toolbox composed of matrix proteins, enzymes, ion channels, and species-specific genes has been proposed (Yarra et al., 2021). However, the role of regulatory factors on shell growth, and how they influence "shell toolbox" genes, and the response to environmental change is unknown. Recently long non-coding RNA

were identified as a class of regulatory factors determining shell growth (Peng et al., 2023).

In our previous bivalve mantle transcriptome studies, we identified neuropeptides and their putative G protein-coupled receptors (GPCRs) and suggested they may be regulators of mantle function (Cardoso et al., 2016, 2020; Li et al., 2021). In addition, orthologues of the vertebrate calcitonin (CALC) system involved in calcium homeostasis, were identified in the mantle of *Mytilus galloprovincialis* (Cardoso et al., 2020) and *M. gigas* (Schwartz et al., 2019), and a role in calcium mobilization for shell production was proposed. Nonetheless, how CALC and other neuropeptides of the mantle interact to regulate shell growth has not yet been established and if neuropeptides of the bivalve nervous system have a function remains to be established. In this study, we explored the role of neuropeptides in shell growth and tested the hypothesis that they do this by modulating the mantle's function. We used as a model the symmetrical bivalve, the Mediterranean mussel, *M. galloprovincialis* we a) explored and characterized the mantle neuropeptidome and compared it to other bivalves, b) looked at the distribution of neurosecretory and neuropeptide fibres between the mantle and nerve ganglia, and c) conducted functional characterization of candidate neuropeptide genes to assess if they modified shell production by the mantle.

2.3. Material and methods

2.3.1 Animals and sampling

Mediterranean mussels (*M. galloprovincialis*) were collected from the Ria Formosa (Faro, Portugal, 37º00'32''N, 7º59'40''W) under the ICNF license 327 / 2022 / CAPT. Adult mussels (5.05 ± 0.32 cm long, 8.31 ± 1.34 g wet weight) were transported live to the Aquatic Organisms Experimental Laboratory at the Centre for Marine Science (CCMAR) where they were manually cleaned. Animals were acclimated for at least one week to the experimental system composed of 5-liter glass aquarium filled with 4 liters of aerated seawater (37 ppt, pH = 8.1 ± 0.1) from the bivalve's natural environment at ambient temperature (20 - 22°C). During the acclimation period and experimental trials, mussels were fed daily (0.002 g / g body weight) with a mixture of a commercial dry microalgae (PHYTOBLOOM, Necton, Portugal). No mortality occurred during the acclimation or experimental period.

For tissue sampling, animals were placed on ice and the adductor muscle was severed with a sterile blade to allow the two valves to open. Samples from the mantle edge in the region most distal from the umbo (from here on designated as, the mantle) and CPG ganglia from control and experimental animals were collected, snap-frozen in dry ice, and stored at - 80°C until analysis. Mantle samples from control adult mussels were also collected and stored at - 80°C for transcriptome analysis and fixed overnight in 4% paraformaldehyde at 4 ºC for immunohistochemistry.

2.3.2 Shell regeneration experiments

Two holes next to each other (distance ~ 1 cm) were manually drilled (~ 2 - 3 mm in diameter) in the posterior edge of the shell of *M. galloprovincialis* without damaging the mantle. Three experimental challenges were performed (Supplementary Figure 2.1).

Experiment 1. Determination of the timeline for shell regeneration after damage

The results of the first experiment were used to plan the subsequent experimental trials. Six animals (n = 6) were used, and shell regeneration was monitored at 1-, 5-, 9-, 12-, 16- and 20-days post-damage by taking digital images of the damaged region in live animals to calculate the percentage of shell repair across time. The repaired area in each drilled hole / individual was calculated using the program ImageJ version 1.52a and the percentage of shell growth for each animal was taken as the average of the shell regrowth area in the two holes and calculated according to the formula: % hole area = (shell growth area / total hole area) × 100%.

Because the mantle is involved in shell formation, we also aimed to characterize mantle mobility during the shell repair process the same experiment was repeated and the inner side of the valve was observed at 1-, 5-, 9-, 12-, 16- and 20-days post-damage. Animals were placed on ice and then the two valves were separated by carefully cutting the adductor muscle with a blade. Digital photographs of the mantle attached to the inner side of the left valve of the damaged shell were taken. To confirm the presence of newly grown shell (covering the hole) and to detect any changes related to the shell repair process in the inner shell surface, the mantle was

gently detached from the shell and digital images were taken (Supplementary Figure 2.1B).

Experiment 2. Identification of candidate neuropeptide transcripts associated with shell regeneration

In this experiment the expression of candidate neuropeptide genes (Supplementary Figure 2.1C) was determined in mantle tissue collected immediately below the drilled holes (n = 6 samples / group) and in the CPG ganglia (n = 3 samples / group, and each sample contained the CPG from 2 individuals) from control (non-drilled) and shell drilled (SD) animals at 12-, 24- and 36-hours post damage (SD-group).

Ten neuropeptide transcripts were selected for in-depth analysis based on the following criteria: a) expression and possible function in the mantle, as indicated by existing literature, b) the diversity of encoded mature peptides in the precursor genes, c) previously reported neuroregulatory activity in Mollusca and/or other invertebrates, d) the identification of a potential cognate receptor in the mantle transcriptome, and e) unknown mature peptide function.

The selected neuropeptide precursor candidates were: 1) the two calcitonin-like peptide precursors (CALCI and CALCII), previously suggested to have a role in the regulation of calcium movements across the mantle (Cardoso et al., 2020). 2) The AST-C precursor proposed as a candidate immune factor in the mantle (Li et al., 2021). 3) Four members of the RF-amide family, a large, functionally diverse family

of peptides in Mollusca (Kuroki et al., 1993; Zatylny-Gaudin and Favrel, 2014), including the FxRI-amide peptide precursor that encodes 12 mature peptides and plays an important role as a neurotransmitter and neuromodulator in invertebrates (Price and Greenberg, 1977), LFRF-amide peptide precursor which encodes 6 matures peptides and has inhibitory activity in Mollusca neurons (Zatylny-Gaudin and Favrel, 2014), the CCK/SK peptide precursor for which a putative receptor was found in the mantle transcriptome (data not shown) and the LFRY-amide peptide precursor a new member of the RF-amide family for which no function has been assigned. 4) The Mollusca Myomodulin precursor which encodes 10 putative mature peptides and is involved in the regulation of reproduction (Lopez et al., 1993; Kellett et al., 1996). 5) The Lophotrochozoan APGW-amide peptide precursor which encodes 9 mature peptides and regulates reproduction in gastropods (Kuroki et al., 1990) and 6) the LRNFV-amide peptide precursor which encodes 11 peptides with no known function.

Experiment 3. The role of the nerve ganglia in shell regeneration

To identify which nerve ganglia was involved in shell repair, a preliminary experiment was conducted. The commissure between the paired CPG (CPG-group) and between the paired VG (VG-group) ganglia was cut (Supplementary Figure 2.1D). This was done by placing animals on ice, and slightly opening their shells with a clam shell opener. Using a fine needle, the body tissues were gently separated to expose the ganglia. The CPG and VG commissures were cut using fine scissors. Then two holes were drilled in each valve as previously described, and the animals were immediately placed in seawater. The CPG and VG were targeted because, a) both CPG and VG are

proposed to innervate the mantle edge and control mantle movement (Kotsyuba et al., 2020), b) neuropeptide precursors have previously been identified in both ganglia in other bivalve transcriptome studies (Adamson et al., 2015; Zhang et al., 2018), and c) the CPG and VG ganglia are easy to access and manipulate. Each group (control, CPG-group and VG-group) contained 8 animals and the repair rate of the holes in the left and right valves of the CPG-sectioned group was monitored and measured at 0-, 5- and 10-days after drilling, while for the VG-sectioned group it was monitored at days 0 and 7. To understand the impact of ganglia damage on mantle movement the third shell repair experiment was repeated and the mantle on the inner side of the left valve was observed at 2-, 5-, 9- and 20-days after the damage and photographed as described above. Additionally, a group in which both CPG and VG commissures were severed (CPG+VG-group) was established, and shell repair and mantle movement were monitored. No mortality was observed in any of the experimental groups during the experiment.

After examining the regrowth of shells when the ganglia were severed, it was determined that damage to the CPG-ganglia commissure had the most significant inhibitory effect on shell repair. To further investigate the relationship between the CPG and the mantle, another experiment was conducted. Adult mussels (n = 48 total) were randomly assigned to three groups (n = 16 mussels / group): 1) intact control animals (C), 2) shell-damaged group (SD-group) with an intact nervous system, and 3) group with shell damage and a severed commissure between the CPG ganglia (CPG-group). On day 0, the mantle tissue beneath the drilled holes was collected from

the SD-group and CPG-group (n = 8 mussels / group) and from the C group (n = 8 mussels). The trial duration was determined based on the results of experiment one. At day 0 and at the end of the 10th day the mantle (located below the drilled shell or its equivalent position in the control group) was collected from all experimental groups for analysis of changes in gene transcript expression.

All the experimental trials were carried out during October - December 2021 under natural photoperiod (winter in the Algarve) and at ambient room temperature (20 - 22ºC). Half of the water in each aquarium was renewed every two days and the aquaria were manually cleaned. The regenerating shell in each drilled hole was inspected at each sampling timepoint under a stereoscope (Motic, SMZ-171, China) equipped with a digital camera (Visicam 6 Plus, VWR, Portugal). Digital images of the shells were taken from the mussels of experiment 1 (n = 6 mussels / time point) at 0, 1-, 5-, 9-, 12-, 15- and 20-days post-drilling and from experiment 3 on day 0, 5 and day 10 (n = 8 mussels / time point) and the repaired area in each drilled hole/individual was calculated using the program ImageJ version 1.52a. The percentage of shell growth in each animal was calculated by averaging the shell regrowth area in the two holes and using the formula: % hole area = (shell growth area / total hole area) × 100%.

2.3.3 Total RNA extraction and cDNA synthesis

Total RNA was extracted using an ENZA kit (VWR, USA) and any contaminating genomic DNA was removed by treating with Precision DNase as recommended by the manufacturer (Primer design, UK). For total RNA extraction,

the collected tissue composed of the mantle and CPG ganglia with the commissure nerves from control and experimental animals were thawed on ice in lysis buffer and then mechanically disrupted using a Tissue lyser II (Qiagen, Germany) with two iron beads (5 mm) for 3 min at room temperature. The concentration and quality of the extracted total RNA were assessed by determining their absorbance using a NanoDrop (Thermo Scientific, USA) and by agarose gel (1 %) electrophoresis.

For cDNA synthesis, DNase-treated total RNA (500 ng) was denatured at 65°C for 5 min and quenched on ice for 5 min. The reactions for cDNA synthesis were carried out in a final reaction volume of 20 µl and contained 10 ng of pd (N) 6 random hexamers (Jena Bioscience, Germany), 2 mM dNTPs (ThermoScientific, USA), 100 U of RevertAid Reverse Transcriptase and 8 U Ribolock RNAse inhibitor (ThermoScientific). Reaction conditions were as follows: 10 min at 20 °C; 60 min at 42 °C and finally 5 min at 70 °C. The quality and uniformity of the synthesised cDNA for all samples were assessed by amplification of mussel 18S ribosomal subunit (18S rRNA) using specific primers (Table 2.1) and the following thermocycle: 95°C, 3 min; 25 cycles (95°C, 20 sec; 60°C, 20 sec; 72°C, 20 sec); 72°C, 5 min. The reaction products were assessed by agarose gel (2 %) electrophoresis.

Table 2.1- List of primers used in qRT-PCR analysis for the bivalve *M. galloprovincialis.*

Transcript		**Sequence (5' → 3′)**
CALCI	Fwd	TGGTTGAAACTTACATGTGGTT
	Rev	CATTCTTCTTCAATGACGTCA

CALCII	Fwd	AAACGGGCGTGCAATCTTG
	Rev	CGAATGTTCTTTAGGTCAAGGC
CCK/SK	Fwd	CCGGTGCGATATTTCTGTAGG
	Rev	ACACATTGTGCACTTACCGT
LFRY-amide	Fwd	TAGAATTATGTGCTGAAGGGA
	Rev	ATATTGCTGTAATCCTGAAGGA
APGW-amide	Fwd	CATCTTCAGATGAGTCGAGTG
	Rev	CTTCGGAATCGAACAACATATC
Myomodulin	Fwd	ATTAACCCAGGACCTCGTCC
	Rev	TCTTCTGTGAGGTATCTACC
LFRF-amide	Fwd	TTGGACACCAGGACGATAAC
	Rev	CTAATTCCTCCTCACGACCA
FxRI-amide	Fwd	CAAGATGGGACCTGAATATG
	Rev	GATTTAACTCAGCACTCCTC
ASTC	Fwd	GCAGTTTCAAGAGCAGGAAGCCT
	Rev	GGCATTGCACATGGCTTCGTTT
LRNFV-amide	Fwd	TGCGTACACTATCTTCTGGT
	Rev	AATTCAAACCACGGAAGCAC
18S	Fwd	GTGCTAGGGATTGGGGCTTG
	Rev	TAGTAACGACGGGCGGTGTG
EF1 α	Fwd	GAAGGCTGAGGGTGAACGTG
	Rev	TCCTGGGGCATCAATAATGG

2.3.4 Mantle transcriptomes and analysis

The mantle from the left and right valve of control adult *M. galloprovincialis* (n = 6 samples / shell side) was collected and total RNA was extracted using an ENZA kit (VWR, USA) as described above. Library preparation and sequencing were performed by Novogene Europe. Before library production, the total RNA integrity of the samples was assessed using an RNA Nano 6000 Assay Kit for a Bioanalyzer 2100

system (Agilent Technologies, CA, USA) and only samples that passed a pre-established threshold for the RNA integrity (RIN > 8.0) were used for library preparation (n = 3 samples / shell side and each sample was composed of a pool of total RNA from two individuals). Sequencing was performed with an Illumina NovaSeq 6000 and 150 base paired-end reads were generated.

Mantle transcriptomes were analysed in Galaxy (https://usegalaxy.eu/) and annotated in R-studio. The quality of the transcriptome was assessed using FastQC (Version 0.72) with the default parameters (Andrews, 2010) and Trimmomatic (Version 0.36.5) was used to trim low-quality reads (Bolger et al., 2014). Clean reads from the two mantle valves were combined and mapped to the annotated reference genome of *M. galloprovincialis* (NCBI Accession: GCA_900618805.1) in GenBank using HISAT2 (Version 2.1.0, default settings) and transcript counts generated with StringTie (Version 1.3.6, default settings). Sequences were deposited in SRA with the project PRJNA995578 in Nº. SAMN36494222. The mantle transcriptomes were generated in the context of another project, which provides in-depth analysis of the data. In the present study, the transcriptomes were exclusively used to identify putative neuropeptide-encoding genes, which were not the focus of the other study.

2.3.5 Sequence database searches and annotations

The presence of putative neuropeptide precursor genes in the predicted proteins of the *M. galloprovincialis* genome at NCBI (GCA_900618805.1) was established by searching the database using as the query the deduced neuropeptide precursor orthologues from the Pacific oyster (*M. gigas*, now renamed *Megallana gigas*) and the

scallop (*M. yessoensis*) (Stewart et al., 2014; Zhang et al., 2018; Réalis-Doyelle et al., 2021). A total of 110 bivalve neuropeptide precursor genes (Supplementary Table 2.1), 60 from *M. gigas* and 50 from *M. yessoensis* were used to search the predicted proteins of *M. galloprovincialis* (taxid:29158) using the blastp programme and hits with an e value < -10 were retrieved and analysed. To identify candidate neuropeptide genes with the potential to regulate mantle function, *M. galloprovincialis* mantle transcriptome reads were mapped to the annotated genome. Only genes identified in more than one of the mantle transcriptome libraries generated for the right or left valve (n = 3 samples / each valve) were included in subsequent analysis. Additionally, assembled, and annotated *M. galloprovincialis* mantle transcriptomes (SRP 063654) available "in-house" (Bjärnmark et al., 2016) were also searched for the neuropeptide sequences since the reference genome annotation (NCBI, GCA_900618805.1) available for *M. galloprovincialis* is incomplete (Gerdol et al., 2020).

The identity of the retrieved *M. galloprovincialis* putative neuropeptide coding genes was confirmed by characterization of the deduced protein precursors and localization of the predicted mature peptides by a) the identification in the flanking sequences of monobasic, dibasic, or tribasic consensus cleavage sites (RR, KR, KK) and b) identification of conserved mature peptide motifs (Stewart et al., 2014; Zhang et al., 2018). The *M. galloprovincialis* peptide precursors were aligned with the orthologues from *M. gigas* and *M. yessoensis* using the multiple sequence alignment programme clustal omega with the default settings (Madeira et al., 2022) to confirm sequence homologies and the deduced mature peptides were annotated.

2.3.6 Immunofluorescence

Immunofluorescence was performed to a) characterize the neuropeptide secretory fibres in the mantle and b) analyse the organization of the nerve fibres in the ganglia (CPG and VG) and mantle during shell repair and after severing the CPG commissure in mussels. Mantle, CPG ganglion and VG ganglion tissue samples were equilibrated with a graded series of sucrose solutions (from 10% to 30%) and stored at - 20°C until use. To prepare the tissue for sectioning, they were embedded in an optimal cutting temperature (OCT, VWR, Portugal) medium and frozen at - 20°C overnight. Serial sections of 14 μm were prepared using a cryostat (NX50 cryostat, Thermo Scientific, Waltham, MA, USA) and mounted on glass slides (treated with APES; Sigma-Aldrich, Madrid, Spain) before being stored at - 20°C.

For immunofluorescence, slides were washed 3 times in PBS for 15 min and then incubated in OCT blocking solution (Tris-Carrageenan-Triton X buffer, 0.1M Tris buffer containing 0.7% Carrageenan and 0.5% Triton X-100, pH 7.6) containing 3% sheep serum (Sigma-Aldrich, Madrid, Spain) for 2 hours at 4 ºC. The primary antisera utilized were anti-FMRF (rabbit polyclonal, Immunostar, 20091) diluted 1:1000 in PBS, anti-β-tubulin (mouse monoclonal, Sigma, T-4026) diluted 1:250 in PBS and anti-5-HT (rabbit polyclonal, Sigma, S-5545) diluted 1:400 in PBS (Table 2.2). The specificity of the primary antisera used in the study has previously been validated in other studies of invertebrates (Nikishchenko et al., 2022; Yurchenko and Dyachuk, 2022).

Table 2.2. Primary and secondary antibodies used.

Antibody	Host species	Source	Dilution before use
FMRF_amide	Rabbit (polyclonal)	Immunostar(20091)	1:1000
β-tubulin	Mouse (monoclonal)	Sigma (T-4026)	1:250
Serotonin (5-HT)	Rabbit (polyclonal)	Sigma (S-5545)	1:400
Alexa Fluor 546-anti-rabbit IgG	Donkey	Molecular Probes, Eugen (A-11035)	1:400
Alexa Fluor 546-anti-mouse IgG	Donkey	Molecular Probes, Eugen (A-11030)	1:400

Mantle tissue sections were incubated with FMRF, serotonin and β-tubulin antisera and the CPG and VG sections were incubated with serotonin and β-tubulin antisera. For all tissue sections incubation with the primary antisera at the optimal dilution was overnight at 4°C, rinsed twice in PBS for 5 min and then incubated with the secondary antisera in the dark and in all subsequent steps of the procedure. The secondary antisera were Alexa Fluor 546-conjugated anti-rabbit IgG (Molecular Probes, Eugen, Oregon; A-11035) for the FMRF and serotonin antisera, and Alexa Fluor 546-conjugated anti-mouse IgG (Molecular Probes, Eugen, Oregon; A-11030) for the β-tubulin antisera. The sections were incubated with the appropriate secondary antisera for 2 hours at room temperature in the dark and then washed twice in PBS (3 minutes per wash) and the nuclei stained with a solution of DAPI (1:20000 dilution, Sigma, St. Louis, MO, USA) for 5 min. After two washes of 3 minutes in PBS, tissue sections were mounted in glycerol-gelatine (Sigma-Aldrich, GG1, Madrid, Spain) and analysed using a fluorescence microscope (Zeiss Axioimager Z2, Carl Zeiss Group)

coupled to a digital camera (Axiocam ICC3) linked to a computer for digital image analysis.

2.3.7 Quantitative PCR

Changes in neuropeptide gene expression during shell repair were assessed in the RNA extracted from mantle tissue below the drilled area and in the CPG-ganglia by quantitative real-time PCR (qPCR) using SsoFast EvaGreen Supermix (BIO-RAD, Portugal). A 5 µl final reaction volume was prepared with 200 nM of forward and reverse gene-specific primers (Table 2.1) and 1 µl of template cDNA (diluted 1:3). The expression of elongation factor 1-alpha (ef1α) and 18S ribosomal subunit (18s) transcripts in *M. galloprovincialis* cDNA (diluted 1:50 and 1:500, respectively) did not vary between samples and so they were used as reference genes. Duplicate reactions were performed (< 5% variation between replicates) using a CFX Connect Real-Time PCR Detection System for 384-well microplates (BIO-RAD). Cycling conditions were 95 ºC, 30 sec; 44 cycles (95 ºC for 5 sec and 10 sec at the primer annealing temperature, Table 2.1). To detect non-specific products and primer dimers melting curves were performed. q-PCR efficiencies and R^2 (coefficient of determination) were established (Table 2.1) and gene expression levels were calculated. Data was normalized using the geometric mean of the reference genes. All amplicons were sequenced to confirm reaction specificity.

2.3.8 Enzymatic assays

The effect of the experimental manipulations on the activity of mantle carbonic

anhydrase activity the enzyme that generates bicarbonate from metabolic carbon dioxide and so regulates the formation of the mineralized calcium carbonate crystals in the shell was determined (Müller et al., 2013; Rodriguez-Navarro et al., 2019; Cardoso et al., 2020).

2.3.8.1 Mantle protein extracts

Protein extracts were prepared from the mantle of both valves for the enzymatic assays. Mantle samples from the control (C), SD-group and CPG-group mussels at 0 and 10 days were used. Mantle protein extracts were prepared in sterile SW by mechanically disrupting the tissue using a Tissue lyser II (Qiagen, Germany) with two iron beads (5 mm) for 3 min at room temperature. The amount of SW added was 10 times the tissue weight to obtain a final concentration of 0.1 mg /µl of the protein extract. The lysate was centrifuged for 15 min at 13000 rpm and the supernatant was transferred to a clean tube and stored at - 80ºC until use. Samples were used within 4 days of preparation.

2.3.8.2 Esterase activity

Esterase activity in the mantle (n = 8 samples / group) was quantified in protein extracts using a colorimetric assay that measured the conversion of the substrate 4-nitrophenyl acetate to p-nitrophenolate. Assays were performed using the method previously described (Cardoso et al., 2019, 2020). In brief, 10 µl of mantle edge protein extracts (0.1 mg / µl) were added to 290 µl of the substrate (0.05 M 4-Nitrophenyl acetate (Acros Organics, USA) in Tris-HCl (pH 7.4) for 20 minutes in

the dark with gentle agitation. Reactions were performed at RT in duplicate for each of the extracts prepared. Esterase activity was stopped by placing the reactions on ice for 5 min and the absorbance was read at 405 nm (Biotek Synergy 4, USA). The amount of p-nitrophenolate produced was quantified using a standard curve prepared from p-nitrophenol (from 0 to 200 µM). Bovine CA isoenzyme II (0.1 mg / ml) (SIGMA-ALDRICH) was used as the positive control.

2.3.8.3 Acid phosphatase activity

Acid phosphatase activity (n = 8 samples / group) in mantle protein extracts was determined using 96 well-plates (GREINER, Germany) and a tartrate-resistant acid phosphatase (TRAP) assay as described in (Cardoso et al., 2020). Briefly, 10 µl of the mantle edge protein extract (0.1 mg / µl) was added to 190 µl of TRAP buffer (20 mM para nitrophenyl (pNPP, SIGMA-ALDRICH), 20 mM tartrate in 0.1 M Na-acetate buffer, pH 5.3) and incubated for 20 min at RT with agitation. Reactions were stopped with 2 M NaOH and measured at 405 nm using a microplate reader (BIOTEK SYNERGY 4). The amount of pNPP converted into p-nitrophenol (pNP) was calculated using a pNP standard curve (from 0 to 200 µM) prepared as outlined above.

2.2.8.4 Alkaline phosphatase activity

Alkaline phosphatase (ALP) activity (n = 8 samples / group) in mantle protein extracts was determined using 96 well-plates (GREINER, Germany) according to the protocol described in (Cardoso et al., 2020). Briefly, 10 µl of the mantle protein

extract (0.1 mg / µl) was added to 190 µl of ALP buffer (5 mM paranitrophenylphosphate - pNPP, Sigma-Aldrich -, 0.1 M Tris-HCl - pH 9.5 - 1 mM MgCl2, and 0.1 mM ZnCl). For ALP reactions, the samples were incubated with agitation at 30 ºC in the dark for 30 min. The reactions were stopped by adding 200 µl of 2 M NaOH and 150 µl of the reaction mix from each well was transferred in duplicate to a 96-well plate and absorbance was measured at 405 nm using a microplate reader (BIOTEK SYNERGY 4). The amount of pNPP converted into pNP was calculated using a pNP standard curve (from 0 to 200 µM) prepared as outlined above.

2.3.9 Peptide injections

To assess if the candidate peptides identified regulate shell formation, a shell damage-repair assay was carried out in bivalves. Several neuropeptides were selected as candidates for shell growth, based on the following criteria a) in shell damage-repair assays they had a significantly modified gene expression compared to the control individuals, and/or b) they had a significantly modified gene expression after the commissure of the CPG ganglia was severed (see section 2.3.2 for experiments).

In *M. galloprovincialis* with two holes drilled in the right and left valve, candidate peptides were injected into the adductor muscle using a micro-syringe (Hamilton Gastight Syringes, Germany) with a 23 G needle and their effect on mantle function and shell formation was assessed. Candidate peptides that were tested included CALCIIa (H-CTWGGGMSDEMCSTVDIDEIQRSFQVIHDRNSP-amide),

which is encoded in the *M. galloprovincialis* CALCII precursor, a candidate regulatory factor of shell mineralisation (Cardoso et al., 2020) and the MYOc peptide (AMPMLRL-amide, repeated 3 times inside the Myomodulin precursor). The peptide CALCIa (H-ACNLGLNSHHCALADLDNQLQS REWLSNGHSP-amide) was also tested because it is the duplicate of CALCIIa (Cardoso et al., 2020) and a further peptide CCK/SK (QGDWDLDYGLGGGRW-amide) was included as a negative control because its expression was unrelated to shell growth and the peptide was synthesised without the sulphate group, so it does not activate its receptor.

All the peptides were synthesized with a purity > 95% by HPLC analysis. Modifications including N-terminal acetylation, C-terminal amidation and appropriate disulphide bonds were included for CALC peptides and for Myoc and CCK/SK the peptides were amidated (GL Biochem Ltd, Shanghai, China). All peptides were re-suspended in sterile 1x PBS before the assays. To choose the best concentration of peptide for the in vivo assays, optimization studies with three concentrations (10^{-4}, 10^{-5} and 10^{-6} M) were initially tested, by injecting (50 µl) of them into the adductor muscle and monitoring shell regrowth for 5 days. In the PBS group, PBS alone (50 µl) was administrated. A control group was included to represent the normal repair process (no manipulation). For the trial, a peptide concentration of 10^{-5} M was chosen. Only the peptides (CALCIa, CALCIIa and MYOc) that affected shell growth were tested. CCK/SK, which had no effect in the optimization trials, was excluded (Supplementary Figure 2.2). Thirty *M. galloprovincialis* were randomly divided into 5 groups of 6 animals each and placed in 10 L tanks filled with seawater from their

natural habitat. Peptides and PBS injections (50 µl) were administered every 48 hours throughout the experimental.

Experiments were run under the conditions described above (section 2.3.1) except that the temperature of the seawater was 25 - 27ºC and the photoperiod was that for August in the Algarve. No mortality was observed during the experiments. The regenerated shell inside the holes drilled in each valve was observed daily under a stereomicroscope and photographed using a digital camera (Visicam 6 Plus, VWR, Portugal). The shell repair rate was calculated on day-15 after the start of the experiments from six (n = 6 animals) biological replicates per group and was the average of the two holes in the two valves (right and left) of each animal. This experiment was repeated independently twice.

2.3.10 Scanning electron microscopy (SEM)

Regenerated shells from *M. galloprovincialis* were washed with distilled water, air-dried, and used for SEM imaging. Shell samples were mounted on stubs coated with gold (JEOL, JFC1200, JSM Electron Microscopes, Tokyo, Japan), and observed using a scanning electron microscope (JEOL, JSM5200-LV, JSM Electron Microscopes, Tokyo, Japan) with a high-energy beam of 25 kV, and images were acquired after 90 seconds exposure using digital software.

2.3.11 Statistical analysis

Statistical analysis was performed using GraphPad Prism version 8.0 for Mac OS X (US, www.graphpad.com). One-Way ANOVA and Two-Way ANOVA with a

Sidak's multiple comparisons test were used. All the results are shown as mean ± standard error of the mean (SEM). One-Way ANOVA was used to identify significant differences between experimental groups in the enzymatic assays and shell repair experiments. Two-Way ANOVA was utilized to determine significant differences in gene expression between groups and to assess the impact of the peptides on shell growth. The significance threshold was set at $p < 0.05$.

2.4. Results

2.4.1 Neuropeptide precursors in M. galloprovincialis

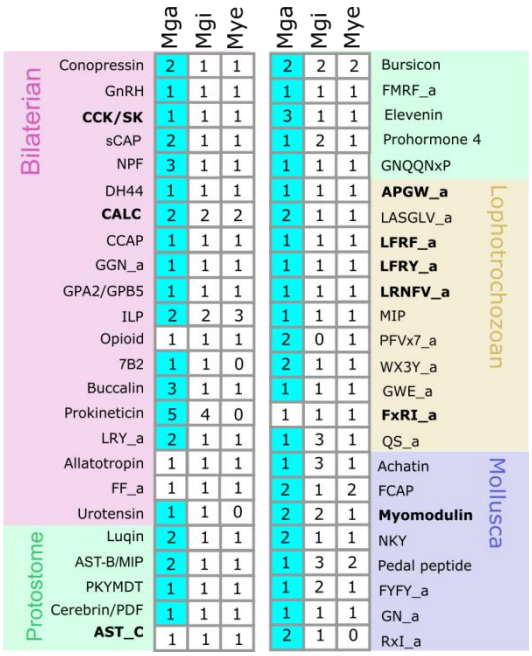

Figure 2.1: Minimum neuropeptidome in the *M. galloprovincialis* genome. Comparisons of the number of *M. galloprovincialis* (Mga) neuropeptide gene transcripts with *M. gigas* (Mgi) (Stewart et al., 2014; Réalis-Doyelle et al., 2021) and *M. yessoensis* (Mye) (Zhang et al., 2018). The numbers inside the boxes represent the number of genes. The accession numbers of the predicted peptide precursors, length and number of mature peptides are available in Supplementary Table 2.1. The complete neuropeptide precursor sequences and deduced mature peptides for *M. galloprovincialis* are available in Supplementary Figure 2.3 and the sequence alignment of the deduced mature peptides between Mga, Mgi and Mye are available in Supplementary Figure 2.4. The peptide precursors found in the mantle

transcriptomes are marked in blue and those selected for genes expression and functional analysis are in bold.

To explore the diversity of neuropeptide precursors found in the *M. galloprovincialis* genome and to identify those expressed in the mantle, the neuropeptide gene set was obtained from the genome and then their expression was determined in the mantle by analyzing transcriptomes. Sequencing of the 6 mantle cDNA libraries (n = 3 samples / each shell side) of control adult mussels yielded an average number of reads of 43771022 per library with an average GC content of 38%. They were combined and mapped against the *M. galloprovincialis* annotated genome and yielded a total of 83135 genes. This suggests that approximately 62% of the genes predicted in the *M. galloprovincialis* genome (a total of 134183 predicted genes) are expressed in the mantle (Peng et al., 2023).

Searches in the *M. galloprovincialis* annotated genome using full-length peptide precursors or deduced mature peptide sequences from other bivalves identified at least 48 neuropeptide gene family members that were orthologues of neuropeptide genes and precursors found in *M. gigas* and *M. yessoensis* (Figure 2.1, Supplementary Table 2.1). To confirm genome predictions and identify additional neuropeptide families or family members that have not been identified in the available annotated genome, annotated mantle transcriptomes available "in house" were searched and 6 additional neuropeptide precursor transcripts (Allatostatin C, Allatotropin, CALCI, FF-amide, FxRI-amide and opioid) were identified (Bjärnmark et al., 2016; Cardoso et al., 2020; Li et al., 2021).

In *M. galloprovincialis* most neuropeptide genes corresponded to a single protein precursor but for some multiple precursors were predicted (Figure 2.1, Supplementary Figure 2.3 and Supplementary Table 2.1). Two protein precursors were predicted for 16 neuropeptides gene families: Bursicon, Calcitonin (CALC), Conopressin, Feeding Circuit-Activating Peptide (FCAP), Insulin-like peptide (ILP), LASGLV_amide, Luqin, LRY-amide, Allatostatin B / Myoinhibiting peptides (AST-B/MIP), Myomodulin, neuropeptide KY (NKY), PFVx7, RxI_amide, small Cardioactive Peptide (sCAP) and WX3Y_amide peptide, three protein precursors were retrieved for Buccalin, Elevenin and neuropeptide F (NPF) and five for the Prokineticin neuropeptide gene (Figure 2.1, Supplementary Table 2.1 and 2.2). Most of the predicted protein precursors resulted from alternative exon splicing events of a single gene (Supplementary Table 2.2). However, in the case of Bursicon, CALC, ILP, PFVx7 and Prokineticin the predicted peptide precursors arose from different genes (Supplementary Table 2.2).

Precursors encoding neuropeptide genes that are conserved across bilaterians (19), Protostomes (5), Lophotrochozoans (16) and Mollusca (8) were identified (Figure 2.1). Comparisons between the bivalve species *M. gigas, M. yessoensis* and *M. galloprovincialis* suggested that the number of neuropeptide precursors and encoded mature peptides was species-specific (Figure 2.1, Supplementary Table 2.1, Supplementary Figure 2.4). In *M. galloprovincialis* the largest and most peptide - rich neuropeptide precursor was the pedal peptide precursor and a single gene encoding the peptide precursor was found. The predicted peptide precursor encoded 23 mature

peptides. In *M. gigas*, 3 different genes encoding the pedal precursors have been described and the predicted peptide precursors encoded a different number of mature peptides (27,11 and 16 peptides) (Stewart et al., 2014).In *M. yessoensis* two gene orthologues encoding the pedal precursors were described and encoded 9 and 7

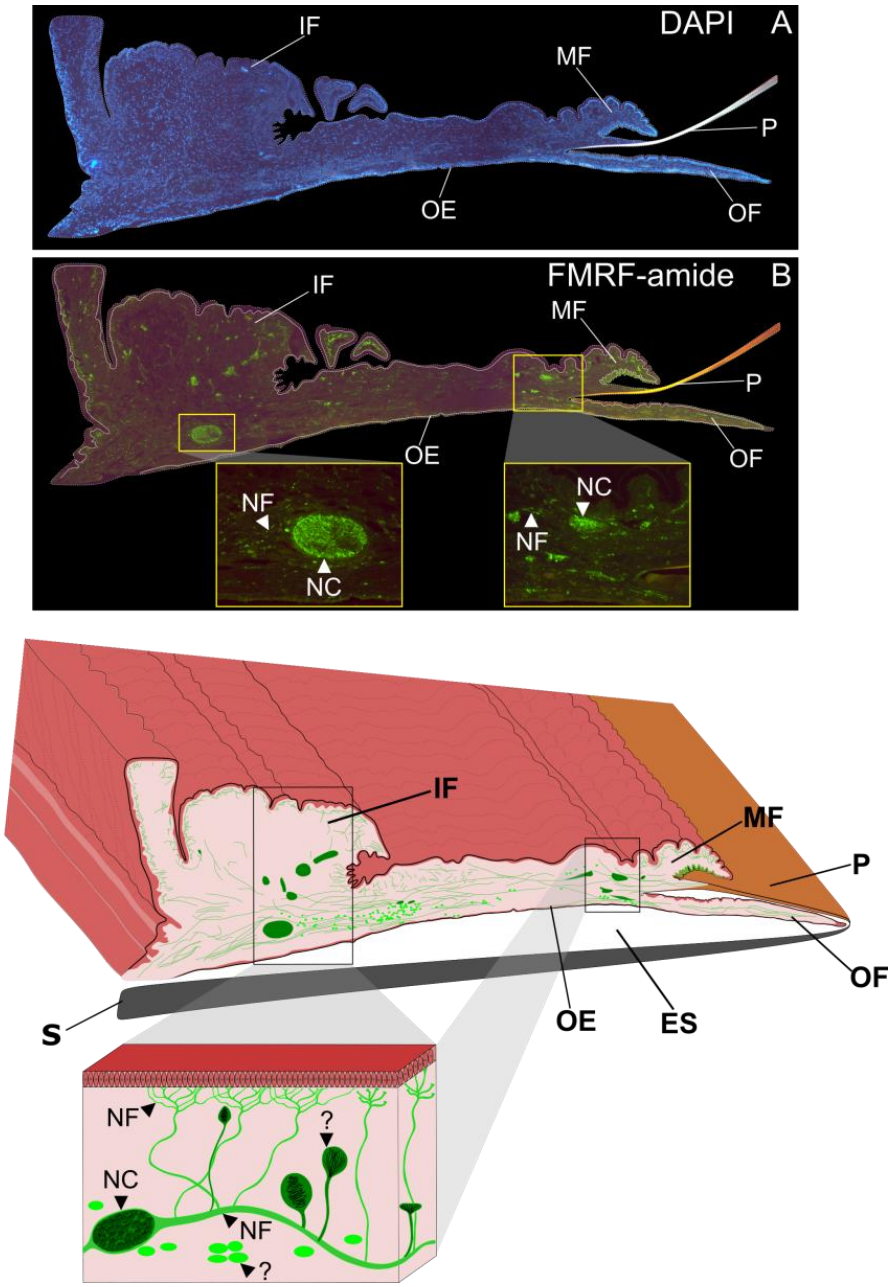

Figure 2.2: Immunohistochemistry of the *M. galloprovincialis* mantle. A) DAPI staining, B) immunostaining with the FMRF antibody, C) illustration of the distribution of the neuropeptide fibers in mantle. The three structural folds of the mantle edge are represented. White arrows indicate the neural nodes within the mantle

body. OF - outer fold; MF - middle fold; IF - inner fold, P - periostracum, OE- outer epithelial cell layer, NC - neuro cell clusters, NF-nerve fibres, S-shell, ES-extrapallial space. The scale is indicated in the images. Stained sections from histology were analysed using light or fluorescence microscopy and a Zeiss Axioimager Z2 (Carl Zeiss Group) coupled to a digital camera (Axiocam ICC3) linked to a computer for digital image analysis. The magnification used was 100X for the combined overall tissue images, and 200X for the detailed images.

mature peptides (Zhang et al., 2018) (Supplementary Table 2.1). Other examples of predicted peptide precursors encoding multiple peptides were the bivalve FMRF-amide precursors which encoded 16, 14 and 27 mature peptides in *M. galloprovincialis*, *M. gigas* and *M. yessoensis*, respectively (Figure 2.1, Supplementary Table 2.1, Supplementary Figure 2.4).

Interrogation of adult *M. galloprovincialis* mantle transcriptomes identified at least 45 neuropeptide transcripts that belonged to 41 different neuropeptide gene families (Supplementary Table 2.3). Of all the neuropeptide gene families identified only members of Bursicon, GWE-amide and Neuropeptide prohormone 4 gene families were not identified. Ten (10) neuropeptide precursors were selected for gene expression analysis and functional studies to explore their involvement in mantle-shell production and biomineralization (Figure 2.1, Supplementary Figure 2.3).

2.4.2 Detection of neuropeptide fibres in M. galloprovincialis mantle

We used antisera commercially available, which were previously validated for use in molluscs (Kotsyuba et al., 2020) (Figure 2.2). The mantle of *M. galloprovincialis* is made up of three distinct folds: the outer fold (OF), middle fold (MF), and inner fold (IF). FMRF immunopositive fibers were found in the inner mantle and in the mantle margin, indicating that this tissue is highly innervated, and contains a complex network of FMFR fibres. Additionally, concentrated nerve tracts

of varying size were detected within the inner mantle tissue (Figure 2.2). This confirmed that the mantle in *M. galloprovincialis* is highly innervated and suggested that it is regulated by the ganglia and indicates that neuropeptides such as FMRF may play an important role.

2.4.3 The impact of ganglia damage on shell regeneration

2.4.3.1 Implementation of an in vivo M. galloprovincialis shell regeneration model

To study the potential role of neuropeptides in mantle function, we have examined their potential involvement in shell production. For this purpose, we established an experimental model to observe shell damage and repair in living bivalves. In our experiment, we drilled a hole in both shell valves and monitored the

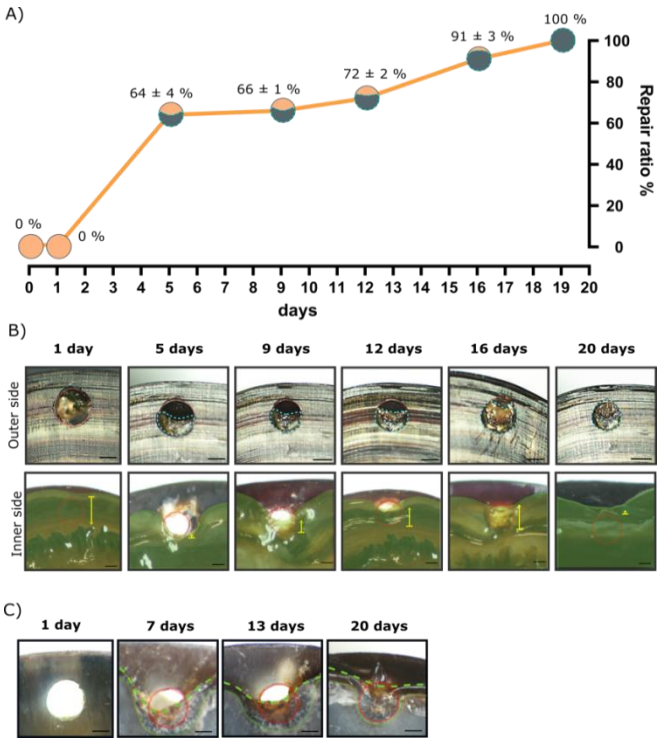

Figure 2.3: Shell re-generation after damage in *M. galloprovincialis*. A) Timeline of the shell repair process. Images were analysed to calculate the percentage (%) shell repair ratio using Image J. The blue dashed line represents the outline of the newly grown shell. The orange line in the graph represents the progress of shell repair and

the circles provide an illustrated view of the proportion (%) of the damaged shell that was repaired across time. The percentage presented is the average of the results of six different individuals. B) Digital images of the outer and inner shell side during shell repair. Outer shell side images illustrate hole coverage with the newly grown shell and inner shell side images illustrate the movement of the mantle during shell repair. The green shaded area represents the mantle, the red circles denote the edge of holes drilled in the shell, and the yellow arrows indicate the direction of mantle movement. C) Inner shell morphology during repair. The green line represents the baseline where the new shell begins to grow, the dashed green line represents the front of the newly deposited shell. The red circles indicate the hole position. The scale bar indicates 1 mm.Moreover, no differences were observed in the rate of shell regrowth when the left and right drilled valves were compared suggesting that shell regeneration occurred at a similar rate after damage in both valves (Figure 2.4A).

shell regeneration process. After 20 days the hole in the valve was fully repaired with new shell (Figure 2.3A). Normal shell regeneration occurred at a variable rate across time (Figure 2.3A) and the most intense period of repair occurred within the first days after the shell was drilled and by the 5th day more than half (64 ± 4 %) of the hole was covered by newly grown shell. The subsequent repair rate was slower, and it took a further 15 days (until day 20), for the drilled hole to be totally covered (Figure 2.3A). Observations of the mantle movements during shell repair were carried out during the initial stages of shell repair. After drilling, the mantle edge retracted and surrounded the hole (Figure 2.3B). After the shell was repaired, the mantle slowly returned to its original position before drilling. Twenty (20) days after drilling, when the hole was completely covered by a thin mineralized layer, the mantle was close to its original position before drilling as seen in Figure 2.3B. During the shell repair process morphological changes were observed in the prismatic layer of the inner shell surface surrounding the anterior region of the drilled hole (Figure 2.3C). Light microscopy revealed that an irregular matrix structure was formed during repair.

To assess the potential regulatory role of the nervous ganglia on shell repair / growth, the nerve commissure that connects the left and right CPG ganglion (CPG-group) and the left and right VG ganglion (VG-group) were severed, and shell regeneration was monitored in the drilled shell (Figure 2.4 and Supplementary Figure 2.5).

2.4.3.2 Severing the CPG in vivo impairs shell-regeneration in M. galloprovincialis

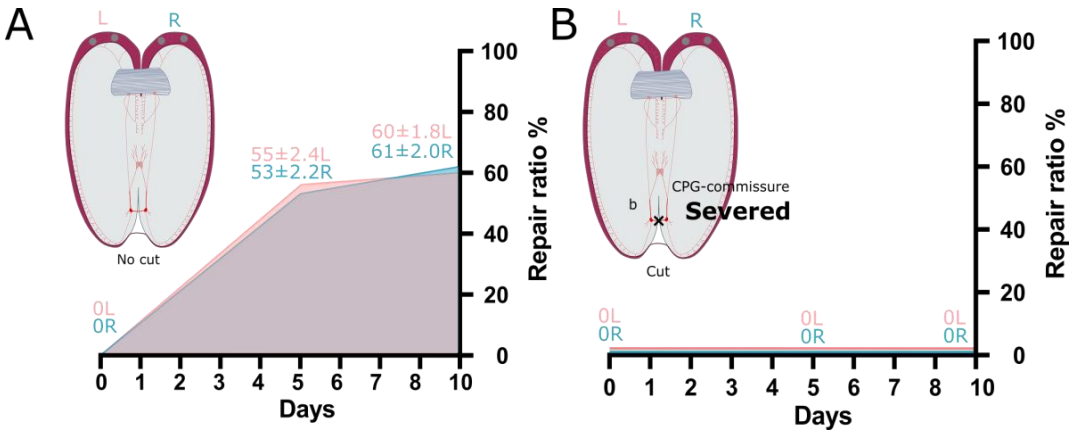

Figure 2.4: Effect of ganglia commissure damage on shell regrowth. The nerve commissure that connects the CPG ganglia was severed and the process of shell-regrowth was observed for 10 days in both left and right valves. The repair of holes in the shell was monitored at 0, 5 and 10-days post-drilling, A) in animals (n = 8) in which holes were drilled in the shell (control-group) or B) in animals (n = 8) with drilled shells and severed ganglia (CPG-group). Two holes were made in each valve - the right valve is represented in blue; the left valve is represented in pink, using a stereomicroscope (Motic, SMZ-171, China) equipped with a digital camera (Visicam 6 Plus, VWR, Portugal). The percentage (%) of shell repair was calculated using Image J. No differences in the rate of shell repair were observed between the two valves. Shell repair was arrested in the animals in which the nerve commissure that connects the two CPG was severed.

Both the CPG and VG were independently severed since both nerve ganglia are suggested to control mantle function (Benjamin et al., 2021). After severing the ganglia, the effect on shell regrowth was monitored using the approach outlined in section 2.3.1. In *M. galloprovincialis*, regrowth of the shell was stopped in both the right and left valves when the CPG was severed during the experiments (Figure 2.4A

and B). In contrast, when the VG ganglia commissure was severed shell regrowth occurred as normal in both the left and right valves and the repair rate was identical to the control group after 7 days (Supplementary Figure 2.5A and B). Visual inspection of the severed CPG or VG ganglia revealed that the nerve connections were not re-established for the duration of the experiment (data not shown). The results indicate that the CPG ganglia is essential for shell regrowth and may regulate the shell-related activities of the mantle. While the VG ganglia does not appear to have an important role.

To verify if the effects of the severed CPG on shell regrowth were due to modified mantle movement, mussels with a severed CPG were observed across the 20

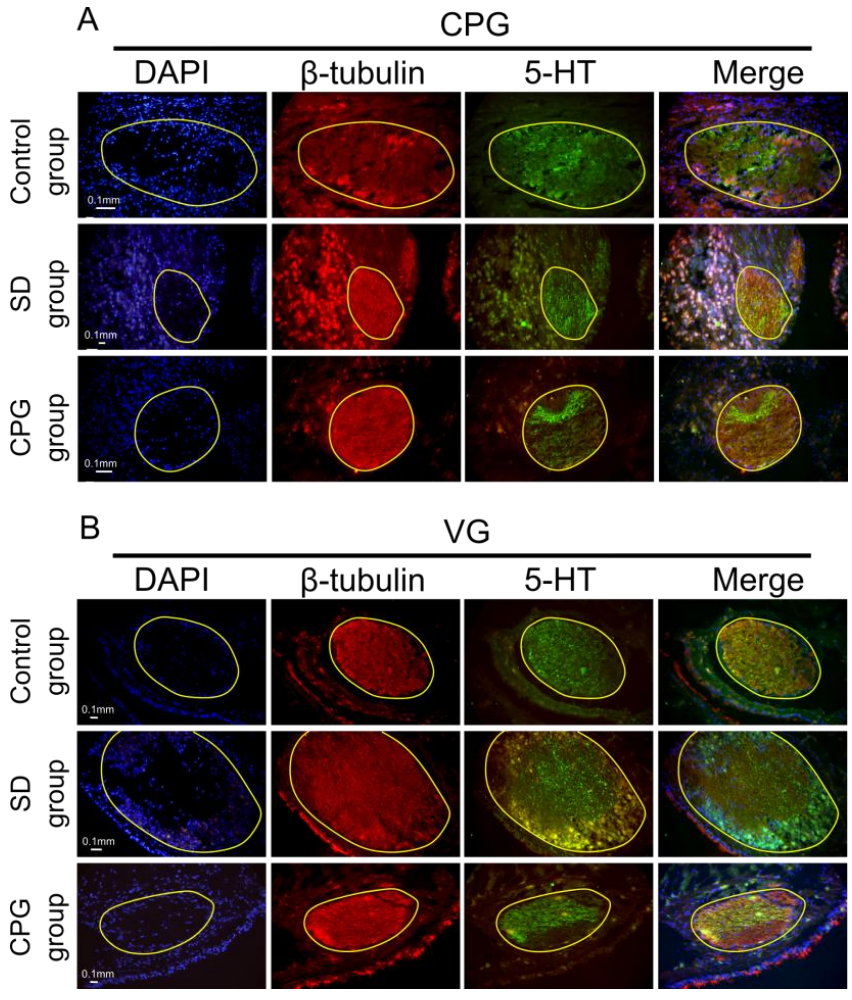

Figure 2.5: Immunohistochemistry of *M. galloprovincialis* CPG and VG during shell regrowth. A) CPG ganglion, B) VG ganglion. The image shows immunostaining with DAPI and with anti- β-tublin and anti 5-HT. SD-group- shell damage, CPG-group- shell damage with severed CPG ganglia after 24 hours post damage. The scale bar is indicated. Stained sections were analyzed using light or fluorescence microscopy and a Zeiss Axioimager Z2 (Carl Zeiss Group) coupled to a digital camera (Axiocam ICC3) linked to a computer for digital image analysis. The magnification used was 400X.

days of the experiment. The results showed that cutting the commissure of the GPG or VG ganglia did not have any effect mantle movement (Supplementary Figure 2.5C).

2.4.3.3 CPG and VG ganglia reorganization after severing the ganglia or during shell damage

Immunohistochemistry was performed to analyze the impact of shell damage or cutting the commissure (CPG only) on neurons and nerve tracts in the CPG and VG ganglion and mantle at the initial stages of shell repair (24h). Anti β-tubulin was used to analyze the overall nervous tissue organization and anti-5-HT to characterize the distribution of the neurotransmitter neurons/fibers (Figure 2.5). In shell-damaged animals, the CPG ganglion showed a reorganized pattern. The immunopositive neurons for β-tubulin and 5-HT showed that the ganglion were re-organized compared to intact control animals (Figure 2.5A). Twenty-four (24) hours after shell damage, the CPG ganglion in shell damaged animals was smaller than the control ganglion and contained a compact mass of 5-HT neurons. When the CPG commissure was severed (CPG-group) the shape of the ganglion changed, becoming rounder, and the 5-HT neurons became concentrated in the region localized near the severed commissure (Figure 2.5A). For the VG-group, shell damage increased the ganglion size and 5-HT positive neurons became concentrated in the center of the ganglion (Figure 2.5B).

Notably when the CPG commissure was severed the VG ganglion was affected and it became smaller, and the 5-HT neurons were concentrated on one side (Figure 2.5B).

At the mantle edge, shell damage does not modify the tissue structure, but the distribution of the 5-HT positive fibers was modified. Shell damage increased the number of 5-HT positive fibers in the mantle but in the CPG-group there was a re-distribution of the 5-HT immunopositive nerves, and they became more concentrated in the mantle OF, which is most related with shell formation (Figure 2.6).

2.4.3.4 Activity of biomineralization enzymes in the mantle

To determine the impact of shell damage and the nervous system on "shell toolbox genes" the activity of the biomineralization enzymes: α-carbonic anhydrase (CA) involved in the production of bicarbonate ions essential for crystal

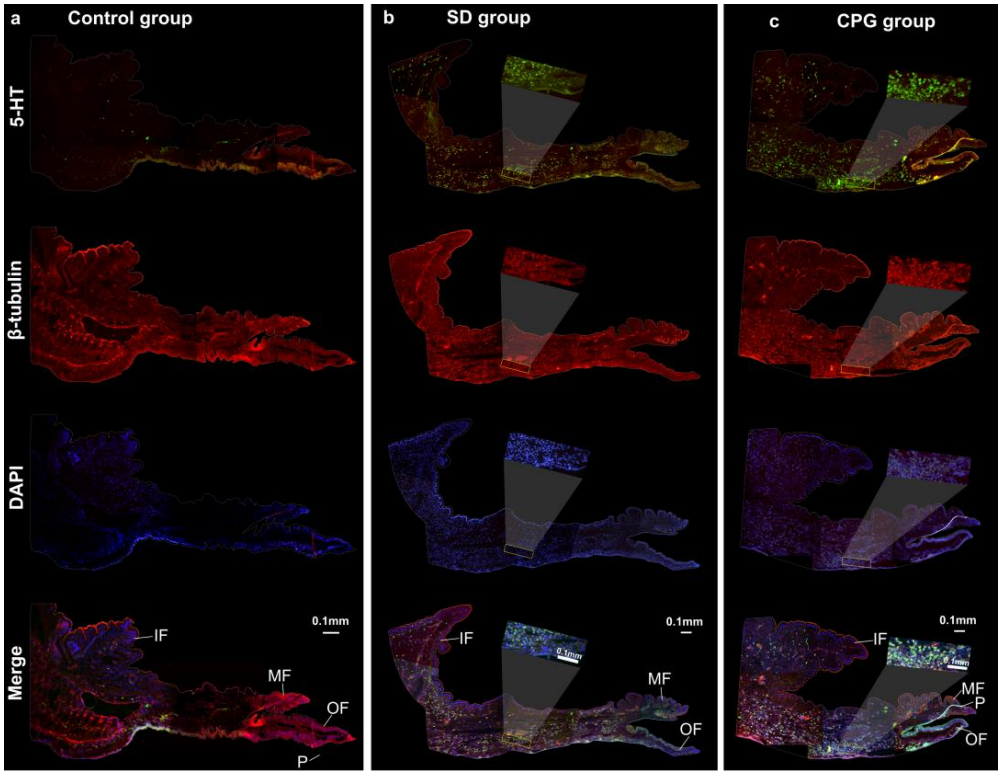

Figure 2.6: Immunohistochemistry of the *M. galloprovincialis* mantle edge during shell regeneration. The image shows immunostaining with DAPI and with anti-β-tublin and anti 5-HT of control, SD-group (shell damage) and CPG-group (shell damage with severed CPG ganglia) 24 hours post damage. The scale bar is indicated and corresponds to 0.1 mm. The stained sections were analyzed using light or fluorescence microscopy and a Zeiss Axioimager Z2 (Carl Zeiss Group) coupled to a digital camera (Axiocam ICC3) linked to a computer for digital image analysis. The magnification used was 200X.

mineralization (Lindskog & Coleman, 1973; Tripp et al., 2001), acid phosphatase (TRAP) which is associated with shell remodelling and alkaline phosphatase (ALP) a shell matrix protein associated with shell formation (Le Roy et al., 2014, 2016) were measured in the mantle 10 days after shell drilling (Figure 2.7A). In the SD-group the activity of CA and TRAP was significantly increased after shell damage ($p < 0.05$) compared to the intact group, but in the CPG-group shell damage caused a significant

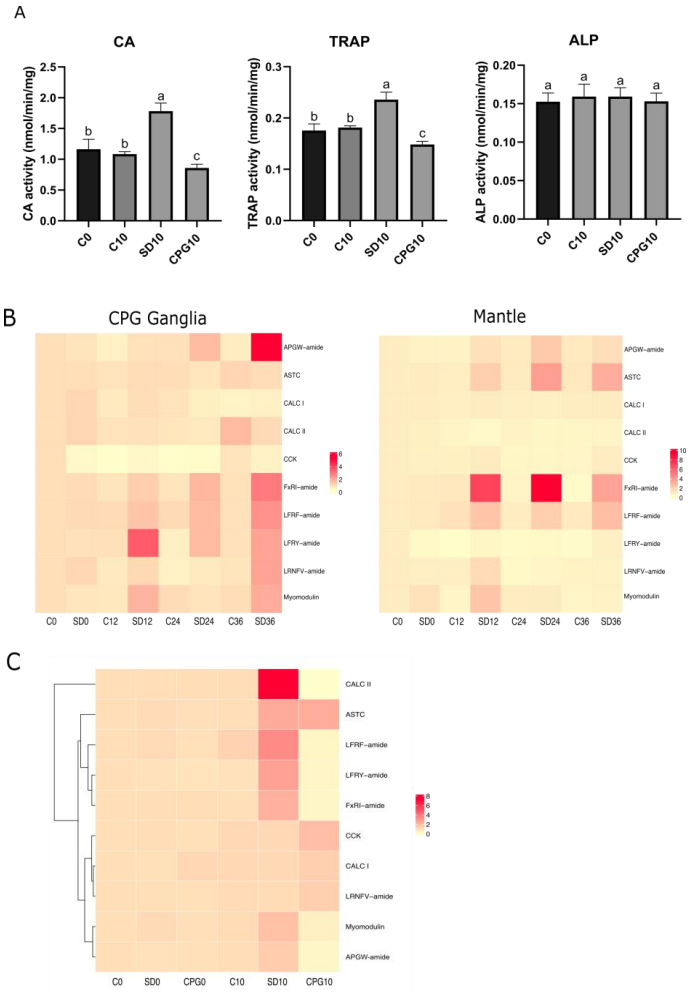

Figure 2.7: Biomineralization enzyme activity and gene expression levels of candidate neuropeptides during shell regeneration. A) Enzyme activity of mantle edge samples (below the hole drilled in the shell) collected at day 0 and 10 days after repair. Three enzymes linked to biomineralization were measured: Alpha-Carbonic anhydrase (CA), Acid phosphatase (TRAP) and Alkaline phosphatase (ALP), in control (intact shell), drilled shells (SD-group) and drilled shells and ganglia damage (CPG-group) mussels. Values represent the mean ± SEM (n = 8 samples / assay) performed in duplicate. Prism GraphPad v5 was used to assess the significance of the differences between the groups using One-Way Anova and Tukey's multiple comparison test. Different letters indicate significantly different groups ($p < 0.05$). B and C) Heat maps representing the clustering of gene expression profiles measured by qRT-PCR of the candidate neuropeptides, during early stages of shell repair in CPG ganglia and mantle (B) (Supplementary Figure 2.6), and in late stages of shell repair in the mantle (C) (Supplementary Figure 2.7). For B) mantle samples were collected from mussels with intact and drilled shells (SD-group) after 0,12-, 24- and 36-hours. For C) mantle samples were collected from control (C), drilled shell (SD-group) and a drilled shell and severed ganglia (CPG-group) mussels at 0 and 10-day after shell damage. Hierarchical clustering of gene expression profiles is represented. In B) and C) gene expression levels were normalized using the geometric mean of two reference genes (EF1α and 18S). For B) ganglia results are shown as the mean of three samples/group (each sample contained the CPG from 2 individuals) and for the mantle represents the mean of six (n = 6) biological replicates per group / sampling point. For C) the results are shown as the mean of eight animals per group/sampling point. Heatmaps were prepared in R-studio software and the normalized values are represented using a colour gradient, from downregulated (yellow) to upregulated (red).

decrease in enzyme activities (Figure 2.7A). This suggests that the activity of mantle cells producing the biomineralization enzymes is likely to be regulated by the nervous system. ALP activity did not change in any of the experimental groups (Figure 2.7A).

2.4.3.5 Neuropeptide gene expression during shell regeneration

To identify potential candidates for shell repair, we selected 10 neuropeptide mantle transcripts for gene expression analysis in the mantle and CPG ganglia during the first 36 hours after shell damage, which represents the initial stages of shell regeneration. Among these, the CALC precursors (CALCI and CALCII) were chosen due to their previously demonstrated potential involvement in shell production (Cardoso et al., 2020).

Expression data confirmed that all candidate precursors were expressed in both the mantle and CPG ganglia and that gene expression in both organs was modified after the shell was damaged (Figure 2.7B, Supplementary Figure 2.6). Expression of gene transcripts for APGW-amide, Myomodulin, LFRF-amide, FxRI-amide, LFRY-amide and LRNFV-amide peptide precursors was significantly increased in response to shell damage ($p < 0.05$) in both the mantle and CPG ganglia. In contrast, the AST-C gene was only significantly upregulated in the mantle ($p < 0.05$). Shell damage did not invoke a significant change in gene expression of CALC (CALCI and CALCII) or the CCK/SK precursors either in the mantle or the CPG ganglia (Figure 2.7B, Supplementary Figure 2.6).

Candidate gene expression in later stages of shell repair was examined in the mantle 10 days after approximately 60% of the drilled holes had been repaired (Figure 2.3). The results showed that the pattern of gene expression was altered in both the SD-group and CPG-group (Figure 2.7C). Six of the 10 candidate neuropeptide precursor genes had a coordinated expression pattern. In the SD-group transcript abundance of the CALCII, LFRY-amide, APWG-amide, Myomodulin, LFRF-amide and FxRI-amide peptide precursor genes was significantly increased ($p < 0.05$), but in the CPG-group expression of the same neuropeptide precursor genes was significantly downregulated ($p < 0.05$). This indicates that the cells expressing these neuropeptide precursors may be regulated by the CPG ganglia. Conversely, no alterations in gene expression were detected for CALCI, LRNFV-amide and CCK/SK peptide precursors in the CPG-group (Figure 2.7C). Expression of the AST-C precursor in the mantle

was significantly increased ($p < 0.05$) in the SD-group and CPG-group suggesting that cells expressing this neuropeptide gene are not under the regulation of the CPG ganglia. Overall, the results indicate that regulation of mantle cells expressing the neuropeptide precursor genes targeted in this study may be regulated by the CPG ganglia. These neuropeptides may be involved in shell growth and repair.

2.4.4 Effect of neuropeptides on shell regeneration and shell microstructure

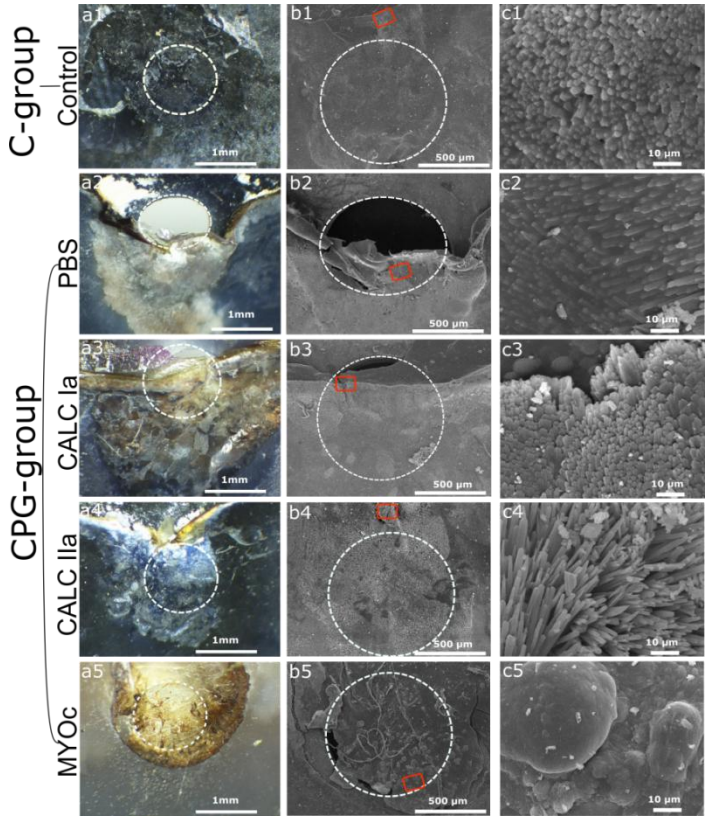

Figure 2.8: Effect of neuropeptide injections on regrowing shell microstructure. Bright field (a) and SEM (b and c) digital images of the inner side of the right valve showing the recovery of the newly grown shell 15 days post-drilling. Bright field images were captured using a stereoscope (Motic, SMZ-171, China) equipped with a digital camera (Visicam 6 Plus, VWR, Portugal). The position of the drilled hole in (a) and (b) is indicated by a dashed circle and the red box. (b) reveals the microstructure of regrown shell analysed by SEM and (c) presents the same shell regrowth region but at a higher magnification. The numbers indicated in the images identifies the different groups: 1) non-injected control, and the CPG-severed group includes 4 different experimental groups: 2) PBS injected, 3) CALCIa injected, 4) CALCIIa injected and 5) MYOc injected. The control group represents the reference group and reveals the normal process of shell repair after damaging the shell by drilling.

To identify the candidate peptides that might be directly involved in shell repair, mature peptides were injected into the adductor muscle of CPG-group animals with damaged shells. The rationale behind this was that by directly adding the peptide, it should be possible to rescue the severed CPG ganglia phenotype, which caused arrested shell repair.

The peptides that were tested included CALCIa, CALCIIa, MYOc and CCK/SK synthetic peptides. We chose CALCIa (encoded in the CALCI precursor) and CALCIIa (encoded in the CALCII precursor) because the precursors exhibited different gene expression profiles in response to shell damage (Figure 2.7C). We selected the MYOc peptide (encoded in the Myomodulin precursor) because its gene expression was similar to that of the CALCII precursor (Figure 2.7C). CCK/SK was used as a negative control since its gene expression was unrelated to shell repair (Figure 2.7C). All peptides except for CCK significantly increased ($p < 0.05$) the rate of shell repair when compared to the drilled CPG-group animals where no peptide was supplied (Supplementary Figure 2.7).

SEM photomicrographs of the inner side of the regenerated shells from the SD-group 15 days after drilling (when the hole was almost fully repaired, Supplementary Figure 8A), showed that it was composed of tightly packed needle-like aragonite, mineralized calcium carbonate prismatic crystals (Figure 2.8A). In the CPG-group that was injected with the CALCIa and CALCIIa mature peptides, SEM photomicrographs revealed the crystal structure of the newly grown shell was

similar to the SD-group. The number of crystals formed in the newly regenerated shell in the CALCIa injected group was like the control and was higher than in the CALCIIa group where the crystals seemed to be sparser resulting in a porous-like structure in the regenerated shell (Supplementary Figure 2.8B). Injections with the MYOc peptide promoted hole repair after 15 days (Supplementary Figure 2.8A) but the microstructure did not contain typical biomineralized prismatic crystals and was mostly organic tissue (Figure 2.8, Supplementary Figure 2.8B).

2.5. Discussion

Neuropeptides are signalling molecules and modulators of neuronal activity that regulate a diversity of physiological processes. Sequencing of bivalve nerve ganglia transcriptomes and genomes has identified a large variety of neuropeptide precursors, but their functions are poorly documented (Zhang et al., 2018; Kim et al., 2019b; Réalis-Doyelle et al., 2021). Neuropeptides that are homologues of those described in nerve ganglia of other bivalves were found in the mantle of *M. galloprovincialis* and associated with shell production and immunity (Cardoso et al., 2016, 2020, 2024; Li et al., 2021). Ganglia transcriptomes are not yet available for the mussel and the origin and potential regulation of the neuropeptide transcripts in mantle remains elusive. Here we demonstrate that neuropeptides and the nervous system innervating the mantle seem to be key factors regulating the mantle's function in shell production. The change in expression of neuropeptide genes in the mantle during shell repair or when it was impaired by damage to the CPG ganglia revealed an intriguing functional

link between the CPG ganglia and the shell secretory activity of the mantle. Of note was the capacity of peptides of the CALC neuropeptides (CALCIa and CALCIIa) and MYOc to rescue shell repair when it was inhibited by cutting the commissure between the CPG ganglia. Several other putative neuropeptides responsive to shell drilling or CPG ganglia damage were identified as potential candidates for regulation of shell production by the mantle. Even though the neuroendocrine cells and putative neurosecretory cells responsible for neuropeptide expression in the mantle were not identified, in this study the evidence obtained indicates that neuropeptide gene expression in the mantle was responsive to shell status and most likely involves the nervous system.

M. galloprovincialis mantle innervation and regulation

The mantle is a multifunctional tissue involved in activities such as sensing, secretion, immunity, movement and feeding (Morton, 1983; Beninger et al., 1999; Windoffer et al., 1999; Allam and Espinosa, 2016). However, the best-known function of the mantle is the production of the biomineralized shell, and the most active region is the mantle edge (Yonge, 1957, 1983). The mantle edge is composed of three folds with heterogeneous function, the inner and middle folds have sensory and contractile activities, and the outer fold secretes the shell. The outer fold is contiguous with the outer mantle epithelium, and transports ions, matrix proteins, chitin and carbohydrates that create the shell scaffold and biomineralization of calcium carbonate (Richardson et al., 1981; Addadi and Weiner, 1992; Morton and Peharda, 2008; Audino et al., 2015). Furthermore, mantle transcriptomes (Peng et al.,

2023) revealed that the highly active mantle edge in *M. galloprovincialis* expressed a diversity of neuropeptide transcripts that were homologues of those in oyster (*M. gigas*) and scallop (*M. yessoensis*) ganglia (Zhang et al., 2018; Réalis-Doyelle et al., 2021). Of the 48 neuropeptide gene families identified in the *M. galloprovincialis* genome only members of 3 gene families (Bursicon, GWE-amide and Neuropeptide prohormone 4) were not detected in mantle transcriptomes.

Although the nervous system in gastropods and cephalopods is relatively well characterised, it is much less studied in bivalves. In gastropods and cephalopods, the center nervous system (CNS) and the main components of their sensory system such as eyes (optical lobes) and tentacles are localized in the head region. In gastropods seven pairs of ganglia, that regulate different organs are concentrated in the head region, and in the cephalopods which is the invertebrate with the most complex nervous system, they have large and well-developed brains divided into lobes (Budelmann, 1995). In the bivalves a much simpler nervous system exists and is distributed throughout their body. Bivalves have no brain, and the nervous system consists of three pairs of symmetrical ganglia, the CPG, VG and PG, that project to, and innervate different parts of the body (Kotsyuba et al., 2020). The CPG innervates the labial palps, anterior adductor muscle and the anterior mantle and sensory organs, the VG innervates the gills, heart, posterior adductor muscle, siphons, and posterior mantle (Bullough, 1958; Galtsoff, 1964; Grizel, 2003; Beninger and Le Pennec, 2006; Gosling, 2015) and the PG regulates the muscular foot, that is involved in locomotion and digging (Ponder et al., 2019).

In the scallop (*P. yessoensis*), a bivalve, mapping by histochemistry of the nervous system revealed that the VG projects to and innervates the posterior region of the mantle margin (Matsutani and Nomura, 1984). Our immunofluorescence experiments revealed like in other bivalves the anterior and posterior mantle edge and inner mantle in *M. galloprovincialis* was highly innervated, particularly with FMRF an important biomarker of the nervous system in molluscs and other invertebrates (Saleuddin and Dillaman, 1976; Cottrell, 1993; Santama and Benjamin, 2000; Zatylny-Gaudin and Favrel, 2014). However, the results of the nerve sectioning experiment in the present study suggested that the CPG have a more pronounced role in regulating shell growth than the VG in *M. galloprovincialis*. Furthermore, the effect on shell growth of cutting the commissure of the CPG was not due to loss of mantle movement since the mantle crept forward and accompanied the repair of the drilled hole. Based on the results of the immunofluorescence with dense FMRF and 5-HT nerve clusters and the sectioning of the ganglia we propose a) that a mantle autonomous neurosecretory network exists and b) inputs from the CPG regulate shell secretion and repair.

A diversity of neuropeptide precursors in the mantle modulates shell production

Biomineralization is a biologically controlled process by which living organisms generate mineralized structures (Saleuddin and Wilbur, 2012). The evolution of processes that regulate shell production has been associated with the diversity, expansion and success of the molluscs, and chitin has been implicated in this process (Weiss et al., 2006, 2013; Weiss, 2012). In *M. galloprovincialis* with damaged shells

the highest rates of shell growth regrowth occurred within the first 5 days of damage and more than 60% of the hole in the shell valve was covered with biomineralized material. Using several different experimental approaches, we gathered evidence in the mussel that the ganglia is involved in the regulation of shell formation. Specifically, we identified neuropeptide precursors with a significantly modified gene expression from early stages of shell repair and these included APWG-amide, Myomodulin, LFRF-amide, FxRI-amide and LFRY-amide precursors that were previously described to regulate reproduction and growth in Mollusca (Lange et al. , 1998; Hoek et al., 2005; Bernay et al., 2006; Koene, 2010; Morishita et al., 2010). The two mussel CALC peptide precursors we previously linked to shell biomineralization, CALCIa and CALCIIa (Cardoso et al., 2020), rescued the shell secretory ability of *M. galloprovincialis* mantle in individuals with a cut CPG commissure. Furthermore, the injection of CALCIa, and CALCIIa promoted the formation of the tightly packed needle-like aragonite, mineralized calcium carbonate prismatic crystals characteristic of the nacreous layer (Kobayashi and Samata, 2006). In contrast, although MYOc promoted shell repair regular crystals were not formed, and an amorphous mass covered the hole. Further experiments will be required to better characterise the role in shell growth of the neuropeptides found in the bivalve mantle.

A large proportion of the predicted neuropeptide precursors (25 precursors out of 48) in the mantle encoded multiple mature peptides that based on their structure and the presence of conserved motifs are likely to be bioactive. Several of the candidate

neuropeptide precursors tested to assess if they modify shell production encoded multiple mature peptides with different sequences and for which a function has not yet been assigned in *M. galloprovincialis*. Our results and those of other studies, namely the demonstration that oyster CALC activates oyster CALCRs in vitro, the presence of CALC peptides in the VG and the abundant repertoire of neuropeptide transcripts in bivalve mantle transcriptomes (Schwartz et al., 2019) support our hypothesis that peptides are regulatory factors of shell production.

Calcitonin is a key biomineralization regulatory factor in *M. galloprovincialis*

The involvement of the CALCII precursor, which encodes the peptide CALCIIa that was previously associated with calcium mobilization in the mussel mantle was confirmed (Cardoso et al., 2020), since it was highly up regulated in the mantle during shell repair, which suggests that it may act as local regulator. Severing the commissure between the CPG ganglia caused a change in the expression of several candidate neuropeptide precursor genes in the mantle edge and biomineralization enzyme activity was inhibited. We showed that the administration of the neuropeptides CALCIa, CALCIIa and MYOc rescued the arrested shell repair phenotype and restored shell growth. However, although the shell growth stimulated by CALCIa and CALCIIa had a similar morphological and structural appearance to the control (tightly packed calcium carbonate prismatic crystals), the shell in the MYOc stimulated repair was non-crystalline and seemed to correspond to organic matrix. We previously demonstrated that the calcitonin system can modify biomineralization enzymes and calcium movements in mantle epithelial cells

(Cardoso et al., 2020) and in the present study we demonstrated an intact nervous connection with the ganglia is required for shell secretion.

Neuropeptide receptors of the GPCR family, that shared conserved sequence and structure with the vertebrates and other invertebrates GPCRs, have been described in bivalves and other molluscs (Jékely, 2013; Mirabeau and Joly, 2013; Elphick et al., 2018; Cardoso et al., 2024), but few have been functionally characterized. In bivalves CALCRs have been deorphanized in *M. gigas* and *M. galloprovincialis* and they are expressed in the mantle (Schwartz et al., 2019; Cardoso et al., 2020). In *M. gigas* two CALC (Cragi-CT1b and Cragi-CT2b) orthologues of the mussel CALCIb and CALCIIb peptides (which we did not study) activated two cognate GPCRs (Cg-CT-R and Cragi-CTR2) in *M. gigas* (Schwartz et al., 2019). However, the peptides Cragi-CT1a and Cragi-CT2dp, which are orthologues of the *M. galloprovincialis* peptides we studied (CALCIa and CALCIIa) did not activate these receptors, suggesting that CALC peptides that are encoded within the same precursor may have different biological roles. In *M. galloprovincialis* six CALCRs have been described and a receptor for CALCIIa peptide was deorphanized and receptor gene expression is sensitive to changes in salinity of the environmental water (Cardoso et al., 2020). Receptors for AST-C (Díaz et al., 2019; Jiang et al., 2022) , CCK (Janssen et al., 2008; Yu and Smagghe, 2014; Schwartz et al., 2018), LFRF-amide peptides (Yoon et al., 2022), myomodulin peptides (Bigot et al., 2014), FxRI-amide (Pedder et al., 2001) have been identified in Mollusca but few have been deorphanized and characterized in bivalves. In summary, neuropeptides are well represented in the

mantle and nervous system of the mussel and most likely other bivalves and through their action via specific receptors in the mantle cells regulate shell production.

2.6. Conclusion

Shell production and biomineralization is a complex mechanism and its regulation is largely unknown. Here we provide functional evidence that neuropeptides play an important regulatory role in shell growth in bivalves. We found that in the bivalve *M. galloprovincialis* the mantle was a highly innervated organ with neuropeptide secreting fibers which are likely involved in shell production. Analysis of publicly available mantle transcriptomes revealed a high proportion of neuropeptides encoded in the genome of a diversity of bivalves were expressed and encoded for multiple mature peptides in the mantle of *M. galloprovincialis*. Furthermore, the gene expression of some neuropeptide precursors in the mantle changed during shell production and when the CPG commissure was severed suggesting these processes are linked. We identified a putative regulatory link between nerve ganglia and mantle neuropeptide gene expression and mantle biomineralized enzyme activity. In mussels with arrested shell growth caused by severing the CPG ganglia (but not VG) the arrested phenotype could be rescued by injection of neuropeptides into the adductor muscle. The present results confirm previous studies proposing that the CALC peptide system is a key regulatory system in mussel shell growth since in mussels with a damaged shell, CALCIa and CALCIIa induced the formation of shell with a similar crystalline structure to intact shells. The

peptide, Myomodulin, contributed to repair of the damaged shell but not crystals formed and instead an amorphous mass was produced in *M. galloprovincialis*. Overall, we provide strong evidence that neuropeptides and the nervous system regulate mantle function and shell growth in *M. galloprovincialis* and most likely other bivalves.

2.7. Supplementary materials

All the supplementary materials are provided in the Annex I in digital format.

CHAPTER 3

Nervous regulation of shell biomineralization uncovered in the Mediterranean mussel (*Mytilus galloprovincialis*)

Nervous regulation of shell biomineralization uncovered in the Mediterranean mussel (*Mytilus galloprovincialis*)

Manuscript in preparation (submission 2024)

Acknowledgements

This study received Portuguese national funds from FCT - Foundation for Science and Technology through institutional projects UIDB/04326/2020, UIDP/04326/2020 and LA/P/0101/2020, and from the operational programmes CRESC Algarve 2020 and COMPETE 2020 through the projects EMBRC.PT ALG-01-0145-FEDER-022121 and BIODATA.PT ALG-01-0145-FEDER-022231 and from the FCT-funded project FCT-AGAKHAN/ 541666287/2019HealthyBi4 Namibe. ZL was supported by a PhD scholarship from the China Scholarship Council. MP was supported by a PhD scholarship from Shanghai Ocean University (China).

Nervous regulation of shell biomineralization uncovered in the Mediterranean mussel (*Mytilus galloprovincialis*)

Zhi Li[1], Maoxiao Peng[1], João CR Cardoso[1*] and Deborah M Power[1,2,3*]

[1]Comparative Endocrinology and Integrative Biology, Centre of Marine Sciences, Universidade do Algarve, Campus de Gambelas, 8005-139 Faro, Portugal

[2]International Research Center for Marine Biosciences, Ministry of Science and Technology, Shanghai Ocean University, Shanghai, China

[3]Key Laboratory of Exploration and Utilization of Aquatic Genetic Resources, Ministry of Education, Shanghai Ocean University, Shanghai, China

3.1. Abstract

Biomineralization in marine bivalves is regulated by multiple mechanisms, but the involvement of the nervous system has not been reported. In this study, we used the symmetrical Mediterranean mussel *Mytilus galloprovincialis* to determine if the cerebropleural ganglia (CPG) is involved in the regulation of biomineralization. Analysis of the right and left mantle transcriptomes in *M. galloprovincialis* revealed gene expression differed and was not symmetric, and that disruption of the CPG commissure significantly modified the abundance and number of biomineralization-related DEGs. Filtering and comparison of genes using DNASeq2 and WGCNA identified 81 significantly regulated target genes modified when the CPG was severed including many long non-coding RNA. Notably, the DE genes identified did not belong to previously established members of the shell biomineralization toolbox and the high number of lncRNAs suggests they play a key role in the regulation of shell biomineralization. We propose that the circumpallial nerve innervating the mantle receives inputs from the CPG and that this coordinates and integrates across bivalves shell production by the right and left mantle.

Keywords: bivalve, cerebroplural ganglia, lncRNA, mantle transcriptome, regulation, shell biomineralization

3.2. Introduction

Bivalves belong to the phylum Mollusca, the second-largest animal phylum after insects (Wanninger and Wollesen, 2019), they are one of the most diverse branches of molluscs and display an exuberant diversity of shapes, colours, sizes and habitats. They are characterized by the presence of two calcareous valves (a.k.a. the shell), a feature that is proposed to have contributed to their notable evolutionary success and widespread distribution (Raible et al., 2005; Ponder et al., 2019). The presence of two mineralized valves (a.k.a. shells) that enclose and protect the soft body is a core anatomical structure used to classify bivalves. The mantle, which covers and creates an interface between the shell and the soft body is the primary shell-forming organ in both juvenile and adult bivalves (Clark et al., 2010; Marin et al., 2012; Suzuki and Nagasawa, 2013). Shell growth depends on the secretory activity of the mantle and the biomineralization toolbox includes enzymes, ion transport proteins, and shell matrix proteins (SMP) (Clark et al., 2020). The shell in bivalves is composed of calcium carbonate ($CaCO_3$) crystals, that account for approximately 95% of the total shell weight. Although the mechanisms and dynamics of shell formation remain enigmatic, molecular data from shell and mantle proteomes as well as mantle transcriptomes have uncovered candidate proteins and regulatory factors involved in shell construction and turnover (Marie et al., 2012; Bjärnmark et al., 2016; Clark et al., 2020).

Bivalve resilience across time is clear when considering that the earliest fossil records of bivalves' date back to at least the early Cambrian period, 530 million years

ago (Ponder et al., 2019). In the past 500 million years, the Earth experienced two ocean acidification events, accompanied by complex changes in atmospheric and ocean geochemistry, including two glacial periods (Kump et al., 2009; Zeebe, 2012). Despite these profound environmental changes, the bivalves evolved and persisted, and their fossilized shells provide a record across time of climate change (Aucour et al., 2003; Yan et al., 2014). The utility of fossilized shells to gain insight into the Earth's carbon cycle (Munari et al., 2013) is linked to the fact that when atmospheric carbon dioxide (CO_2) dissolves in the ocean it combines with calcium ions to form $CaCO_3$ the most abundant chemical found in the calcareous shell of bivalves (Caron and Jackson, 2008).

The process by which living organisms generate hard calcified structures is called biomineralization and is one of the most fascinating processes in the animal kingdom. Mineralized skeletons composed of $CaCO_3$ can be traced back to the late Proterozoic era (Knoll, 2003) and have been attributed to the evolutionary success of the phylum Mollusca (Marin et al., 2012; Bieler et al., 2014). In mussels (*Mytilus*) the shell is composed primarily of $CaCO_3$ which is present in two main crystalline polymorphic forms: the nacreous layer (aragonite platelets) and the prismatic layer (calcite prisms) (Uozumi and Suzuki, 1979; Marin et al., 2007; Checa, 2018). The anatomical and functional organization of the mantle into multiple folds at its outer limit seems to be linked to the formation of the $CaCO_3$ crystals found in the shell (Salas et al., 2022). The outer mantle fold is involved in the formation of calcite and aragonite, and the inner mantle fold is responsible for the formation of the aragonite shell layer (Owen

et al., 1953; Kadar et al., 2009). The periostracum (inner epithelial cells of the outer mantle fold) is the surface on which calcium carbonate is deposited (Beedham, 1958; Beedham and Trueman, 1968). Although the core genes, proteins and structural domains/motifs of the shell biomineralization toolbox are conserved in bivalves, the rich variety of shell shapes and colors is considered a highly species-specific outcome of the exploitation of SMPs (Peck et al., 2015; Clark, 2020). Emerging evidence has revealed that long noncoding RNA (lncRNAs) are involved in the local modulation of shell biomineralization in molluscs (Cai et al., 2022; Zheng et al., 2023). However, if there are regulatory processes that coordinate shell biomineralization at an organismal level is unclear. Although the recent identification of neuropeptides and their putative G protein-coupled receptors (GPCRs) in the mantle edge, suggests they may be regulatory factors that coordinate mantle function (Cardoso et al., 2016, 2020).

The endocrine regulation in organisms with an open circulatory system, such as invertebrates, involves the neuroendocrine system that delivers neuropeptides and proteins via the nervous system directly to their site of action. In adult bivalves the central nervous system (CNS) consists of paired cerebroplural (CPG), visceral (VG), and pedal (PG) ganglia (Stefano and Aiello, 1975; Stefano et al., 1976; Meechonkit et al., 2010). The VG are usually fused and connected to the CPG via longitudinal lateral cords. These neural structures innervate most of the visceral organs. The PG innervates the foot and is connected to the CPG via the ventral (pedal) cords (Bullock and Horridge, 1965; Wanninger, 2015). Accordingly, the nervous system of adult bivalves is tetraneural, consisting of two prominent pairs of longitudinal neurite

bundles (cords) ganglionated to varying extents (Siniscalchi et al., 2004; Meechonkit et al., 2010; Schmidt-Rhaesa et al., 2015; Wanninger, 2015). In the previous chapter, we revealed that the mantle has abundant neural fibers and neural cell networks. Additionally, when the commissure of the CPG nerve ganglia was severed, this significantly modified the expression of neuropeptide genes and reduced the activity of enzymes involved in biomineralization (Li et al., 2021). Evidence was provided suggesting that neuropeptides play a role in the modulation of shell growth, although the coupling of molecules, pathways and processes to regulate shell growth was not directly demonstrated.

The objective of the present study was to evaluate how nervous innervation of the mantle modulates its function in shell growth and biomineralization by analyzing transcriptomes of the left and right mantle of the bilaterally symmetrical Mediterranean mussel (*M. galloprovincialis*). Three experimental treatments were established: unmanipulated mussels, mussels with a sanded shell, and mussels with a severed CPG commissure and a sanded shell, and transcriptomes from the right and left mantle were generated. A 24-hour time frame was selected for the experiments so that the immediate response of the mantle to shell sanding and CPG ganglia damage could be evaluated. Global gene transcription patterns were observed and analyzed to evaluate the status of gene expression in the mantle. The identification of a novel regulatory loop between the nerve ganglia and the mantle provides evidence about how bivalves coordinate and integrate regulation of the mantle to generate and maintain symmetrical shell growth.

3.3. Materials and methods

3.3.1. Animal experimentation and sampling

Adult Mediterranean mussels (*M. galloprovincialis*) (5.05 ± 0.32 cm long, 8.31 ± 1.34 g wet weight) were collected from the Ria Formosa, Portugal (37°00'32"N, 7°59'40"W, ICNF license 327 / 2022 / CAPT). The animals were transported live to the Aquatic Organisms Experimental Laboratory at the Center for Marine Sciences (CCMAR). Prior to the experiment, they were acclimated for one week in 5-liter plastic aquariums containing 4 liters of aerated seawater (salinity 37 ppt, pH = 8.1 ± 0.1). The experiments were conducted in January under normal light and temperature conditions for the Algarve, Portugal (13 - 17°C) in an open circuit system. No mortality occurred during acclimation or the experimental period.

To collect tissue samples, the animals were placed on ice, and the adductor muscle was cut with a sterile scalpel blade to allow both valves to open. Samples from the posterior mantle edge (referred to as the mantle from this point onwards, Figure 3.1) of both the control and experimental animals were collected, flash-frozen in dry ice, and stored at - 80°C until analysis. The number of biological replicates used in experiments is indicated in the next section.

3.3.2. Challenge experiments, shell sanding and CPG sectioning

To assess the influence of the CPG ganglia in mussels on target gene expression in the mantle, three experimental groups (n = 6 animals / group) were established: 1) intact shells (control-C), 2) sanded shell (T) to stimulate shell regrowth, and 3) severed CPG commissure and sanded shell (CPG). Shells were thinned by mechanical

sanding of the external surface at the edge of both the right and left valve. After manipulation the mussels in the experiment were maintained in an open seawater circuit for 24 hours using the conditions described in 3.3.1. No mortality was observed during the experiment (Figure 3.1).

3.3.3. RNA extraction and RNA-Seq library

The mantle of the left (ML) and right (MR) valves of adult *M. galloprovincialis* (n = 6 samples / group / shell side) from control and the treatment groups were collected, and total RNA (tRNA) was extracted for RNA-seq library construction. Prior to RNA extraction, the heavily pigmented connective tissue at the edge of the

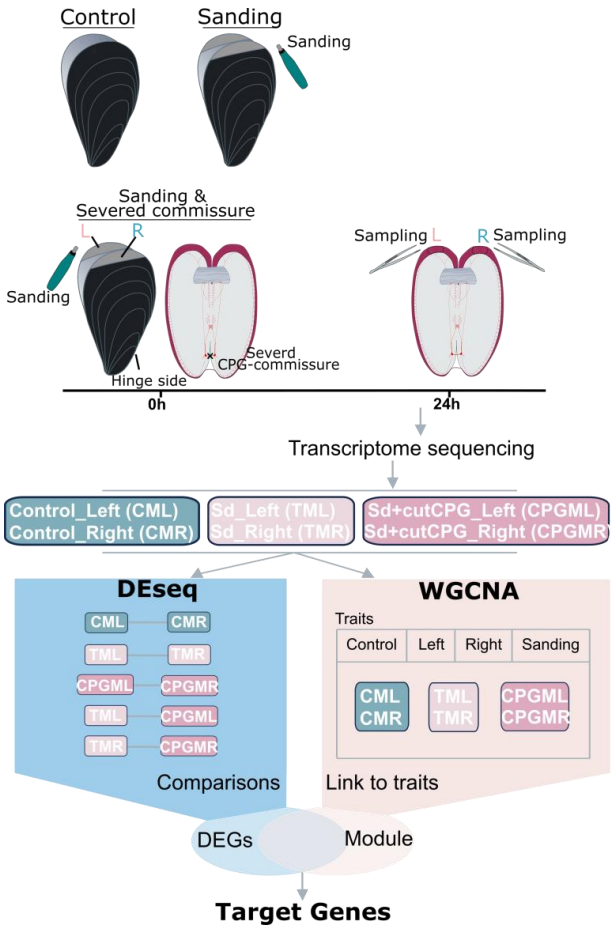

Figure 3.1. Workflow of the strategy to screen target DEGs in the mantle of control mussels, mussels with a sanded shell and a sanded shell and severed CPG commissure. In all experiments, the edge of the left and right valves were sanded using a handheld electric drill. In the cerebropleural ganglia (CPG) severing experiments, the CPG commissure was severed with fine dissection scissors after the valves were sanded. Samples from the edge of the left and right mantles were collected 24 hours after treatment for transcriptome sequencing from control (control mantle right, CMR and control mantel left, CML) and the experimental groups, shell sanded (shell sanded right mantle, TMR and shell sanded left mantle, TML) and shell sanded+severed CPG commissure (right shell sanded and severed CPG, CPGMR and left shell sanded and severed CPG, CPGML). The sample raw data were analyzed in DEseq and WGCNA analysis in parallel. After identifying the shell-sanded related gene module, target genes were filtered by comparing the genes identified in the most strongly supported module and genes identified by DEseq. Different colored boxes represent different groups: blue boxes for control - C (right CM and left CR), pink boxes for shell sanded - TM (right TMR and left TML), and light pink boxes for shell sanded + severed CPG commissure - CPGM (right CPGMR and left CPGML).

mussel mantle was carefully peeled off using a surgical blade, since melanin and other pigments interfere with the quality of the extracted RNA. Total RNA (tRNA) was extracted using an ENZA kit (VWR, USA). For tRNA extraction, the mantle tissues from control (n = 6 samples) and the experimental groups (n = 6 samples /group) were thawed on ice in lysis buffer and homogenized for 3 minutes at room temperature using a bead beater with two iron beads (5 mm). DNase treatment was performed after tRNA was isolated using a Precision DNase kit (Primer design, UK) to remove any contaminating genomic DNA following the manufacturer's protocol. The concentration and quality of the extracted tRNA were assessed using a NanoDrop (Thermo Scientific, USA) and measuring the absorbance at 280 nm, 260 nm and 230 nm and by agarose gel (1%) electrophoresis.

The samples used for RNA-seq library construction consisted of pools of tRNA (2 μg) from two (2) individuals/experimental groups (1 μg total RNA / animal), with three (3) replicates for library preparation per treatment group and for the right (RM) and left mantle (LM). Library preparation and sequencing were performed by

Novogene Europe. Prior to library generation, sample tRNA integrity was assessed using an RNA Nano 6000 Assay Kit on a Bioanalyzer 2100 system (Agilent Technologies, CA, USA), and only samples passing a pre-set RNA integrity value threshold (RIN > 8.0) were evaluated. Sequencing was conducted using an Illumina NovaSeq 6000 platform, generating 150-base pair end reads.

3.3.4. Transcriptome quality control, genome mapping and transcript counts

The transcriptome of the mantle was analyzed in Galaxy (https://usegalaxy.eu/) and annotated in R-studio. FastQC (http://www.bioinformatics.babraham.ac.uk /projects/fastqc) and FastP (https://github.com/OpenGene/fastp) programs were used to assess the quality of the raw reads of the sequencing library, with quality assessment showing "no contaminants or adapters". The Trimmomatic tool (Bolger et al., 2014) was employed to remove low-quality reads (short reads and unpaired reads). The "paired-end reads" option was selected to join the forward and reverse reads of each individual sample. The mantle transcriptome reads were mapped to the reference genome (NCBI accession number: GCA_900618805.1) using data from the NCBI database (https://www.ncbi.nlm.nih.gov) and Hisat2 (Kim et al., 2019a) using the default parameters. The StringTie tool (Pertea et al., 2015) was applied to assemble and quantify transcripts from the BAM files provided by Hisat2. Gene expression was calculated using FPKM values.

3.3.5. Identification and analysis of differentially expressed genes (DEGs)

The DESeq2 package (Love et al., 2014) in R Studio was used to calculate

differentially expressed genes (DEGs) based on the total counts of each library. The P-values were adjusted using q-values (Storey and Tibshirani, 2003), and a threshold q-value of < 0.05 and a log2 (fold change) > 1 was set to identify genes with significant differential expression. Two analysis approaches were established to attain the defined objectives: i) comparison of the left and right mantle transcriptomes of the right versus the left mantle in control mussel (CML_vs_CMR), the right and left mantle transcriptome in mussels with sanded shells (TML_vs_TMR), and the left versus the right mantle transcriptomes of mussels with a sanded shell and cut CP ganglia (CPGML_vs_CPGMR). The comparisons were to determine the gene composition of the left and right mantle transcriptomes and the impact on mantle gene expression of shell repair and severing the CPG commissure; ii) comparison of gene expression between the left and right mantle of shell sanded mussels or shell sanded mussels with a severed CPG commissure (TML_vs_CPGML and TMR_vs_CPGMR). To determine which DEGs identified in the two comparisons (i and ii) were common, the DEGs obtained were compared and common genes identified. To establish the similarity between the global transcriptome of the left and right mantle samples during preliminary exploratory data analysis, principal component analysis (PCA) was conducted using the psych, reshape2, factoextra, and ggplot2 packages (Revelle, 2011; Wickham, 2016; Kassambara, 2017).

3.3.6. Weighted gene co-expression network analysis (WGCNA) to identify shell sanded modules

WGCNA is a systems biology method that explores the relationship between

genes and associated traits by identifying co-expression modules and hub genes within a network. WGCNA uses a soft thresholding power (β) approach to assess the similarity of gene expression profiles, which avoids the limitations of arbitrarily setting correlation coefficients. In this study, the parameters for module identification were set as follows: the soft thresholding power (β) was set to 6, the minimum number of genes per module was set to 30, and the minimum correlation coefficient between module members and the eigengene was 0.3. Modules below a certain distance threshold were merged, using a merging threshold set to 0.45.

3.3.7. Target gene selection and functional annotation

To understand the regulatory relationship between the shell sanded and severed CPG commissure, a comparative analysis of the DEGs (TMR_vs_CPGMR and TML_vs_CPGML) identified using DESeq2 and gene module correlation with shell sanded using WGCNA was established. The DEGs obtained were filtered using the gene annotation assigned and genes involved in shell biomineralization, and genes related to the nervous system/neural tissue were identified. The expression levels of DEGs in each of the mantle regions were represented as heat maps. To verify the similarities between the DEGs obtained for the experimental group comparisons, preliminary exploratory data analysis using PCA was performed in the psych, reshape2, factoextra, and ggplot2 package.

DE coding (DEc) transcripts were annotated using blastp against NCBI (nr) and Swiss-Prot databases, respectively. DE non-coding (DEnc) transcripts were annotated by mapping against the genome, and by confirming them using blastx against

Swiss-Prot databases and CPC2 lncRNA prediction tool (https://cpc2.gao-lab.org/). DEc in *M. galloprovincialis* were annotated for subcellular localization using: 1) SignalP 5.0 (http://www.cbs.dtu.dk/services/SignalP/) for detection of the signal peptide, 2) TMHMM v.2.0 (http://www.cbs.dtu.dk/services/TMHMM/) for detection of transmembrane domains and 3) DeepLoc v2.0 (http://www.cbs.dtu.dk/services/DeepLoc/) for prediction of the subcellular localization. The identification of target neuropeptide genes in the DEGs was obtained by interrogating them with the genes identified and reported in Chapter II of the thesis. Protein domains were identified using Pfam (ver 34.0) (https://pfam.xfam.org/) and 7tm domain containing protein coding genes were considered as GPCR. The deduced putative extracellular and molluscan shell matrix proteins (SMPs, https://data.bas.ac.uk/full-record.php?id=GB/NERC/BAS/PDC/01132) annotated in the DEc obtained were used to search the Pfam database (https://pfam.xfam.org) so that DE mantle genes encoding shell specific protein domains could be identified. To identify DEGs encoding membrane transporter proteins, searches were performed against the Transporter Classification Database (TCDB, https://tcdb.org/) using BLASTp. Deduced proteins of DE mantle genes expressed in the Nucleus were identified by searching against the Animal Transcription Factor database (AnimalTFDB3.0, http://bioinfo.life.hust.edu.cn/AnimalTFDB/) and putative transcription factors were verified using the Transcription Factor Prediction tool with the default parameters.

3.3.8. Detection of potential cis-regulatory modules related to shell formation and CPG regulation

At the chromosome level of the *M. galloprovinciallis* genome (NCBI accession number: GCA_037788925.1 (MytGallo_primary_0.1), mantle protein-coding and non-coding DEGs were mapped. The 14 chromosomes of *M. galloprovinciallis* were visualized using the advanced Circos program (version 1.0986) in TBtools (Chen et al., 2020) and mapped using the chromoMap package (version 0.3) in R-studio (Anand and Rodriguez Lopez, 2019). DEGs located upstream or downstream of DEnc genes within 100 kb were selected as candidate cis-regulatory genes. Detailed mapping of the candidate cis-regulatory modules (DEnc-DEc genes) was performed using the gggenes package (version 0.4.1) in R-studio (Wilkins, 2019).

3.3.9. Statistical analysis

The statistical tests for transcriptome analysis are indicated in the respective sections of the MS.

3.4. Results

3.4.1 RNA-seq analysis

The raw RNA-Seq data for 18 samples across 6 groups (Figure 3.1) using the Illumina system produced transcriptomes with an average of 40 to 50 million clean paired-end reads (Supplementary Table 3.1). The Q20 of clean reads for the samples was greater than 96%, Q30 was greater than 90%, and the GC content ranged from 35% to 42%, which is similar to the GC content of the genome. The clean reads were

mapped to the reference genome using HISAT2, and the number of reads mapped for each sample exceeded 76%, and unique mapped reads ranged between 42% to 54 % (Supplementary Table 3.1).

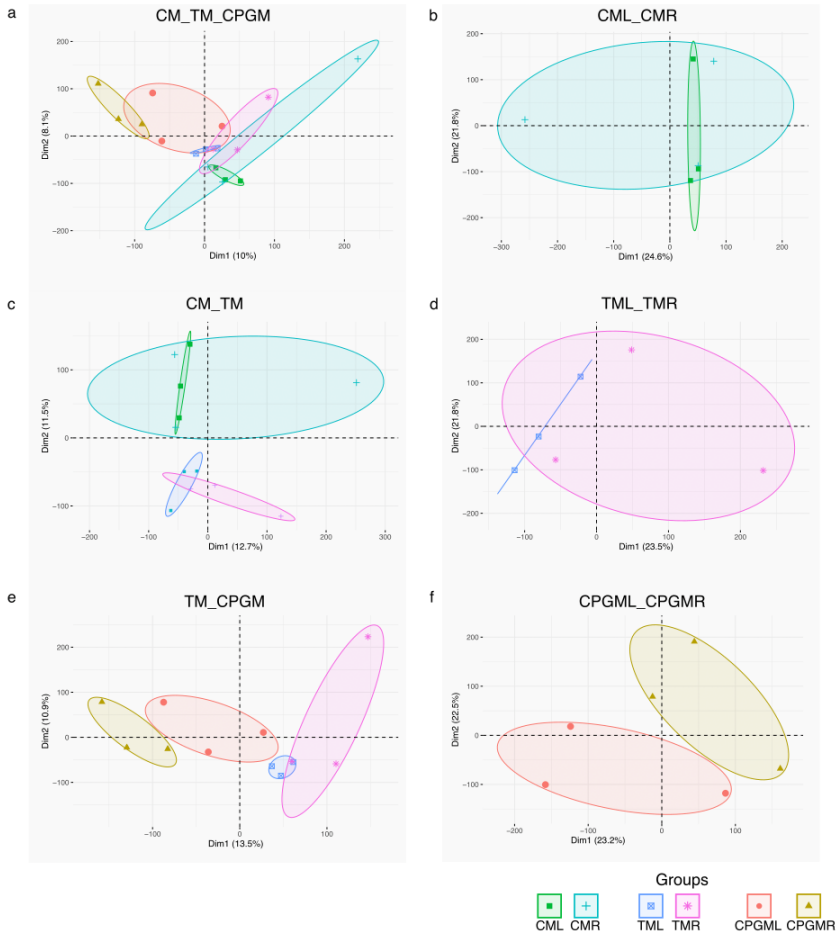

Figure 3.2. PCA plots of the global gene transcriptome of the mantle. a) PCA plot of all mantle samples used in this study. b) PCA plot of all samples from the C group mantle. c) PCA plot of all samples from the C group and T group. d) PCA plot of all samples from the T group. e) PCA plot of all samples from the T group and CPG group. f) PCA plot of all samples from the CPG group. Different colors and symbols represent different conditions, and each ellipse represents the 0.95 confidence interval for condition. C - control group, T - shell sanding group, CPG - shell sanding + severed CPG commissure group.

PCA of the global mantle transcriptomes for each treatment group revealed that within the 0.95 confidence interval with the exception of the CPGMR group the other five groups partially overlapped (Figure 3.2A). Comparison of the three treatment groups, CML, TML, and CPGML revealed they partially overlapped with each other

(Figure 3.2B). However, for the right mantle edge, TMR and CMR partially overlapped, and CPGMR clustered independently (Figure 3.2C).

3.4.2 DEGs Associated with shell formation in M. galloprovinciallis

The DEG analysis using DESeq2 with a threshold of log2 fold change > 1 and P < 0.05 identified a different number of DE genes for treatment group comparisons (Supplementary Table 3.2). In the analysis of the control mantle, CML vs CMR, 45 DEGs were identified, and 13 and 32 were up regulated in the left and right mantle, respectively. In the shell sanded mantle, TML vs TMR, 86 DEGs were identified, and 33 and 53 were upregulated in the left and right mantle, respectively. In the mantle transcriptomes of animals in which the CPG ganglia commissure was severed (CPGML vs CPGMR), there were 106 DEGs of which 63 were more abundant in the left mantle and 45 were more abundant in the right mantle (Figure 3.3A). Comparing the DEGs identified in the left and right mantle across the three treatment groups (VENN diagram) to understand the response of genes on the left and right sides of the mantle to shell sanding and severing of the CPG commissure revealed very little overlap. The non-coincident DEGs indicated that the challenges elicited a significantly different response in the left and right mussel mantle (Figure 3.3B). In the control group (C), there were 44 different DEGs between the left and right sides of the mantle. The shell sanded group (T) had 83 specific DEGs in the mantle between the left and right sides, while the left and right mantle of mussels with a sanded shell and severed CPG commissure (CPG) had 104 different DEGs.

LncRNA and protein-coding genes accounted for 20.44% and 79.55% of the DEGs in CML_vs_CMR, respectively, with protein-coding genes most abundant in the left mantle. In TML_vs_TMR, lncRNA and protein-coding genes accounted for 27.91% and 72.09% of DEGs, respectively, and protein-coding genes were most abundant in the right mantle. In the mussel group with a severed CPG ganglia commissure, lncRNA and protein-coding genes accounted for 26.17% and 73.83% of DEGs, respectively, and protein-coding genes were more abundant in the left mantle (Figure 3.3C).

To investigate the specific response of the mantle when the ganglia commissure was severed, DEG analysis was performed separately on the left and right valve of the mantle in the two treatment groups. The results showed that in the left valve comparison of TML vs CPGML there were 267 DEGs, of which 99 were upregulated (severed CPG abundance) and 168 downregulated (T abundance) (Figure 3.4A). In contrast, in the comparison of the mantle transcriptomes of the right valve, TMR vs CPGMR, the number of DEGs was almost twice that of the left valve, with 552 DEGs identified, of which 259 were upregulated (severed CPG abundance) and 293 were downregulated (T abundance) (Figure 3.4A).

A comparison of the DEGs identified in the analysis of the left and right valve in the T group and CPG group (Venn diagram), identified 41 common genes (Figure 3.4B). Comparison of shell sanded with and without CPG sectioning identified 226 DEGs that were specific to the left mantle of the CPG group and 511 DEGs specific to the mantle of the CPG group. In TML_vs_CGML, lncRNAs and protein-coding

genes accounted for 43.34% and 56.66% of DEGs, respectively, and in the CPG sectioning 11.02% were lncRNAs and 25.85% were protein-coding. In the right mantle transcriptomes, the comparison of TMR_vs_CPGMR, revealed lncRNAs and protein-coding genes accounted for 40.88% and 59.12% of DEGs, respectively, with CPG sectioning abundant 19.16% lncRNAs and 27.91% protein-coding.

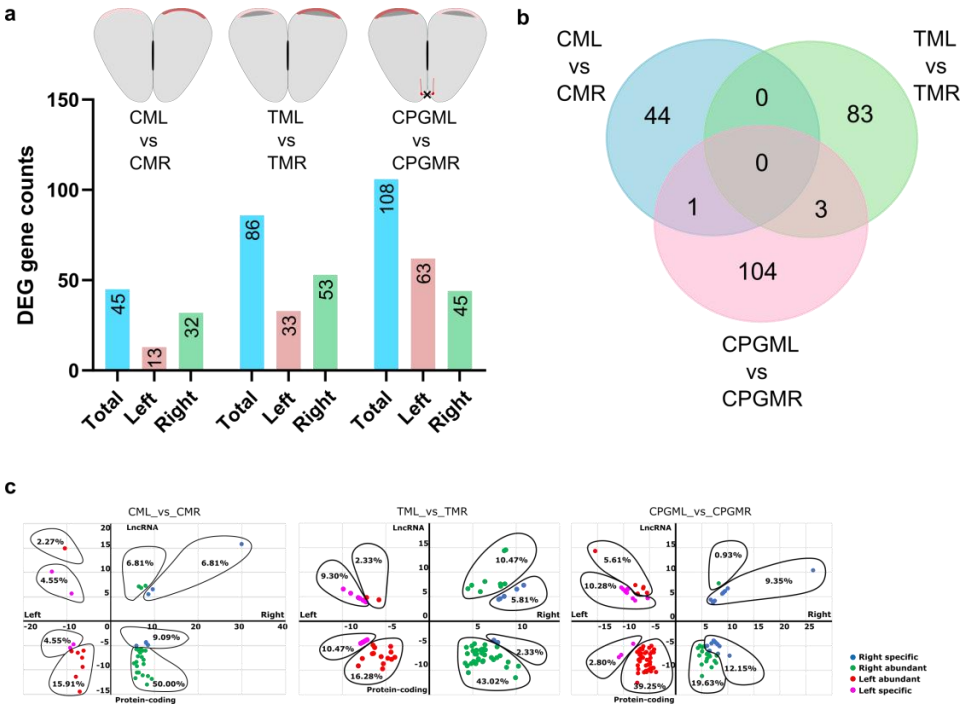

Figure 3.3. DEseq2 analysis of the left and right mantle transcriptome of *M. galloprovincialis*. a) Bar plot of DEGs in the *M. galloprovincialis* left and right mantles for each experimental group. Blue, red and green indicate the total number of genes and the genes most abundant in the left and right mantle, respectively. The schematic diagram in the upper panel shows the differences in the expression abundance of DEGs in the left and right mantles under the three conditions (control, shell sanding, shell sanded+severed CPG commissure). The dark gray area indicates the location of shell sanded, and the red area indicates the edge of the mantle. The darker the red, the higher the abundance of DEGs. b) Venn plot shows the overlapping DEGs between CML vs CMR, TML vs TMR, and CPGML vs CPGMR. c) Distribution and expression of DEGs in the left and right mantle for each experimental group. The chart shows the DEGs in each valve of the mantle (Left and Right) and the proportion that are protein-coding or lncRNA. The X-axis represents the significant changes in DEGs (log2 fold change) in each valve (Left and Right) of the mantle, and the Y-axis represents their abundance and distribution (log2 base mean). Dots represent identified DEGs and are color-coded based on their abundance in the mantle: blue represent right specific genes and green represent highly abundant genes in the right valve; pink represent left specific genes and red represent highly abundant genes in the left mantle. Percentage values indicate the proportion of DEGs

in each comparison. C - control group, T - shell sanding group, CPG - severed CPG commissure group + shell sanding.

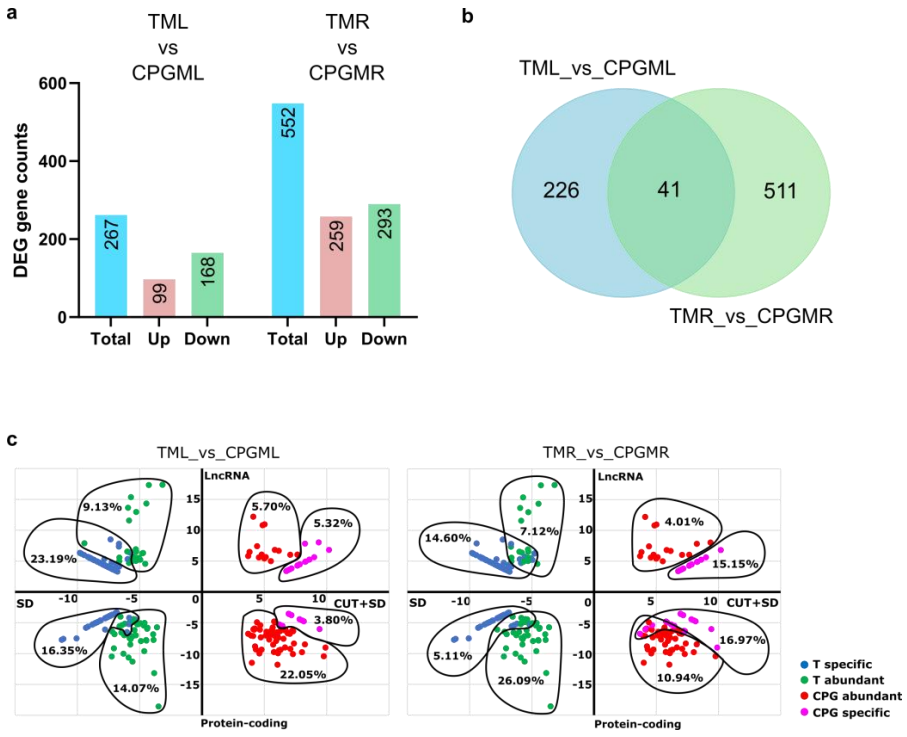

Figure 3.4. Severed CPG commissure related DEseq2 analysis. a) Bar plot of DEGs in the left and right mantles that are specific to severing the CPG. Blue and red indicate the total number of genes that are upregulated (T abundance), and downregulated (severed CPG commissure abundance), respectively. b) Venn plot showing the overlapping DEGs between TML vs CPGML and TMR vs CPGMR. c) Distribution and expression of DEGs in the T and CPG group mantle. The X-axis represents the significant change in mantle DEGs (log2 fold change) between the sanded and sanded+severed CPG commissure (T and CPG group), and the Y-axis represents DEG gene types by log2 base mean that positive values in lncRNA and negative values in protein coding gene. Dots are color-coded based on their abundance in the mantle: blue (T specificity) and green (G abundance), pink (severed CPG commissure specificity) and red (severed CPG commissure abundance). Percentage values indicate the proportion of DEGs in each comparison. TML/R- shell sanded left/right, CPGML/R - severed CPG commissure +shell sanded left/right.

3.4.3 WGCNA identifies target modules correlated with shell formation

To further explore the relationship between the challenge response (trait) and genes, genes with FPKM (reads per kilobase of exon per million reads mapped) expression levels less than 1 were filtered out, and the remaining genes were used for WGCNA analysis. A gene cluster tree was constructed with 13 stable expression

modules (Figure 3.5A, Supplementary Table 3.2). To identify modules related to the shell sanded condition (shell formation), a module-trait relationship analysis was conducted (Figure 3.5B). The brown module was significantly ($p < 0.05$) and positively correlated (co-efficient 0.72) with the shell sanded treatment. No significant correlations were detected for other treatments and groups. A total of 4961 genes were obtained in the brown module. Comparing the expression profile of the control and shell sanded groups in the module, a partial overlap in genes existed between CML and CMR and TML and TMR (Figure 3.5C). Comparison of the results for the left mantle only, or the right mantle only, revealed there were no common genes between each of the comparisons CML and TML and CMR and TMR (Figure 3.5C).

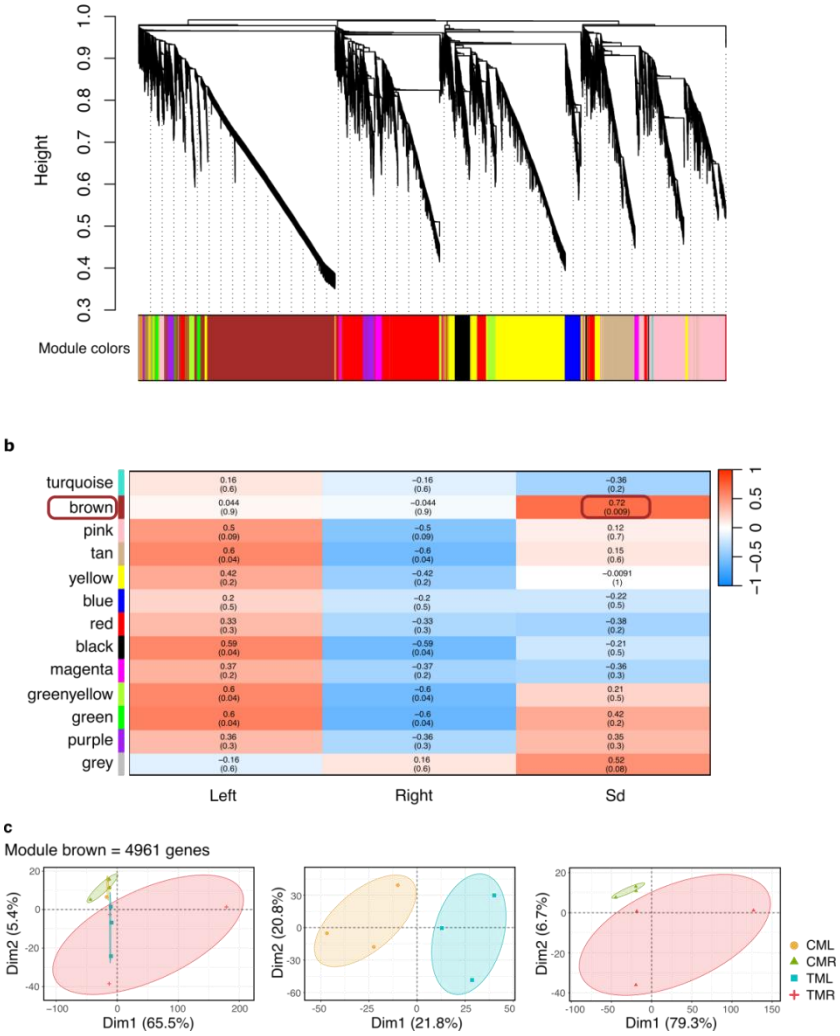

Figure 3.5. Shell sanded correlation module genes from WGCNA analysis in mantle expression data. a) Gene dendrogram obtained by average linkage hierarchical clustering. Height indicates the dissimilarity between genes, which was based on topological overlap. The colour row underneath the dendrogram shows the module assignment determined by the Dynamic Tree Cut. WGCNA analysis identified 13 modules marked by specific colours across the dataset. b) Module-shell sanding correlations and corresponding P-values (in parenthesis). The colour scale shows module-trait correlation from -1 (blue) to 1 (red). The boxes indicate the modules that were selected since they had the highest significance correlation with the T trait. c) Selected module gene expression pattern (PCA plots) in the dataset. The PCA plots represent the expression profiles of module members in each sample, showed as the mutual distance relationship of points after dimensionality reduction clustering. Different colours represent the four experimental conditions, and each ellipse represents the 0.95 confidence range of the samples under that condition.

3.4.4 The target modules for shell formation

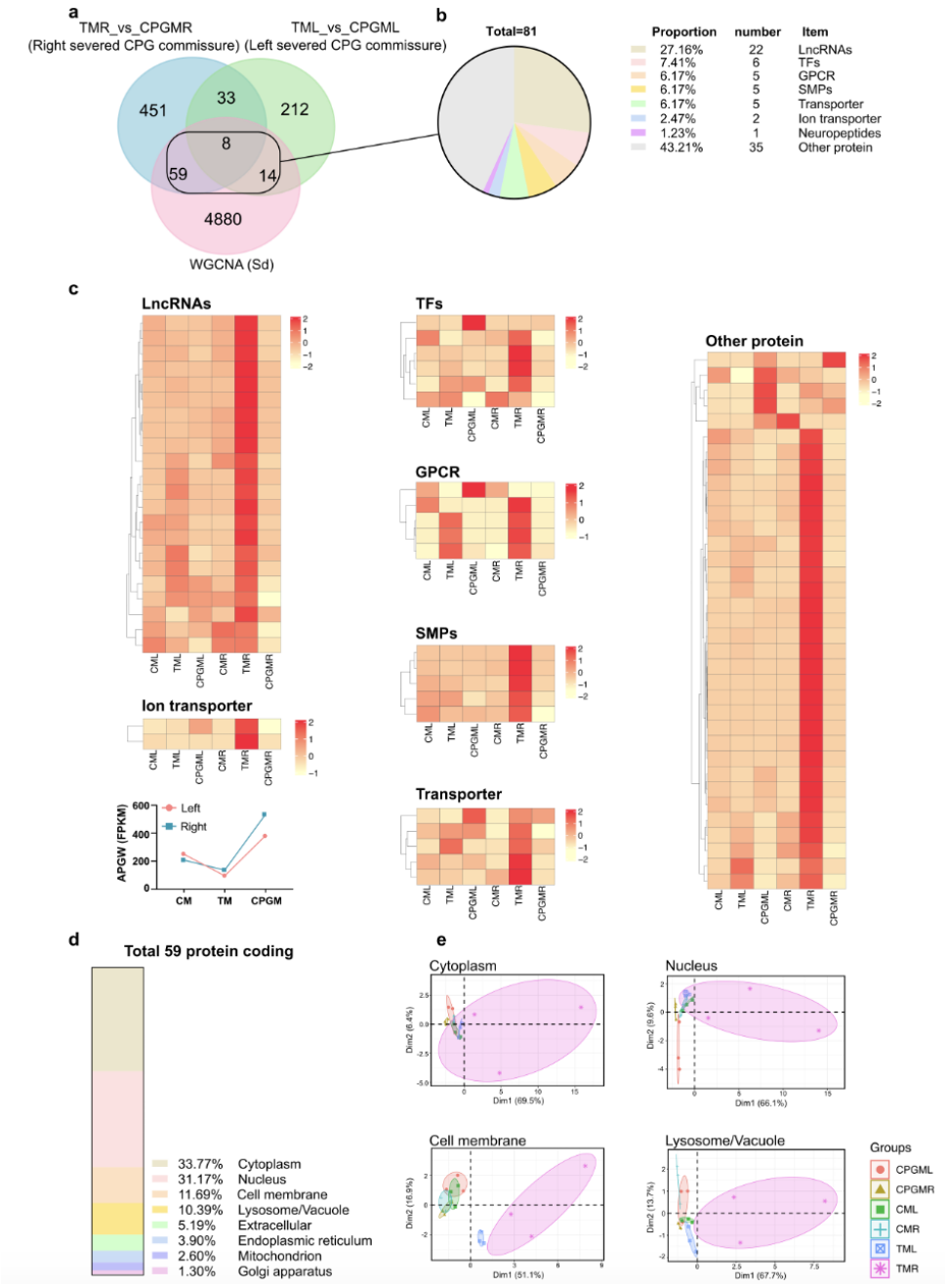

Figure 3.6. Target gene screening and its expression profile and functional annotation. a) Venn diagram showing the overlapping analysis of shell sanded relation module genes and DEGs of severed CPG commissure. The box indicates that the 81 target genes screened meet the following two conditions at the same time: i) gene significant correlation with shell sanding, ii) gene significant differential expression after severing the CPG commissure. b) Pie chart shows the functional composition of target genes. Different colors represent the annotation of functional items, and the proportions and gene quantities are show at the side. c) The expression profile of target genes in the mantle samples. The heatmap represents the expression of genes in CML, TML, CPGML, CMR, TMR and CPGMR in each item. Colours in the heatmap from yellow to deep red represent increasing gene expression (normalized FPKM value in row). One of the line graphs represents the expression (FPKM value) of APGW_amide which is a neuropeptide. d) The subcellular annotation of the 55 protein-coding genes identified. The stacked plots show the proportion of gene localization in subcellular organelles. e) The PCA plots represent the gene expression profiles in samples which localization in top four subcellular organelles, showed as the mutual distance relationship of points after dimensionality reduction clustering. Different colours represent the six experimental conditions, and each ellipse represents the 0.95 confidence range of the samples under that condition.

To identify candidate genes regulated by the CPG and related to shell formation, we compared the genes found in the shell formation-related modules identified by WGCNA with the DEGs from DESeq2 in TMR_vs_CPGMR and TML_vs_CPGML (Figure 3.6A). The comparison identified 81 candidate genes that were significantly modified when the shell was sanded, and the CPG commissure severed. The target genes were clustered under 8 categories, “other proteins” 43.21% (35 genes), lncRNAs 27.16% (22 genes), transcription factors (TFs) 7.41% (6 genes), GPCRs 6.17% (5 genes), SMPs 6.17% (5 genes), Transporter 6.17% (5 genes), Ion transporter 2.47% (2 genes) and only 1 neuropeptide gene (1.23% of the identified candidate genes, Figure 3.6B, Supplementary Table 3.3 - 3.4).

A heatmap of the expression levels of the target genes in the 8 categories revealed that most genes had a higher expression level in the right mantle compared to the left, with significantly higher expression in TMR. However, after the CPG commissure was severed, the expression levels of the significantly upregulated genes decreased to

those of the C group. The expression significantly decreased in TM but significantly increased in CPGM. While 1 GPCR and TF encoding gene were significantly reduced in the TM and significantly increased in CPGM in the left mantle (Figure 3.6C).

The putative subcellular localization of the 55 protein-coding genes showed that the top four locations were: 33.77% in the cytoplasm, 31.17% in the nucleus, 11.69% in the cell membrane, and 10.39% in the lysosome/vacuole (Figure 3.6D, Supplementary Table 3.5). PCA analysis revealed that the Top four subcellular locations for genes of the left and right mantle in the CPGM group were different as they clustered independently. For example, the genes mapped to the cytoplasm in the left and right mantle of the CM group formed 2 separate groups; genes mapped to the cell membrane of the left and right mantle in the TM group formed 2 separate groups and genes mapped to the lysosome/vacuole, in the left and right mantle were separated in all three groups (Figure 3.6E).

3.4.5 The candidate cis-regulatory module of shell formation

All target genes (81) were mapped to the chromosome level genome of *M. galloprovinciallis*. The density of mapping varied, in MgaLG5 the highest number of genes (14) were mapped and in MgaLG14 the lowest number of genes (4) were mapped (Supplementary Figure 3.1). A total of 6 potential lncRNA cis-regulatory gene modules were obtained from the target gene mapping. Two modules were identified in MgaLG12 and one module in MgaLG7, 10, 11 and 13, respectively. Further analysis of the mapped target genes indicated that the cis-regulatory modules

related to shell formation included lncRNAs, GPCRs, and transcription factors (TFs) (Figure 3.7, Supplementary Table 3.6).

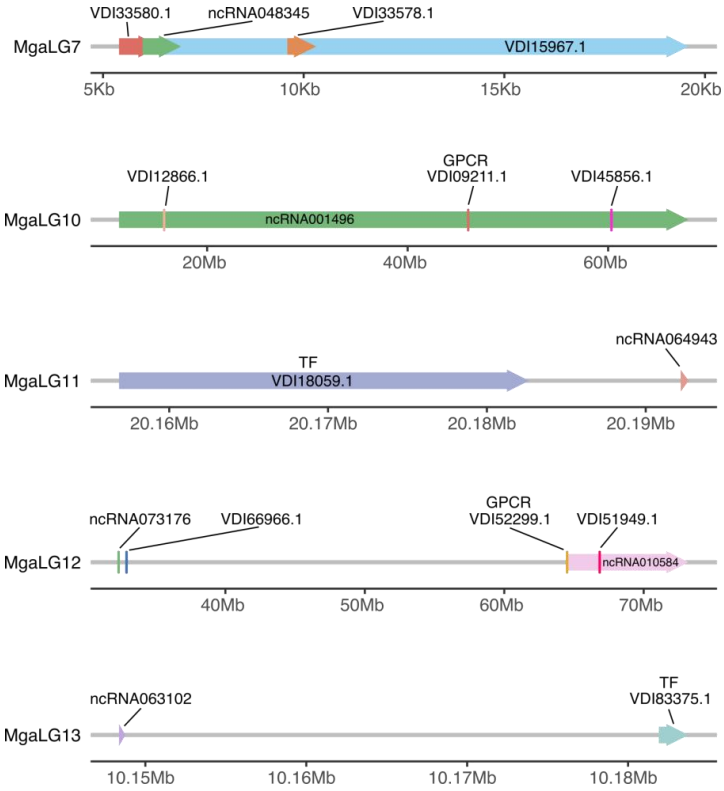

Figure 3.7. Cis-regulation module genes in mantle target genes. Mapping of the target genes in the chromosome level genome of *M. galloprovincialis* using gggenes package in R-studio. The gene position, coding and non-coding is annotated by arrows and the direction of the arrows indicates the gene orientation. The accession number and probable gene identity is provided when possible.

3.5. Discussion

The biomineralized shell is an important structure for bivalves, and the mantle is the crucial tissue for the formation of the calcified shell (Huang and Li, 1991). In this study, mussel shells were damaged by sanding and to test the influence of the nervous system on the shell the CPG commissure was severed. The results give new insights into mantel function in shell symmetric bivalves since we report for the first time that gene expression in the left and right mantles was not symmetrical. In the context of

shell sanding, cutting the commissure between the left and right CPGs resulted in a shift from high gene expression in the right mantle to high gene expression in the left mantle, with significant differences in expression patterns between the two sides. Based on these observations we infer that the nervous system plays a role in shell formation. Comparative analysis of the genes related to biomineralization and sectioning the CPG commissure identified 81 target genes. Notably, lncRNAs accounted for the largest proportion of DE genes, emphasizing the significant role of lncRNAs in regulating shell structure. This study provides strong evidence supporting a regulatory link between ganglia and the mantle, with lncRNAs playing an important role in regulating shell formation.

The conserved function of the mantle despite the divergent characteristics of the shell in bivalves has been assigned to their rapidly evolving shell secretome. This has been interpreted to mean that although core biomineralization toolbox genes are conserved in bivalves, but their utilization in shell construction varies across species (Aguilera et al., 2017; Clark et al., 2020). The $CaCO_3$ crystals in bivalve shells are shaped in the extrapallial fluid and the organic (proteins, polysaccharides, and chitin) and inorganic materials are secreted by the mantle (Kobayashi and Samata, 2006; Santini et al., 2011; Cardoso et al., 2019). Interestingly, the shells of mussels are constructed in two independent extrapallial spaces formed by independent mantles, and a regional difference in shell construction rate (Bjärnmark et al., 2016) was found around the edge of the mantle. Considering the above observations in the context of the high symmetry of the left and right shells of mussels, we hypothesize that

secretion of the shell by the mantle must be coordinated. Further, based on the results of our study we propose that innervation of the mantle by the nervous system is crucial to assure that the two shells and their circumference grow at a similar rate and in this way maintain shell symmetry.

Early studies characterizing the nervous system in bivalves analysed it from an anatomical perspective and revealed the distribution of ganglia, nerve centers, nerve fibers, and their interactions (Ponder et al., 2019). The overall organization of the nervous system in bivalve species is generally conserved, with the loss, gain or prominence of structures dictated by their differing anatomies and life histories. An example, of this is the oysters in which the foot has been lost, and the pedal ganglia, which innervates the foot has also been lost (Galtsoff, 1964; Grizel, 2003). The distribution of neurons, and mapping of neurotransmitters, neuropeptides, and related enzymes reveals the role of the nervous system in locomotion of bivalves, and involves the foot and mantle (Field, 1922; Matsutani and Nomura, 1984; Too and Croll, 1995; Kotsyuba et al., 2020).

The innervation of the bivalve mantle seems to vary with stage and in the larvae the peripheral nervous system is prominent (Saleuddin and Dillaman, 1976; Audino et al., 2015). However, studies on the scallop (*Pecten tenuicostatus*) revealed that the circum-mantle nerve is the most important nerve in the mantle edge. This nerve extends along the entire extension of the mantle and is responsible for innervating the mantle folds and organs (Drew, 1906). Furthermore, the anterior dorsolateral part of the circum-mantle nerve is formed by fibers from the CPG, while the ventral and

posterior areas of the mantle edge are innervated by long fibers from the visceral ganglia (Drew, 1907; Dakin, 1928). Strong serotonergic immunoreactivity was detected in the circumpallial nerve of juvenile scallops (*Nodipecten nodosus*), as well as in projections towards mantle organs (Audino et al., 2015). In the mussel, *M. edulis*, serotonin-like nerves extending along the mantle were detected in larval stages, and catecholaminergic-like cells were identified in the mantle of *Placopecten magellanicus* (Croll et al., 1997). The development of a circumpallial nerve in the mantle ensures this large organ receives integrated inputs and outputs that regulate its sensory function and muscles. However, the function of the nervous system/ganglia in regulating the mantle and shell biomineralization is unstudied (Kotsyuba et al., 2020).

In Chapter II, I showed that neuropeptides and the nervous system regulate the mantle's function and shell growth in *M. galloprovincialis*. Following on from this the present chapter reported the meta-analysis of the global transcriptome of the mantle of the left and right valves in *M. galloprovincialis* and indicated that the right mantle had consistently more DE genes irrespective of the challenge (sanded shell or a combination of sanded shell and cut CPG commissure). This indicates that in the symmetrical bivalve *M. galloprovincialis*, the gene expression of the left and right mantle was not symmetrical. Furthermore, the DE genes identified did not belong to the previously established shell biomineralization toolbox. Notably, after the commissure between the CPG was severed, gene expression shifted from high abundance in the right valve to high abundance in the left valve. An explanation for this phenomenon may lie in the role and organization of the of the circumpallial nerve

and studies of its innervation of the left and right mantles are urgent. We speculate that the nerve regulates the symmetrical growth of the shell by coordinating the gene expression of the left and right mantles.

This study yielded 81 conserved candidate genes presumably related to the regulation by the CPG of shell production since transcriptomes from shell sanded and shell sanded, and sectioning of the CPG commissure were co-analyzed. The bivalve toolbox that determines the formation, composition, and morphology of their shells (Yarra et al., 2021) includes lncRNAs, enzymes, SMPs, ion transporters, TFs, GPCRs and neuropeptides(Jackson and Degnan, 2016). In previous studies, we demonstrated that the CALC system including the peptides and receptors (GPCR) are present in the bivalve mantle and may be part of the regulatory system of shell mineralization (Cardoso et al., 2019). In this study, the results of gene expression analysis demonstrated that two ion transporters, lncRNAs (18 / 22), five SMPs, TFs (4 / 6), GPCRs (4 / 5) were annotated target genes that responded to shell sanding and had significantly elevated expression in the right mantle. However, after severing the CPG commissure, the expression of the identified candidate genes returned to normal. It is worth noting that CPG regulation of the mantle biomineralization toolbox genes does not resemble our previous study of the asymmetric shell in oyster where asymmetric regulation of SMPs was found (Peng et al., 2023). We speculate that after shell damage in mussel, the CPG promoted the up-regulation of biomineralization genes in the left and right mantle in response to the damage. When the CPG commissure was severed, this signaling pathway was disrupted, preventing the transmission of repair

instructions to the mantle, and leading to an absence of a specific response to the damage. Only eight DEGs were shared between the left and right mantle, while 59 genes were specific to the right mantle of mussels with damaged shells. The eight shared DE genes in the right and left mantle coded for GPCRs, lncRNA and a neuropeptide. Combined with the inhibition of shell growth and expression of neuropeptide genes after severing the CPG commissure (Chapter II), we speculate that the inhibition of shell regrowth may be caused by the disruption of the molecular signaling pathway for mantle biomineralization normally received and processed by the CPG. This suggests that shell growth and shell shape (asymmetric / symmetric) is governed by the nervous innervation of the mantle.

LncRNAs have been identified that function in diverse biological processes in molluscs, including immunity in *M. gigas*, the stress response in *Pomacea canaliculata* (Sun and Feng, 2018; Xiao et al., 2022), regulation of muscle growth in the Pacific abalone, *Haliotis discus hannai* (Huang et al., 2018), gametogenesis in *M. gigas* (Wang et al., 2022), and an association with larval development in the *M. gigas* (Yu et al., 2016). In the bivalve *M. gigas*, chorion peroxidase and its cis-acting lncRNA TCONS_00951105 plays a key role in melanin biosynthesis in the shell of the oyster (Feng et al., 2018). In the Manila clam (*Ruditapes philippinarum*), differentially expressed mRNAs and their interacting lncRNAs are thought to be involved in melanin synthesis and the porphyrin metabolism pathways in the shell (Chen S, 2023). Recent studies have provided preliminary evidence of a role for lncRNAs in bivalve biomineralization. In the pearl oyster (*P. fucata*), a lncRNA,

MSEN2, was associated with the regulation of the immune response and nacre formation (Zhang et al., 2020a). Another lncRNA named lncMPEG1, was related to irregular crystal growth on the inner surfaces of the prismatic and nacreous layers in the shell of *P. fucata* (Cai et al., 2022). In the present study, a series of novo candidate lncRNA were identified furthermore an unexpected observation was that the abundance of protein-coding genes was not significantly different between the left and right mantle, but there was a highly significant change in the abundance of lncRNA in the left (upregulated) and right mantle (Figure 3.4C). We propose that the results obtained in relation to lncRNA highlight a cell autonomous role for these molecules in the regulation of shell construction. However, they also indicate that they are involved in mediating the response seen when the CPG ganglia commissure was sectioned since they represented a large proportion (27%) of the responsive genes. Further work will be required to explore the functions of lncRNA and if they are regulated by the mantle nervous system.

A recent study by (Peng et al., 2023), clearly highlights the role for lncRNA in shell production in the Pacific oyster. Using meta-analysis of transcriptome data during larval shell development, shell repair and adult mantle evidence was gathered revealing that lncRNAs can regulate shell growth and experimental studies pinpointed novel biomineralization target genes and identified and confirmed the function of cis-regulatory lncRNA modules (Peng et al., 2023). The present study also predicted cis-regulatory modules in the mantle and identified the potential interaction between candidate lncRNA and protein coding genes. Intriguingly, a total of five

cis-regulatory modules that target GPCRs and TFs were identified. Based on the results of our study, we hypothesis that the way by which the CPG regulates the biomineralization function of the mantle may include the regulation of lncRNA that act on GPCRs genes and TFs in the nucleus. Among these, neuropeptides might also play a crucial role in this pathway, as neuropeptides usually exist and function as GPCR ligands.

3.6. Conclusion

The transcriptome results of this study indicate that severing the CPG ganglia commissure disrupts the balance in gene expression between the right and left mantle and that mantle biomineralization is not limited in scope to the established biomineralization toolbox genes. Long non-coding RNAs appear to be crucial in the regulation of shell formation by the CPG since their expression was highly responsive and they were differential expressed along with protein coding genes in the left and right mantles. Overall, the results provide new evidence for the existence of regulatory pathways between the mantle and the nervous system and that it modulates and coordinates biomineralization of the left and right shell to maintain bilateral symmetry.

3.7. Supplementary materials

All the supplementary materials are provided in the Annex II in digital format.

CHAPTER 4

Evolution and potential function in molluscs of neuropeptide and receptor homologues of the insect allatostatins

Evolution and potential function in molluscs of neuropeptide and receptor homologues of the insect allatostatins

Manuscript published on Frontiers in Endocrinology (2021)

Acknowledgements

This study was funded by Portuguese Foundation for Science and Technology (FCT) through project UIDB/04326/2020. ZL was supported by a PhD scholarship from the China Scholarship Council. MP was supported by a PhD scholarship from Shanghai Ocean University (China).

Evolution and potential function in molluscs of neuropeptide and receptor homologues of the insect allatostatins

Zhi Li[1+], João CR Cardoso[1*+], Maoxiao Peng[1+], João PS Inácio[1] and Deborah M Power[1,2,3*]

[1]Comparative Endocrinology and Integrative Biology, Centre of Marine Sciences, Universidade do Algarve, Campus de Gambelas, 8005-139 Faro, Portugal

[2]International Research Center for Marine Biosciences, Ministry of Science and Technology, Shanghai Ocean University, Shanghai, China

[3]Key Laboratory of Exploration and Utilization of Aquatic Genetic Resources, Ministry of Education, Shanghai Ocean University, Shanghai, China

4.1. Abstract

The allatostatins (ASTs), AST-A, AST-B and AST-C, have mainly been investigated in insects. They are a large group of small pleotropic alloregulatory neuropeptides that are unrelated in sequence and activate receptors of the rhodopsin G-protein coupled receptor family (GPCRs). The characteristics and functions of the homologue systems in the molluscs (Buccalin, MIP and AST-C-like), the second most diverse group of protostomes after the arthropods, and of high interest for evolutionary studies due to their less rearranged genomes remains to be explored. In the present study their evolution is deciphered in molluscs and putative functions assigned in bivalves through meta-analysis of transcriptomes and experiments. Homologues of the three arthropod AST-type peptide precursors were identified in molluscs and produce a larger number of mature peptides than in insects. The number of putative receptors were also distinct across mollusc species due to lineage and species-specific duplication. Our evolutionary analysis of the receptors identified for the first time in a mollusc, the cephalopod, GALR-like genes, which challenges the accepted paradigm that AST-AR/buccalin-Rs are the orthologues of vertebrate GALRs in protostomes. Tissue transcriptomes revealed the peptides, and their putative receptors have a widespread distribution in bivalves and in the bivalve *Mytilus galloprovincialis*, elements of the three peptide-receptor systems are highly abundant in the mantle an innate immune barrier tissue. Exposure of *M. galloprovincialis* to lipopolysaccharide or a marine pathogenic bacterium, *Vibrio harveyi*, provoked significant modifications in the expression of genes of the peptide precursor and receptors of the AST-C-like system in the mantle suggesting

involvement in the immune response. Overall, our study reveals that homologue of the arthropod AST-systems in molluscs are potentially more complex due to the greater number of putative mature peptides and receptor genes. In bivalves they have a broad and varying tissue distribution and abundance, and the elements of the AST-C-like family may have a putative function in the immune response.

Keywords: Allatostatins, GPCRs, molluscs, function, immunity

4.2. Introduction

Molluscs are the second most diverse animal group after the insects and belong to the speciose Lophotrochozoan clade. Their success is linked to their adaptation to a wide variety of habitats, and they are found from the abysses of the sea to mud flats and even as parasites dwelling in other animals. Unlike the more popular protostome models of the nematodes and insects that have substantial genome rearrangements and gene loss (Raible et al., 2005; Miller and Ball, 2009; Takahashi et al., 2009; Simakov et al., 2013), the molluscs have a more similar genome organisation and gene repertoire to deuterostomes. Their success, exquisite diversity in form and function and less rearranged genomes makes the molluscs of particular interest for evolutionary studies directed at deciphering the evolution, diversification and role of neuroendocrine factors (Simakov et al., 2013; Wang et al., 2017).

The allatostatins (AST) are a diverse group of small neuropeptides that have low sequence conservation but have overlapping functions as insect allatoregulatory peptides (Audsley and Weaver, 2009). Three AST peptide families exist and are named allatostatin A (AST-A), B (AST-B) and C (AST-C). They were first described in insects as inhibitors of the biosynthesis by the corpora allatum (CA) gland, of juvenile hormone (JH), an important regulator of arthropod development and reproduction (Lorenz et al., 1995; Nässel, 2002; Stay and Tobe, 2007; Verlinden et al., 2015). Currently the ASTs are now recognized to be involved in a diversity of other activities and play a key role in arthropod physiology (Verlinden et al., 2015; Wu et al., 2020) and immunity (Bachtel et al., 2018; Wang et al., 2019; Xu et al.,

2021). The ASTs are best studied in insects and despite the relatively low gene sequence conservation between the AST families their function and distribution has been conserved. This provides an interesting opportunity to assess if functional constraints have shaped AST evolution in the same way across the protostomes.

The members of each AST family derive from distinct precursor proteins that are assumed to undergo proteolytic cleavage to generate multiple peptides with a similar structure and sequence. The exception is the precursor of AST-C which encodes a single peptide. AST peptides bind and activate members of the rhodopsin G-protein coupled receptor (GPCR) superfamily. AST-A and AST-C activate receptors of the rhodopsin-gamma GPCR cluster while AST-B activates receptors of the rhodopsin-beta GPCR cluster (Mirabeau and Joly, 2013; Elphick et al., 2018; Gerdol et al., 2020). Sequence orthologues of ASTs and of their receptors have been identified in other protostomes outside the arthropod phylum, such as the molluscs, the second most diverse protostome phylum after the arthropods. The evolution and function of the AST families in molluscs that lack a CA are at present poorly described (Cropper et al., 1988; Miller et al., 1993; Vilim et al., 1994; Kim et al., 2006; Veenstra, 2010; Stewart et al., 2014; Adamson et al., 2015; Ahn et al., 2017; Zhang et al., 2018; De Oliveira et al., 2019).

AST-A was the first AST to be described and was initially isolated from the cockroach, *Diploptera punctata* (Pratt et al., 1989; Woodhead et al., 1989) and the peptides are characterized by a conserved C-terminal FGL-amide motif. In arthropods a single peptide precursor exists and it is mostly expressed in the nervous system and

mid-gut (Felix et al., 2015; Chen et al., 2016) and depending on the species encodes a differing number of peptides from 14 to 13 in Blatoidea (*Periplaneta americana* and *Diploptera punctata*) to 4 to 5 in Diptera (*Drosophila melanogaster* and *Anopheles gambiae*) (Felix et al., 2015). The regulation of JH biosynthesis by AST-A was demonstrated in cockroaches, termites and crickets and across the insects the most conserved physiological role for this peptide is regulation of food intake, inhibition of insect gut motility and regulation of digestive enzyme metabolism (Fuse et al., 1999; Robertson et al., 2012; Vanderveken and O'Donnell, 2014; Hentze et al., 2015; Chen et al., 2016). Recently we and others revealed that in the blood-feeding mosquitos the AST neuropeptides and GPCRs may regulate blood digestion and reproduction (Felix et al., 2015; Christ et al., 2018). A single AST-A receptor (AST-AR) has been described in arthropods but in *Diptera* there are two receptor genes, that shared a common evolutionary origin with the vertebrate KISS (KISSR) and galanin (GALR) receptors (Lenz et al., 2000; Mirabeau and Joly, 2013; Felix et al., 2015; Cardoso et al., 2016). In molluscs, buccalins are orthologues of insect AST-A, and were first identified and functionally described in the gastropod *Aplysia californica* where they regulate muscle contraction and feeding (Cropper et al., 1988; Miller et al., 1993). Currently buccalins have been reported in several molluscs where they are suggested to regulate reproduction and spawning in the Sydney rock oyster (*Saccostrea glomerata*) (Van In et al., 2016) and in the Mediterranean mussel (*Mytilus galloprovincialis*) their presence in the mantle has been linked to a role in shell formation (Cardoso et al., 2016).

The functions of AST-B and AST-C peptides have received much less attention. AST-B are encoded by a precursor that in different species generates a variable number of small peptides. In *D. melanogaster* the AST-B precursor gives rise to 5 peptides but in *Rhodnius prolixus* 12 peptides are generated (Broeck, 2001) and they are characterized by the presence of two conserved tryptophan residues and a C-terminal amide (WxW-amide). AST-B peptides were first isolated from the brain-corpora cardiaca-corpora allata-suboesophageal ganglion complex of the migratory locust, *Locusta migratoria* and were shown to inhibit hindgut and oviduct contractions, and thus were initially named myoinhibiting peptides (MIPs) (Schoofs et al., 1996). The allatostatic properties of AST-B/MIP peptides were only discovered after their isolation in the two-spotted cricket (*Gryllus bimaculatus*) (Lorenz et al., 1995). Subsequently other functions have been identified for AST-B/MIP including regulation of ecdysis in the silkworm (*Bombyx mori*) (Hua et al., 1999; Kim et al., 2006),the circadian clock in Drosophila (*D. melanogaster*) (Kolodziejczyk and Nässel, 2011), feeding and locomotion in the cockroach (*Leucophaea maderae*) (Schulze et al., 2012), reproduction in the locust (*Locusta migratoria*) (Schoofs et al., 1996) and the immune response of the green mud crab (*Scylla paramamosain*) (Xu et al., 2021). In insects, the AST-B/MIP precursor is most commonly found in the nervous system (Davis et al., 2003; Lange et al., 2012; Schulze et al., 2012). The functions of AST-B/MIP have also been described in other protostomes such as annelids (where they are known only as MIP) but not in molluscs and they were found to regulate larval settlement and feeding (Williams et al., 2015). The AST-B/MIP peptides

activate the same GPCRs that are activated by insect sex peptide (Kim et al., 2010; Yamanaka et al., 2010; Vandersmissen et al., 2013) and they are proposed to be proximate with the orphan receptors, GPR142 and GPR139, in vertebrates (Mirabeau and Joly, 2013; Elphick et al., 2018).

AST-C was first isolated from the head of the tobacco hornworm (*Manduca sexta*) (Kramer et al., 1991) and unlike other insect ASTs, the precursor produces a single peptide, although other genes, ASTC double C and triple C exist in the genomes of some arthropods including insects (Veenstra, 2009, 2016). The AST-C mature peptide has a conserved C-terminal PISCF motif (Weaver and Audsley, 2009; Coast and Schooley, 2011; Verlinden et al., 2015). The function of AST-C varies and includes inhibition of muscle contraction, feeding suppression, reduced fecundity and inhibition of ovarian development and regulation of circadian activities (Price et al., 2002; Matthews et al., 2008, 2010; Down et al., 2010; Díaz et al., 2019; Liu et al., 2019). In *D. melanogaster* AST-C was also recently proposed to regulate nociception and immunity (Bachtel et al., 2018). Receptors for AST-C are proposed to have a common origin with the vertebrate Somatostatin receptors (SSR) (Kreienkamp et al., 2002; Cardoso et al., 2012; Mirabeau and Joly, 2013).

The present study revisits and enriches understanding of AST peptide and receptor evolution in the molluscs and takes a comparative genomics approach integrating results from previous genome and transcriptome studies (Veenstra, 2010; Jékely, 2013; Mirabeau and Joly, 2013; Stewart et al., 2014; Adamson et al., 2015; De Oliveira et al., 2019). To elucidate the potential functions of the AST families and

GPCRs in molluscs we searched bivalve transcriptomes and targeted their potential role in the mantle, a multifunctional tissue well recognized for its contribution to shell production (Cardoso et al., 2005, 2016, 2019, 2020; Bjärnmark et al., 2016; Clark et al., 2020) and with an emerging role as an innate immune barrier (Allam and Raftos, 2015; Allam and Espinosa, 2016). Taking into consideration the emerging role of AST family members in immunity of insects (Bachtel et al., 2018; Wang et al., 2019; Xu et al., 2021), the response of specific AST family members on the mantle of the Mediterranean mussel (*M. galloprovincialis*) exposed to an immune challenge with bacteria lipopolysaccharide (LPS) and heat inactivated *Vibrio harveyi*, a common pathogenic bacteria of the marine environment, was established (Beaz-Hidalgo et al., 2010; Romero et al., 2014; Zhang et al., 2020b).

4.3. Methods

4.3.1 Sequence database searches

Receptors

Searches for the homologues of the insect AST-GPCRs (AST-AR, AST-BR and AST-CR) were performed in molecular data available for nine representative species of the Mollusca phyla using the deduced protein sequences of the previously identified *M. galloprovincialis* buccalin receptor (buccalin-R, previous AST-AR (Cardoso et al., 2016) and *D. melanogaster* AST-BR (NP_001284892.1) and AST-CRs (*Drostar1*, AAG54080.1 and *Drostar2*, AAL02125.1). Searches were performed against molecular data available in NCBI (https://www.ncbi.nlm.nih.gov)

using blastp in the species-specific sub-datasets available for five bivalves: two members of the *Mytilidae* family, *M. galloprovincialis* (taxid:29158) and *Mytilus coruscus* (taxid:42192), two members of the *Ostreidae* family, *Magallana gigas (*taxid:29159) and *Crassostrea virginica* (taxid:6565) and one member of the *Pectinide* family, the scallop *Mizuhopecten yessoensis* (taxid:6573); three gastropods, *Aplysia californica* (taxid:6500) of the *Aplysidae* family, *Biomphalaria glabrata* (taxid:6526) of the *Planorbidae* family and *Lottia gigantea* (taxid:225164) of the *Lottidae* family; and also one cephalopod the octopus *Octopus bimaculoides* (taxid:37653).

To increase the number of receptor sequences from the phyla Mollusca, selected genomes of representatives of different orders available from the NCBI Genomes database (https://www.ncbi.nlm.nih.gov/genome/) were also procured using the tblastn algorithm with the *M. galloprovincialis* deduced protein sequences of AST receptors as the query (Supplementary Table 4.1). The available genome assemblies of the Polyplacophora class were also searched. All molluscs mentioned above and the general non-redundant protein sequences (nr) database at NCBI were also searched with the Capitella teleta GALR-like (ELU13887.1) for other protostome orthologues.

For comparative analysis, sequence searches were also performed in other Lophotrochozoan phyla namely, the brachiopod *Lingula anatina* (taxid:7574), two annelids *Capitella teleta* (taxid:283909) and *Platynereis dumerilii* (taxid:6359) and in three arthropods of the Ecdysozoans namely, the diptera *Anopheles gambiae*

(taxid:7165), the coleoptera *Tribolium castaneum* (taxid:7070) and the branchiopod *Daphnia pulex* (taxid:6669). Sequences for the homologue receptors in the vertebrates, human (*Homo sapiens*, taxid:9606), spotted gar (*Lepisosteus oculatus*, taxid:7918) and for the invertebrate deuterostome, the amphioxus (*Branchiostoma floridae*, taxid:7739) were retrieved for comparison with the Lophotrochozoan and Ecdysozoan sequences. Sequence hits with a cut off < e^{-30} were retrieved, and their identity was confirmed by searching against the *D. melanogaster* (taxid:7227) and *H. sapiens* (taxid:9606) databases.

Searches were also performed in mantle transcriptomes available from the Mediterranean mussel (*M. galloprovincialis*, SRP 063654) (Bjärnmark et al., 2016) and the hard-shelled mussel (*M. coruscus*, kindly provided by Yifeng Li and Jin-Long Yang, SHOU, China) to identify the corresponding gene transcripts. Putative receptors were retrieved based on their sequence similarity (cut off < e^{-30}) with *M. galloprovincialis* and *D. melanogaster* homologues or using transcriptome annotations. All sequences retrieved were translated using the Expasy translate tool (https://web.expasy.org/translate/) and their identity confirmed as described above.

Peptide precursors

Mollusca buccalin precursors (Cardoso et al., 2016) and *M. galloprovincialis* and *M. coruscus* orthologues of the insect AST-B/MIP and AST-C peptide precursors were initially obtained by exploring the species-specific mantle transcriptome annotation available "in house". The deduced protein sequence of MIP-like and AST-C-like were used to identify the corresponding coding genes and additional gene

isoforms. The mussel precursor protein sequences were translated with the Expasy translate tool (https://web.expasy.org/translate/) and the localization of the predicted mature peptides were manually deduced by a) the identification of monobasic, dibasic, or tribasic consensus cleavage sites (RR, KR, KK) and b) the identification of the conserved mature peptide motifs such as the two conserved tryptophan (W) residues (W(X)W-amide) in AST-B/MIPs and the two conserved cysteine (C) residues in AST-Cs. The mature peptides and the full peptide precursors were procured in other molluscans (bivalves, gastropods cephalopods and the polyplacophoran) using a similar strategy. Homologues from other representatives of the lophotrochozoan clade such as one brachiopod and two annelids were also characterized for comparisons (Supplementary Figure 4.1).

4.3.2 Sequence comparisons and phylogenetic analysis

Multiple sequence alignments (MSA) of the deduced peptides and receptor sequences were performed using the MUSCLE algorithm available in Aliview 1.18. (Larsson, 2014). For phylogenetic analysis the receptor alignments were manually inspected, and sequence gaps removed, and the edited alignments were used to construct Bayesian Inference (BI) and Maximum Likelihood (ML) phylogenetic trees. The AST-AR and AST-CR (members of the Rhodopsin g family) trees and the AST-BR trees (members of Rhodopsin b family) included sequences from representatives of 27 molluscs (11 bivalves, 11 gastropods, 4 cephalopods, 1 polyplacophors), 1 brachiopod, 2 annelids, 1 cephalochordate and 2 vertebrates (Supplementary Table 4.1) and were built in the CIPRES Science Gateway v3 using

an LG model (selected using model test-ng 0.1.5) since they best fitted the data (Miller et al., 2010). The BI trees were built in MrBayes (Ronquist et al., 2012) run on XSEDE v3.2.7a with 1.000.000 generation sampling and probability values to support tree branching. The ML trees were built with the RAxML v8.2.12 (Stamatakis, 2014) method with 100 bootstrap replicates. The BI tree was mid-rooted according to previous models proposed for receptor sequence evolution (Mirabeau and Joly, 2013), and AST-BRs were rooted with the *H. sapiens* (NP_000721) and *L. oculeatus* (XP_006629714) cholecystokinin receptor type A (CCKAR) branch. To build the phylogenetic trees for the AST-Rhodopsin g family GPCRs the sequences of the metazoan KISSRs and GALRs were also included as they are suggested to have evolved from the same ancestral gene as protostome AST-ARs (sequences obtained from (Cardoso et al., 2016) and also from database searches using the predicted receptor proteins of *M. galloprovincialis* as queries. For the trees of the AST-Rhodopsin b family GPCRs the related protostome receptors from the FMRFamide (FMRFaR), RGWamide (RGWaR), Proctolin (ProctR) and Myosupressin/Myomodulin (MyoR) families were also included as well as the vertebrate sequence orthologues GPR142 and GPR139 from *H. sapiens* (GPR142, NP_001318005.1 and GPR139, NP_001002911.1) and *L. oculeatus* (GPR142, XP_006635495 and GPC139, XP_006637109) (Mirabeau and Joly, 2013; Elphick et al., 2018; Thiel et al., 2021).

Receptor sequence alignments and percentage of sequence identity was displayed and calculated in the GenDoc programme (http://www.nrbsc.org/gfx/genedoc/). The

mature peptide alignments were established using Clustal W (https://www.genome.jp/tools-bin/clustalw). Receptor structures were predicted in Protter (http://wlab.ethz.ch/protter) using the default settings and the outputs annotated in Inkscape to highlight the conserved aa positions across species. The receptor signal peptide was predicted using the SignalP-5.0 Server (Almagro Armenteros et al., 2019) and the DeepLoc1 server was used to explore protein cellular localization (Almagro Armenteros et al., 2017).

4.3.3 Neighbouring gene analysis (short range synteny)

The neighbouring gene environments of the annelid *C. teleta* GALR-like and buccalin-R that map to SuperContig CAPTEscaffold_148 (scaffold_148) and SuperContig CAPTEscaffold_45 (scaffold_45), respectively and *H. sapiens* GALRs and *D. melanogaster* AST-ARs (DAR1 and DAR2) were characterized to infer potential ancestral origin and to support the identification of the new protostome sister clade of the deuterostome GALRs. Ten genes upstream and downstream of the *C. teleta* gene loci were collected and they were used to search for gene homologues in the *H. sapiens* GALR1 (chromosome 18), GALR2 (chromosome 17), GALR3 (chromosome 22) and KISSR (chromosome 19) and in *D. melanogaster* DAR1 (chromosome X) and DAR2 (chromosome 3R) genome regions. The BioMart tool available from Ensembl was used to compare the *C. teleta* and *D. melanogaster* genome regions. The deduced C. teleta AST-AR and GALR-like neighbouring protein sequences were searched against the species-specific *H. sapiens* (taxid:9606) and *D. melanogaster* (taxid:7227) datasets available from NCBI

(https://www.ncbi.nlm.nih.gov). The gene loci of the top protein hits (with the lowest e value) were retrieved based on the genome assemblies available from NCBI (*D. melanogaster*, Release 6.32, and *H. sapiens*, GRCh38.p13). The *O. bimaculoides* GALR-like genome region on SuperContig KQ419625 was also analysed and the five neighbouring genes were retrieved and searched against *C. teleta* and *H. sapiens* genomes.

4.3.4 Animal manipulation and sampling

Mediterranean mussels (*M. galloprovincialis*) were obtained from a local producer in the Ria Formosa (Olhão, Portugal). For the experimental immune challenge mussels (length 4.35 ± 0.34 cm, soft body dry mass 1.61 ± 0.46 g) were transported live to the Centre of Marine Sciences (CCMAR) where they were cleaned and acclimatized for a week in 5 litres of aerated seawater (SW) prior to the immune challenge at 20 - 22ºC. Animals were fed daily with a mixture of a commercial dried microalgae diet (PHYTOBLOOM, Necton, Portugal). For tissue sampling animals were opened by cutting the adductor muscle and mantle edge from the region most distal to the umbo (referred to as the posterior region) was dissected out and snap frozen in dry ice and stored at - 80ºC for RNA extraction. For tissue distribution, cDNA samples (n = 3 samples for each tissue) from gills, digestive gland, mantle edge and haemolymph available in the lab were used.

4.3.5 Immune challenge

Mussels were exposed to heat-inactivated *V. harveyi* by introducing them into the

bathing seawater. The *V. harveyi* (kindly donated Dr M. Manchado, IFAPA, Puerto Santa Maria, Spain) was grown in TSB medium supplemented with 1% NaCl and the number of cfu / ml was determined on TSA/1% NaCl agar plates. For the bacterial challenge 5 x 107 cfu / ml of the heat inactivated bacteria suspended in 1 L of sterile seawater was used. The *V. harveyi* bacteria was heat inactivated by boiling the culture for 2 hours.

For the challenge experiments mussels (n = 80) were randomly distributed in triplicate tanks. The experiments were performed in 2 L plastic tanks containing 1 L of filtered seawater (0.45 mm) that was collected from their natural environment. Each of the control (3 tanks) and exposed (3 tanks) tanks contained 12 - 13 individuals (total 40 animals per group). The seawater in the experimental tanks was constantly aerated with aquarium air-pumps and the temperature was 20 - 22ºC, pH was 8.1 ± 0.1 and salinity 37 ppt and the experiments were conducted under natural photoperiod for March 2021 in the Algarve. Control mussels were maintained in seawater and transferred after 15 h to new tanks and the immune challenged mussels were exposed for 15 h to heat-inactivated *V. harveyi* (5 x 107 cfu / liter) and then transferred to new tanks containing clean filtered seawater. Specimens (n = 6 samples per time point) from control and challenged tanks were sampled (as outlined above) at 0, 6, 12, 24 and 36h post exposure. Animals were not fed during the experiment and no mortality was observed.

4.3.6 RNA extraction and cDNA synthesis

Total RNA (tRNA) from control and immune challenged mantle edge was

extracted using an E.Z.N.A kit (VWR, USA) and DNase treatment was performed after elution using a Precision DNase kit (Primer design, UK) according to the manufactures protocol. For extraction, collected tissues were defrosted in the lysis buffer and homogenized by mechanical disruption with two iron beads (5 mm) using a Tissue lyser II Qiagen and 1 cycle of 3 min at room temperature.

Table 4.1. List of primers used in qRT-PCR analysis for the bivalve *M. galloprovincialis*.

Transcript		**Sequence (5' →3')**	**T (ºC)**	**Efficiency**	**R^2**
AST-C-like	Fwd	GCAGTTTCAAGAGCAGGAAGCCT	66ºC	95.6%	0.996
	Rev	GGCATTGCACATGGCTTCGTTT			
AST-CR-like VDI53419.1	Fwd	AAACATCGGAAGAGAGGCT	60ºC	92.9%	0.999
	Rev	GCATTTCCAATCAGACCGGC			
AST-CR-like VDI15122.1	Fwd	TACGGACGAATTCGAAAACGG	62ºC	96.2%	0.995
	Rev	ATTACCAACCAATCCACCGAC			
AST-CR-like VDI08560.1	Fwd	AACACATCCAGTGCTGTCGC	na	na	na
	Rev	CGCCTTATTGAATGCCATACC			
AST-CR-like VDI13242.1	Fwd	CGTCATTCTGCGTTCATCCA	na	na	na
	Rev	CCAAAAAGCCAGAATCGCAG			
TLRa	Fwd	TCATACCTGGGGCCTGCATA	62ºC	99.7%	1

	Rev	GTGGCGTCGGTGTTTCAATG			
LYG1	Fwd	TGCAGTGTGATGTCCGAGTC	62ºC	95.3%	0.996
	Rev	GTATGCTGCCACTCCACCTT			
C345i	Fwd	CCAGCACCAAACTGTCCACT	62ºC	100.3%	0.995
	Rev	ACGATTCGTCCCGTCTCATC			
18S	Fwd	GTGCTAGGGATTGGGGCTTG	60ºC	95.5%	0.999
	Rev	TAGTAACGACGGGCGGTGTG			
EF1 α	Fwd	GAAGGCTGAGGGTGAACGTG	60ºC	96.2%	0.996
	Rev	TCCTGGGGCATCAATAATGG			

na- not amplified

For cDNA synthesis, DNase treated tRNA (500 ng) was denatured at 65ºC for 5 min and quenched 5 min on ice. Reactions were carried out for a 20 µl final volume with 10 ng of pd (N) 6 random hexamers (Jena Bioscience, Germany), 2 mM dNTPs (ThermoScientific, USA), 100 U of RevertAid Reverse Transcriptase and 8 U Ribolock RNAse inhibitor (ThermoScientific). Reaction conditions were: 10 min, 20 ºC; 60 min, 42 ºC; 70 ºC, 5 min. The quality of the cDNA produced was assessed by amplification of mussel ribosomal subunit 18s rRNA using specific primers (Table 4.1) and the following thermocycle: 95°C, 3 min; 25 cycles (95°C, 20 sec; 60 °C, 20 sec; 72 °C, 20 sec); 72 °C, 5 min.

4.3.7 Tissue expression analysis

Tissue expression analysis

To characterize the tissue distribution publicly available control tissue transcriptomes of four bivalves: *M. galloprovincialis*, *M. coruscus*, *M. gigas* and *M. yessoensis* were retrieved and analyzed. Public transcriptome data available for control tissues including the gills, muscle, mantle, digestive gland/hepatopancreas, haemocytes and nerve ganglia were searched using the species-specific nucleotide sequences identified for the peptide precursors and receptors. Searches were carried out using Blastn and the corresponding sequence read archive (SRA, https://www.ncbi.nlm.nih.gov/sra/) for each of the species analyzed (Supplementary Table 4.2). Maximum target sequences were adjusted to 1000 and sequence hits with > 98% nucleotide identity were selected. FPKM counts were calculated taking into consideration the number of reads, gene length and the transcriptome sequencing depth.

The involvement of the bivalve homologues of the arthropod ASTs and receptors in the immune response was initially assessed using mantle edge transcriptomes of *M. galloprovincialis* challenged with Lipopolysaccharide (LPS, *E. coli* LPS 0111 : B4, Sigma-Aldrich, USA) a major component of the outer membrane of Gram-negative bacteria. Candidate transcripts were identified by exploring available in-house DEG data (p-adj < 0.05, log2-fold > 2) for the mantle edge transcriptomes of control *M. galloprovincialis* (injected with 1 x PBS) and LPS exposed *M. galloprovincialis* (injected with 50 ml of 0.5 mg / ml of bacterial LPS in the adductor mussel) from

samples collected in the context of another study.

To further explore the involvement of the AST-C-like system in the bivalve response to pathogenic marine bacteria, expression analysis of the *M. galloprovincialis* members was assessed using cDNA (n = 3 samples) from normal tissues (gills, digestive gland, mantle edge and haemocytes) and from the mantle edge of control and exposed specimens to heat-inactivated pathogen, *V. harveyi*, at 0 (n = 6 samples), 6 (n = 6 samples), 12 (n = 6 samples), 24 (n = 6 samples) and 36 h (n = 6 samples) post exposure. Specific primers for the *M. galloprovincialis* AST-C-like peptide precursors and for four AST-CR-like were designed and the PCR products were sequenced, and their identity confirmed (Table 4.1). It was not possible to design specific primers for the AST-CR-like VDI60978.1 as its sequence was smaller and the predicted nucleotide coding region was highly identical to other AST-CR-like (97%). The activation of the immune response in *M. galloprovincialis* was confirmed by determining the expression of three humoral factors that have previously been shown in bivalves to respond to Vibrio spp., Toll-receptor TLRa (Xu et al., 2018), Lysozyme goose-type 1 LYG1 (Wang et al., 2012) and complement-factor C345i (Peng et al., 2022)in cDNA of the mantle edge of control (n = 3 samples) and exposed (n = 3 samples) specimens from 0, 6 and 12 h post exposure (Table 4.1).

Changes in gene expression were assessed by quantitative real-time PCR (qRT-PCR) using SsoFast EvaGreen Supermix (Bio-Rad, Portugal) in a 10 µl final reaction volume containing 200 nM of forward and reverse gene specific primers (Table 4.1) and 2 µl of template cDNA (diluted 1:2). Elongation factor 1-alpha (EF1α)

and 18s ribosomal subunit (18S) were used as reference genes (cDNA diluted 1:50 and 1:500, respectively). QRT-PCR analysis was performed in duplicate reactions (< 5% variation between replicates) using a CFX Connect™ Real-Time PCR Detection System for 96-well microplates (Bio-Rad). Cycling conditions were 95 ºC, 30 sec; 44 cycles of 95 ºC, 5 sec; the most appropriate primer annealing temperature, 10 sec (Table 4.1). Melting curves were performed to detect the presence of non-specific products and primer dimers. Reverse transcriptase (RT-) and PCR control reactions were included in each PCR plate to confirm the absence of genomic or PCR contamination. QRT-PCR efficiencies and R^2 (coefficient of determination) were established (Table 4.1), and data was normalized using the geometric mean of the expression levels of the reference genes.

4.3.8 Statistical analysis

Results are presented as the mean ± SEM. Statistical differences were detected using One-Way ANOVA for the tissue distribution and for gene expression between the control and immune challenged mussels with Two-Way ANOVA using a Sidak's multiple comparison test. Analysis was executed using GraphPad Prism version 8.0 for Mac OS X (USA, www.graphpad.com).

4.4. Results

Nomenclature

The AST neuropeptides were named due to their inhibitory (allatostatic) actions on JH biosynthesis from the insects CA gland. In molluscs no equivalent organ has

been described and JH is specific to insects. In molluscs the sequence orthologues of the arthropod AST-A are known as buccalin and in annelids the orthologues of the arthropod AST-B/MIP are known as MIP. For the lophotrochozoan AST-Cs no nomenclature has yet been proposed. Throughout the manuscript we use the existing lophotrochozoan nomenclature and have named AST-C as AST-C-like (Table 4.2).

Table 4.2. Nomenclature adopted for the molluscan neuropeptide homologues of the arthropod AST peptides and receptors.

	Arthropoda		Mollusca	
	peptide	receptor	peptide	receptor
Allatostatin A	AST-A	AST-AR	Buccalin	Buccalin-R
Allatostatin B/ myoinhibitory peptide	AST-B/ MIP	AST-B/ MIP-R	MIP	MIP-R
Allatostatin C	AST-C	AST-CR	AST-C-like	AST-CR-like

Orthologues of the arthropod AST precursors and receptors in the molluscs

Sequence homologues of the three arthropod AST peptide precursors and receptors were found in the 27 mollusc species included in the study and the number of peptide precursors genes and predicted mature peptides and putative receptor genes varied across the species (Figure 4.1, Supplementary Table 4.1, Supplementary Figure 4.1A, 4.1B and 4.1C). In other lophotrochozoan phyla the peptide precursors shared a similar organization to the molluscs (Supplementary Figure 4.1A).

Buccalin precursors and buccalin receptors

The Mollusca buccalin precursors are the orthologues of the arthropod AST-As

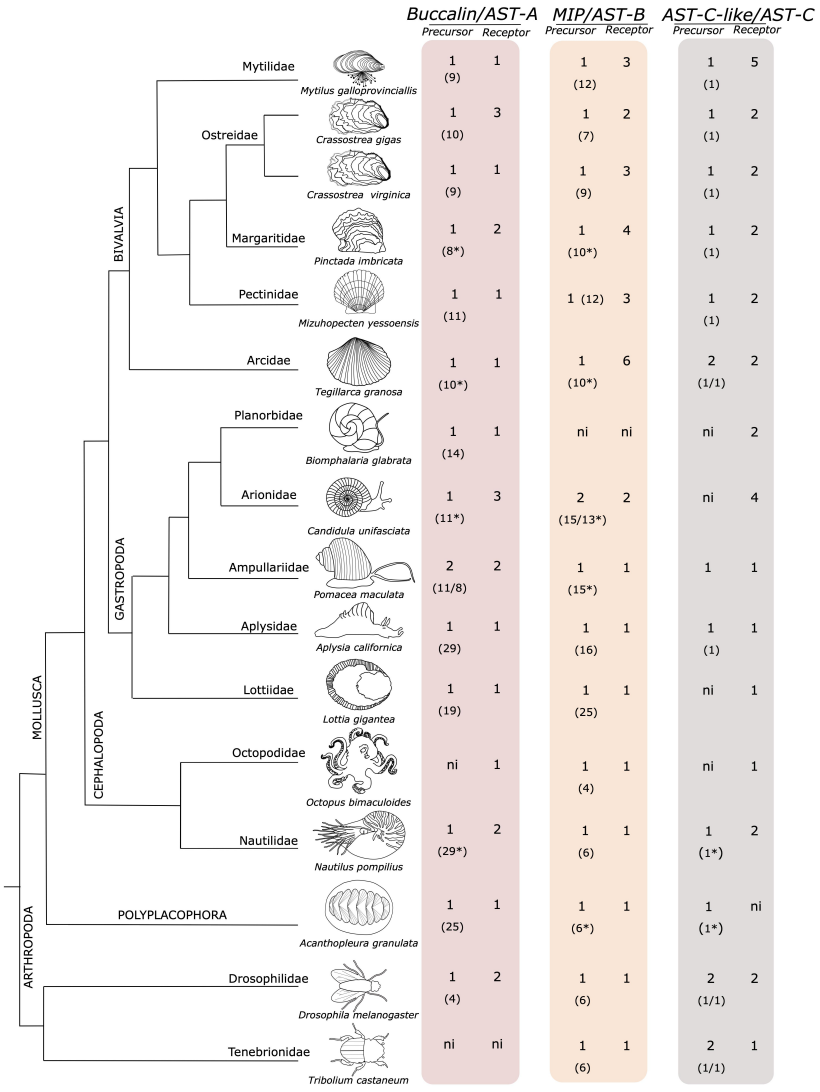

Figure 4.1. The molluscan orthologues of the arthropod ASTs precursors and receptors. The number of peptide precursors and receptors retrieved are indicated. The predicted number of deduced mature peptides produced by each peptide precursor is represented within brackets "( )". The dendrogram represents the evolutionary relationship of the species and was manually designed taking into consideration the studies of (113 - 116). The insect *D. melanogaster* and *T. castaneum* are also represented for comparisons. The figure is not drawn to scale. Ni - not identified. Complete peptide precursor sequences are available from Supplementary Figure 4.1. * deduced from an incomplete precursor sequence.

and a single precursor gene was found in most molluscs and encoded for multiple mature peptides (Figure 4.1 and Supplementary Figure 4.1A). The exception was the gastropod *Conus ventricosus* (CM031604.1 and CM031615.1) and *Pomacea*

maculata (XP_025108540.1 and XP_025087986.1) where two putative genes were found. The number of buccalin-R was more variable and while most species possessed a single buccalin-R gene, other species genomes contained two receptor genes (the bivalves *Pinctada imbricata*, *Margaritifera margaritifera*; the gastropods *Alviniconcha marisindica*, *Haliotis laevigata*, *Pomacea maculata* and the cephalopod *Nautilus pompilius* but the bivalve *M. gigas* and the gastropod *Candidula unifasciata* contained three buccalin-R genes. The majority of the mollusca duplicate buccalin-R genes were localized within the same genome region and thus are likely to be tandem gene duplicates (Supplementary Table 4.1).

The buccalin precursors encoded for a different number of peptides. In the *Mytilidae* family 7 mature peptides were predicted in *M. coruscus* and 9 in *M. galloprovincialis*. In the *Ostreidae* family, the buccalin precursors have the potential to generate 10 mature peptides in *M. gigas* and *M. hongkongensis* and 9 in *C. virginica* and in the *Pectinidae*, *P. yessoensis*, 11 mature peptides were predicted (Supplementary Figure 4.1A). In other bivalves, such as the *Margaritifera margaritífera* (*Margaritiferidae* family), *Pinctada imbricata* (*Pteriidae* family) and in *Tegillarca granosa* (*Arcidae* family) at least 8, 8 and 10 putative mature peptides were encoded, and the full-length precursors still remains to be isolated. No buccalin precursor genes were retrieved from the bivalves *Sinonovacula constricta* and *Ruditapes philippinarum* genomes.

The buccalin precursor in the gastropod *A. californica* (*Aplysiidae* family) contained the largest number of predicted peptides (29 mature peptides) and the

Gigantopelta aegis (*Peltospiridae* family) precursor was the second most rich. In the cephalopod *O. bimaculoides* and most cephalopod genomes explored our searches failed to identify the buccalin precursor except in the *Nautilus pompilius* (*Nautilidae* family) where 29 peptides were predicted (Supplementary Figure 4.1A). In the polyplacophore *Acanthopleura granulata* a single the buccalin precursor was found (Supplementary Figure 4.1A).

Previously, a putative buccalin-like precursor with a similar organization to the buccalin precursor was identified since it generates a series of highly identical V-amide mature peptides with a conserved PFDRLASGLV/I-amide sequence (Cardoso et al., 2016) (Supplementary Figure 4.2). These buccalin-like peptides were recently reclassified and proposed as a new Mollusca neuropeptide family, the LASGLI/V-amide peptide family (Zhang et al., 2018; Oliveira et al., 2019). For this reason, the buccalin-like peptides (LASGLI/V-amide peptide) were excluded from the present analysis.

MIP precursors and MIP receptors

In Mollusca a single MIP-B peptide precursor encoding multiple peptides was found (Supplementary Figure 4.1B) in most species, the exception was the gastropod, *C. unifascia*ta, where two precursors were retrieved. The number of MIP-R receptors was variable (Figure 4.1). A single receptor gene was found in the gastropods, cephalopods and in the polyplacophore genomes analysed but gene number was very variable in bivalves where multiple receptors were found with 3 in *M. galloprovincialis* and 6 in *T. granosa* (Supplementary Table 4.1). No MIP or MIP-R

were found in the gastropod *B. glabrata*. In bivalves, the number of mature MIP peptides varied from 11 in the *Mytilidae* to 12 in the *Pectinidae* (Figure 4.1 and Supplementary Figure 4.1B). The gastropod peptide precursors encoded the greatest number of peptides, and 25 MIP mature peptides were predicted in *L. gigantea* and 16 in *A. californica*. In other gastropods the minimum number of mature peptides found was 8 but most precursors were deduced from the species genomes and were incomplete and it seems likely that more peptides may be produced. In the cephalopod *O. bimaculoides* the MIP precursor encoded the least number of peptides (only 4) but in other taxa at least 6 peptides existed (Supplementary Figure 4.1B). In the polyplacophore a single MIP precursor was found, which encoded for at least 6 mature peptides.

AST-C-like and AST-C-like receptors

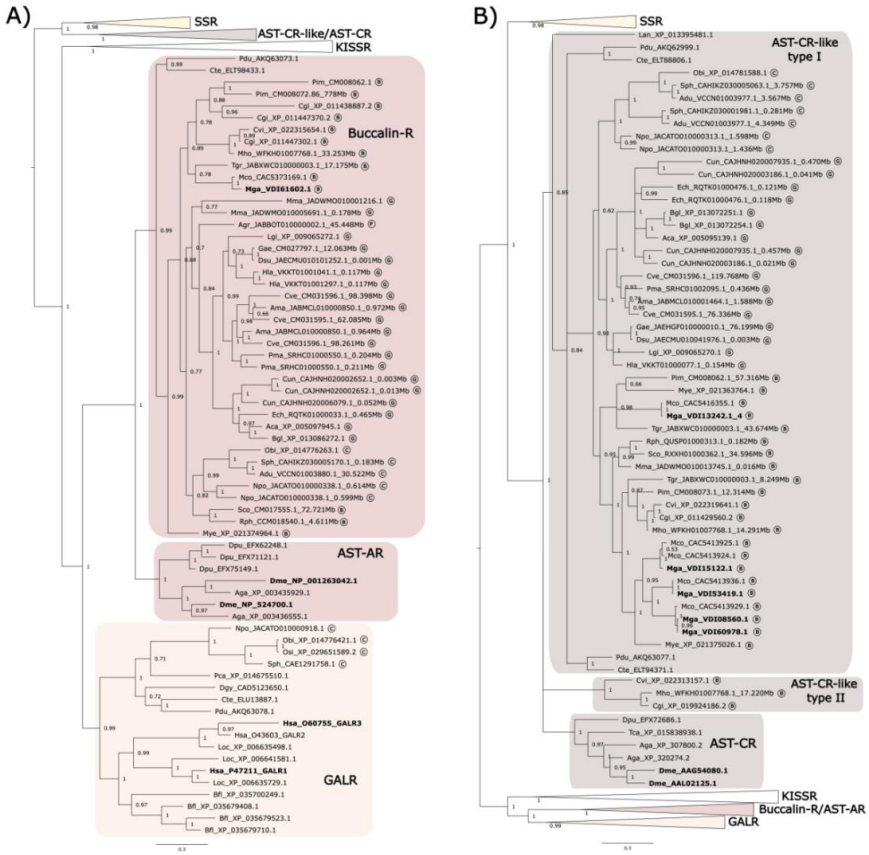

Figure 4.2. Phylogenetic trees of the Molluscan Buccalin and AST-C-like receptors and orthologues from other lophotrochozoans, ecdysozoans and deuterostomes. The tree was built using the Bayesian inference (BI) method with 1,000,000 generations and posterior probability values and was constructed using an LG model. A tree with a similar topology was also obtained using the Maximum likelihood (ML) method (Supplementary Figure 4.3). The AST-AR and AST-CR tree was mid-rooted taking into consideration the clustering of the sequences. Circled letters indicate: B - bivalves; G - gastropods, C - cephalopods; P - polyplacophore species used in the analyses. The sequences that were retrieved from non-annotated genomes have the putative localization (Mbp) indicated.

In Mollusca a single AST-C-like peptide precursor that encodes for a single mature peptide was found in all the species analyzed (Figure 4.1, Supplementary Figure 4.1C). The only exception was for the bivalve *T. granosa* where two identical mature peptides precursor genes localized in the same genomic fragment (JABXWC010000007.1) were found. In contrast, in other molluscs receptor number was variable and 5 putative AST-CR-likes were retrieved from bivalves of the *Mytilidae* family and four were also found in the gastropod *C. unifasciata* (*Arionidae* family). The other representatives of the diverse Mollusca classes possessed 1 to 2 AST-CR-like (Figure 4.1). Genes encoding the AST-C-like peptide precursors were not predicted in available protein coding gene data for *M. galloprovincialis* and *M. coruscus* but searches in mantle transcriptomes identified a single AST-C-like gene transcript in *M. coruscus* which mapped with 100% identity to the genome (CM029607.1). An orthologue sequence was identified in the genome of *M. galloprovincialis* (UYJE01007806.1) when the *M. coruscus* AST-C-like sequence was used for searches.

Phylogeny of the Mollusca receptors

The retrieved receptors from Mollusca were compared with the orthologue

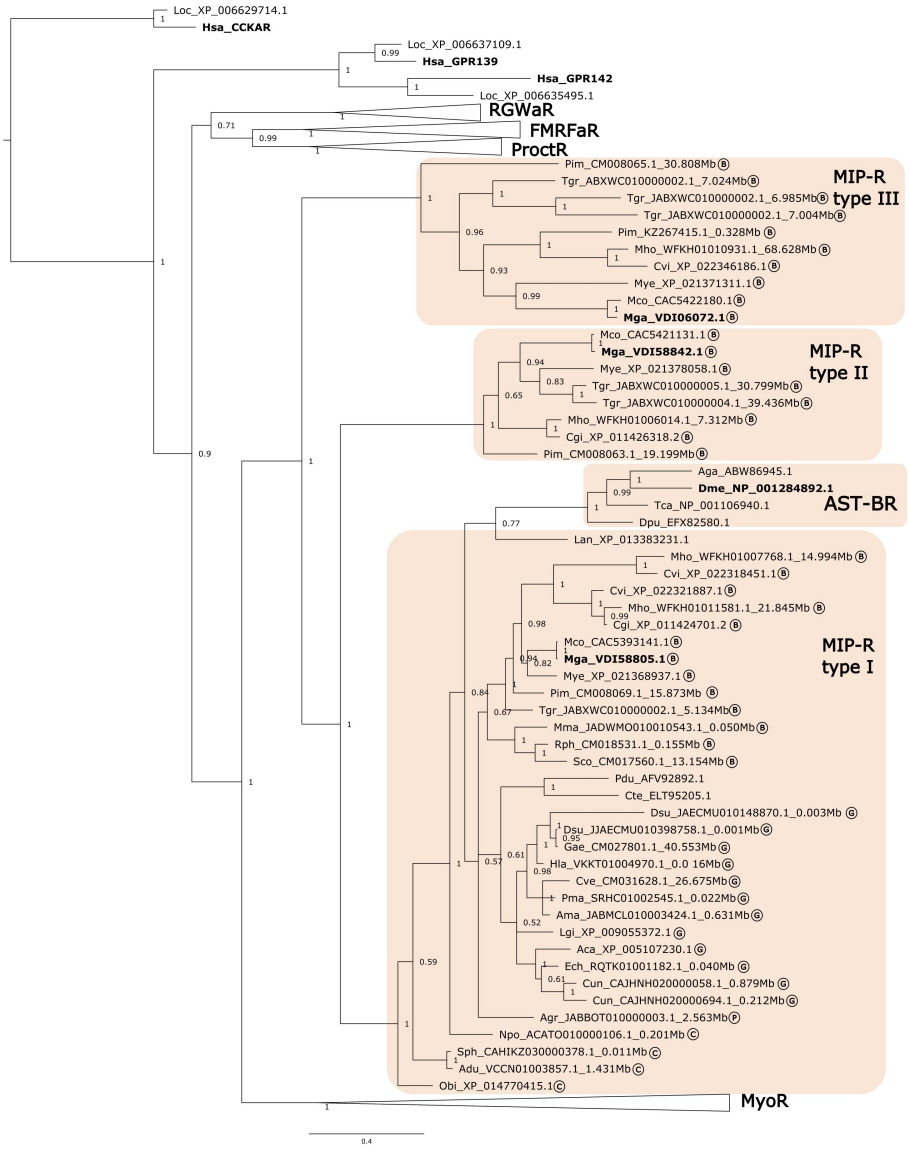

Figure 4.3. Phylogenetic tree of the Molluscan MIP receptors and orthologues from other lophotrochozoans, ecdysozoans and deuterostomes. The tree was built using the Bayesian inference (BI) method with 1,000,000 generations and posterior probability values and was constructed with an LG model. A tree with a similar topology was also obtained using the Maximum likelihood (ML) method (Supplementary Figure 4.3). The receptor clusters of FMRFamide (FMRFaR), RGWamide (RGWaR), Proctolin (ProctR) and Myosupressin/Myomodulin (MyoR) were collapsed. The AST-BR tree was rooted with the *H. sapiens* (NP_000721) and *L. oculeatus* (XP_006629714) cholecystokinin receptor type A (CCKAR). Circled letters indicate: B- bivalves; G-gastropods, C- cephalopods; P- polyplacophore species used in the analysis. The sequences that were retrieved from non-annotated genomes have the putative localization (Mbp) indicated.

receptors in other lophotrochozoans, arthropods and deuterostomes by building BI phylogenetic trees (Figure 4.2A and B, Figure 4.3). The ML tree had a similar branch

topology (Supplementary Figure 4.3A and B). The protostome buccalin-R/AST-AR and AST-CR-like/AST-CR family members belonged to the GPCR-rhodopsin g subfamily. The protostome MIP-R/AST-BRs family members belonged to the GPCR-rhodopsin b subfamily. All the Mollusca sequences within each receptor family clustered together based on their sequence homology in the phylogenetic trees and the lophotrochozoan receptors formed sister branches with the arthropod receptor homologues. The receptors of the *Mytilidae* family, *M. galloprovincialis* and *M. coruscus*, always clustered in proximity and the same was observed for the Ostreidae family, *M. gigas* and *C. virginica*. Clustering of the Mollusca receptors revealed that the variable number of members found within each family resulted from lineage and species-specific duplication events.

Buccalin-R

The topology of the phylogenetic tree confirmed that no Buccalin-R/AST-ARs existed in deuterostomes and that Mollusca as well as other protostome receptors shared a common origin with the metazoan KISSR and GALR (Liu et al., 2010; Mirabeau and Joly, 2013; Kim et al., 2014; Felix et al., 2015; Cardoso et al., 2016) (Figure 4.2A). Our searches also confirmed that homologues of the deuterostome KISSRs exist in bivalves and gastropods and that GALR-like sequences were only found in cephalopods. The cephalopod GALR-like sequences clustered with the annelid GALR-like from *C. teleta* (ELU13887) and *P. dumelii* (AKQ63078) and with the deuterostome GALRs (Figure 4.2A) irrespective of the phylogenetic tree building method. This reveals for the first time the presence in Mollusca of a

GALR-like clade, which is apparently absent from the bivalves, gastropods and polyplacophore.

MIP-R

Homologues of the arthropod AST-BRs (MIP-Rs) were identified in molluscs and other lophotrochozoans and the clustering of the retrieved bivalve sequences suggested that there were three MIP-R subtypes (Figure 4.3). Type I MIP-Rs was assigned to the Mollusca receptors that were present in most species and that clustered with the other lophotrochozoans and in the same branch as the arthropod AST-BRs. The other two MIP-R clusters were named type II and type III and contained sequences from bivalves (Figure 4.3). Identification of 3 MIP-R subtypes in bivalves and their absence from other protostomes suggests that they emerged prior to the divergence of the ecdysozoan and lophotrochozoan lineages (Figure 4.3). The protostome RGWaR, FMRFaR, ProctR and MyoR that are proposed to have radiated from the same common ancestor as MIP-R/AST-BRs were included in phylogenetic tree (Mirabeau and Joly, 2013; Elphick et al., 2018; Thiel et al., 2021) and the tree topology confirmed that all receptors shared a common origin with the orphan deuterostome GPR139/142 (Mirabeau and Joly, 2013; Elphick et al., 2018).

AST-CR-like

The arrangement of the sequences within the Mollusca AST-CR-like branch confirmed that the receptors shared a common origin with vertebrate SSRs (Figure 4.2B). A large gene family expansion occurred within the *Mytilidae* family and

originated four of the five receptor isoforms retrieved from *M. galloprovincialis* and *M. coruscus*. In addition, the clustering of one of the *Ostreidae* duplicate receptors from *M. gigas*, *C. virginica* and *M. hongkongensis* in distinct branches from the other lophotrochozoan receptors suggested that the two gene copies were under different evolutionary pressure (Figure 4.2B). Genome mapping revealed that the duplicate *Ostreidae* receptor genes mapped in proximity in the same genome fragment and are likely to be the result of a tandem gene duplication (Supplementary Table 4.1).

Buccalin, MIP and AST-C-like mature peptides in molluscs

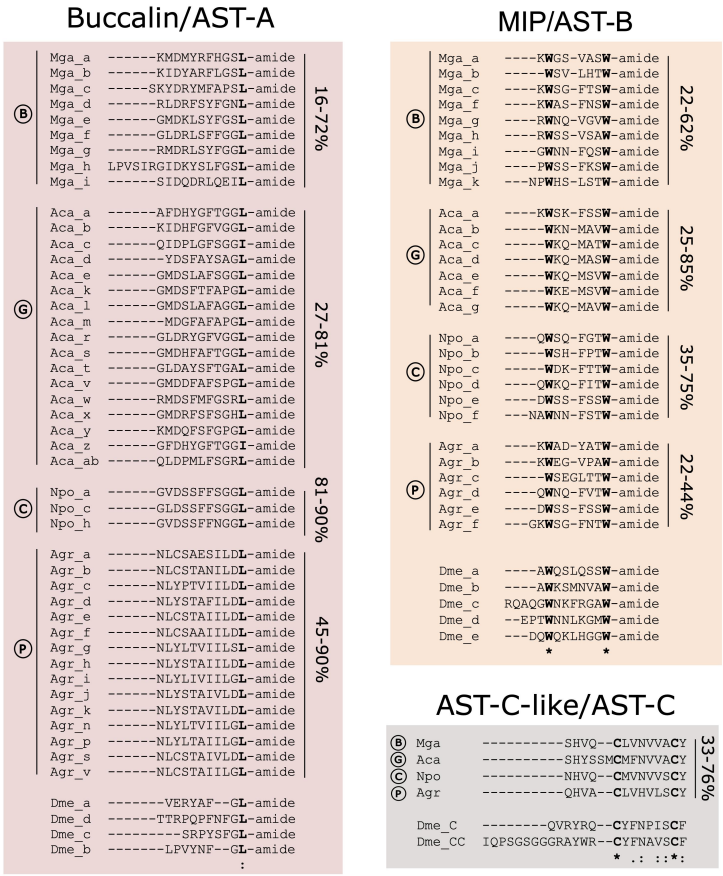

Figure 4.4. Molluscan Buccalin, MIP and AST-C-like mature peptide sequences. Identical peptides arising from the same peptide precursor are not represented. The deduced peptides were named with a letter (a to z) based on their position within the peptide precursor. The percentage of amino acid sequence identity of the mature

peptides encoded by the same precursor in each species is indicated at the side for each peptide group. The bivalve (B) *M. galloprovincialis* (Mga), gastropod (G) *A. californica* (Aca), cephalopod (C) *N. pompilius* (Npo) and polyplacophore (P) *A. granulata* (Agr) mature peptides and the *D. melanogaster* (Dme) peptides are represented for comparison. Totally conserved amino acids are marked in bold. "*" indicates total amino acid conservation, ":" indicates a site belonging to groups exhibiting strong similarity and "." indicates a site belonging to a group exhibiting weak similarity. Full-length peptide precursor sequences are available in Supplementary Figure 4.1

Buccalin, MIP and AST-C-like mature peptides in molluscs

Buccalin mature peptides

In molluscs the buccalin precursors encoded L-amide (as found in *A. californica* (Miller et al., 1993) and the peptide precursors encoded a different number of peptides (Supplementary Figure 4.1A). The gastropod and the cephalopod *N. pompilius* precursors encoded for the largest number of mature peptides (Figure 4.1 and Supplementary Figure 4.1). The bivalve and cephalopod buccalin precursors encoded for a conserved C-terminal L-amide peptide (like *D. melanogaster* AST-A) (Figure 4.4) but in gastropods it also encoded I-amide peptides and all predicted peptides were less than 55% identical in sequence to the *D. melanogaster* AST-A. The number of predicted peptides in the buccalin precursor varied across the molluscs. In bivalves, the buccalin precursor in the representatives of the *Mytilidae* family, encoded 9 in *M. galloprovincialis* and 7 in *M. coruscus* mature L-amide peptides that all had different sequences (Figure 4.4, Supplementary Figure 4.1A).

In gastropods, the *A. californica* buccalin precursor encoded for the largest number of predicted peptides (29 mature peptides) and 25 were L-amine and the 3 remaining were C-terminal I-amide and produce 17 different peptides (Figure 4.4).

Other gastropods precursors only encoded L-amide peptides (*G. aegis*, *A. marisindica*, *C. ventricosus*, *D. subfuscus*, *P. maculata*, *H. laevigata*, *E. chlorotica*) but the *B. glabrata* precursor only encoded I-amide peptides (11 in total) (Supplementary Figure 4.1A). In *O. bimaculoides* and other cephalopod genomes our searches failed to identify the buccalin precursor except in *N. pompilius* and 29 L-amide peptides were predicted, and most of them were identical in sequence and only 3 different types of mature peptides were produced (Figure 4.4, Supplementary Figure 4.1A). The buccalin precursor in the polyplacophore *A. granulata* encoded 25 L-amide peptides with 15 different sequences (Figure 4.4, Supplementary Figure 4.1A). Conservation of the mollusc mature peptides encoded within the precursor was distinct and the amino acid sequence identity of the *M. galloprovincialis* mature peptides varied from 16 - 72% and the predicted Mga_c and Mga_i peptides were most divergent and Mga_g was the most conserved (72% aa identical) with Mga_d, e and f.

MIP mature peptides

The MIP precursors in common with the mollusc buccalin precursor have the potential to generate multiple peptides by proteolysis of a single polypeptide precursors and the highest peptide numbers were identified in the gastropods (Figure 4.1, Figure 4.4, Supplementary Figure 4.1B). For MIP a single peptide precursor was found and in the bivalve *Mytilidae* the number of mature peptides varied from 11 in *M. coruscus* to 12 in *M. galloprovincialis* but in the gastropod *C. unifasciata* two MIP precursors existed and they encoded for different peptides (Figure 4.1, Supplementary Figure 4.1B). The mollusca MIP mature peptides varied from 7 - 9 aa in length and

the sequence identity in the *M. galloprovincialis* precursor revealed that 3 peptides (Mga_c, d and e) were identical and the peptides overall, shared 22 to 62% aa identity (Figure 4.4). The MIP precursor in *A. californica* produced 16 peptides of which 7 had different sequences and overall, they shared 25-85% aa identity. The gastropod *L. gigantea* MIP precursor was the most peptide rich (25 MIPs in total) and it encoded putative mature peptides of different sizes, and the majority were slightly longer (12 aa) than most molluscan peptides due to their extended N-terminal region (Supplementary Figure 4.1B). The same occurred for the cephalopod *S. pharaonic* and *A. dux* MIPs but *N. pompilius* had peptides of a similar length to other mollusca MIPs and all the encoded peptides (6) differed and the same was true for the polyplacophore *A. granulata* (Figure 4.4 and Supplementary Figure 4.1). All the mollusc mature peptides possessed two conserved tryptophan (W) residues separated by 4 - 7 aa residues (W(x4 - 7)W, where x represents any aa). In *D. melanogaster* there were five AST-B/MIP peptides that contained two conserved W residues separated by 6 aa (W(x6)W). The 12 MIP mature peptides in the bivalve *M. galloprovincialis* shared 38 to 78% aa sequence identity with the *D. melanogaster* orthologues.

AST-C-like mature peptides

A single AST-C-like peptide was encoded by the AST-C precursor and in the molluscs analysed, the peptide was 13 - 15 aa in length (Figure 4.4, Supplementary Figure 4.1C). AST-C in molluscs like AST-C and AST-CC of *D. melanogaster* possessed two conserved cysteine (C) residues that form a disulphide bond in the

peptide (Figure 4.4). Within molluscs the aa conservation varied from 33 to 76% and the mollusc AST-C-like mature peptide shared higher sequence conservation with *D. melanogaster* AST-C (25 - 33%) than with AST-CC (13 - 17%).

Structure of the Mollusca receptors

The Mollusca receptors shared a conserved protein structure with their homologues from *D. melanogaster* and *H. sapiens* and receptors possessed seven transmembrane domains linked by three extracellular loops that alternated with three intracellular loops (Figure 4.5, Supplementary Figure 4.4A, 4.4B and 4.4C). Multiple sequence alignments of the mollusc receptors with the other protostome

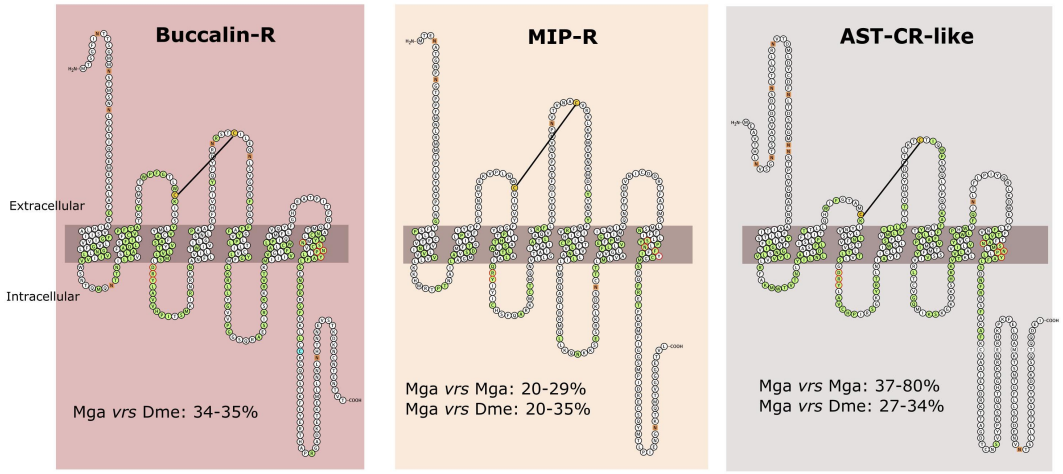

Figure 4.5. Structure and amino acid sequence conservation of the Mollusca Buccalin, MIP and AST-C-like receptors with the orthologues from other species. The figure represents the predicted receptor structure in the cell membrane. The receptors represented are the bivalve *M. galloprovincialis* Buccalin-R (VDI61602), MIP-R (VDI58805) and AST-CR-like (VDI08560). Receptor structure was obtained from Protter and the cell membrane is represented by the grey bar. Amino acids that were highly conserved across species and present in the full-length receptor sequence alignments (available from Supplementary Figures 4.4) are marked in green and the N-glycosylation motifs are represented by orange squares. The motif DRY and NSxxNPxxY (where x represents any aa) within TM7 that are required for receptor activation are outlined in red, the two conserved cysteine residues which might be responsible for the formation of a disulphide bond are highlighted in yellow and the C-terminal cysteine residue for potential palmitoylation after TM7 is in blue. The percentage (%) of amino acid sequence identity between the *M. galloprovincialis* (Mga) receptors and *D. melanogaster* (Dme) homologues is indicated.

homologues revealed that the TM domains shared the highest sequence conservation across species and the conserved aa motifs involved in receptor activation, DRY in ICL2 between TM3 and TM4 and NSxxNPxxY (where x represents any aa) within TM7 were present (Fritze et al., 2003; Rovati et al., 2007) (Figure 4.5, Supplementary Figure 4.4A and 4.4C). The exception was the protostome MIP-Rs in which DRY was mutated to QRY (Glutamine) and degeneration of the motif in TM7 occurred (Figure 4.5, Supplementary Figure 4.4B).

Two conserved cysteine residues, which potentially form a disulphide bond between ECL1 and ECL2 and determine receptor structure and stability were conserved in the mollusc and arthropod receptors. A C-terminal cysteine residue for potential palmitoylation after TM7, which is a characteristic of the rhodopsin-GPCRs, was also identified in the Buccalin-Rs and AST-CRs-like (Figure 4.5). No signal peptide was predicted for the *M. galloprovincialis* receptors or the *D. melanogaster* homologues except for DAR1. However, DeepLoc1 analysis predicted a cell membrane localization for the *M. galloprovincialis* receptors. Several N-glycosylation sites were found in the N-terminal region of *M. galloprovincialis* and other bivalve receptors (Figure 4.5 and Supplementary Figure 4.4A, 4.4B and 4.4C).

The deduced protein sequence of *M. galloprovincialis* and *M. coruscus* Buccalin-Rs shared 96% aa identity, 40 - 54% identity with the homologues from the Ostreidae family and 34 - 35% with the two receptor homologues in *D. melanogaster* (DAR1 and DAR2). The three *M. galloprovincialis* MIP-Rs were only 25 - 29% identical suggesting that they may have different functions. The *M. galloprovincialis*

type I receptor was most similar to *D. melanogaster* AST-BR (35%), while the other paralogues type II and type III only shared 20% identity with *D. melanogaster* AST-BR. The amino acid sequence of the five *M. galloprovincialis* AST-CR-like shared between 37 to 80% identity and VDI08560.1 and VDI60978.1 (that arose due to a recent gene duplication) shared the highest aa sequence identity. The *M. galloprovincialis* and *M. coruscus* AST-CR-like shared 36 - 94% aa identity and 27 to 34% aa identity with the two *D. melanogaster* receptors.

Comparisons of the gene environment of Buccalin-R and GALR-like with the homologue regions in human and *D. melanogaster*

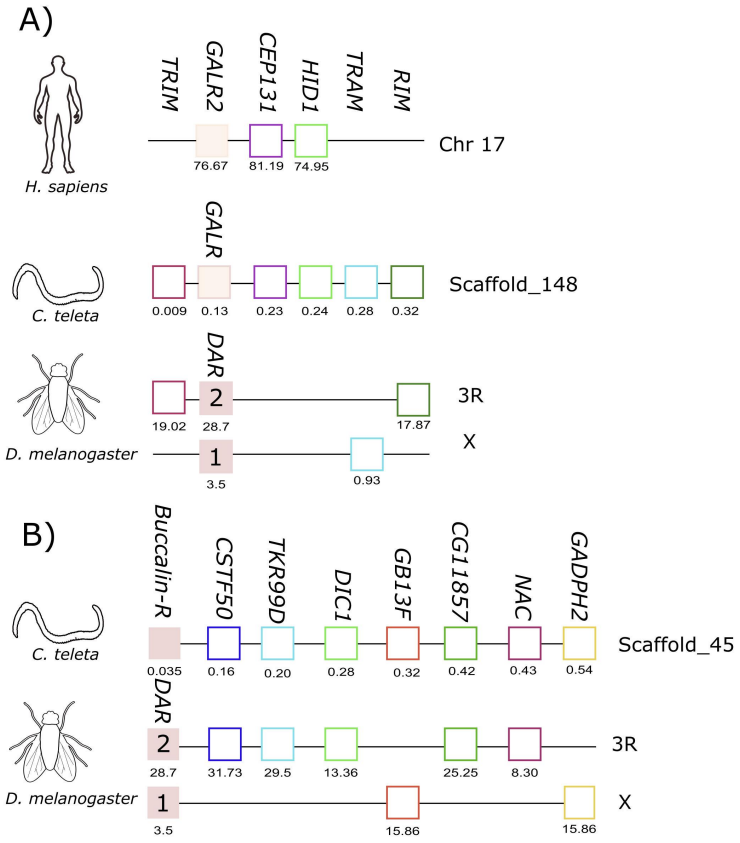

Figure 4.6. Short-range gene synteny of the *C. teleta* GALR-like (A) and Buccalin-R (B) with *D. melanogaster* and *H. sapiens*. Predicted genes are represented by coloured boxes and full blue boxes represent the genes of the GALR

and Buccalin-R/AST-AR family. *Orthologue* neighbouring genes are indicated in the same colour. The genes are mapped on chromosomes based on their predicted position (Mbp) in the genome assemblies. Only genes that were conserved in the homologous genome regions are represented. Tripartite motif family (TRIM); CCR4-NOT transcription complex subunit 3 (CNOT3), *Centrosoma*l Protein 131 (CEP131), HID1 Domain Containing (HID1), Translocation Associated Membrane Protein 1 (TRAM), Rab3 interacting molecule (RIM), WD repeat-containing protein 55 homolog (CSTF50), Tachykinin-like receptor at 99D (TKR99D), Mitochondrial dicarboxylate transporter (DIC1), Guanine nucleotide-binding protein subunit beta-1 (GB13F), NAC transcription factor (NAC), Glyceraldehyde - 3phosphate dehydrogenase 2 (GADPH2).

Previously, our studies on the characterization of the Buccalin-R / AST-ARs and the sequence homologues of the vertebrate KISSR and GALRs in Arthropods and Mollusca suggested that they were most closely related to the metazoan KISSRs (Felix et al., 2015; Cardoso et al., 2016). However, the topology of the present phylogenetic trees (Figure 4.2A) that included a larger number of molluscan representatives indicated that the protostomes, arthropod AST-ARs and lophotrochozoan Buccalin-Rs, tended to cluster with the vertebrate GALRs (Figure 4.2A). Moreover, a novel receptor clade containing homologues of the deuterostome GALRs were identified in molluscs (cephalopods), annelids and other lophotrochozoans. To gain further insight into the relationship of the lophotrochozoan Buccalin-R and GALR-like members with the KISSR/GALR, the gene environment in the annelid *C. teleta* and *O. bimaculoides*, which have the two receptor types was characterized (Figure 4.6). The *O. bimaculoides* GALR-like gene mapped to a short genome fragment (SuperContig KQ419625) and only 5 gene neighbours were mapped, and searches against *C. teleta* and the human genome regions failed to identify gene homologues in the neighbourhood of the GALR-like and GALRs genes.

In *C. teleta* the GALR-like homologue mapped to scaffold_148 and gene

homologues of human CEP131 and HID1 located near the loci of human GALR2 in chromosome 17 were identified (Figure 4.6A). In addition, homologues of three other neighbouring genes were found in *D. melanogaster* AST-AR chromosomes, TRIM and RIM in proximity with the DAR2 gene on chromosome 3R and TRAM in proximity with DAR1 on chromosome X. This suggests that the *C. teleta* GALR-like genome region shares similarity with both arthropod AST-AR and human GALR2 genome regions.

The *C. teleta* AST-AR genome region was also characterized, and the gene mapped to scaffold_45 and shared conserved homologue neighbouring genes with the *D. melanogaster* DAR1 and DAR2 genome regions suggesting that both annelid Buccalin-R and insect AST-AR shared a common origin (Figure 4.6B). No homologue neighbouring genes of *C. teleta* AST-AR loci were found in the proximity of the human GALR1 (chromosome 18), GALR2, GALR3 (chromosome 22) or KISS1R (chromosome 19) genome regions. Comparison of the gene environment of human KISSR and AST-ARs in *D. melanogaster* (chromosomes 3R and X) and *A. gambiae* (chromosome 2R) using the conserved neighbouring genes previously identified, PTBP1, EVIL5L, DOT1L and ODF3L2 (Felix et al., 2015), failed to retrieve putative homologues in the annelid C. teleta KISSR-like and GALR-like genome regions.

Expression analysis in the bivalves and targets of immunity

Transcriptome data available for the bivalves, *M. galloprovincialis*, *M. coruscus*, *M. gigas* and *M. yessoensis* (Supplementary Table 4.2) was used to infer potential

function in molluscs. The expression profile obtained suggested that buccalin, MIP and AST-C-like peptide precursors and receptors have a widespread tissue distribution and that they seemed to be most abundant in the mantle (Figure 4.7). Of the tissue transcriptomes analysed the haemocytes had the lowest expression except for the MIP system in *M. gigas*. The widespread tissue distribution and different relative abundance (RPKM) of the peptides and receptors suggests that they may have

Buccalin system

			Gills	Digestive gland	Mantle	Haemocytes	Muscle	Nerve ganglia
M. galloprovincialis	Precursor	VDI48108.1	1,98	0,29	2,03	0	0,6	
	Receptor	VDI61602.1	0,66	0	1,38	0	0,54	na
M. coruscus	Precursor	CAC5362126.1	1,15	0,23	1,43	0	0,63	
	Receptor	CAC5373169.1	0,06	0	0,58	0	0,16	na
C. gigas	Precursor	XP_011425482.2	2,26	2,28	2,15	0	1,57	
	Receptor	XP_011447302.1	1,48	2,58	2,19	1	1,15	na
		XP_011447370.2	1,48	2,58	2,19	1	1,15	
		XP_011438887.2	0,01	0,6	0,03	0,7	0	
M. yessoensis	Precursor	AXN93469.1	1,43	0,08	2,34	0,12	0,01	3,09
	Receptor	XP_021374964.1	0,46	0,01	0,69	0	0	1,65

MIP system

			Gills	Digestive gland	Mantle	Haemocytes	Muscle	Nerve ganglia
M. galloprovincialis	Precursor	VDI26375.1	1,85	0,53	2,01	0	0,41	
	Receptor	VDI06072.1	0	0	1	0	0	na
		VDI58805.1	1,02	0,63	1,45	0	1,21	
		VDI58842.1	1,57	0,01	1,54	0	0,57	
M. coruscus	Precursor	CAC5388310.1	0,3	0,06	0,37	0	0	
	Receptor	CAC5393141.1	0,43	0	0,29	0	0	na
		CAC5421131.1	0,4	0,05	0,41	0	0	
		CAC5422180.1	0,05	0	0,9	0	0	
C. gigas	Precursor	XP_011417556.2	0,81	2,66	2,46	1,85	0,48	
	Receptor	XP_011424701.2	1,95	2,82	1,87	1,79	1,08	na
		XP_011426218.2	0,38	1,73	2,31	2,99	2,83	
M. yessoensis	Precursor	AXN93470.1	0	1,23	0,04	0,19	0,06	3,24
	Receptor	XP_021368937.1	0,03	0	0,91	0	0	1,64
		XP_021378058.1	0,62	0	1,5	0	0	1,93
		XP_021371311.1	0,98	0,44	1,87	0	0	1,32

AST-C-like system

			Gills	Digestive gland	Mantle	Haemocytes	Muscle	Nerve ganglia
M. galloprovincialis	Precursor	na	1,21	1,90	1,38	0,00	0,37	
	Receptor	VDI08560.1	0,56	0,12	1,08	0,00	0,08	na
		VDI13242.1	0,00	1,00	0,43	0,00	0,00	
		VDI15122.1	0,01	0,00	0,17	0,00	0,00	
		VDI53419.1	0,61	0,48	1,08	0,00	0,77	
		VDI60978.1	0,35	0,10	1,05	0,00	0,10	
M. coruscus	Precursor	na	0,86	1,26	1,11	0,05	0,88	
	Receptor	CAC5413924.1	0,00	0,00	0,00	0,00	0,88	
		CAC5413925.1	0,00	0,00	0,00	0,00	0,85	na
		CAC5413929.1	0,07	0,00	0,84	0,00	0,06	
		CAC5413936.1	0,04	0,07	0,00	0,00	0,00	
		CAC5416355.1	0,09	0,06	0,00	0,00	0,00	
C. gigas	Precursor	XP_011412814.1	0,38	1,73	1,06	0,78	0,00	
	Receptor	XP_011429560.1	1,08	2,52	2,24	0,85	2,12	na
		XP_019924186.1	2,13	2,64	2,73	1,63	2,67	
M. yessoensis	Precursor	XP_021356393.1	0,98	0,42	1,87	0,00	0,00	3,18
	Receptor	XP_021363764.1	0,00	0,02	0,00	0,17	0,00	1,15
		XP_021375026.1	0,03	0,27	0,17	0,00	0,01	1,65

Figure 4.7. Expression levels (FPKM) of the Buccalin, MIP and AST-C-like systems in four bivalves. Data for *M. galloprovincialis*, *M. coruscus*, *M. gigas* and *M. yessoensis* was obtained by screening publicly available transcriptome data (SRA database) for gills, muscle, mantle, digestive gland/hepatopancreas, haemocytes and nerve ganglia (Supplementary Table 4.2). FPKM counts were calculated having in

consideration the number of reads, gene length and the transcriptome sequencing depth. Only tissues common to all species are represented. Expression data for *M. gigas* mantle corresponded to the average of inner (SRX093415) and outer (SRX093411) transcriptomes and for the *M. yessoensis* muscle the average of smooth (n = 3) and striated (n = 3) muscles. Other *M. yessoensis* transcriptome data also reflect the average FPKM of 2 to 3 datasets (except the nerve ganglia). Colour grading highlights differences in transcript abundance in the tissue libraries analyzed. na- not available

different functions (Figure 4.7). In *M. yessoensis* all homologues of the arthropod ASTs and receptors were present in the nerve ganglion (transcriptome, SRR6407589), and were far more abundant in this tissue than in the mantle (Figure 4.6). Analysis of a mantle transcriptome of *M. galloprovincialis* challenged with bacterial LPS revealed that only the AST-CR-like (VDI60978.1), was significantly down-regulated 12h post challenge (Supplementary Figure 4.5). These results suggest that the bivalve AST-C-like system may be involved in the immune response, as described in arthropods. To test this hypothesis *M. galloprovincialis* were challenged with the pathogenic marine bacteria *V. harveyi.*

Exposure of *M. galloprovincialis* to an immune challenge and response of the AST-C-like system in mantle

Quantitative PCR (qRT-PCR) analysis of *M. galloprovincialis* tissues confirmed the AST-C-like precursor and two AST-CR-like (VDI53419.1 and VDI15122.1) were detectable in the mantle (Figure 4.8). Other tissues such as the gills, the digestive gland and the haemocytes also expressed the peptide precursor and receptors. The abundance of AST-C-like was similar in all tissues analysed. AST-CR-like VDI15122.1 was significantly more expressed in the gills compared to haemocytes ($p < 0.05$) and AST-CR-like VDI53419.1 was significantly more expressed ($p < 0.01$) in

the gills than in other tissues. AST-CR-like VDI53419.1 was most abundant and its expression in tissue was approximately 10-fold higher than the other receptor gene VDI15122.1 and the gene encoding the peptide precursor (Figure 4.8). No amplification product was obtained for VDI08560.1 and VDI13242.1. The AST-CR-like gene, VDI60978.1, which shared 97% identity with VDI08560.1 was not analysed as isoform specific qRT-PCR primers could not be designed.

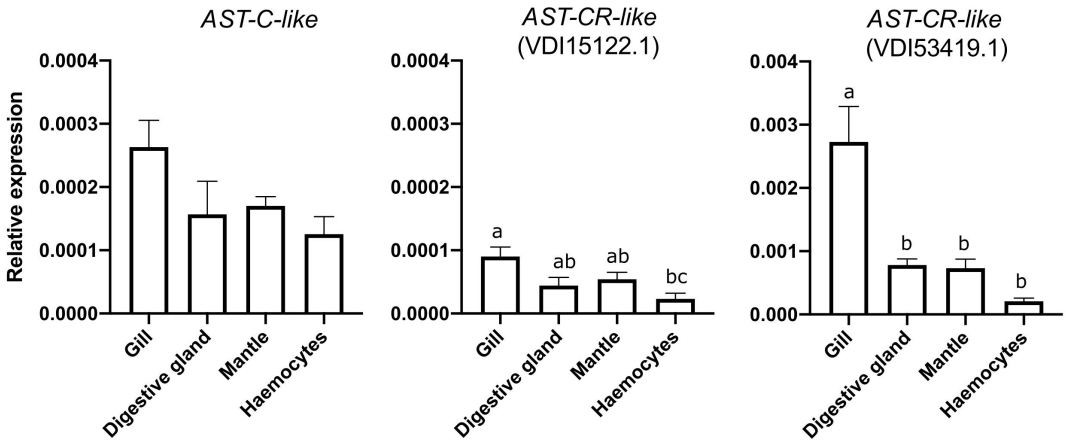

Figure 4.8. Tissue distribution of the AST-C-like precursor and two receptor transcripts in the bivalve *M. galloprovincialis*. Gene expression levels were normalized using the geometric mean of two reference genes (EF1α and 18S). The results are represented as the mean ± SEM of three (n = 3) biological replicates. Significant differences are denoted by different letters and statistical analysis was determined using One-Way ANOVA in GraphPad Prism version 8.0.0 software for Mac OS X.

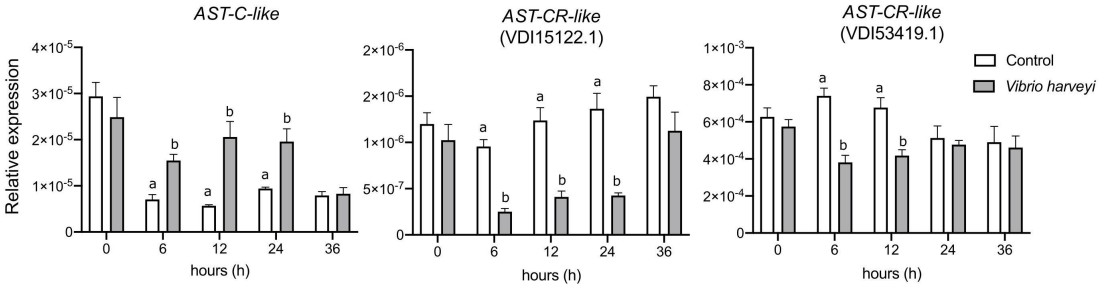

Figure 4.9. Effect of an immune challenge on AST-C-like precursor and receptor expression in the mantle of the bivalve *M. galloprovincialis*. Mantle edge samples were collected at 0, 6, 12, 24 and 36 hours after exposure to heat-inactivated *V.*

harveyi. The expression of two AST-CRs-like (VDI15122.1 and VDI53419.1) was analyzed. Gene expression levels were normalized using the geometric mean of two reference genes (EF1α and 18S). The results are presented as the mean ± SEM of six (n = 6) biological replicates per group / sampling point. Significant differences are denoted by different letters between control and immune challenged mussel mantle at each timepoint were detected using two-way ANOVA and a Sidak's multiple comparison test in GraphPad Prism version 8.0.0 software for Mac OS X.

To assess if the AST-C-like system was modified by an immune challenge, the immune response of *M. galloprovincialis* to heat-killed *V. harveyi* was assessed by measuring by qRT-PCR the change in expression of innate immune-related genes. TLRa was significantly up-regulated 6h ($p < 0.001$) and 12 h ($p < 0.05$) after an immune challenge and LYG1 was significantly down-regulated at 6 h ($p < 0.05$) and complement-like C345i was not significantly changed (Supplementary Figure 4.6). The AST-C-like peptide precursor and receptor expression was modified after exposure to heat-killed *V. harveyi* (Figure 4.9). The AST-C-like precursor was significantly up-regulated 6 h ($p < 0.05$), 12 h ($p < 0.0001$) and 24 h ($p < 0.01$) after an immune challenge. AST-CR-like VDI15122.1 was down-regulated at 6 h ($p < 0.01$), 12 h ($p < 0.001$) and 24 h ($p < 0.0001$) and AST-CR-like VDI53419.1 was down-regulated at 6 h ($p < 0.0001$) and 12 h ($p < 0.01$) after exposure to heat-killed *V. harveyi* (Figure 4.9). The qRT-PCR expression data corroborated the LPS transcriptome data of the AST-C-like system (peptide precursor and receptors) under an immune challenge in *M. galloprovincialis*.

4.5. Discussion

The homologues of the arthropods AST-A, AST-B/MIP and AST-C systems and

their function have been poorly described in the second largest animal phylum, the Mollusca. To better understand the peptide and receptor evolution and function a comparative approach was taken paying particular attention to the shelled molluscs (the bivalves) a group of ecologically and commercially important species. In molluscs, homologues of the three arthropod peptide groups (named buccalin, MIP and AST-C-like) and their corresponding receptors were identified. The sequence similarity between the mollusc and insect peptides and receptors was low but aa motifs involved in peptide and receptor structure were well conserved. In molluscs the peptide precursor and receptors evolved via lineage and species-specific events with receptor gene family expansions found in some species. The buccalin and MIP precursors encoded several mature peptides with differing aa sequences and sizes suggesting that they may have differing affinity or potencies for the corresponding receptors and may modulate distinct biological functions. Expression of all elements of the buccalin, MIP and AST-C-like systems were detected in the bivalve mantle and changes in the AST-C-like peptide and receptor transcripts in response to a bacterial immune challenge in *M. galloprovincialis* revealed that this neuropeptide system may contribute to the immune response in Mollusca.

Diversity of Mollusca peptides and receptors

In molluscs homologue peptide precursors and receptors of the arthropod AST-systems were found. The potential peptides produced, and their putative receptors were more numerous than in *D. melanogaster* and other insects. In common with the insects and other arthropods AST-A and AST-B/MIP, the buccalin and MIP

mature peptides in Mollusca were encoded by long protein precursors containing multiple mature peptides with distinct amino acid sequences but well conserved motifs important for bioactivity (Miller et al., 1993; Veenstra, 2010; Cardoso et al., 2016; Zhang et al., 2018; Oliveira et al., 2019; Sharker et al., 2020). The results of phylogenetic analysis from the present and previous studies (Mirabeau and Joly, 2013; Cardoso et al., 2016; Elphick et al., 2018) revealed that the Mollusca and Arthropoda receptors shared a common origin. The general sequence and structural conservation of the mollusc peptides and receptors with the arthropod AST systems homologues suggests functional conservation is likely across the protostomes.

In molluscs, buccalins were originally isolated from neuronal elements in the accessory radula closer (ARC) muscle of the gastropod *A. californica* and regulate food-induced arousal (Cropper et al., 1988). In arthropods including insects a single gene for the AST-A precursor has been described. In *D. melanogaster* the AST-A peptides share a conserved FGL-amide terminus but the sequences of the orthologue peptides in molluscs was very different although a conserved L-amide C-terminus existed but, in some gastropods and cephalopods I-amide C-terminal peptides were also found. A second AST-A peptide precursor previously proposed to contain buccalin-like peptides that terminated with a V-amide (Cardoso et al., 2016) was exclusive to molluscs and has recently been assigned to the LASGLV-amide family (Veenstra, 2010; Zhang et al., 2018; Oliveira et al., 2019). The two buccalin precursors recently described in the gastropod Pacific abalone (*Haliotis discus hanna*) are authentic as they both encode C-terminal L-amide peptides (Sharker et al., 2020)

as well as the *C. ventricosus* and *P. maculate* precursors identified in this study. The longest and most peptide rich buccalin precursors were found within the gastropods, in the cephalopod *N. pompilius* and in the polyplacophore *A. granulata*. In bivalves, the number of buccalin L-amide peptides varied from 7 to 11 and peptide sequence conservation within each species precursor was distinct and may indicate they have different functions. Despite the large variety of putative buccalins only a single homologue of the arthropod AST-AR was found in most of the species analyzed suggesting that alternative receptors activated by buccalins may exist. It would be interesting to test if molluscan buccalins are the cognate peptide activators of the KISSR/GALR-like since protostome AST-A and AST-ARs are proposed to share a common evolutionary origin with the metazoan KISSR and GALRs (Lenz et al., 2000; Mirabeau and Joly, 2013; Felix et al., 2015; Cardoso et al., 2016; Elphick et al., 2018). Putative KISSR-like and GALR-like were identified in molluscs and in annelids (this study and (Felix et al., 2015; Cardoso et al., 2016)) but our searches in Mollusca failed to identify orthologues in the genome of several of the species.

The MIP peptide precursors in molluscs in common with arthropod homologues encodes for multiple peptides with a similar structure. All mollusc and arthropod deduced mature peptides were C-terminal amides and possessed two conserved tryptophan residues previously shown to be important for peptide bioactivity (Coast and Schooley, 2011). However, the consensus W(X6 / 7)W-amide sequence in Arthropoda AST-B/MIP peptides (Verlinden et al., 2015) was modified to W(X4-7)W-amide in Mollusca MIPs. Gastropod MIP precursors produced the largest

variety of peptides and in *L. gigantea* 25 peptides were predicted, which was 5 times higher than in the insect *D. melanogaster*. Like the insects, *D. melanogaster* and *T. castaneum* a single AST-BR/MIPR was identified in most gastropods and in cephalopods. In contrast, bivalves possessed three receptor type genes that arose prior to the divergence of the molluscs and arthropods by gene duplication. In insects, AST-B/MIP share the same receptor as insect sex peptide, a.k.a. accessory gland peptide, which in *D. melanogaster* is 36 aa in length. The single gastropod *A. californica* MIP-R has been deorphanized but the species MIP peptides (Kim et al., 2010) and the newly identified bivalve MIP-Rs (type II and III) found in this study remain to be characterized with the MIP peptides as the obvious choice of ligand. The degeneration of functionally important rhodopsin-family receptor motifs such as DRY (in ICL2) and NSxxNPxxY (where x represents any aa) within TM7 previously reported in arthropod AST-BR/MIP-R also existed in the mollusc homologue receptors (Fritze et al., 2003; Rovati et al., 2007; Verlinden et al., 2015). MIP and MIP-R were present in all species analysed, except *B. glabrata* and it is unclear if this was due to the genome quality or if they were deleted from the genome.

In molluscs the AST-C-like peptide precursor generated a single peptide as observed in arthropods. The AST-C mature peptides were characterised by two conserved cysteine motifs in arthropods (Veenstra, 2010, 2016; Zhang et al., 2018; De Oliveira et al., 2019; Sharker et al., 2020), which were proposed to determine peptide structure and function and they were also conserved in mollusc AST-C-like suggesting they may be important for function. Nonetheless, despite superficial

sequence similarities the evolutionary model underpinning the AST-C/AST-C-like systems in arthropods and molluscs diverged. In arthropods three genes encode three different peptide precursors (AST-C, CC and CCC) (Veenstra, 2016; Chang et al., 2018)and generally only one or two AST-CR exist (Kreienkamp et al., 2002; Mayoral et al., 2010; Caers et al., 2012). In the case of molluscs, a single gene encodes the peptide precursor (except in the gastropod *C. unifasciata* that contains two identical mature peptide genes), but a larger number of putative AST-CR-like exist compared to arthropods. In molluscs the receptor number was generally conserved apart from in the bivalves and specifically the *Mytilidae* family where lineage and species-specific events caused expansion of the AST-CR-like (type I). The oysters possessed the protostome AST-CR-like type I and an additional AST-CR-like type II that according to the phylogeny diverged from other lophotrochozoan receptors. Genome analysis of the lophotrochozoans revealed that they are tandem duplicates with the AST-CR-like type I gene suggesting that after gene duplication in the ancestral *Ostreoidea* the AST-CR-like type II duplicate considerably diverged.

The identification in molluscs of homologues of the arthropod AST peptide precursors with the potential to produce multiple mature peptides with distinct sequences and of AST-Rs that emerged from lineage/species-specific expansions in molluscs suggests that the diversity and complexity of this neuropeptide system is higher than in arthropods. The functional role of the arthropod AST-like system in the molluscs and other Lophotrochozoans remains to be studied but its diversity suggests it may be pluripotent. In the future, deorphanization of the multiple receptors within

the Mollusca with the corresponding peptides will help to understand the peptide-receptor interactions and provide a route towards the establishment of functional studies.

Evolutionary scenarios for the protostome AST-like system and discovery of GALR-like receptors in molluscs

The lack of sequence conservation and distinct peptide precursor organization of the three protostome AST-like peptide families (AST-A/buccalin, AST-B/MIP and AST-C/AST-C-like) is indicative of their different evolutionary origins. This contrasts with the common evolutionary origin proposed for cognate receptor families. The presence of both peptide precursors and receptors in arthropods and molluscs suggested that they emerged prior to the ecdysozoans-lophotrochozoan divergence and shared a common origin and functional conservation with homologue systems in vertebrates. The protostome AST-A/Buccalin systems are homologues of the highly studied deuterostome GALR/KISS systems and the AST-C/AST-C-like system is suggested to be the counterpart of the vertebrate SST-system in protostomes (Kreienkamp et al., 2002; Caers et al., 2012; Cardoso et al., 2012; Jékely, 2013; Mirabeau and Joly, 2013; Felix et al., 2015). For AST-B/MIP no homologue neuropeptide system has been described but receptor clustering with the vertebrate orphan receptors, GPR139/142, suggests that they may be evolutionary related. The function of GPR139/142 is poorly understood, and in mammals GPR139 is mostly expressed in the CNS and is suggested to regulate movement and food consumption/metabolism (Vedel et al., 2020).

In our study we uncovered a novel mollusc GALR-like clade which only persisted in cephalopods. Previously we showed that putative GALR-like receptors were also present in annelids (Felix et al., 2015; Cardoso et al., 2016) and the identification of homologues in other lophotrochozoans revealed that the GALR-like receptor clade emerged early but was selectively deleted from the genomes of several species. The GALR-like is the protostome orthologue of the deuterostome GALRs and changes the currently accepted paradigm that AST-AR/Buccalin-R are the protostome GALR representatives. In a previous study we proposed that the AST-ARs/Buccalin-Rs were more related with KISSR than with the GALRs. However, the inclusion of more family members in the present study clustered the mollusca and other lophotrochozoan Buccalin-Rs and insect AST-ARs closer to the GALRs suggesting an alternative evolutionary scenario. Comparisons of the gene environment of AST-AR and GALRs in the annelid (*C. teleta*), insect (*D. melanogaster*) and vertebrate (*H. sapiens*) revealed orthologue genes. The GALR-like genome region in *C. teleta* possessed genes shared in the genome region flanking arthropod AST-AR and human GALR2 suggesting that the protostome GALR-like and vertebrate GALR genome regions are related and that the ancestral genes of metazoan GALR and protostome AST-ARs may have emerged from a common genome region in the early bilaterian genome prior to the protostome and deuterostome divergence. The Buccalin-R genome regions in *C. teleta* only shared genes with the equivalent AST-AR genome regions in *D. melanogaster* and no orthologues were found in human GALR or KISSR genome regions. Nonetheless, the

evolutionary scenario that gave rise to the protostome ancestral AST-ARs, metazoan KISSR and GALR genes is difficult to resolve since protostomes and deuterostomes are suggested to have diverged approximately 535 million years ago (Budd and Jensen, 2017; Budd and Mann, 2020) according to fossil records and global, lineage and species-specific genome events may have blurred evolutionary traits.

AST-C-like system and mantle immune function in *M. galloprovincialis*

In protostomes innate immunity is the main defence against pathogens. This system provides an immediate and effective response and depends on haemocytes that circulate in the haemolymph and humoral factors like lysozymes, complement-like molecules, peptidoglycan-recognition proteins (PGRPs) amongst others (Allam and Raftos, 2015; Schultz and Adema, 2017; Bouallegui, 2019). Recent studies have revealed that immune factors in bivalves and molluscs are highly diverse due to species-specific expansions (Allam and Raftos, 2015; Zhang et al., 2015; Gerdol, 2017; Moreira et al., 2018; M Batista et al., 2019; Rosani et al., 2019; Vogeler et al., 2021; Peng et al., 2024). The diversity of bivalves, their adaptation to highly diverse environments, the plethora of pathogenic microorganism to which they are exposed, and their very different susceptibilities makes them excellent model systems to understand how environmental adaptation has shaped the immune system.

In arthropods, the role of the AST families in immunity is poorly resolved. In the haemolymph of the cockroach *Diploptera punctate* ASTs were suggested to be important regulatory peptides of the immune response (Skinner et al., 1997) and in *Litopenaeus vannamei*, transcripts for the three AST peptide precursors (AST-A,

AST-B/MIP and AST-C) were up-regulated in the haemocytes 6 hours after infection with the white spot syndrome virus (Wang et al., 2019). In *Scylla paramamosain* both AST-B/MIP and AST-BR/MIP-R were significantly induced in haemocytes and in the hepatopancreas after immune challenge and animals treated with AST-B/MIP had increased expression of pro-inflammatory cytokines and immune-effectors and receptor knock-down impaired the innate immune response to bacterial proliferation (Xu et al., 2020, 2021). The only report that links the AST-C system to immunity was performed in *D. melanogaster* where ASTC-R1 and R2 were up-regulated by pathogenic bacteria and ASTC-R2 knock-down significantly decreased survival (Bachtel et al., 2018). The effect of the AST-C system was linked to modulation of the "inhibition of immune deficiency" (Imd) pathway (Bachtel et al., 2018). The Imd pathway controls anti-bacterial peptide gene expression in the fat body in response to gram-negative bacterial infections and the pathway is suggested to be similar to the mammalian TNF-a pathway (Khush et al., 2001; Davoodi et al., 2019).

The orthologues of the arthropod AST families had a particularly high expression in the bivalve mantle (Zhang et al., 2012; Moreira et al., 2015; Bjärnmark et al., 2016; Wang et al., 2017; Yang et al., 2021) a mucosal surface where host-pathogen interactions are initially established (Allam and Espinosa, 2016). Expression analysis (qRT-PCR and transcriptome analysis) indicated that the AST-C-like system was highly expressed in the bivalve mantle and mantle transcriptome data revealed modified AST-CR-like expression after a bacterial LPS challenge. The activation of the immune response in *M. galloprovincialis* exposed to a pathogen challenge was

revealed by the significantly modified mantle expression of TLRa and LYG1 and was associated with a significant change in expression of the AST-C-like system. However, in contrast to what was described in *D. melanogaster* down-regulation of the receptors occurred in *M. galloprovincialis* mantle. The basis for the divergent response of the AST-C/AST-C-like system between *D. melanogaster* and *M. galloprovincialis* was not determined but may result from the character of the immune challenge used. In molluscs, homologues of the vertebrate TNF-a and TNFR have been described and shown to respond to infection (Zoysa et al., 2009; Li et al., 2009). However, if the AST-C-like system in bivalves modulates TNF-a and TNFR is unstudied and further work using targeted gene knock-down approaches or overexpression studies and defining the peptide-receptor pairs and their response to different pathogens will be required to characterize in detail the molecular basis of the innate immune response.

4.6. Conclusion

Peptide and receptor homologues of the arthropod AST-A, AST-B and AST-C types existed in molluscs. The diversity of AST peptides and receptor members found, and their widespread tissue distribution in molluscs suggests they are pluripotent factors that modulate a diversity of physiological processes. The mature peptides and receptor members (Buccalin, MIP and AST-C-like) were distinct across mollusc species, and this suggests that the AST families may be as complex as the neuropeptide system described in insects and other arthropods.

Phylogenetic analysis confirmed that receptors are specific to protostomes and emerged early in evolution prior to the Lophotrochozoa and Ecdysozoa divergence. In a previous study (Cardoso et al., 2016) we proposed that AST-ARs/Buccalin-Rs were most closely related to the metazoan KISSRs. In the present study by including AST-CRs in the phylogenetic analysis we found that they grouped with metazoan GALRs. Short-range gene linkage analysis of annelid genomes (the only protostomes where genes for Buccalin-R, GALR and KISSR persisted) confirmed that AST-AR and GALRs may be more evolutionary proximate, and we revised our previous evolutionary model for the protostome AST-ARs/Buccalin-Rs. In addition, we revealed for the first time the existence of Mollusca GALR-like genes in cephalopod genomes, and they were also present in annelids and a few other lophotrochozoans. This reveals that AST-AR/Buccalin-Rs evolved as a separate lineage and are not the orthologues of vertebrate GALRs as previously accepted.

Peptide precursors that encode for multiple mature peptides that diverge in sequence and the existence of lineage and species-specific duplicate receptors in molluscs suggests that the function of the Buccalin, MIP and AST-C-like systems may be distinct across species and that adaption to different environments may have affected gene evolution. Meta-analysis of tissue transcriptomes revealed that the Buccalin, MIP and AST-C-like systems have a broad tissue distribution and varying abundance in several different bivalves, indicating it is an omniscient regulatory factor of the molluscan neuropeptide repertoire. The administration of an immune challenge to *M. galloprovincialis* significant changed the expression of the

AST-C-like peptide and receptor genes supporting its role in immunity and hinting at conservation of this function across protostomes. Overall, our study provides for the first time a comparison of the homologues of the three arthropod AST-systems across different molluscs and contributes to a better understanding of their evolution and function in protostomes.

4.7. Supplementary materials

All the supplementary materials are provided in the Annex III in digital format.

CHAPTER 5

General discussion

5.1. General discussion

The phylum Mollusca is the second largest phylum after Arthropoda. Mollusca, particularly the bivalves are of increasing economic importance to the aquaculture food industry, and they also play significant ecological roles in marine environments. Bivalves are major components of global benthic and planktonic (larval) marine ecosystems. The shell is a hallmark of bivalves and this naturally biomineralized structure is crucial for their survival. Their shells are primarily composed of minerals (95% $CaCO_3$), with biomineralized crystals deposited within an organic matrix made of proteins and polysaccharides, which is secreted by the mantle. Although a "biomineralization toolbox" of the shell has been characterized, the regulation of shell growth and biomineralization still remains poorly understood. The mantle is innervated by ganglia containing neuropeptides and other factors (such as neurotransmitters), but if they regulate mantle function and shell formation is still unclear. Understanding the role of these factors in mantle function and the complex mechanisms controlling mantle physiology and shell formation is a challenge in biology.

The present thesis aimed to advance the state of the art about the regulation of shell production in bivalves. The thesis is focused on an economically important bivalve: the Mediterranean mussel (*M. galloprovincialis*), a bivalve with a symmetrical shell, that has a regular shape, is brittle and composed primarily of calcium carbonate. The study investigated the role of neuropeptide genes on the bivalve mantle and the organization and some of the functions of the *M.*

galloprovincialis nervous system. The regulatory effects of neuropeptides on the mantle and shell formation were explored, as well as the role of the nervous system/ganglia on biomineralization toolbox genes. Specifically, the discussion is divided into three aspects: 1) exploration of the mantle transcriptome of *M. galloprovincialis*, to identify the diversity of neuropeptide precursor genes expressed in the mantle and the effect of the nervous ganglia on mantle neuropeptide expression and function during shell regeneration (Chapter 2); 2) Establishment of approaches to determine the role of the nervous system in shell formation by analyzing changes in the mantle transcriptome of *M. galloprovincialis* with intact and damaged ganglia commissure, and identify biomineralization genes regulated by the nerve ganglia (CPG), and the putative role of lncRNA during shell biomineralization (Chapter 3). 3) Explore the function of the Allatostatin system in the *M. galloprovincialis* mantle (Chapter 4).

5.1.1 Neuropeptides regulate bivalve shell regeneration (Chapter 2)

Bivalve shells exhibit diverse forms, patterns, and colours (Paula and Silveira, 2009). The mantle is the main organ that builds the shell in bivalves, with shell growth depending on its secretions (Marin et al., 2012; Suzuki and Nagasawa, 2013). To understand how the shell is produced, various bivalve mantle transcriptomes and proteomes have been produced (Bjärnmark et al., 2016; Carini et al., 2019). Analyzes of the molecular resources established that a conserved "biomineralization toolbox" exists in bivalves for shell production, and it includes enzymes, matrix proteins, ion channels, and species-specific genes (Yarra et al., 2021). Studies on gastropod shell

production suggests that the neuroendocrine system may controls shell formation. In *Helisoma*, shell damage has been found to alter the appearance of neurosecretory cells in the VG, and differences in shell growth are related to neurosecretory activity in the brain (Dillaman et al., 1976; Saleuddin and Kunigelis, 1984). In the mantle transcriptome of bivalves, neuropeptides and their putative receptors have been identified, and may act as regulators of mantle function (Cardoso et al., 2016; Li et al., 2021). Additionally, it has been concluded that homologues of the mammalian CALC systems my regulate calcium uptake and turnover and may be key factors in shell formation by the mantle of *M. galloprovincialis* (Cardoso et al., 2020). However, the interaction between calcitonin and other neuropeptides in the mantle, as well as their mode of action in regulating shell growth remains unknown. Taking into consideration that the role of neuropeptides and the bivalve nervous system in shell formation was the focus of this thesis. A combination of experiments and multiple analytical approaches in this thesis revealed that neuropeptides are key regulators of bivalve shell growth.

The nervous system in bivalves is not well characterized and, in this thesis, new insights about the innervation of the mantle were provided through immunochemistry using *M. galloprovinciallis* as the representative species. The results revealed that the mantle in *M. galloprovincialis* like in other species is organized into three folds, which are likely to have specific functions based on previous studies in bivalves (Yonge, 1957, 1983). FMRF immunopositive fibers in *M. galloprovinciallis* revealed that the mantle is highly innervated by a complex network of secretory and

neuropeptide fibers and contains large clusters of cell bodies, as reported in other molluscs (Saleuddin and Dillaman, 1976; Audino et al., 2015). Analysis of a previously generated mussel (*M. galloprovincialis*) mantle transcriptome (Peng et al., 2023) showed that the mantle edge, a region primarily associated with shell growth, expressed a large number of neuropeptide transcripts. Homologues of some of the neuropeptide transcripts in the *M. galloprovincialis* mantle were identified in the ganglia the Pacific oyster (*M. gigas*) and the scallop (*M. yessoensis*). Taken together the present and previous results in bivalves indicate the existence of an evolutionary conserved CPG-mantle neuroendocrine regulatory network in bivalves.

Biomineralization is a biologically controlled process in which organisms produce mineralized structures (Saleuddin and Wilbur, 2012). This thesis developed a shell damage - repair model in *M. galloprovincialis* and found that it takes 20 days for the shell to be completely repaired, and the highest rate of shell repair occurred in the first 5 days after damage (the repair rate is more than 60%) and was associated with the synthesis of a thin layer of biomineralized materials. Neuropeptide precursors with a significantly altered gene expression in the mantle and CPG were identified during early stages of shell repair, including APWG-amide, myodulin, LFRF-amide, FxRI-amide, and LFRY-amide precursors. These peptides have previously been described to regulate mollusc reproduction and growth (Lange et al., 1998; Bernay et al., 2006; Koene, 2010; Morishita et al., 2010). The results with the shell regrowth model indicate that shell damage and regeneration are associated with significant ($p < 0.05$) changes in the expression of some candidate neuropeptide genes in the mantle

and CPG. To test if the changing patterns of gene expression had functional consequences the CALC neuropeptides, CALCIa and CALCIIa, were injected into (*M. galloprovincialis* and were found to promote the formation of closely packed needle-like aragonite, prismatic crystals of mineralized calcium carbonate. Peptides found in the mantle transcriptome but not hitherto attributed shell repair-related functions such as MYOc, promoted shell repair but not crystal formation. Further experiments are needed to better characterize the role of the multiple neuropeptides found in bivalve mantle transcriptomes to determine their function.

Currently, studies of the nervous system structure and function in bivalves are not sufficiently comprehensive. The neural system has a very variable anatomy and organization in bivalves, but the common elements are a network of nerve fibers that interlink three pairs of symmetrical ganglia to different parts of the body (CPG, VG and PG) (Kotsyuba et al., 2020). Neuropeptide precursors have been identified associated with reproduction and growth in transcriptomes and proteomes of nerve ganglia in the Pacific oyster and scallop (Zhang et al., 2018; Réalis-Doyelle et al., 2021). In this thesis, the CPG was analysed from the perspective of its role in shell formation and using transcriptomics numerous neuropeptide precursor genes were identified suggesting they have an important role in the nervous system of bivalves. The CPG in bivalves is similar to the cerebral ganglia in gastropods because they innervate some of the same areas (adductor muscles, visceral nerve ring). Additionally, they innervate the anterior part of the mantle (via the anterior pallial nerve) and the labial palps, mouth, and esophagus (Ponder et al., 2019).

Earlier studies of bivalves identified the nervous system from an anatomical perspective and indicated that the posterior mantle is mainly regulated by the VG (Siniscalchi et al., 2004). However, the present study found that severing the commissure of the CPG ganglia hindered shell repair, while severing the commissure of the VG ganglia did not have this effect. This indicates that the nerve fibers projecting from the CPG ganglia regulate the function of the posterior mantle in *M. galloprovincialis* and highlights the need for more studies. Although the secretory function of the mantle is crucial for shell repair, this thesis provides evidence that the movement of the mantle is also important for shell regeneration but is not affected by damage to the VG or CPG commissure. Thus, damage to the commissure between the bilateral CPG ganglion directly affected the secretory activities associated with shell formation by the mantle edge but it did not affect the motor circuit fibers controlling mantle movement. After severing the commissure between the CPG ganglia, alterations were observed in the nerve tracts and cell bodies in the mantle, as well as in the organization of the nerve fibers and cell bodies of the CPG and VG ganglia. This suggests that the coordinated growth and maintenance of the bilateral bivalve shell by the mantle in the *M. galloprovincialis* is regulated by the nervous system including the ganglia. I propose that this regulatory study exists across the bivalves when the anatomical organization of their nervous system is considered and represents a fruitful field for future studies. To sum up, this thesis provides histological, molecular, and functional evidence demonstrating the role of the nervous system and neuropeptides in shell formation in the *M. galloprovincialis*. The

identified mechanism is likely to be conserved across bivalves and shelled molluscs since they share a similar nervous system, a common mantle biomineralization toolbox and shell structure.

5.1.2 Genes related to shell biomineralization in the mantle transcriptome are regulated by nerve ganglia (CPG) (Chapter 3)

Biomineralization is one of the oldest and most fascinating processes in the animal kingdom, dating back to the late Proterozoic era (Knoll, 2003). The evolutionary success of molluscs is attributed to their protective shells composed of $CaCO_3$. The mantle, located beneath the shell, is responsible for biomineralization, making it the most crucial tissue in this process (Uozumi and Suzuki, 1979; Marin et al., 2007). In the previous chapter of this thesis, I demonstrated the significant regulatory role of the nervous system and neuropeptides in shell formation, with the CPG ganglia being particularly crucial in regulating shell regeneration. To further elucidate the connection between the CPG ganglia, bivalve mantle, and shell biomineralization, I conducted a transcriptome analysis of the mantle. Here, the left and right sides of the bivalve mantle were analyzed separately something that has not previously been reported in symmetric bivalves. The results showed that the number and abundance of genes in the right mantle were higher than in the left mantle. Shell sanding did not change this trend, but severing the CPG commissure significantly increased the differentially expressed genes (DEGs) between the left and right sides, and the trend changed such that the number and abundance of genes were higher on

the left side. This raises interesting questions about the mechanisms behind whole organism co-ordination of shell growth. I hypothesize that *M. galloprovincialis* mantle gene expression is not completely symmetrical or synchronous and that the CPG likely plays a regulatory role in coordinating the expression of genes in the left and right mantle.

Although shell formation in molluscs is considered an extracellular process controlled by an organic matrix, evidence suggests that the mantle tissue may directly regulate shell turnover (Checa et al., 2016a, 2016b). Shell regeneration/repair is a critical process in shell formation. In current research, shell regeneration induced by artificial damage is widely used to reveal the shell formation process because regenerated shells are similar to normal shells (Chen et al., 2018; Crane et al., 2021; George et al., 2022). Therefore, in the experiments reported in this thesis, deliberate and standardized shell damage was applied to investigate gene regulation in the mantle related to shell regeneration. Using WGCNA analysis, genes associated with shell sanding were identified in the left and right mantle of *M. galloprovincialis* with sanded shells or sanded shells and a damaged CPG commissure. A comparative analysis of the genes associated with damage to the CPG commissure identified 81 genes associated with both biomineralization and nervous tissue. The biomineralization toolbox (Jackson and Degnan, 2016) genes identified included TFs, GPCRs, SMPs, transporters, ion transporters, neuropeptides, and lncRNA and were significantly increased in the right mantle after shell sanding but decreased to normal levels after severing the CPG commissure. Furthermore, prediction of the subcellular

localization of the gene products revealed a significant separation of candidate genes in the cell membrane between the left and right sides. Considering the transcriptome results and the results about neuropeptides, I speculate that membrane proteins such as GPCRs, ion transporters, and transporters may regulate shell biomineralization and are controlled by the CPG since they were affected when the commissure was cut. In previous studies, the host group identified the CALC receptor (GPCR) in the bivalve mantle and demonstrated that this system is a candidate regulator of shell mineralization (Cardoso et al., 2020) and the identified ion transporters regulate the concentration of ions such as calcium and carbonate, important for the mineral phase (Wilbur and Saleuddin, 1983).

Importantly, lncRNAs make up 27.16% of the candidate DEGs in sanded shells or sanded shells with a severed CPG commissure, the highest proportion aside from other unannotated proteins. Recent studies by Peng et al. have provided evidence that lncRNAs can regulate shell growth and identified new biomineralization candidate genes and regulatory lncRNAs (Peng et al., 2023). Experimental evidence from other studies also found lncRNAs in the bivalve mantle transcriptome and linked them to the regulation of shell formation (Zhang et al., 2020a; Cai et al., 2022). Based on the existing evidence, I hypothesize that lncRNAs are local regulatory factors and that the nervous system coordinates the biomineralization process in the two valves of the bivalve. Future studies should test the applicability of this hypothesis to assess regulatory processes in *M. galloprovincialis* but also across the bivalves in general.

In conclusion, a meta-analysis of the mantle transcriptome in *M.*

galloprovinciallis identified genes related to biomineralization and suggested that the CPG likely regulates these genes in the mantle. Additionally, lncRNAs were highly enriched among the candidate differential expressed genes involved in the biomineralization process, and this highlights their importance in this process (Chapter 3). However, the organization and integration of the shell producing function of the mantle on the right and left side of the animal and locally remains unclear, as does their regulation and this will be a key focus for future research.

5.1.3 The AST-C family has a putative function in immunity in bivalve (Chapter 4)

Neuropeptides play different roles in molluscs, most of which are related to growth, reproduction, sexual behavior or others. However, many mollusc neuropeptides still do not have an identified cognate receptor. In chapter 4, the function of one of the better studied neuropeptide systems, the Allatostatin system, which is present in the mantle was studied. Allatostatin (AST) is a large family of diverse, multifunctional neuropeptides, originally described in insects to be inhibitors of juvenile hormone (JH) (Lorenz et al., 1995; Nässel, 2002). There are three AST peptide families, which share very little sequence similarity, named Allatostatin A (AST-A), B (AST-B), and C (AST-C). AST peptides and peptide precursors have been isolated from various arthropods, where they likely regulate a diversity of physiological activities (Verlinden et al., 2015; Wu 2020). In arthropods, they have been shown to play a role in immunity (Bachtel et al., 2018; Wang et al., 2019; Xu et al., 2021). However, in Mollusca, the genes, molecules and functions of the AST system are relatively poorly described. To better understand the evolution and

function of neuropeptides and receptors of AST in Mollusca, we specifically focused on a bivalve, *M. galloprovincialis*, and studied the neuropeptides of the AST system.

In previous studies, molluscan homologue peptide precursors and receptors of the arthropod AST system were identified. Several of the peptides in Molluscs, share conservation of amino acid sequences that are crucial for their activity in insects (Miller et al., 1993; Cardoso et al., 2016). In my thesis phylogenetic analyses of the AST receptors suggests that the AST receptors in molluscs and arthropods share a common origin, as well as a conserved function. In contrast to the common evolutionary origin of the AST receptor family, the three AST peptide families had low sequence conservation and their different peptide precursor structures and phylogeny suggested that they had different evolutionary origins. The AST-A/Buccalin system is homologous to the vertebrate GALR/KISS system in deuterostomes, while the AST-C system corresponds to the vertebrate SST system (Kreienkamp et al., 2002; Cardoso et al., 2012; Mirabeau and Joly, 2013; Felix et al., 2015). Although the homologue neuropeptide system of AST-B has not been described, the clustering of the receptors with vertebrate GPR139/142 suggests the cognate peptides may be of evolutionary relevance (Vedel et al., 2020).

It is well known that the primary defense of bivalves against pathogen attack is innate immunity, which relies on circulating blood cells and humoral factors in the haemolymph. Research indicates that due to species-specific expansions, the immune factors of bivalves and molluscs are highly diversified (Allam and Raftos, 2015; Rosani et al., 2019). Bivalves exhibit strong adaptability to a wide diversity of

environments and encounter a plethora of pathogens in their surroundings, thus how they adapt to their environment and how this has shaped their immune systems is of utmost importance. AST is considered an important regulatory peptide for the immune response in the hemolymph of cockroaches (Skinner et al., 1997). In crustaceans, specifically the shrimp *Penaeus vannamei*, AST has also been reported to respond to immune challenges. Specifically, following White Spot Syndrome Virus infection, the gene transcripts of three AST peptide precursors (AST-A, AST-B, and AST-C) are up-regulated in hemocytes (Wang et al., 2019).

In chapter 4, the transcriptomes of four bivalve species were analyzed, and the results indicated that the AST system is particularly highly expressed in the mantle, with high expression also observed in the gills, digestive gland, and nerve ganglia. Transcriptome data from the mantle showed that AST-CR expression changed after LPS challenge. A role in the immune response for AST-CR was reported in Drosophila and pathogen exposure up-regulated ASTC-R1 and R2, and when ASTC-R2 was knocked down it significantly reduced survival rates (Bachtel et al., 2018). To investigate the potential role of the AST system in the bivalve immune response, I exposed *M. galloprovincialis* to heat-inactivated *V. harveyi* in seawater and examined the response of immune-related genes. The results showed that in *M. galloprovincialis* exposed to pathogen challenge, TLRa and LYG1 were up-regulated in the mantle, and this was significantly associated with changes in the expression of the AST-C system. These results with the mantle support the role of AST-C in immunity and suggest that this function is conserved in protostomes. This study is the

first to compare the three AST systems in different molluscs and decipher their evolution and the function of members of the AST system in protostomes. The study reported in chapter 4 only scratches the surface of the functional diversity of the AST system in the bivalve mantle and opens up a new avenue for future research on the function of other neuropeptide systems.

5.2. Conclusion and future perspectives

In summary, this thesis research provides new insights into the function of the mantle and provides evidence supporting a crucial role for neuropeptides in regulating shell growth in bivalves. Damage to the CPG commissure affected shell regrowth and neuropeptide expression in the mantle. This indicates that neuropeptides and the nervous system regulate mantle function and shell growth in bivalves and reveals a probable role in local control of shell growth but also in coordinating the growth of the two shells in symmetric bivalves. This study supports the existence of a mantle-nervous regulatory system controlling shell growth. I hypothesize based on my results that genes regulating biomineralization in the mantle, may be under the regulation of the CPG.

From the immunofluorescence results, the shell-producing tissue, the mantle, is highly innervated and contains neuropeptide (FMRF)-positive fibers. Various genes for neuropeptides were detected in the mantle transcriptome, and their gene expression changed during shell regrowth and after severing the CPG commissure, indicating a potential link between the ganglia and the mantle. It was observed that

after damaging the CPG commissure, the shell did not regrow. However, shell regrowth was observed when CALC peptides were applied, confirming its regulatory role in the mantle and the involvement the CALC peptide system on biomineralization

It is well known that the mantle regulates shell formation and biomineralization in bivalves. Our transcriptome analysis indicates that in the bivalve *M. galloprovincialis* that has symmetric valves, gene expression in the left and right mantle is asymmetric, and damaging the CPG commissure altered the abundance and number of DEGs between the two sides. Applying WGCNA analysis identified biomineralization-related genes, and when compared to genes regulated by the CPG commissure, a significant portion were lncRNAs. After the CPG commissure was severed, genes that were significantly up-regulated in *M. galloprovincialis* with sanded shells to provoke shell repair were detected at basal levels despite the damage to the shell. I hypothesize that the CPG regulates biomineralization-related genes, supporting the existence of a mantle-nervous regulatory system and highlighting the importance of lncRNAs in the biomineralization process of bivalves.

The work in this thesis lays the foundation for an interesting and complex study of regulatory processes determining the mantles function in shell biomineralization. In the future, I aim to further clarify the distribution and functional evolution of the nervous system in bivalves and other phylogenetically informative Mollusca in the following aspects:

1) Locate, label, and classify the characteristic cell types in the ganglia (CPG, VG, mantle node) with the aim of obtaining the molecular characteristics of nerve cells at

the cellular level and using them for comparative analysis between species.

2) Screen and validate the regulatory mechanisms of target neuropeptides and lncRNA in the ganglia-mantle system.

3) Explore the biological significance of the asymmetric expression of mantle factors regulated by CPG. Although future work is challenging, it is crucial for understanding the evolution of the nervous system and functions in molluscs, and it may even provide fundamental insights into the functional mechanisms of the bilaterally symmetrical nervous system in humans (vertebrate).

Bibliography

Abdraba, A. M., and Saleuddin, A. S. M. (2000). Protein synthesis in vitro by mantle tissue of the land snail *Otala lactea*: possible insulin-like peptide function. *Can J Zool* 78, 1527–1535.

Adamson, K. J., Wang, T., Zhao, M., Bell, F., Kuballa, A. V, Storey, K. B., et al. (2015). Molecular insights into land snail neuropeptides through transcriptome and comparative gene analysis. *BMC Genomics* 16, 1–15.

Addadi, L., and Weiner, S. (1992). Control and design principles in biological mineralization. *Angewandte Chemie International Edition in English* 31, 153–169.

Aguilera, F., McDougall, C., and Degnan, B. M. (2014). Evolution of the tyrosinase gene family in bivalve molluscs: independent expansion of the mantle gene repertoire. *Acta Biomater* 10, 3855–3865.

Aguilera, F., McDougall, C., and Degnan, B. M. (2017). Co-option and de novo gene evolution underlie molluscan shell diversity. *Mol Biol Evol* 34, 779–792.

Ahn, S.-J., Martin, R., Rao, S., and Choi, M.-Y. (2017). Neuropeptides predicted from the transcriptome analysis of the gray garden slug *Deroceras reticulatum*. *Peptides (N.Y.)* 93, 51–65.

Aiello, E. (1970). Nervous and chemical stimulation of gill cilia in bivalve molluscs. *Physiol Zool* 43, 60–70.

Aiello, E. (1990). Nervous control of gill ciliary activity in *Mytilus edulis*. *Neurobiology of*

Mytilus edulis 10, 189–208.

Allam, B., and Espinosa, E. P. (2016). Bivalve immunity and response to infections: are we looking at the right place? *Fish Shellfish Immunol* 53, 4–12.

Allam, B., and Raftos, D. (2015). Immune responses to infectious diseases in bivalves. *J Invertebr Pathol* 131, 121–136.

Almagro Armenteros, J. J., Sønderby, C. K., Sønderby, S. K., Nielsen, H., and Winther, O. (2017). DeepLoc: prediction of protein subcellular localization using deep learning. *Bioinformatics* 33, 3387–3395.

Almagro Armenteros, J. J., Tsirigos, K. D., Sønderby, C. K., Petersen, T. N., Winther, O., Brunak, S., et al. (2019). SignalP 5.0 improves signal peptide predictions using deep neural networks. *Nat Biotechnol* 37, 420–423.

Alves, M. G., and Oliveira, P. F. (2013). Effects of non-steroidal estrogen diethylstilbestrol on pH and ion transport in the mantle epithelium of a bivalve *Anodonta cygnea*. *Ecotoxicol Environ Saf* 97, 230–235.

Anand, L., and Rodriguez Lopez, C. M. (2019). chromoMap: an R package for interactive visualization and annotation of chromosomes. *Biorxiv*, 605600.

Andrews, S. (2010). FastQC: a quality control tool for high throughput sequence data. Available at: https://www.bioinformatics.babraham.ac.uk/projects/fastqc/.

Aranaz, I., Acosta, N., Civera, C., Elorza, B., Mingo, J., Castro, C., et al. (2018). Cosmetics and cosmeceutical applications of chitin, chitosan and their derivatives. *Polymers (Basel)* 10, 213.

Arivalagan, J., Yarra, T., Marie, B., Sleight, V. A., Duvernois-Berthet, E., Clark, M. S., et al. (2017). Insights from the shell proteome: biomineralization to adaptation. *Mol Biol Evol* 34, 66–77.

Aucour, A.-M., Sheppard, S. M. F., and Savoye, R. (2003). 13C of fluvial mollusk shells (Rhône River): A proxy for dissolved inorganic carbon? *Limnol Oceanogr* 48, 2186–2193.

Audino, J. A., Marian, J. E. A. R., Wanninger, A., and Lopes, S. G. B. C. (2015). Mantle margin morphogenesis in *Nodipecten nodosus* (Mollusca: Bivalvia): new insights into the development and the roles of bivalve pallial folds. *BMC Dev Biol* 15, 1–22.

Audsley, N., and Weaver, R. (2009). Neuropeptides associated with the regulation of feeding in insects. *Gen Comp Endocrinol* 162, 93–104.

Avdelas, L., Avdic-Mravlje, E., Borges Marques, A. C., Cano, S., Capelle, J. J., Carvalho, N., et al. (2021). The decline of mussel aquaculture in the European Union: causes, economic impacts and opportunities. *Rev Aquac* 13, 91–118.

Bachtel, N. D., Hovsepian, G. A., Nixon, D. F., and Eleftherianos, I. (2018). Allatostatin C modulates nociception and immunity in Drosophila. *Sci Rep* 8, 7501.

Bailey, C. H., Bartsch, D., and Kandel, E. R. (1996). Toward a molecular definition of long-term memory storage. *Proceedings of the National Academy of Sciences* 93, 13445–13452.

Barreda, D. R., Hanington, P. C., Walsh, C. K., Wong, P., and Belosevic, M. (2004). Differentially expressed genes that encode potential markers of goldfish macrophage

development in vitro. *Dev Comp Immunol* 28, 727–746.

Bayne, B. L. (1971). Some morphological changes that occur at the metamorphosis of the larvae of *Mytilus edulis*., in *The Fourth European Marine Biology Symposium*, (Cambridge University Press), 259–280.

Bayne, B. L. (1979). Assessing effects of marine pollution. *Nature* 280, 14–15.

Bayne, B. L., Thompson, R. J., and Widdows, J. (1976). Physiology: I. *Marine mussel their ecology and physiology. Bayne, BL, Ed. Cambridge Scientific Press: UK*.

Beaz-Hidalgo, R., Balboa, S., Romalde, J. L., and Figueras, M. J. (2010). Diversity and pathogenecity of Vibrio species in cultured bivalve molluscs. *Environ Microbiol Rep* 2, 34–43.

Beedham, G. E. (1958). Observations on the mantle of the *Lamellibranchia*. *J Cell Sci* 3, 181–197.

Beedham, G. E., and Trueman, E. R. (1968). The cuticle of the Aplacophora and its evolutionary significance in the Mollusca. *J Zool* 154, 443–451.

Beninger, P. G., and Le Pennec, M. (2006). "Structure and function in scallops," in *Developments in aquaculture and fisheries science*, (Elsevier), 123–227.

Beninger, P. G., Veniot, A., and Poussart, Y. (1999). Principles of pseudofeces rejection on the bivalve mantle: integration in particle processing. *Mar Ecol Prog Ser* 178, 259–269.

Benjamin, P. R., Kemenes, G., and Staras, K. (2021). "Molluscan Nervous Systems," in

Encyclopedia of Life Sciences, 1–15. doi: https://doi.org/10.1002/9780470015902.a0029277

Berland, S., Delattre, O., Borzeix, S., Catonné, Y., and Lopez, E. (2005). Nacre/bone interface changes in durable nacre endosseous implants in sheep. *Biomaterials* 26, 2767–2773.

Bernay, B., Baudy-Floc'h, M., Zanuttini, B., Zatylny, C., Pouvreau, S., and Henry, J. (2006). Ovarian and sperm regulatory peptides regulate ovulation in the oyster *Crassostrea gigas*. *Molecular Reproduction and Development: Incorporating Gamete Research* 73, 607–616.

Bieler, R., Mikkelsen, P. M., Collins, T. M., Glover, E. A., González, V. L., Graf, D. L., et al. (2014). Investigating the Bivalve Tree of Life–an exemplar-based approach combining molecular and novel morphological characters. *Invertebr Syst* 28, 32–115.

Bigot, L., Beets, I., Dubos, M.-P., Boudry, P., Schoofs, L., and Favrel, P. (2014). Functional characterization of a short neuropeptide F-related receptor in a lophotrochozoan, the mollusk *Crassostrea gigas*. *Journal of Experimental Biology* 217, 2974–2982.

Bjärnmark, N. A., Yarra, T., Churcher, A. M., Felix, R. C., Clark, M. S., and Power, D. M. (2016). Transcriptomics provides insight into *Mytilus galloprovincialis* (Mollusca: Bivalvia) mantle function and its role in biomineralisation. *Mar Genomics* 27, 37–45.

Blaschko, H., and Milton, A. S. (1960). Oxidation of 5-hydroxytryptamine and related compounds by *Mytilus* gill plates. *Br J Pharmacol Chemother* 15, 42–46.

Boisson, F., Cotret, O., and Fowler, S. W. (1998). Bioaccumulation and retention of lead in the mussel *Mytilus galloprovincialis* following uptake from seawater. *Science of the total environment* 222, 55–61.

Bolger, A. M., Lohse, M., and Usadel, B. (2014). Trimmomatic: a flexible trimmer for Illumina sequence data. *Bioinformatics* 30, 2114–2120.

Bottjer, D. J. (1981). Periostracum of the gastropod Fusitriton oregonensis: natural inhibitor of boring and encrusting organisms. *Bull Mar Sci* 31, 916–921.

Bouallegui, Y. (2019). Immunity in mussels: an overview of molecular components and mechanisms with a focus on the functional defenses. *Fish Shellfish Immunol* 89, 158–169.

Broeck, J. Vanden (2001). Neuropeptides and their precursors in the fruitfly, *Drosophila melanogaster*. *Peptides (N.Y.)* 22, 241–254.

Budd, G. E., and Jensen, S. (2017). The origin of the animals and a 'Savannah'hypothesis for early bilaterian evolution. *Biological reviews* 92, 446–473.

Budd, G. E., and Mann, R. P. (2020). Survival and selection biases in early animal evolution and a source of systematic overestimation in molecular clocks. *Interface Focus* 10, 20190110.

Budelmann, B. U. (1995). "The cephalopod nervous system: what evolution has made of the molluscan design," in *The nervous systems of invertebrates: An evolutionary and comparative approach: With a coda written by TH Bullock*, (Springer), 115–138.

Bullock, T., and Horridge, G. A. (1965). Structure and function in the nervous systems of invertebrates.

Bullough, W. S. (1958). Practical invertebrate anatomy.

Cadet, P. (2004). Nitric oxide modulates the physiological control of ciliary activity in the marine mussel *Mytilus edulis* via morphine: novel mu opiate receptor splice variants. *Neuro Endocrinol Lett* 25, 184–190.

Caers, J., Verlinden, H., Zels, S., Vandersmissen, H. P., Vuerinckx, K., and Schoofs, L. (2012). More than two decades of research on insect neuropeptide GPCRs: an overview. *Front Endocrinol (Lausanne)* 3, 151.

Cai, C., He, Q., Xie, B., Xu, Z., Wang, C., Yang, C., et al. (2022). Long non-coding RNA LncMPEG1 responds to multiple environmental stressors by affecting biomineralization in pearl oyster *Pinctada fucata martensii*. *Front Mar Sci* 9, 1014810.

Canadell, J. G., Le Quéré, C., Raupach, M. R., Field, C. B., Buitenhuis, E. T., Ciais, P., et al. (2007). Contributions to accelerating atmospheric CO2 growth from economic activity, carbon intensity, and efficiency of natural sinks. *Proceedings of the national academy of sciences* 104, 18866–18870.

Cao, L., and Caldeira, K. (2008). Atmospheric CO2 stabilization and ocean acidification. *Geophys Res Lett* 35.

Cardoso, J. C. R., Clark, M. S., Viera, F. A., Bridge, P. D., Gilles, A., and Power, D. M. (2005). The secretin G-protein-coupled receptor family: teleost receptors. *J Mol*

Endocrinol 34, 753–765.

Cardoso, J. C. R., Félix, R. C., Bjärnmark, N., and Power, D. M. (2016). Allatostatin-type A, kisspeptin and galanin GPCRs and putative ligands as candidate regulatory factors of mantle function. *Mar Genomics* 27, 25–35.

Cardoso, J. C. R., Félix, R. C., Ferreira, V., Peng, M., Zhang, X., and Power, D. M. (2020). The calcitonin-like system is an ancient regulatory system of biomineralization. *Sci Rep* 10, 7581.

Cardoso, J. C. R., Félix, R. C., Fonseca, V. G., and Power, D. M. (2012). Feeding and the rhodopsin family g-protein coupled receptors in nematodes and arthropods. *Front Endocrinol (Lausanne)* 3, 157.

Cardoso, J. C. R., Ferreira, V., Zhang, X., Anjos, L., Félix, R. C., Batista, F. M., et al. (2019). Evolution and diversity of alpha-carbonic anhydrases in the mantle of the Mediterranean mussel (*Mytilus galloprovincialis*). *Sci Rep* 9, 10400.

Cardoso, J. C. R., Mc Shane, J. C., Li, Z., Peng, M., and Power, D. M. (2024). Revisiting the evolution of family B1 GPCRs and ligands: Insights from mollusca. *Mol Cell Endocrinol*, 112192.

Carini, A., Koudelka, T., Tholey, A., Appel, E., Gorb, S. N., Melzner, F., et al. (2019). Proteomic investigation of the blue mussel larval shell organic matrix. *J Struct Biol* 208, 107385.

Caron, J.-B., and Jackson, D. A. (2008). Paleoecology of the greater phyllopod bed community, Burgess Shale. *Palaeogeogr Palaeoclimatol Palaeoecol* 258, 222–256.

Carter, J. G. (1990). Evolutionary significance of shell microstructure in the *Palaeotaxodonta, Pteriomorphia* and *Isofilibranchia* (Bivalvia: Mollusca). *Skeletal biomineralization: patterns, processes and evolutionary trends* 1, 135–296.

Catapane, E. J. (1982a). Demonstration of denervation supersensitivity: a pharmacological approach. *Comparative Biochemistry and Physiology Part C: Comparative Pharmacology* 72, 353–355.

Catapane, E. J. (1982b). Demonstration of the peripheral innervation of the gill of the marine mollusc by means of the aluminum formaldehyde histofluorescence technique. *Cell Tissue Res* 225, 449–454.

Catapane, E. J. (1982c). The peripheral innervation of the gill of the marine mollusc demonstrated by the aluminium-formaldehyde (ALFA) histofluorescence method. *Cell Tissue Res* 225, 449–454.

Catapane, E. J. (1983). Comparative study of the control of lateral ciliary activity in marine bivalves. *Comparative Biochemistry and Physiology Part C: Comparative Pharmacology* 75, 403–405.

Catapane, E. J., Collins, E. D., Marcano, J. A., and Stefano, G. B. (1980). Denervation produces supersensitivity of a serotonergically innervated structure. *Eur J Pharmacol* 62, 111–115.

Catapane, E. J., Stefano, G. B., and Aiello, E. (1979). Neurophysiological correlates of the dopaminergic cilio-inhibitory mechanism of *Mytilus edulis*. *Journal of Experimental Biology* 83, 315–323.

Catapane, E. J., Thomas, J. A., Stefano, G. B., and Paul, D. F. (1981). Effects of temperature and temperature acclimation on serotonin-induced cilio-excitation of the gill of *Mytilus edulis*. *J Therm Biol* 6, 61–64.

Chandra Rajan, K., Meng, Y., Yu, Z., Roberts, S. B., and Vengatesen, T. (2021). Oyster biomineralization under ocean acidification: From genes to shell. *Glob Chang Biol* 27, 3779–3797.

Chang, J., Zhao, J., and Tian, X. (2018). In silico prediction of neuropeptides in *Hymenoptera parasitoid* wasps. *PLoS One* 13, e0193561.

Checa, A. (2000). A new model for periostracum and shell formation in *Unionidae* (Bivalvia, Mollusca). *Tissue Cell* 32, 405–416.

Checa, A. G. (2018). Physical and biological determinants of the fabrication of molluscan shell microstructures. *Front Mar Sci* 5, 353.

Checa, A. G., Macías-Sánchez, E., Harper, E. M., and Cartwright, J. H. E. (2016a). Organic membranes determine the pattern of the columnar prismatic layer of mollusc shells. *Proceedings of the Royal Society B: Biological Sciences* 283, 20160032.

Checa, A. G., Macías-Sánchez, E., and Ramírez-Rico, J. (2016b). Biological strategy for the fabrication of highly ordered aragonite helices: the microstructure of the cavolinioidean gastropods. *Sci Rep* 6, 25989.

Chen, C., Chen, H., Zhang, Y., Thomas, H. R., Frank, M. H., He, Y., et al. (2020). TBtools: an integrative toolkit developed for interactive analyses of big biological data. *Mol Plant* 13, 1194–1202.

Chen, J., Reiher, W., Hermann-Luibl, C., Sellami, A., Cognigni, P., Kondo, S., et al. (2016). Allatostatin A signalling in *Drosophila* regulates feeding and sleep and is modulated by PDF. *PLoS Genet* 12, e1006346.

Chen, Y., Liu, C., Li, S., Liu, Z., Xie, L., and Zhang, R. (2018). Repaired shells of the pearl oyster largely recapitulate normal prismatic layer growth: A proteomics study of shell matrix proteins. *ACS Biomater Sci Eng* 5, 519–529.

Cherkasov, A. S., Grewal, S., and Sokolova, I. M. (2007). Combined effects of temperature and cadmium exposure on haemocyte apoptosis and cadmium accumulation in the eastern oyster *Crassostrea virginica* (Gmelin). *J Therm Biol* 32, 162–170.

Christ, P., Hill, S. R., Schachtner, J., Hauser, F., and Ignell, R. (2018). Functional characterization of the dual allatostatin-A receptors in mosquitoes. *Peptides (N.Y.)* 99, 44–55.

Clark, M. S. (2020). Molecular mechanisms of biomineralization in marine invertebrates. *Journal of Experimental Biology* 223, jeb206961.

Clark, M. S., Peck, L. S., Arivalagan, J., Backeljau, T., Berland, S., Cardoso, J. C. R., et al. (2020). Deciphering mollusc shell production: the roles of genetic mechanisms through to ecology, aquaculture and biomimetics. *Biological Reviews* 95, 1812–1837.

Clark, M. S., Thorne, M. A. S., Vieira, F. A., Cardoso, J. C. R., Power, D. M., and Peck, L. S. (2010). Insights into shell deposition in the Antarctic bivalve *Laternula elliptica*: gene discovery in the mantle transcriptome using 454 pyrosequencing. *BMC Genomics* 11, 1–14.

Coast, G. M., and Schooley, D. A. (2011). Toward a consensus nomenclature for insect neuropeptides and peptide hormones. *Peptides (N.Y.)* 32, 620–631.

Cottrell, G. A. (1993). The wide range of actions of the FMRFamide-related peptides and the biological importance of peptidergic messengers. *Comparative molecular neurobiology*, 279–285.

Crane, R. L., Diaz Reyes, J. L., and Denny, M. W. (2021). Bivalves rapidly repair shells damaged by fatigue and bolster strength. *Journal of Experimental Biology* 224, jeb242681.

Croll, R. P., Jackson, D. L., and Voronezhskaya, E. E. (1997). Catecholamine-containing cells in larval and postlarval bivalve molluscs. *Biol Bull* 193, 116–124.

Crook, R. J., and Walters, E. T. (2011). Nociceptive behavior and physiology of molluscs: animal welfare implications. *ILAR J* 52, 185–195.

Cropper, E. C., Miller, M. W., Tenenbaum, R., Kolks, M. A., Kupfermann, I., and Weiss, K. R. (1988). Structure and action of buccalin: a modulatory neuropeptide localized to an identified small cardioactive peptide-containing cholinergic motor neuron of *Aplysia californica*. *Proceedings of the National Academy of Sciences* 85, 6177–6181.

Cuif, J.-P., Dauphin, Y., and Sorauf, J. E. (2010). Biominerals and fossils through time. *Cambridge University Press*.

Dakin, W. J. (1928). The anatomy and phylogeny of *Spondylus*, with a particular reference to the lamellibranch nervous system. *Proceedings of the Royal Society of London. Series B, Containing Papers of a Biological Character* 103, 337–354.

Davis, N. T., Blackburn, M. B., Golubeva, E. G., and Hildebrand, J. G. (2003). Localization of myoinhibitory peptide immunoreactivity in *Manduca sexta* and *Bombyx mori*, with indications that the peptide has a role in molting and ecdysis. *Journal of experimental biology* 206, 1449–1460.

Davoodi, S., Galenza, A., Panteluk, A., Deshpande, R., Ferguson, M., Grewal, S., et al. (2019). The immune deficiency pathway regulates metabolic homeostasis in *Drosophila*. *The Journal of Immunology* 202, 2747–2759.

Díaz, M. M., Schlichting, M., Abruzzi, K. C., Long, X., and Rosbash, M. (2019). Allatostatin-C/AstC-R2 is a novel pathway to modulate the circadian activity pattern in *Drosophila*. *Current biology* 29, 13–22.

Dillaman, R. M., Saleuddin, A. S. M., and Jones, G. M. (1976). Neurosecretion and shell regeneration in *Helisoma duryi* (Mollusca: Pulmonata). *Can J Zool* 54, 1771–1778.

Doney, S. C., Fabry, V. J., Feely, R. A., and Kleypas, J. A. (2009). Ocean acidification: the other CO2 problem. *Ann Rev Mar Sci* 1, 169–192.

Down, R. E., Matthews, H. J., and Audsley, N. (2010). Effects of Manduca sexta allatostatin and an analog on the pea aphid *Acyrthosiphon pisum* (Hemiptera: Aphididae) and degradation by enzymes from the aphid gut. *Peptides (N.Y.)* 31, 489–497.

Drew, G. A. (1906). The habits, anatomy, and embryology of the Giant Scallop,(*Pecten tenuicostatus*, Mighels). University of Maine.

Drew, G. A. (1907). The circulatory and nervous systems of the giant scallop (*Pecten*

tenuicostatus, Mighels), with remarks on the possible ancestry of the *Lamellibranchiata*, and on a method for making series of anatomical drawings. *Biol Bull* 12, 225–258.

Dyrynda, E. A., Law, R. J., Dyrynda, P. E. J., Kelly, C. A., Pipe, R. K., and Ratcliffe, N. A. (2000). Changes in immune parameters of natural mussel *Mytilus edulis* populations following a major oil spill (Sea Empress[1], Wales, UK). *Mar Ecol Prog Ser* 206, 155–170.

Dyrynda, E. A., Pipe, R. K., Burt, G. R., and Ratcliffe, N. A. (1998). Modulations in the immune defences of mussels (*Mytilus edulis*) from contaminated sites in the UK. *Aquatic Toxicology* 42, 169–185.

Eghianruwa, Q. A., Osoniyi, O. R., Maina, N., and Wachira, S. (2019). Bioactive Peptides from Marine Molluscs–A Review. *Int J Biochem Res Rev* 27, 1–12.

Ellis, I., and Kempf, S. C. (2011). Characterization of the central nervous system and various peripheral innervations during larval development of the oyster *Crassostrea virginica*. *Invertebrate Biology* 130, 236–250.

Elphick, M. R., Mirabeau, O., and Larhammar, D. (2018). Evolution of neuropeptide signalling systems. *Journal of Experimental Biology* 221, jeb151092.

Erspamer, V., and Anastasi, A. (1962). Structure and pharmacological actions of eledoisin, the active endecapeptide of the posterior salivary glands of Eledone. *Experientia* 18, 58–59.

Faller, S., Rothe, B. H., Todt, C., Schmidt-Rhaesa, A., and Loesel, R. (2012). Comparative

neuroanatomy of *Caudofoveata, Solenogastres, Polyplacophora,* and *Scaphopoda* (Mollusca) and its phylogenetic implications. *Zoomorphology* 131, 149–170.

Fang, D., Xu, G., Hu, Y., Pan, C., Xie, L., and Zhang, R. (2011). Identification of genes directly involved in shell formation and their functions in pearl oyster, *Pinctada fucata*. *PLoS One* 6, e21860.

Felix, R. C., Trindade, M., Pires, I. R. P., Fonseca, V. G., Martins, R. S., Silveira, H., et al. (2015). Unravelling the evolution of the allatostatin-type A, KISS and galanin peptide-receptor gene families in bilaterians: insights from *Anopheles* mosquitoes. *PLoS One* 10, e0130347.

Felton, C. M., and Johnson, C. M. (2014). Dopamine signaling in *C. elegans* is mediated in part by HLH-17-dependent regulation of extracellular dopamine levels. *G3: Genes, Genomes, Genetics* 4, 1081–1089.

Feng, D., Li, Q., Yu, H., Kong, L., and Du, S. (2018). Transcriptional profiling of long non-coding RNAs in mantle of *Crassostrea gigas* and their association with shell pigmentation. *Sci Rep* 8, 1436.

Field, I. A. (1922). *Biology and Economic Value of the Sea Mussel Mytilus edulis* . US Government Printing Office.

Floyd, P. D., Li, L., Rubakhin, S. S., Sweedler, J. V, Horn, C. C., Kupfermann, I., et al. (1999). Insulin prohormone processing, distribution, and relation to metabolism in *Aplysia californica*. *Journal of Neuroscience* 19, 7732–7741.

Franchini, A., Ottaviani, E., and Caselgrandi, E. (1985). Biogenic amines in the snail brain

of *Helicella virgata* (Gastropoda, Pulmonata). *Brain Res* 347, 132–134.

Frank, W., Ponder, L., David, R. P., and Juliet, M. (2019). Biology and evolution of the mollusca. CRC PRESS.

Friedrich, S., Wanninger, A., Brückner, M., and Haszprunar, G. (2002). Neurogenesis in the mossy chiton, *Mopalia muscosa* (Gould)(Polyplacophora): evidence against molluscan metamerism. *J Morphol* 253, 109–117.

Fritze, O., Filipek, S., Kuksa, V., Palczewski, K., Hofmann, K. P., and Ernst, O. P. (2003). Role of the conserved NPxxY (x) 5, 6F motif in the rhodopsin ground state and during activation. *Proceedings of the National Academy of Sciences* 100, 2290–2295.

Fuse, M., Zhang, J. R., Partridge, E., Nachman, R. J., Orchard, I., Bendena, W. G., et al. (1999). Effects of an allatostatin and a myosuppressin on midgut carbohydrate enzyme activity in the cockroach *Diploptera punctata*. *Peptides (N.Y.)* 20, 1285–1293.

Galtsoff, P. S. (1964). *The American oyster, Crassostrea virginica gmelin*. US Government Printing Office.

Gazeau, F., Gattuso, J.-P., Dawber, C., Pronker, A. E., Peene, F., Peene, J., et al. (2010). Effect of ocean acidification on the early life stages of the blue mussel *Mytilus edulis*. *Biogeosciences* 7, 2051–2060.

George, M. N., O'Donnell, M. J., Concodello, M., and Carrington, E. (2022). Mussels repair shell damage despite limitations imposed by ocean acidification. *J Mar Sci Eng* 10, 359.

Geraerts, W. P. M. (1976). Control of growth by the neurosecretory hormone of the light green cells in the freshwater snail *Lymnaea stagnalis*. *Gen Comp Endocrinol* 29, 61–71.

Gerdol, M. (2017). Immune-related genes in gastropods and bivalves: a comparative overview. *Invertebrate Survival Journal* 14, 95–111.

Gerdol, M., Moreira, R., Cruz, F., Gómez-Garrido, J., Vlasova, A., Rosani, U., et al. (2020). Massive gene presence-absence variation shapes an open pan-genome in the Mediterranean mussel. *Genome Biol* 21, 1–21.

Goh, S. L., and Davey, K. G. (1976). Localization and distribution of catecholaminergic structures in the nervous system of *Phocanema decipiens* (Nematoda). *Int J Parasitol* 6, 403–411.

Gopurappilly, R., Ogawa, S., and Parhar, I. S. (2013). Functional significance of GnRH and kisspeptin, and their cognate receptors in teleost reproduction. *Front Endocrinol (Lausanne)* 4, 24.

Gosling, E. (2008). *Bivalve molluscs: biology, ecology and culture*. John Wiley & Sons.

Gosling, E. (2015). *Marine bivalve molluscs*. John Wiley & Sons.

Gricourt, L., Bonnec, G., Boujard, D., Mathieu, M., and Kellner, K. (2003). Insulin-like system and growth regulation in the Pacific oyster *Crassostrea gigas*: hrIGF-1 effect on protein synthesis of mantle edge cells and expression of an homologous insulin receptor-related receptor. *Gen Comp Endocrinol* 134, 44–56.

Gricourt, L., Mathieu, M., and Kellner, K. (2006). An insulin-like system involved in the

control of Pacific oyster *Crassostrea gigas* reproduction: hrIGF-1 effect on germinal cell proliferation and maturation associated with expression of an homologous insulin receptor-related receptor. *Aquaculture* 251, 85–98.

Grizel, H. (2003). An atlas of histology and cytology of marine bivalve molluscs. *An atlas of histology and cytology of marine bivalve molluscs.*

Guilgur, L. G., Moncaut, N. P., Canário, A. V. M., and Somoza, G. M. (2006). Evolution of GnRH ligands and receptors in *gnathostomata*. *Comp Biochem Physiol A Mol Integr Physiol* 144, 272–283.

Guo, Y., Wang, L., Zhou, Z., Wang, M., Liu, R., Wang, L., et al. (2013). An opioid growth factor receptor (OGFR) for [Met5]-enkephalin in *Chlamys farreri*. *Fish Shellfish Immunol* 34, 1228–1235.

Hanington, P. C., Barreda, D. R., and Belosevic, M. (2006). A novel hematopoietic granulin induces proliferation of goldfish (*Carassius auratus*) macrophages. *Journal of Biological Chemistry* 281, 9963–9970.

Harayashiki, C. A. Y., Márquez, F., Cariou, E., and Castro, Í. B. (2020). Mollusk shell alterations resulting from coastal contamination and other environmental factors. *Environmental Pollution* 265, 114881.

Harper, E. M., and Skelton, P. W. (1993). The Mesozoic marine revolution and epifaunal bivalves. *Scripta Geologica, Special Issue* 2, 127–153.

Hartenstein, V. (2016). The central nervous system of invertebrates. *The Wiley Handbook of Evolutionary Neuroscience*, 173–235.

Haszprunar, G. (1988). On the origin and evolution of major gastropod groups, with special reference to the *Streptoneura*. *Journal of Molluscan Studies* 54, 367–441.

Hentze, J. L., Carlsson, M. A., Kondo, S., Nässel, D. R., and Rewitz, K. F. (2015). The neuropeptide allatostatin A regulates metabolism and feeding decisions in *Drosophila*. *Sci Rep* 5, 11680.

Herlitze, I., Marie, B., Marin, F., and Jackson, D. J. (2018). Molecular modularity and asymmetry of the molluscan mantle revealed by a gene expression atlas. *Gigascience* 7, giy056.

Hickman, R. W., and Gruffydd, L. D. (1971). The histology of the larvae of *Ostrea edulis* during metamorphosis., in *Fourth European marine biology symposium*, (Cambridge University Press New York), 281–294.

Hodgkin, A. L., and Huxley, A. F. (1939). Action potentials recorded from inside a nerve fibre. *Nature* 144, 710–711.

Hodgkin, A. L., and Huxley, A. F. (1945). Resting and action potentials in single nerve fibres. *J Physiol* 104, 176.

Hoek, R. M., Li, K. W., Van Minnen, J., Lodder, J. C., De Jong-Brink, M., Smit, A. B., et al. (2005). LFRFamides: a novel family of parasitation-induced-RFamide neuropeptides that inhibit the activity of neuroendocrine cells in *Lymnaea stagnalis*. *J Neurochem* 92, 1073–1080.

Hoffman, J. I., Peck, L. S., Hillyard, G., Zieritz, A., and Clark, M. S. (2010). No evidence for genetic differentiation between Antarctic limpet *Nacella concinna* morphotypes.

Mar Biol 157, 765–778.

Hökfelt, T., Broberger, C., Xu, Z.-Q. D., Sergeyev, V., Ubink, R., and Diez, M. (2000). Neuropeptides—an overview. *Neuropharmacology* 39, 1337–1356.

Hosseini, S. F., Rezaei, M., and McClements, D. J. (2022). Bioactive functional ingredients from aquatic origin: A review of recent progress in marine-derived nutraceuticals. *Crit Rev Food Sci Nutr* 62, 1242–1269.

Hua, Y.-J., Tanaka, Y., Nakamura, K., Sakakibara, M., Nagata, S., and Kataoka, H. (1999). Identification of a prothoracicostatic peptide in the larval brain of the silkworm, *Bombyx mori*. *Journal of Biological Chemistry* 274, 31169–31173.

Huang, J., Li, L., Jiang, T., Xie, L., and Zhang, R. (2022). Mantle tissue in the pearl oyster *Pinctada fucata* secretes immune components via vesicle transportation. *Fish Shellfish Immunol* 121, 116–123.

Huang, J., Luo, X., Zeng, L., Huang, Z., Huang, M., You, W., et al. (2018). Expression profiling of lncRNAs and mRNAs reveals regulation of muscle growth in the Pacific abalone, *Haliotis discus hannai*. *Sci Rep* 8, 16839.

Huang, L. J., and Li, H. D. (1991). Observation of the phase transition in the growth of a biomineralized calcium carbonate. *Biochem Biophys Res Commun* 176, 654–659.

Illanes–Bucher, J. (1979) Recherches cytologiques et expérimentales sur la neurosécrétion de la moule *Mytilus edulis* L. (Mollusque, Lamellibranche). Thèse de 3eme cycle. Université de Caen, France.

Jackson, D. J., and Degnan, B. M. (2016). The importance of evo-devo to an integrated

understanding of molluscan biomineralisation. *J Struct Biol* 196, 67–74.

Jackson, D. J., McDougall, C., Woodcroft, B., Moase, P., Rose, R. A., Kube, M., et al. (2010). Parallel evolution of nacre building gene sets in molluscs. *Mol Biol Evol* 27, 591–608.

Jacob, D. E., Wirth, R., Soldati, A. L., Wehrmeister, U., and Schreiber, A. (2011). Amorphous calcium carbonate in the shells of adult *Unionoida*. *J Struct Biol* 173, 241–249.

Janssen, T., Meelkop, E., Lindemans, M., Verstraelen, K., Husson, S. J., Temmerman, L., et al. (2008). Discovery of a cholecystokinin-gastrin-like signaling system in nematodes. *Endocrinology* 149, 2826–2839.

Jékely, G. (2013). Global view of the evolution and diversity of metazoan neuropeptide signaling. *Proceedings of the National Academy of Sciences* 110, 8702–8707.

Jékely, G., Melzer, S., Beets, I., Kadow, I. C. G., Koene, J., Haddad, S., et al. (2018). The long and the short of it–a perspective on peptidergic regulation of circuits and behaviour. *Journal of Experimental Biology* 221, jeb166710.

Jiang, H.-M., Yang, Z., Xue, Y.-Y., Wang, H.-Y., Guo, S.-Q., Xu, J.-P., et al. (2022). Identification of an allatostatin C signaling system in mollusc *Aplysia*. *Sci Rep* 12, 1213.

Johannesson, B. (1986). Shell morphology of *Littorina saxatilis Olivi*: the relative importance of physical factors and predation. *J Exp Mar Biol Ecol* 102, 183–195.

Jong-Brink, M., Ter Maat, A., and Tensen, C. P. (2001). NPY in invertebrates: molecular

answers to altered functions during evolution. Peptides (N.Y.) 22, 309–315.

Joubert, C., Piquemal, D., Marie, B., Manchon, L., Pierrat, F., Zanella-Cléon, I., et al. (2010). Transcriptome and proteome analysis of *Pinctada margaritifera* calcifying mantle and shell: focus on biomineralization. *BMC Genomics* 11, 1–13.

Jurenka, R., and Nusawardani, T. (2011). The pyrokinin/pheromone biosynthesis-activating neuropeptide (PBAN) family of peptides and their receptors in Insecta: evolutionary trace indicates potential receptor ligand-binding domains. Insect Mol. Biol. 20, 323–334.

Kadar, E., Lobo-da-Cunha, A., and Azevedo, C. (2009). Mantle-to-shell $CaCO_3$ transfer during shell repair at different hydrostatic pressures in the deep-sea vent mussel *Bathymodiolus azoricus* (Bivalvia: Mytilidae). *Mar Biol* 156, 959–967.

Kandel, E., and Abel, T. (1995). Neuropeptides, adenylyl cyclase, and memory storage. *Science (1979)* 268, 825–826.

Kaplan, D. L. (1998). Mollusc shell structures: novel design strategies for synthetic materials. *Curr Opin Solid State Mater Sci* 3, 232–236.

Karhunen, T., Airaksinen, M. S., Tuomisto, L., and Panula, P. (1993). Neurotransmitters in the nervous system of *Macoma balthica* (Bivalvia). *Journal of Comparative Neurology* 334, 477–488.

Kassambara, A. (2017). *Practical guide to principal component methods in R: PCA, M (CA), FAMD, MFA, HCPC, factoextra*. Sthda.

Kauffman, E. G. (1979). *Bivalvia*. Berlin, Heidelberg: Encyclopedia of Earth Science. Springer.

Keihan, R., Ghorbani, A. R., Salahinejad, E., Sharifi, E., and Tayebi, L. (2020). Biomineralization, strength and cytocompatibility improvement of bredigite scaffolds through doping/coating. *Ceram Int* 46, 21056–21063.

Kellett, E., Perry, S. J., Santama, N., Worster, B. M., Benjamin, P. R., and Burke, J. F. (1996). Myomodulin gene of *Lymnaea*: structure, expression, and analysis of neuropeptides. *Journal of Neuroscience* 16, 4949–4957.

Khush, R. S., Leulier, F., and Lemaitre, B. (2001). Drosophila immunity: two paths to NF-κB. *Trends Immunol* 22, 260–264.

Kim, D., Paggi, J. M., Park, C., Bennett, C., and Salzberg, S. L. (2019a). Graph-based genome alignment and genotyping with HISAT2 and HISAT-genotype. *Nat Biotechnol* 37, 907–915.

Kim, D.-K., Yun, S., Son, G. H., Hwang, J.-I., Park, C. R., Kim, J. Il, et al. (2014). Coevolution of the spexin/galanin/kisspeptin family: Spexin activates galanin receptor type II and III. *Endocrinology* 155, 1864–1873.

Kim, M. A., Markkandan, K., Han, N.-Y., Park, J.-M., Lee, J. S., Lee, H., et al. (2019b). Neural ganglia transcriptome and peptidome associated with sexual maturation in female Pacific abalone (*Haliotis discus hannai*). *Genes (Basel)* 10, 268.

Kim, Y.-J., Bartalska, K., Audsley, N., Yamanaka, N., Yapici, N., Lee, J.-Y., et al. (2010). MIPs are ancestral ligands for the sex peptide receptor. *Proceedings of the National*

Academy of Sciences 107, 6520–6525.

Kim, Y.-J., Žitňan, D., Cho, K.-H., Schooley, D. A., Mizoguchi, A., and Adams, M. E. (2006). Central peptidergic ensembles associated with organization of an innate behavior. *Proceedings of the National Academy of Sciences* 103, 14211–14216.

Kiss, T., and Pirger, Z. (2006). Neuropeptides as modulators and hormones in terrestrial snails: their occurrence, distribution and physiological significance.

Klausen, C., Chang, J. P., and Habibi, H. R. (2002). Multiplicity of gonadotropin-releasing hormone signaling: a comparative perspective. *Prog Brain Res* 141, 111–128.

Knoll, A. H. (2003). Biomineralization and evolutionary history. *Rev Mineral Geochem* 54, 329–356.

Kobayashi, I., and Samata, T. (2006). Bivalve shell structure and organic matrix. *Materials Science and Engineering: C* 26, 692–698.

Kobayashi, M., and Muneoka, Y. (1990). Structure and action of molluscan neuropeptides. *Zoolog Sci* 7, 801–814.

Kocot, K. M., Cannon, J. T., Todt, C., Citarella, M. R., Kohn, A. B., Meyer, A., et al. (2011). Phylogenomics reveals deep molluscan relationships. *Nature* 477, 452–456.

Kocot, K. M., Poustka, A. J., Stöger, I., Halanych, K. M., and Schrödl, M. (2020). New data from Monoplacophora and a carefully-curated dataset resolve molluscan relationships. *Sci Rep* 10, 101.

Koene, J. M. (2010). Neuro-endocrine control of reproduction in hermaphroditic

freshwater snails: mechanisms and evolution. *Front Behav Neurosci* 4, 167.

Kolodziejczyk, A., and Nässel, D. R. (2011). A novel wide-field neuron with branches in the lamina of the *Drosophila* visual system expresses myoinhibitory peptide and may be associated with the clock. *Cell Tissue Res* 343, 357–369.

Korringa, P. (1976). Farming the cupped oysters of the genus *Crassostrea*.

Kotsyuba, E., and Dyachuk, V. (2023). Role of the neuroendocrine system of marine bivalves in their response to hypoxia. *Int J Mol Sci* 24, 1202.

Kotsyuba, E., Kalachev, A., Kameneva, P., and Dyachuk, V. (2020). Distribution of molecules related to neurotransmission in the nervous system of the mussel *Crenomytilus grayanus*. *Front Neuroanat* 14, 35.

Kramer, S. J., ToSCHI, A., Miller, C. A., Kataoka, H., Quistad, G. B., Li, J. P., et al. (1991). Identification of an allatostatin from the tobacco hornworm *Manduca sexta*. *Proceedings of the national academy of sciences* 88, 9458–9462.

Kreienkamp, H.-J., Larusson, H. J., Witte, I., Roeder, T., Birgul, N., Ho¨ nck, H.-H., et al. (2002). Functional annotation of two orphan G-protein-coupled receptors, Drostar1 and-2, from *Drosophila melanogaster* and their ligands by reverse pharmacology. *Journal of Biological Chemistry* 277, 39937–39943.

Kreiling, J. A., Jessen-Eller, K., Miller, J., Seegal, R. F., and Reinisch, C. L. (2001). Early development of the serotonergic and dopaminergic nervous system in *Spisula solidissima* (surf clam) larvae. *Comp Biochem Physiol A Mol Integr Physiol* 130, 341–351.

Kump, L. R., Bralower, T. J., and Ridgwell, A. (2009). Ocean acidification in deep time. *Oceanography* 22, 94–107.

Kuroki, Y., Kanda, T., Kubota, I., Fujisawa, Y., Ikeda, T., Miura, A., et al. (1990). A molluscan neuropeptide related to the crustacean hormone, RPCH. *Biochem Biophys Res Commun* 167, 273–279.

Kuroki, Y., Kanda, T., Kubota, I., Ikeda, T., Fujisawa, Y., Minakata, H., et al. (1993). FMRFamide-related peptides isolated from the prosobranch mollusc *Fusinus ferrugineus*. *Acta Biol Hung* 44, 41–44.

Kvetnansky, R., Sabban, E. L., and Palkovits, M. (2009). Catecholaminergic systems in stress: structural and molecular genetic approaches. *Physiol Rev* 89, 535–606.

Lacoste, A., Jalabert, F., Malham, S. K., Cueff, A., and Poulet, S. A. (2001b). Stress and stress-induced neuroendocrine changes increase the susceptibility of juvenile oysters (*Crassostrea gigas*) to *Vibrio splendidus*. Appl. Environ.Microbiol.

Lacoste, A., Malham, S. K., Cueff, A., Jalabert, F., Gelebart, F., and Poulet, S. A. (2001c). Evidence for a form of adrenergic response to stress in the mollusc *Crassostrea gigas*. J. Exp. Biol. 204(Pt 7), 1247–1255.

Lane, D. J. W., and Nott, J. A. (1975). A study of the morphology, fine structure and histochemistry of the foot of the pediveliger of *Mytilus edulis* L. *Journal of the Marine Biological Association of the United Kingdom* 55, 477–495.

Lange, A. B., Alim, U., Vandersmissen, H. P., Mizoguchi, A., Vanden Broeck, J., and Orchard, I. (2012). The distribution and physiological effects of the myoinhibiting

peptides in the kissing bug, *Rhodnius prolixus*. *Front Neurosci* 6, 98.

Lange, R. P. J., Joosse, J., and Van Minnen, J. (1998). Multi-messenger innervation of the male sexual system of *Lymnaea stagnalis*. Journal of Comparative Neurology 390, 564–577.

Larsson, A. (2014). AliView: a fast and lightweight alignment viewer and editor for large datasets. *Bioinformatics* 30, 3276–3278.

Le Roy, N., Jackson, D. J., Marie, B., Ramos-Silva, P., and Marin, F. (2014). The evolution of metazoan α-carbonic anhydrases and their roles in calcium carbonate biomineralization. *Front Zool* 11, 1–16.

Le Roy, N., Jackson, D. J., Marie, B., Ramos-Silva, P., and Marin, F. (2016). Carbonic anhydrase and metazoan biocalcification: a focus on molluscs. *Key Eng Mater* 672, 151–157.

Lenz, C., Søndergaard, L., and Grimmelikhuijzen, C. J. P. (2000). Molecular cloning and genomic organization of a novel receptor from *Drosophila melanogaster* structurally related to mammalian galanin receptors. *Biochem Biophys Res Commun* 269, 91–96.

Lethimonier, C., Madigou, T., Muñoz-Cueto, J.-A., Lareyre, J.-J., and Kah, O. (2004). Evolutionary aspects of GnRHs, GnRH neuronal systems and GnRH receptors in teleost fish. *Gen Comp Endocrinol* 135, 1–16.

Li C, Kim K. Neuropeptides[J]. (2008) WormBook: the online review of *C. elegans* biology,

Li, L., Qiu, L., Song, L., Song, X., Zhao, J., Wang, L., et al. (2009). First molluscan TNFR

homologue in Zhikong scallop: molecular characterization and expression analysis. *Fish Shellfish Immunol* 27, 625–632.

Li, Z., Cardoso, J. C. R., Peng, M., Inácio, J. P. S., and Power, D. M. (2021). Evolution and potential function in molluscs of neuropeptide and receptor homologues of the insect allatostatins. *Front Endocrinol (Lausanne)* 12, 725022.

Liao, H., Mutvei, H., Sjöström, M., Hammarström, L., and Li, J. (2000). Tissue responses to natural aragonite (Margaritifera shell) implants in vivo. *Biomaterials* 21, 457–468.

Liu, A., Liu, F., Shi, W., Huang, H., Wang, G., and Ye, H. (2019). C-Type allatostatin and its putative receptor from the mud crab serve an inhibitory role in ovarian development. *Journal of Experimental Biology* 222, jeb207985.

Liu, D. W., Chen, Z. W., and Xu, H. Z. (2008). Effects of leucine-enkephalin on catalase activity and hydrogen peroxide levels in the haemolymph of the Pacific Oyster (*Crassostrea gigas*). Molecules 13, 864–870.

Liu, Z., Li, M., Yi, Q., Wang, L., and Song, L. (2018a). The neuroendocrine-immune regulation in response to environmental stress in marine bivalves. *Front Physiol* 9, 1456.

Liu, Z., Wang, L., Lv, Z., Zhou, Z., Wang, W., Li, M., et al. (2018b). The cholinergic and adrenergic autocrine signaling pathway mediates immunomodulation in oyster *Crassostrea gigas*. *Front Immunol* 9, 284.

Liu, Z., Xu, Y., Wu, L., and Zhang, S. (2010). Evolution of galanin receptor genes: insights from the deuterostome genomes. *J Biomol Struct Dyn* 28, 97–106.

Liu, Z., Zhou, Z., Wang, L., Jiang, S., Wang, W., Zhang, R., et al. (2015). The immunomodulation mediated by a delta-opioid receptor for [Met5]-enkephalin in oyster *Crassostrea gigas*. *Dev Comp Immunol* 49, 217–224.

Loker, E. S., Adema, C. M., Zhang, S., and Kepler, T. B. (2004). Invertebrate immune systems–not homogeneous, not simple, not well understood. *Immunol Rev* 198, 10–24.

Lopez, V., Wickham, L., and Desgroseillers, L.U.C. (1993). Molecular cloning of myomodulin cDNA, a neuropeptide precursor gene expressed in neuron L10 of *Aplysia californica*. *DNA Cell Biol* 12, 53–61.

Lorenz, M. W., Kellner, R., and Hoffmann, K. H. (1995). A Family of Neuropeptides That Inhibit Juvenile Hormone Biosynthesis in the Cricket, *Gryllus bimaculatus* (*). *Journal of Biological Chemistry* 270, 21103–21108.

Louis, V., Besseau, L., and Lartaud, F. (2022). Step in time: Biomineralisation of bivalve's shell. *Front Mar Sci* 9, 906085.

Love, M. I., Huber, W., and Anders, S. (2014). Moderated estimation of fold change and dispersion for RNA-seq data with DESeq2. *Genome Biol* 15, 1–21.

Lutz, R. A., and Kennish, M. J. (1993). Ecology of deep-sea hydrothermal vent communities: A review. *Reviews of geophysics* 31, 211–242.

M Batista, F., M Churcher, A., Manchado, M., Leitao, A., and M Power, D. (2019). Uncovering the immunological repertoire of the carpet shell clam.

Madeira, F., Pearce, M., Tivey, A. R. N., Basutkar, P., Lee, J., Edbali, O., et al. (2022).

Search and sequence analysis tools services from EMBL-EBI in 2022. *Nucleic Acids Res* 50, W276–W279.

Mantione, K. J., Kim, C., and Stefano, G. B. (2006). Morphine regulates gill ciliary activity via coupling to nitric oxide release in a bivalve mollusk: opiate receptor expression in gill tissues. *Med Sci Monit* 12, BR195-200.

Malagoli, D., Mandrioli, M., Tascedda, F., and Ottaviani, E. (2017). Circulating phagocytes: the ancient and conserved interface between immune and neuroendocrine function. Biol. Rev. Camb. Philos. Soc. 92, 369–377.

Marie, B., Joubert, C., Tayalé, A., Zanella-Cléon, I., Belliard, C., Piquemal, D., et al. (2012). Different secretory repertoires control the biomineralization processes of prism and nacre deposition of the pearl oyster shell. *Proceedings of the National Academy of Sciences* 109, 20986–20991.

Marin, F. (2020). Mollusc shellomes: past, present and future. *J Struct Biol* 212, 107583.

Marin, F., Amons, R., Guichard, N., Stigter, M., Hecker, A., Luquet, G., et al. (2005). Caspartin and calprismin, two proteins of the shell calcitic prisms of the Mediterranean fan mussel *Pinna nobilis*. *Journal of Biological Chemistry* 280, 33895–33908.

Marin, F., Le Roy, N., and Marie, B. (2012). The formation and mineralization of mollusk shell. *Front. Biosci* 4, 1099–1125.

Marin, F., Luquet, G., Marie, B., and Medakovic, D. (2007). Molluscan shell proteins: primary structure, origin, and evolution. *Curr Top Dev Biol* 80, 209–276.

Marques, P., Skorupskaite, K., Rozario, K. S., Anderson, R. A., and George, J. T. (2022). Physiology of GNRH and gonadotropin secretion. *Endotext [internet]*.

Matsutani, T., and Nomura, T. (1984). Localization of monoamines in the central nervous system and gonad of the scallop *Patinopecten yessoensis*. *Bulletin of the Japanese Society of Scientific Fisheries* 50, 425–430.

Matthews, H. J., Audsley, N., and Weaver, R. J. (2008). In vitro and in vivo effects of myo-active peptides on larvae of the tomato moth Lacanobia oleracea and the cotton leaf worm *Spodoptera littoralis* (Lepidoptera; Noctuidae). *Archives of Insect Biochemistry and Physiology: Published in Collaboration with the Entomological Society of America* 69, 60–69.

Matthews, H. J., Down, R. E., and Audsley, N. (2010). Effects of Manduca sexta allatostatin and an analogue on the peach-potato aphid *Myzus persicae* (hemiptera: aphididae) and degradation by enzymes in the aphid gut. *Arch Insect Biochem Physiol* 75, 139–157.

Mayoral, J. G., Nouzova, M., Brockhoff, A., Goodwin, M., Hernandez-Martinez, S., Richter, D., et al. (2010). Allatostatin-C receptors in mosquitoes. *Peptides (N.Y.)* 31, 442–450.

McDougall, C., and Degnan, B. M. (2018). The evolution of mollusc shells. *Wiley Interdiscip Rev Dev Biol* 7, e313.

Meechonkit, P., Kovitvadhi, U., Chatchavalvanich, K., Sretarugsa, P., and Weerachatyanukul, W. (2010). Localization of serotonin in neuronal ganglia of the

freshwater pearl mussel, *Hyriopsis (Hyriopsis) bialata*. *Journal of Molluscan Studies* 76, 267–274.

Metz, J. R., Huising, M. O., Leon, K., Verburg-van Kemenade, B. M. L., and Flik, G. (2006). Central and peripheral interleukin-1β and interleukin-1 receptor I expression and their role in the acute stress response of common carp, *Cyprinus carpio* L. *Journal of endocrinology* 191, 25–35.

Meyers, M. A., Chen, P.-Y., Lin, A. Y.-M., and Seki, Y. (2008). Biological materials: Structure and mechanical properties. *Prog Mater Sci* 53, 1–206.

Miller, D. J., and Ball, E. E. (2009). The gene complement of the ancestral bilaterian-was Urbilateria a monster? *J Biol* 8, 1–4.

Miller, M. A., Pfeiffer, W., and Schwartz, T. (2010). Creating the CIPRES Science Gateway for inference of large phylogenetic trees., in *2010 gateway computing environments workshop (GCE)*, (Ieee), 1–8.

Miller, M. W., Beushausen, S., Cropper, E. C., Eisinger, K., Stamm, S., Vilim, F. S., et al. (1993). The buccalin-related neuropeptides: isolation and characterization of an *Aplysia* cDNA clone encoding a family of peptide cotransmitters. *Journal of Neuroscience* 13, 3346–3357.

Miner, B. G., Sultan, S. E., Morgan, S. G., Padilla, D. K., and Relyea, R. A. (2005). Ecological consequences of phenotypic plasticity. *Trends Ecol Evol* 20, 685–692.

Mirabeau, O., and Joly, J.S. (2013). Molecular evolution of peptidergic signaling systems in bilaterians. *Proceedings of the national academy of sciences* 110, E2028–E2037.

Miyamoto, H., Endo, H., Hashimoto, N., Isowa, Y., Kinoshita, S., Kotaki, T., et al. (2013). The diversity of shell matrix proteins: genome-wide investigation of the pearl oyster, *Pinctada fucata*. *Zoolog Sci* 30, 801–816.

Moreira, R., Balseiro, P., Forn-Cuní, G., Milan, M., Bargelloni, L., Novoa, B., et al. (2018). Bivalve transcriptomics reveal pathogen sequences and a powerful immune response of the Mediterranean mussel (*Mytilus galloprovincialis*). *Mar Biol* 165, 1–20.

Moreira, R., Pereiro, P., Canchaya, C., Posada, D., Figueras, A., and Novoa, B. (2015). RNA-Seq in *Mytilus galloprovincialis*: comparative transcriptomics and expression profiles among different tissues. *BMC Genomics* 16, 1–18.

Morishita, F., Furukawa, Y., Matsushima, O., and Minakata, H. (2010). Regulatory actions of neuropeptides and peptide hormones on the reproduction of molluscs. *Can J Zool* 88, 825–845.

Morton, B. (1983). Feeding and digestion in Bivalvia. *The Mollusca. Physiology Part* 2, 65–147.

Morton, B., and Peharda, M. (2008). The biology and functional morphology of *Arca noae* (Bivalvia: Arcidae) from the Adriatic Sea, Croatia, with a discussion on the evolution of the bivalve mantle margin. *Acta Zoologica* 89, 19–28.

Müller, W. E. G., Schröder, H. C., Schlossmacher, U., Neufurth, M., Geurtsen, W., Korzhev, M., et al. (2013). The enzyme carbonic anhydrase as an integral component of biogenic Ca-carbonate formation in sponge spicules. *FEBS Open Bio* 3, 357–362.

Munari, C., Rossetti, E., and Mistri, M. (2013). Shell formation in cultivated bivalves

cannot be part of carbon trading systems: a study case with *Mytilus galloprovincialis*. *Mar Environ Res* 92, 264–267.

Muneoka, Y. (1994). Phylogeneticaspects of structure and action of molluscan neuropeptides. *Perspectives in comparative endocrinology*, 109–118.

Muneoka, Y., Morishita, F., Furukawa, Y., Matsushima, O., Kobayashi, M., Ohtani, M., et al. (2000). Comparative aspects of invertebrate neuropeptides. *Acta Biol Hung* 51, 111–132.

Muzzarelli, R. A. A. (2011). Potential of chitin/chitosan-bearing materials for uranium recovery: An interdisciplinary review. *Carbohydr Polym* 84, 54–63.

Naot, D., and Cornish, J. (2008). The role of peptides and receptors of the calcitonin family in the regulation of bone metabolism. *Bone* 43, 813–818.

Naot, D., Musson, D. S., and Cornish, J. (2019). The activity of peptides of the calcitonin family in bone. *Physiol Rev* 99, 781–805.

Nässel, D. R. (2002). Neuropeptides in the nervous system of *Drosophila* and other insects: multiple roles as neuromodulators and neurohormones. *Prog Neurobiol* 68, 1–84.

Nässel, D. R., and Wegener, C. (2011). A comparative review of short and long neuropeptide F signaling in invertebrates: Any similarities to vertebrate neuropeptide Y signaling *Peptides (N.Y.)* 32, 1335–1355.

Nell, J. A., and Hand, R. E. (2003). Evaluation of the progeny of second-generation Sydney rock oyster *Saccostrea glomerata* (Gould, 1850) breeding lines for resistance to QX disease *Marteilia sydneyi*. *Aquaculture* 228, 27–35.

Newell, R. I. E. (2004). Ecosystem influences of natural and cultivated populations of suspension-feeding bivalve molluscs: a review. *J Shellfish Res* 23, 51–62.

Nikishchenko, V. E., Sayenko, E. M., and Dyachuk, V. A. (2022). First immunodetection of sensory and nervous systems of parasitic larvae (glochidia) of freshwater bivalve Nodularia douglasiae. *Front Physiol* 13, 624.

O'Connor, E. F., Watson III, W. H., and Wyse, G. A. (1982). Identification and localization of catecholamines in the nervous system of *Limulus polyphemus*. *J Neurobiol* 13, 49–60.

Odeleye, T., White, W. L., and Lu, J. (2019). Extraction techniques and potential health benefits of bioactive compounds from marine molluscs: a review. *Food Funct* 10, 2278–2289.

Oliveira, A. L., Calcino, A., and Wanninger, A. (2019). Extensive conservation of the proneuropeptide and peptide prohormone complement in mollusks. *Sci Rep* 9, 4846.

O'Shea, M., and Schaffer, M. (1985). Neuropeptide function: the invertebrate contribution. *Annu Rev Neurosci* 8, 171–198.

Owen, G., Trueman, E. R., and Yonge, C. M. (1953). The ligament in the *Lamellibranchia*. *Nature* 171, 73–75.

Paula, S. M., and Silveira, M. (2009). Studies on molluscan shells: contributions from microscopic and analytical methods. *Micron* 40, 669–690.

Paula, S. M., Huila, M. F. G., Araki, K., and Toma, H. E. (2010). Confocal Raman and electronic microscopy studies on the topotactic conversion of calcium carbonate from

Pomacea lineate shells into hydroxyapatite bioceramic materials in phosphate media. *Micron* 41, 983–989.

Peck, L. S., Clark, M. S., Power, D., Reis, J., Batista, F. M., and Harper, E. M. (2015). Acidification effects on biofouling communities: winners and losers. *Glob Chang Biol* 21, 1907–1913.

Pedder, S. M., Muneoka, Y., and Walker, R. J. (2001). Structure–activity and possible mode of action of S-Iamide neuropeptides on identified central neurons of *Helix aspersa*. *Regul Pept* 101, 131–140.

Pelseneer, P. (1931). Quelques particularités d'organisation chez des Pectinacea., in *Annales de la Societe Royale Zoologique de Belgique*, 12–17.

Peng, C., Zhao, X., Liu, S., Shi, W., Han, Y., Guo, C., et al. (2017). Ocean acidification alters the burrowing behaviour, Ca2+/Mg2+-ATPase activity, metabolism, and gene expression of a bivalve species, *Sinonovacula constricta*. *Mar Ecol Prog Ser* 575, 107–117.

Peng, M., Cardoso, C. R. J., Sorigué, P., and Power, M. D. (2024). Species-specific responses of bivalves to ocean acidification. (unpublish).

Peng, M., Cardoso, J. C. R., Pearson, G., Canário, A. V. M., and Power, D. M. (2023). Core genes of biomineralization and cis-regulatory long non-coding RNA regulate shell growth in bivalves. *J Adv Res*.

Peng, M., Li, Z., Cardoso, J. C. R., Niu, D., Liu, X., Dong, Z., et al. (2022). Domain-dependent evolution explains functional homology of protostome and

deuterostome complement C3-like proteins. *Front Immunol* 13, 840861.

Pertea, M., Pertea, G. M., Antonescu, C. M., Chang, T.-C., Mendell, J. T., and Salzberg, S. L. (2015). StringTie enables improved reconstruction of a transcriptome from RNA-seq reads. *Nat Biotechnol* 33, 290–295.

Ponder, W. F., and Lindberg, D. R. (1997). Towards a phylogeny of gastropod molluscs: an analysis using morphological characters. *Zool J Linn Soc* 119, 83–265.

Ponder, W. F., Lindberg, D. R., and Ponder, J. M. (2019). *Biology and evolution of the mollusca, volume 1*. CRC Press.

Popesku, J. T., Martyniuk, C. J., Mennigen, J., Xiong, H., Zhang, D., Xia, X., et al. (2008). The goldfish (*Carassius auratus*) as a model for neuroendocrine signaling. *Mol Cell Endocrinol* 293, 43–56.

Pratt, G. E., Farnsworth, D. E., Siegel, N. R., Fok, K. F., and Feyereisen, R. (1989). Identification of an allatostatin from adult *Diploptera punctata*. *Biochem Biophys Res Commun* 163, 1243–1247.

Price, D. A., and Greenberg, M. J. (1977). Structure of a molluscan cardioexcitatory neuropeptide. *Science (1979)* 197, 670–671.

Price, M. D., Merte, J., Nichols, R., Koladich, P. M., Tobe, S. S., and Bendena, W. G. (2002). *Drosophila melanogaster* flatline encodes a myotropin orthologue to *Manduca sexta* allatostatin. *Peptides (N.Y.)* 23, 787–794.

Raible, F., Tessmar-Raible, K., Osoegawa, K., Wincker, P., Jubin, C., Balavoine, G., et al. (2005). Vertebrate-type intron-rich genes in the marine annelid *Platynereis dumerilii*.

Science (1979) 310, 1325–1326.

Raineri, M. (1995). Is a mollusc an evolved bent metatrochophore? A histochemical investigation of neurogenesis in *Mytilus* (Mollusca: Bivalvia). *Journal of the Marine Biological Association of the United Kingdom* 75, 571–592.

Raineri, M., and Ospovat, M. (1994). The initial development of gangliar rudiments in a posterior position in *Mytilus galloprovincialis* (Mollusca: Bivalvia). *Journal of the Marine Biological Association of the United Kingdom* 74, 73–77.

Raven, C. P. (2013). *Morphogenesis: the analysis of molluscan development*. Elsevier.

Réalis-Doyelle, E., Schwartz, J., Cabau, C., Le Franc, L., Bernay, B., Rivière, G., et al. (2021). Transcriptome profiling of the Pacific oyster *Crassostrea gigas* visceral ganglia over a reproduction cycle identifies novel regulatory peptides. *Mar Drugs* 19, 452.

Revelle, W. (2011). An overview of the psych package.

Richardson, C. A., Runham, N. W., and Crisp, D. J. (1981). A histological and ultrastructural study of the cells of the mantle edge of a marine bivalve, *Cerastoderma edule*. *Tissue Cell* 13, 715–730.

Robertson, L., Rodriguez, E. P., and Lange, A. B. (2012). The neural and peptidergic control of gut contraction in *Locusta migratoria*: the effect of an FGLa/AST. *Journal of Experimental Biology* 215, 3394–3402.

Rodolfo-Metalpa, R., Houlbrèque, F., Tambutté, É., Boisson, F., Baggini, C., Patti, F. P., et al. (2011). Coral and mollusc resistance to ocean acidification adversely affected by

warming. *Nat Clim Chang* 1, 308–312.

Rodriguez-Navarro, C., Cizer, Ö., Kudłacz, K., Ibañez-Velasco, A., Ruiz-Agudo, C., Elert, K., et al. (2019). The multiple roles of carbonic anhydrase in calcium carbonate mineralization. *CrystEngComm* 21, 7407–7423.

Romero, A., del Mar Costa, M., Forn-Cuni, G., Balseiro, P., Chamorro, R., Dios, S., et al. (2014). Occurrence, seasonality and infectivity of *Vibrio* strains in natural populations of mussels *Mytilus galloprovincialis*. *Dis Aquat Organ* 108, 149–163.

Ronquist, F., Teslenko, M., Van Der Mark, P., Ayres, D. L., Darling, A., Höhna, S., et al. (2012). MrBayes 3.2: efficient Bayesian phylogenetic inference and model choice across a large model space. *Syst Biol* 61, 539–542.

Roots, B. I. (2008). The phylogeny of invertebrates and the evolution of *myelin*. *Neuron Glia Biol* 4, 101–109.

Rosani, U., Domeneghetti, S., Gerdol, M., Pallavicini, A., and Venier, P. (2019). Expansion and loss events characterized the occurrence of MIF-like genes in bivalves. *Fish Shellfish Immunol* 93, 39–49.

Rosell, N. C. (1991). The green mussel (*Perna viridis*) in the Philippines. *Estuarine and marine bivalve mollusk culture*, 297–305.

Rovati, G. E., Capra, V., and Neubig, R. R. (2007). The highly conserved DRY motif of class AG protein-coupled receptors: beyond the ground state. *Mol Pharmacol* 71, 959–964.

Salas, C., de Dios Bueno-Pérez, J., López-Téllez, J. F., and Checa, A. G. (2022). Form and

function of the mantle edge in *Protobranchia* (Mollusca: Bivalvia). *Zoology* 153, 126027.

Saleuddin, A. S. M., and Dillaman, R. M. (1976). Direct innervation of the mantle edge gland by neurosecretory axons in *Helisoma duryi* (Mollusca: Pulmonata). *Cell Tissue Res* 171, 397–401.

Saleuddin, A. S. M., and Kunigelis, S. C. (1984). Neuroendocrine control mechanisms in shell formation. *Am Zool* 24, 911–916.

Saleuddin, A. S. M., Sevala, V. M., Sevala, V. L., Mukai, S. T., and Khan, H. R. (1992). Involvement of mammalian insulin and insulin-like peptides in shell growth and shell regeneration in molluscs. *Hard tissue mineralization and demineralization*, 149–169.

Saleuddin, A. S. M., and Wilbur, K. M. (2012). *The Mollusca: Physiology, Part 2*. Academic Press.

Salvini-Plawen, L. v (1972). Zur Morphologie und Phylogenie der Mollusken: die Beziehungen der Caudofoveata und der Solenogastres als *Aculifera*, als Mollusca und als Spiralia. *Zeitschrift fur wissenschaftliche Zoologie* 184, 205–394.

Samonte, P. B., Gallardo, W. G., Agbayani, R. F., Siar, S. V, Ortega, R. O., Tumaliuan, R. E., et al. (1992). Socio-economic study of oyster (*Crassostrea iredalei*) and mussel (*Perna viridis*) farming in the Western Visayas, Philippines. Asian Fisheries Social Science Research Network. AFSSRN-SEAFDEC/AQD Team.

Santama, N., and Benjamin, P. R. (2000). Gene expression and function of FMRFamide-related neuropeptides in the snail *Lymnaea*. *Microsc Res Tech* 49,

547–556.

Santini, O., Chahbane, N., Vasseur, P., and Frank, H. (2011). Effects of low-level copper exposure on Ca2+-ATPase and carbonic anhydrase in the freshwater bivalve *Anodonta anatina*. *Toxicol Environ Chem* 93, 1826–1837.

Schmidt-Rhaesa, A., Harzsch, S., and Purschke, G. (2015). *Structure and evolution of invertebrate nervous systems*. Oxford University Press.

Schoofs, L., Veelaert, D., Broeck, J. Vanden, and De Loof, A. (1996). Immunocytochemical distribution of locustamyoinhibiting peptide (Lom-MIP) in the nervous system of *Locusta migratoria*. *Regul Pept* 63, 171–179.

Schultz, J. H., and Adema, C. M. (2017). Comparative immunogenomics of molluscs. *Dev Comp Immunol* 75, 3–15.

Schulze, J., Neupert, S., Schmidt, L., Predel, R., Lamkemeyer, T., Homberg, U., et al. (2012). Myoinhibitory peptides in the brain of the cockroach *Leucophaea maderae* and colocalization with pigment-dispersing factor in circadian pacemaker cells. *Journal of Comparative Neurology* 520, 1078–1097.

Schwartz, J., Dubos, M.-P., Pasquier, J., Zatylny-Gaudin, C., and Favrel, P. (2018). Emergence of a cholecystokinin/sulfakinin signalling system in Lophotrochozoa. *Sci Rep* 8, 16424.

Schwartz, J., Réalis-Doyelle, E., Dubos, M.-P., Lefranc, B., Leprince, J., and Favrel, P. (2019). Characterization of an evolutionarily conserved calcitonin signalling system in a lophotrochozoan, the Pacific oyster (*Crassostrea gigas*). *Journal of Experimental*

Biology 222, jeb201319.

Seilacher, A. (1985). Bivalve morphology and function. *Series in Geology, Notes for Short Course* 13, 88–101.

Sharker, M. R., Sukhan, Z. P., Kim, S. C., Rha, S.-J., and Kho, K. H. (2020). In silico prediction of neuropeptides from the neural ganglia of Pacific abalone *Haliotis discus hannai* (Mollusca: Gastropoda). *Eur Zool J* 87, 35–45.

Sharma, V., Srinivasan, A., Nikolajeff, F., and Kumar, S. (2021). Biomineralization process in hard tissues: The interaction complexity within protein and inorganic counterparts. *Acta Biomater* 120, 20–37.

Sheehan, D., and McDonagh, B. (2008). Oxidative stress and bivalves: a proteomic approach. *Invertebrate Survival Journal* 5, 110–123.

Shi, X. (2012). Preliminary on Cholinergic Neuro-Immune Regulatory System in Scallop *Chlamys Farreri*. Dissertation for the Degree of Doctor of Natural Science, Chinese Academy of Sciences.

Simakov, O., Marletaz, F., Cho, S.-J., Edsinger-Gonzales, E., Havlak, P., Hellsten, U., et al. (2013). Insights into bilaterian evolution from three spiralian genomes. *Nature* 493, 526–531.

Siniscalchi, A., Cavallini, S., Sonetti, D., Sbrenna, G., Capuano, S., Barbin, L., et al. (2004). Serotonergic neurotransmission in the bivalve *Venus verrucosa* (Veneridae): a neurochemical and immunohistochemical study of the visceral ganglion and gonads. *Mar Biol* 144, 1205–1212.

Skinner, J. R., Fairbairn, S. E., Woodhead, A. P., Bendena, W. G., and Stay, B. (1997). Allatostatin in hemocytes of the cockroach *Diploptera punctata*. *Cell Tissue Res* 290, 119–128.

Smit, A. B., Vreugdenhil, E., Ebberink, R. H. M., Geraerts, W. P. M., Klootwijk, J., and Joosse, J. (1988). Growth-controlling molluscan neurons produce the precursor of an insulin-related peptide. *Nature* 331, 535–538.

Smith, S. A., Wilson, N. G., Goetz, F. E., Feehery, C., Andrade, S. C. S., Rouse, G. W., et al. (2011). Resolving the evolutionary relationships of molluscs with phylogenomic tools. *Nature* 480, 364–367.

Song, L., Wang, L., Qiu, L., and Zhang, H. (2010). Bivalve immunity. *Invertebrate immunity*, 44–65.

Song, L., Wang, L., Zhang, H., and Wang, M. (2015). The immune system and its modulation mechanism in scallop. Fish Shellfish Immunol. 46, 65–78.

Stamatakis, A. (2014). RAxML version 8: a tool for phylogenetic analysis and post-analysis of large phylogenies. *Bioinformatics* 30, 1312–1313.

Stay, B., and Tobe, S. S. (2007). The role of allatostatins in juvenile hormone synthesis in insects and crustaceans. *Annu. Rev. Entomol.* 52, 277–299.

Stefano, G. B., and Aiello, E. (1975). Histofluorescent localization of serotonin and dopamine in the nervous system and gill of *Mytilus edulis* (Bivalvia). *Biol Bull* 148, 141–156.

Stefano, G. B., Catapane, E., and Aiello, E. (1976). Dopaminergic agents: Influence on

serotonin in the molluscan nervous system. *Science (1979)* 194, 539–541.

Stefano, G. B., and Catapane, E. J. (1979). Enkephalins increase dopamine levels in the CNS of a marine mollusc. *Life Sci* 24, 1617–1621.

Stefano, G. B., Hall, B., Makman, M. H., and Dvorkin, B. (1981). Opioids inhibit potassiumstimulated dopamine release in the marine mussel *Mytilus edulis* and in the cephalopod Octopus bimaculatis. *Science (1979)* 213, 928–930.

Stewart, M. J., Favrel, P., Rotgans, B. A., Wang, T., Zhao, M., Sohail, M., et al. (2014). Neuropeptides encoded by the genomes of the Akoya pearl oyster *Pinctata fucata* and Pacific oyster *Crassostrea gigas*: a bioinformatic and peptidomic survey. *BMC Genomics* 15, 1–16.

Storey, J. D., and Tibshirani, R. (2003). Statistical significance for genomewide studies. *Proceedings of the National Academy of Sciences* 100, 9440–9445.

Sun, W., and Feng, J. (2018). Differential lncRNA expression profiles reveal the potential roles of lncRNAs in antiviral immune response of *Crassostrea gigas*. *Fish Shellfish Immunol* 81, 233–241.

Suo, S., Ishiura, S., and Van Tol, H. H. M. (2004). Dopamine receptors in C. elegans. *Eur J Pharmacol* 500, 159–166.

Suzuki, M., and Nagasawa, H. (2013). Mollusk shell structures and their formation mechanism. *Can J Zool* 91, 349–366.

Suzuki, M., Saruwatari, K., Kogure, T., Yamamoto, Y., Nishimura, T., Kato, T., et al. (2009). An acidic matrix protein, Pif, is a key macromolecule for nacre formation.

Science (1979) 325, 1388–1390.

Takahashi, T., McDougall, C., Troscianko, J., Chen, W.-C., Jayaraman-Nagarajan, A., Shimeld, S. M., et al. (2009). An EST screen from the annelid *Pomatoceros lamarckii* reveals patterns of gene loss and gain in animals. *BMC Evol Biol* 9, 1–17.

Talmage, S. C., and Gobler, C. J. (2010). Effects of past, present, and future ocean carbon dioxide concentrations on the growth and survival of larval shellfish. *Proceedings of the National Academy of Sciences* 107, 17246–17251.

Tantiwisawaruji, S., Rocha, E., Kovitvadhi, U., and Rocha, M. J. (2014). The bivalve nervous system and its relevance for the physiology of reproduction. *Indian J Anat* 3, 14.

Taylor, J. D., Kennedy, W. J., and Hall, A. (1969). The shell structure and mineralogy of the Bivalvia Introduction. Nuculacea—Trigonacea. *Bulletin of the British Museum (Natural History). Zoology. Supplement*, 1–125.

Taylor, J. D., and Layman, M. (1972). The mechanical properties of bivalve (Mollusca) shell structures. *Palaeontology* 15, 73–87.

Teske, P. R., Barker, N. P., and McQuaid, C. D. (2007). Lack of genetic differentiation among four sympatric southeast African intertidal limpets (*Siphonariidae*): phenotypic plasticity in a single species *Journal of Molluscan Studies* 73, 223–228.

Tevesz, M. J. S., and Carter, J. G. (1980). Environmental relationships of shell form and structure of Unionacean bivalves.

Thiel, D., Yanez-Guerra, L. A., Franz-Wachtel, M., Hejnol, A., and Jékely, G. (2021).

Nemertean, brachiopod, and phoronid neuropeptidomics reveals ancestral spiralian signaling systems. *Mol Biol Evol* 38, 4847–4866.

Thomsen, J., Casties, I., Pansch, C., Körtzinger, A., and Melzner, F. (2013). Food availability outweighs ocean acidification effects in juvenile *Mytilus edulis*: laboratory and field experiments. *Glob Chang Biol* 19, 1017–1027.

Too, C. K. L., and Croll, R. P. (1995). Detection of FMRFamide-like immunoreactivities in the sea scallop *Placopecten magellanicus* by immunohistochemistry and Western blot analysis. *Cell Tissue Res* 281, 295–304.

Trudeau, V. L. (1997). Neuroendocrine regulation of gonadotrophin II release and gonadal growth in the goldfish, *Carassius auratus*. *Rev Reprod* 2, 55–68.

Trussell, G. C., and Nicklin, M. O. (2002). Cue sensitivity, inducible defense, and trade-offs in a marine snail. *Ecology* 83, 1635–1647.

Trussell, G. C., and Smith, L. D. (2000). Induced defenses in response to an invading crab predator: an explanation of historical and geographic phenotypic change. *Proceedings of the National Academy of Sciences* 97, 2123–2127.

Tsutsui, K., Bentley, G. E., Kriegsfeld, L. J., Osugi, T., Seong, J. Y., and Vaudry, H. (2010). Discovery and evolutionary history of gonadotrophin-inhibitory hormone and kisspeptin: new key neuropeptides controlling reproduction. *J Neuroendocrinol* 22, 716–727.

Uozumi, S., and Suzuki, S. (1979). " Organic Membrane-Shell" and Initial Calcification in Shell Regeneration. Journal of the Faculty of Science, Hokkaido University. Series 4,

Geology and mineralog. 19, 37–74.

van der Schatte Olivier, A., Jones, L., Vay, L. Le, Christie, M., Wilson, J., and Malham, S. K. (2020). A global review of the ecosystem services provided by bivalve aquaculture. *Rev Aquac* 12, 3–25.

Van In, V., Ntalamagka, N., O'Connor, W., Wang, T., Powell, D., Cummins, S. F., et al. (2016). Reproductive neuropeptides that stimulate spawning in the Sydney Rock Oyster (*Saccostrea glomerata*). *Peptides (N.Y.)* 82, 109–119.

Vandersmissen, H. P., Nachman, R. J., and Broeck, J. Vanden (2013). Sex peptides and MIPs can activate the same G protein-coupled receptor. *Gen Comp Endocrinol* 188, 137–143.

Vanderveken, M., and O'Donnell, M. J. (2014). Effects of diuretic hormone 31, drosokinin, and allatostatin A on transepithelial K^+ transport and contraction frequency in the midgut and hindgut of larval *Drosophila melanogaster*. *Arch Insect Biochem Physiol* 85, 76–93.

Vaughn, C. C., and Hoellein, T. J. (2018). Bivalve impacts in freshwater and marine ecosystems. *Annu Rev Ecol Evol Syst* 49, 183–208.

Vedel, L., Nøhr, A. C., Gloriam, D. E., and Bräuner-Osborne, H. (2020). Pharmacology and function of the orphan GPR139 G protein-coupled receptor. *Basic Clin Pharmacol Toxicol* 126, 35–46.

Veenstra, J. A. (2009). Allatostatin C and its paralog allatostatin double C: the arthropod somatostatins. *Insect Biochem Mol Biol* 39, 161–170.

Veenstra, J. A. (2010). Neurohormones and neuropeptides encoded by the genome of *Lottia gigantea*, with reference to other mollusks and insects. *Gen Comp Endocrinol* 167, 86–103.

Veenstra, J. A. (2016). Allatostatins C, double C and triple C, the result of a local gene triplication in an ancestral arthropod. *Gen Comp Endocrinol* 230, 153–157.

Venier, P., Varotto, L., Rosani, U., Millino, C., Celegato, B., Bernante, F., et al. (2011). Insights into the innate immunity of the Mediterranean mussel *Mytilus galloprovincialis*. *BMC Genomics* 12, 1–19.

Verlinden, H., Gijbels, M., Lismont, E., Lenaerts, C., Broeck, J. Vanden, and Marchal, E. (2015). The pleiotropic allatoregulatory neuropeptides and their receptors: A mini-review. *J Insect Physiol* 80, 2–14.

Vermeij, G. J. (1983). Traces and trends of predation, with special reference to bivalved animals. *Palaeontology* 26, 455–465.

Vilim, F. S., Cropper, E. C., Rosen, S. C., Tenenbaum, R., Kupfermann, I., and Weiss, K. R. (1994). Structure, localization, and action of buccalin B: a bioactive peptide from *Aplysia*. *Peptides (N.Y.)* 15, 959–969.

Vinther, J. (2015). The origins of molluscs. *Palaeontology* 58, 19–34.

Vinther, J., Sperling, E. A., Briggs, D. E. G., and Peterson, K. J. (2012). A molecular palaeobiological hypothesis for the origin of aplacophoran molluscs and their derivation from chiton-like ancestors. *Proceedings of the Royal Society B: Biological Sciences* 279, 1259–1268.

Vogeler, S., Carboni, S., Li, X., and Joyce, A. (2021). Phylogenetic analysis of the caspase family in bivalves: implications for programmed cell death, immune response and development. *BMC Genomics* 22, 1–17.

Voronezhskaya, E. E., Tyurin, S. A., and Nezlin, L. P. (2002). Neuronal development in larval chiton *Ischnochiton hakodadensis* (Mollusca: Polyplacophora). *Journal of Comparative Neurology* 444, 25–38.

Waller, T. R. (1981). Functional morphology and development of veliger larvae of the European oyster, *Ostrea edulis Linné*.

Wang, F., Li, S., Xiang, J., and Li, F. (2019). Transcriptome analysis reveals the activation of neuroendocrine-immune system in shrimp hemocytes at the early stage of WSSV infection. *BMC Genomics* 20, 1–14.

Wang, H., Yu, H., Li, Q., and Liu, S. (2022). Transcription analysis for core networks of lncRNAs–mRNAs: implication for potential role in sterility of *Crassostrea gigas*. *Biology (Basel)* 11, 378.

Wang, L., Song, X., and Song, L. (2018). The oyster immunity. *Dev Comp Immunol* 80, 99–118.

Wang, Q., Zhang, L., Zhao, J., You, L., and Wu, H. (2012). Two goose-type lysozymes in *Mytilus galloprovincialis*: possible function diversification and adaptive evolution.

Wang, S., Zhang, J., Jiao, W., Li, J. I., Xun, X., Sun, Y., et al. (2017). Scallop genome provides insights into evolution of bilaterian karyotype and development. *Nat Ecol Evol* 1, 0120.

Wanninger, A. (2015). *Evolutionary developmental biology of invertebrates 2: lophotrochozoa (Spiralia)*. Springer.

Wanninger, A., and Wollesen, T. (2019). The evolution of molluscs. *Biological Reviews* 94, 102–115.

Weaver, R. J., and Audsley, N. (2009). Neuropeptide regulators of juvenile hormone synthesis: structures, functions, distribution, and unanswered questions. *Ann N Y Acad Sci* 1163, 316–329.

Wen, Z., Gulia, M., Clark, K. D., Dhara, A., Crim, J. W., Strand, M. R., et al. (2010). Two insulin-like peptide family members from the mosquito *Aedes aegypti* exhibit differential biological and receptor binding activities. Mol. Cell. Endocrinol. 328, 47–55.

Weiss, I. (2012). Species-specific shells: chitin synthases and cell mechanics in molluscs. *Zeitschrift für Kristallographie-Crystalline Materials* 227, 723–738.

Weiss, I. M., Lüke, F., Eichner, N., Guth, C., and Clausen-Schaumann, H. (2013). On the function of chitin synthase extracellular domains in biomineralization. *J Struct Biol* 183, 216–225.

Weiss, I. M., Schönitzer, V., Eichner, N., and Sumper, M. (2006). The chitin synthase involved in marine bivalve mollusk shell formation contains a myosin domain. *FEBS Lett* 580, 1846–1852.

Weiss, I. M., Tuross, N., Addadi, L. I. A., and Weiner, S. (2002). Mollusc larval shell formation: amorphous calcium carbonate is a precursor phase for aragonite. *Journal*

of Experimental Zoology 293, 478–491.

Westbroek, P., and Marin, F. (1998). A marriage of bone and nacre. *Nature* 392, 861–862.

Wickham, H. (2016). *ggplot2: elegant graphics for data analysis*. Verlag New York: springer.

Wilbur, K. M., and Saleuddin, A. S. M. (1983). "Shell formation," in *The mollusca*, (Elsevier), 235–287.

Wilk, J., and Bieler, R. (2009). Ecophenotypic variation in the Flat Tree Oyster, *Isognomon alatus* (Bivalvia: Isognomonidae), across a tidal microhabitat gradient. *Marine Biology Research* 5, 155–163.

Wilkins, D. (2019). "gggenes: draw gene arrow maps in 'ggplot2'. R package version 0.4. 0," in *gggenes: draw gene arrow maps in 'ggplot2'. R package version 0.4. 0*.

Williams, E. A., Conzelmann, M., and Jékely, G. (2015). Myoinhibitory peptide regulates feeding in the marine annelid *Platynereis*. *Front Zool* 12, 1–16.

Windoffer, R., Jahn, A., Meyberg, F., Krieger, J., and Giere, O. (1999). Sulphide-induced metal precipitation in the mantle edge of *Macoma balthica* (Bivalvia, Tellinidae)--a means of detoxification. *Mar Ecol Prog Ser* 187, 159–170.

Wolf, H., Backeljau, T., and Verhagen, R. (1998). Spatio-temporal genetic structure and gene flow between two distinct shell morphs of the planktonic developing periwinkle *Littorina striata* (Mollusca: Prosobranchia). *Mar Ecol Prog Ser* 163, 155–163.

Woodhead, A. P., Stay, B., Seidel, S. L., Khan, M. A., and Tobe, S. (1989). Primary

structure of four allatostatins: neuropeptide inhibitors of juvenile hormone synthesis. *Proceedings of the national academy of sciences* 86, 5997–6001.

Wu, K., Li, S., Wang, J., Ni, Y., Huang, W., Liu, Q., et al. (2020). Peptide hormones in the insect midgut. *Front Physiol* 11, 191.

Xiao, Q., Lin, Y., Li, H., Chen, Y., Wei, W., Li, P., et al. (2022). Transcriptome sequencing reveals the differentially expressed lncRNAs and mRNAs in response to cold acclimation and cold stress in *Pomacea canaliculata*. *BMC Genomics* 23, 382.

Xu, M., Wu, J., Ge, D., Wu, C., Chi, C., Lv, Z., et al. (2018). A novel toll-like receptor from *Mytilus coruscus* is induced in response to stress. *Fish Shellfish Immunol* 78, 331–337.

Xu, Z., Wei, Y., Guo, S., Lin, D., and Ye, H. (2020). B-type allatostatin modulates immune response in hepatopancreas of the mud crab *Scylla paramamosain*. *Dev Comp Immunol* 110, 103725.

Xu, Z., Wei, Y., Wang, G., and Ye, H. (2021). B-type allatostatin regulates immune response of hemocytes in mud crab Scylla paramamosain. *Dev Comp Immunol* 120, 104050.

Yamanaka, N., Hua, Y.-J., Roller, L., Spalovská-Valachová, I., Mizoguchi, A., Kataoka, H., et al. (2010). Bombyx prothoracicostatic peptides activate the sex peptide receptor to regulate ecdysteroid biosynthesis. *Proceedings of the National Academy of Sciences* 107, 2060–2065.

Yan, H., Chen, J., and Xiao, J. (2014). A review on bivalve shell, a tool for reconstruction

of paleo-climate and paleo-environment. *Chinese Journal of Geochemistry* 33, 310–315.

Yang, J.-L., Feng, D.-D., Liu, J., Xu, J.-K., Chen, K., Li, Y.-F., et al. (2021). Chromosome-level genome assembly of the hard-shelled mussel *Mytilus coruscus*, a widely distributed species from the temperate areas of East Asia. *Gigascience* 10, giab024.

Yarra, T., Blaxter, M., and Clark, M. S. (2021). A bivalve biomineralization toolbox. *Mol Biol Evol* 38, 4043–4055.

Yarra, T., Gharbi, K., Blaxter, M., Peck, L. S., and Clark, M. S. (2016). Characterization of the mantle transcriptome in bivalves: *Pecten maximus*, *Mytilus edulis* and *Crassostrea gigas*. *Mar Genomics* 27, 9–15.

Yonge, C. M. (1957). Mantle fusion in the *Lamellibranchia*. *Pubblicazioni della Stazione zoologica di Napoli* 29, 151–171.

Yonge, C. M. (1983). Symmetries and the role of the mantle margins in the bivalve Mollusca. *Malacological Review* 16, 1–10.

Yoon, S., Kim, M. A., Lee, J. S., and Sohn, Y. C. (2022). Functional analysis of LFRFamide signaling in Pacific abalone, *Haliotis discus hanna*i. *PLoS One* 17, e0267039.

Yoshida, N., Higashimura, E., and Saeki, Y. (2010). Catalytic biomineralization of fluorescent calcite by the thermophilic bacterium Geobacillus thermoglucosidasius. *Appl Environ Microbiol* 76, 7322–7327.

Yu, H., Zhao, X., and Li, Q. (2016). Genome-wide identification and characterization of long intergenic noncoding RNAs and their potential association with larval development in the Pacific oyster. *Sci Rep* 6, 20796.

Yu, N., and Smagghe, G. (2014). CCK (-like) and receptors: structure and phylogeny in a comparative perspective. *Gen Comp Endocrinol* 209, 74–81.

Yurchenko, O. V, and Dyachuk, V. A. (2022). Characterization of Neurodevelopment in Larvae of the Protobranch *Acila insignis* (Gould, 1861) in Order to Reconstruct the Last Common Ancestor of Bivalves. *Malacologia* 64, 241–255.

Zatylny-Gaudin, C., and Favrel, P. (2014). Diversity of the RFamide peptide family in mollusks. *Front Endocrinol (Lausanne)* 5, 110140.

Zeebe, R. E. (2012). History of seawater carbonate chemistry, atmospheric CO2, and ocean acidification. *Annu Rev Earth Planet Sci* 40, 141–165.

Zenger, K. R., Khatkar, M. S., Jones, D. B., Khalilisamani, N., Jerry, D. R., and Raadsma, H. W. (2019). Genomic selection in aquaculture: application, limitations and opportunities with special reference to marine shrimp and pearl oysters. *Front Genet* 9, 693.

Zha, G., Chen, V. P., Luk, W. K. W., Zou, X., Choi, R. C. Y., and Tsim, K. W. K. (2013). Characterization of acetylcholinesterase in Hong Kong oyster (*Crassostrea hongkongensis*) from South China Sea. *Chem Biol Interact* 203, 277–281.

Zhang, G., Fang, X., Guo, X., Li, L. I., Luo, R., Xu, F., et al. (2012). The oyster genome reveals stress adaptation and complexity of shell formation. *Nature* 490, 49–54.

Zhang, L., Li, L., Guo, X., Litman, G. W., Dishaw, L. J., and Zhang, G. (2015). Massive expansion and functional divergence of innate immune genes in a protostome. *Sci Rep* 5, 8693.

Zhang, M., Wang, Y., Li, Y., Li, W., Li, R., Xie, X., et al. (2018). Identification and characterization of neuropeptides by transcriptome and proteome analyses in a bivalve mollusc *Patinopecten yessoensis*. *Front Genet* 9, 197.

Zhang, W., Mao, J., Yuan, C., Yang, J., Han, B., Wang, X., et al. (2020a). Histological changes in the mantle tissue of the Yesso Scallop *Patinopecten yessoensis* shell infested by Polydora. *J Shellfish Res* 39, 87–97.

Zhang, X.-H., He, X., and Austin, B. (2020b). *Vibrio harveyi*: a serious pathogen of fish and invertebrates in mariculture. *Mar Life Sci Technol* 2, 231–245.

Zhang, Y., Meng, Q., Jiang, T., Wang, H., Xie, L., and Zhang, R. (2003). A novel ferritin subunit involved in shell formation from the pearl oyster (*Pinctada fucata*). *Comp Biochem Physiol B Biochem Mol Biol* 135, 43–54.

Zhao, R., Takeuchi, T., Luo, Y.-J., Ishikawa, A., Kobayashi, T., Koyanagi, R., et al. (2018). Dual gene repertoires for larval and adult shells reveal molecules essential for molluscan shell formation. *Mol Biol Evol* 35, 2751–2761.

Zheng, Z., Hao, R., Yang, C., Jiao, Y., Wang, Q., Huang, R., et al. (2023). Genome-wide association study analysis to resolve the key regulatory mechanism of biomineralization in *Pinctada fucata martensii*. *Mol Ecol Resour* 23, 680–693.

Zieritz, A., Checa, A. G., Aldridge, D. C., and Harper, E. M. (2011). Variability, function

and phylogenetic significance of periostracal microprojections in unionoid bivalves (Mollusca). *Journal of Zoological Systematics and Evolutionary Research* 49, 6–15.

Zoysa, M., Jung, S., and Lee, J. (2009). First molluscan TNF-α homologue of the TNF superfamily in disk abalone: Molecular characterization and expression analysis. *Fish Shellfish Immunol* 26, 625–631.

Zwaan, A., and Mathieu, M. (1992). Cellular biochemistry and endocrinology. *Developments in aquaculture and fisheries science* 25, 223–307.